Searches for light Dark Matter with Spherical Proportional Counters

Konstantinos Nikolopoulos
University of Birmingham

UNIVERSITY OF BIRMINGHAM

ATLAS experiment at CERN

Particle Physics Seminar
October 11th, 2022, CEA-Saclay

This project has received funding from the European Research Council (ERC) under the European Union's Horizon 2020 research and innovation programme under grant agreement 714893-ExclusiveHiggs and under Marie Skłodowska-Curie agreement 841261-DarkSphere, 895168-neutronSPHERE, 101026519-GaGARin

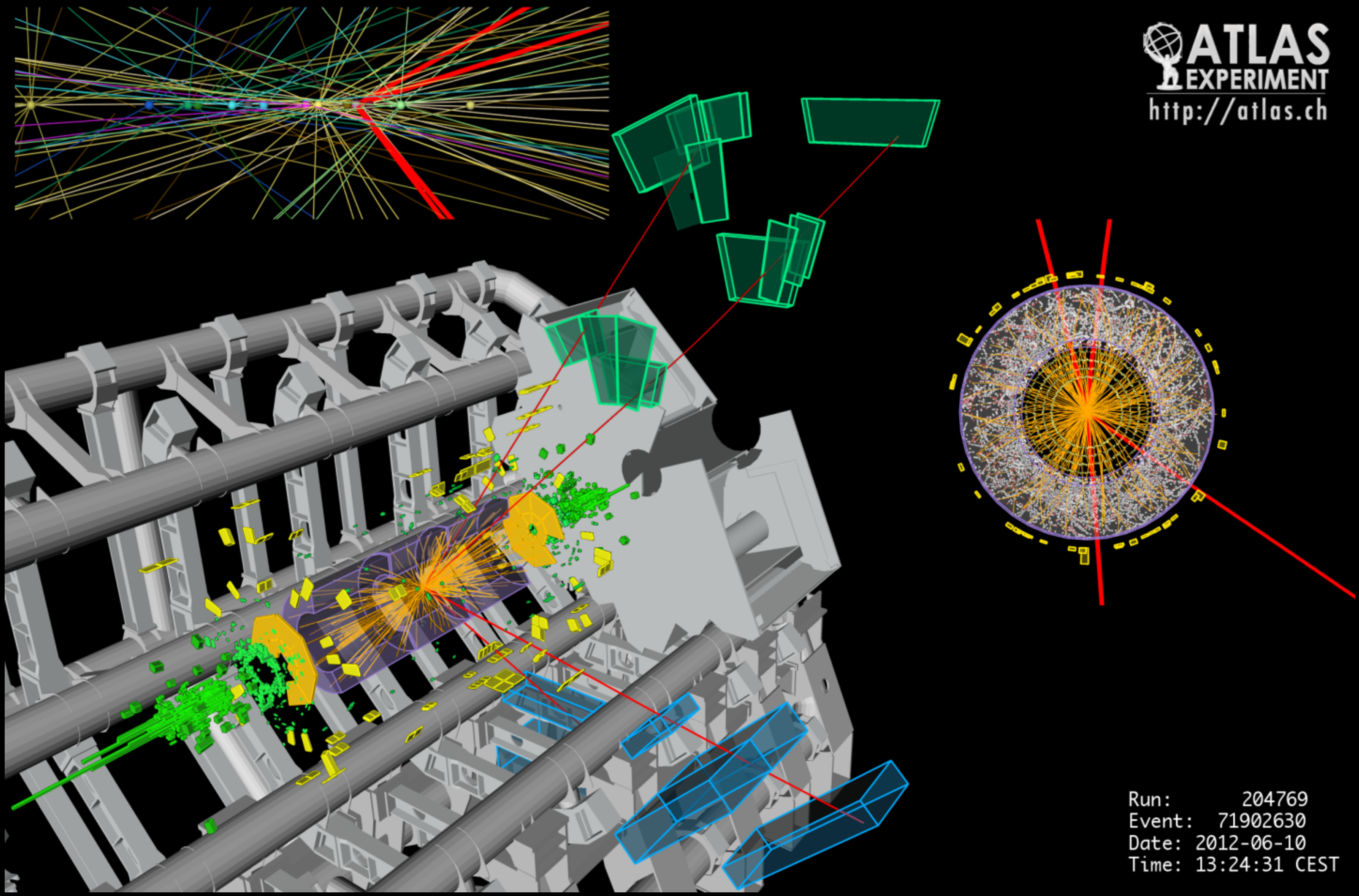
ATLAS
EXPERIMENT
http://atlas.ch
Run: 204769
Event: 71902630
Date: 2012-06-10
Time: 13:24:31 CEST

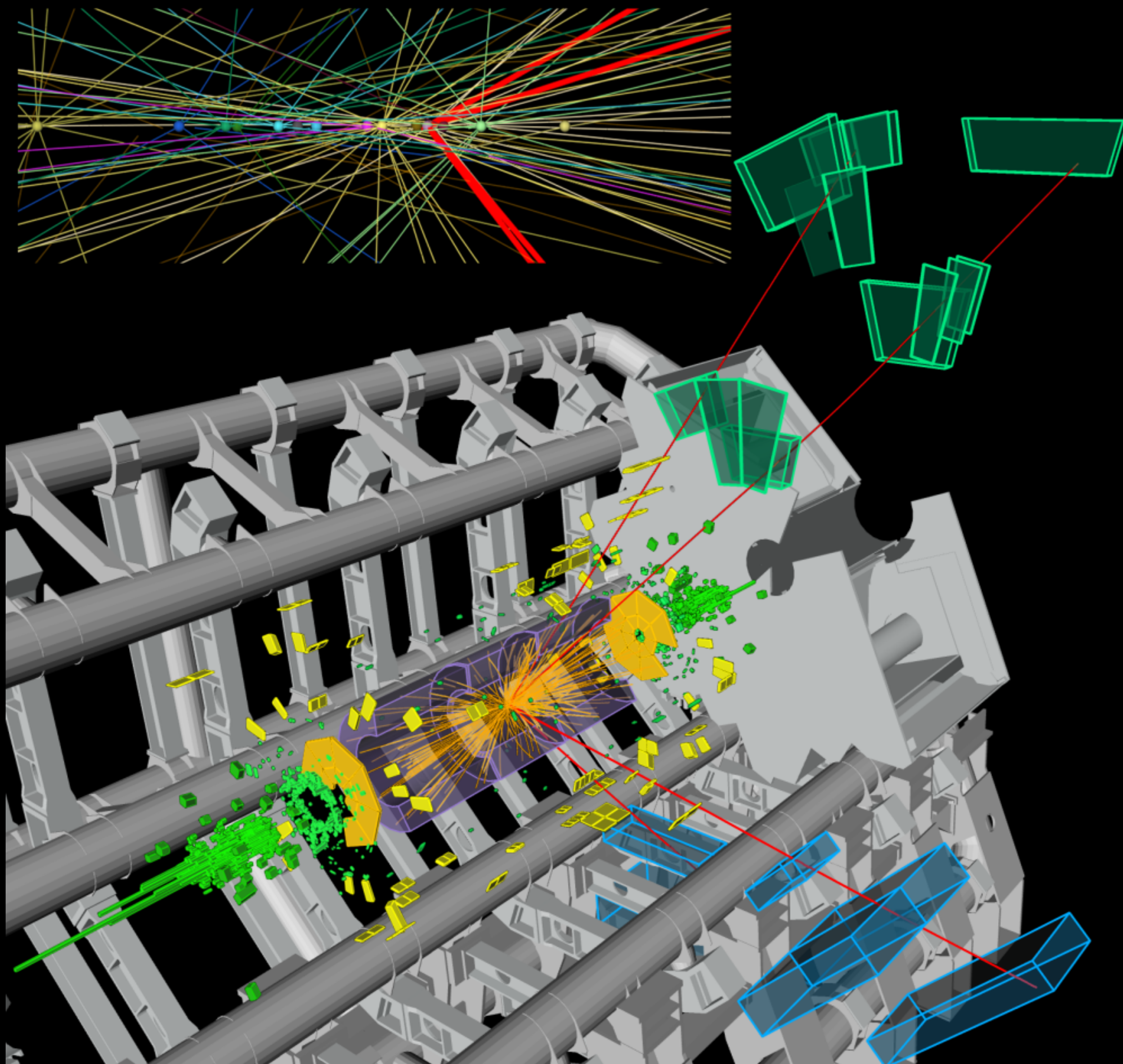

ATLAS EXPERIMENT
http://atlas.ch

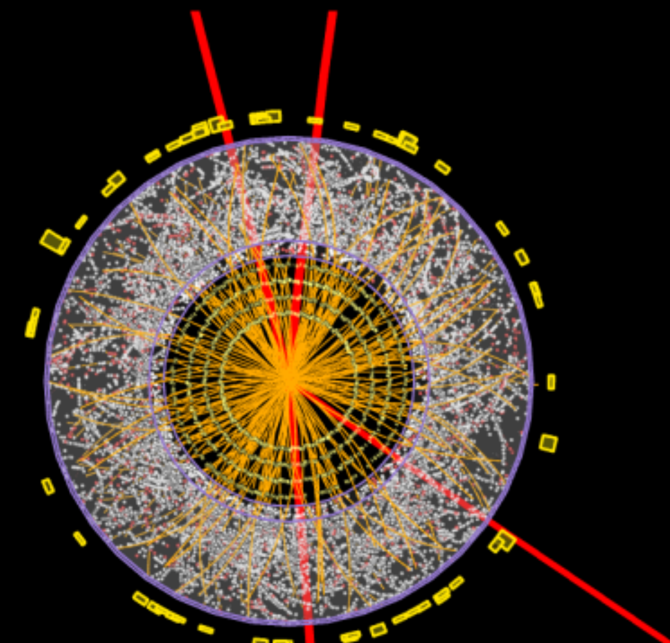

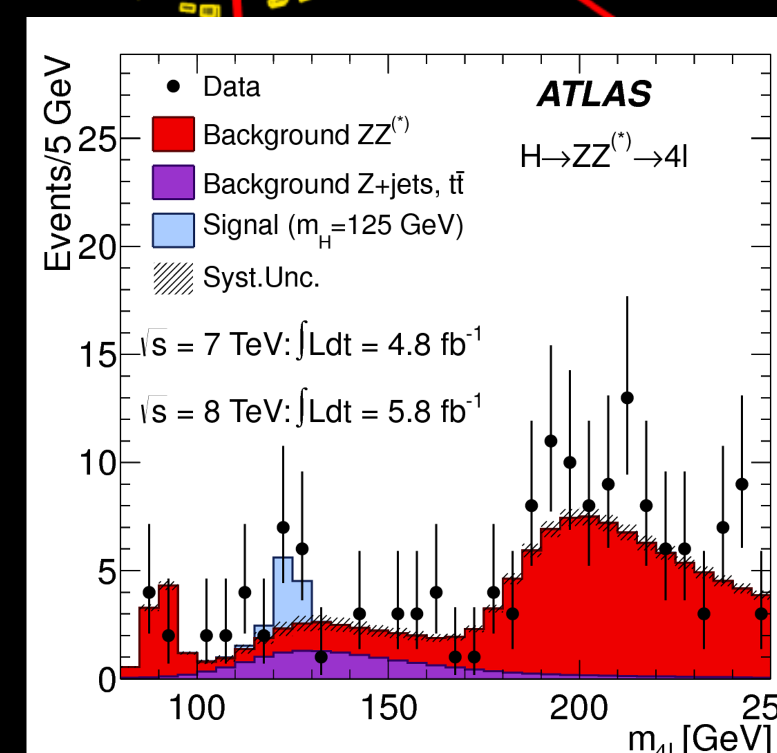

ATLAS EXPERIMENT
http://atlas.ch

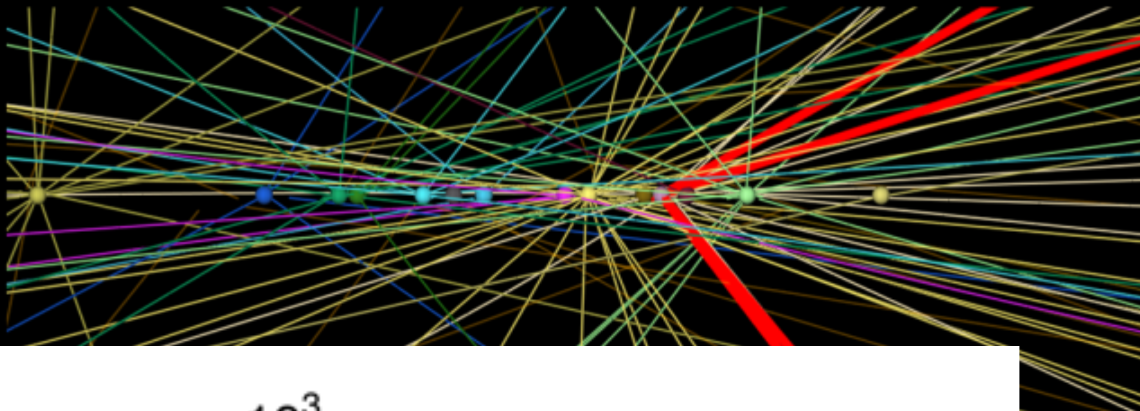

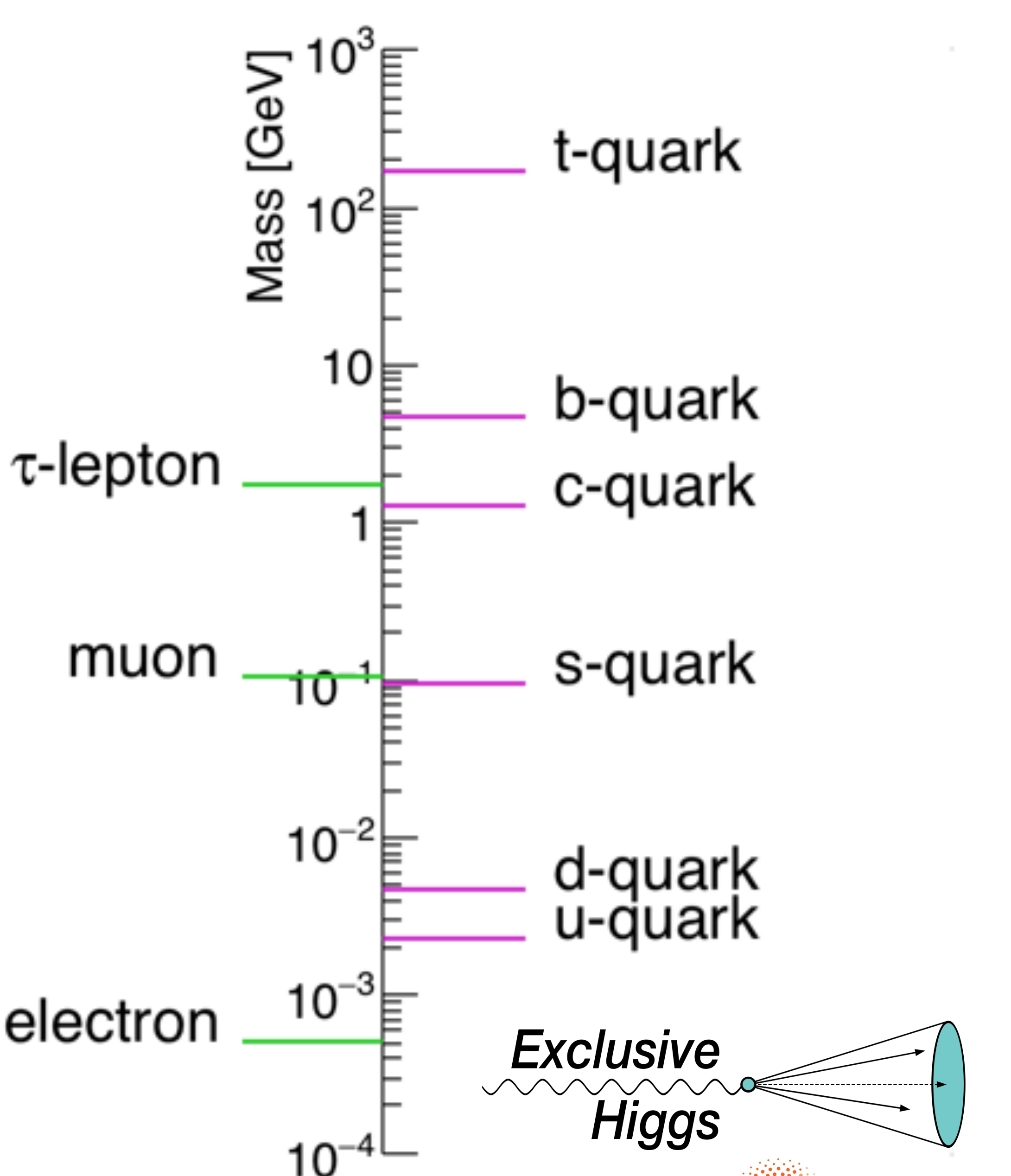

$$\frac{m_e}{m_t} \approx 3 \times 10^{-6}$$

erc
European Research Council
Established by the European Commission

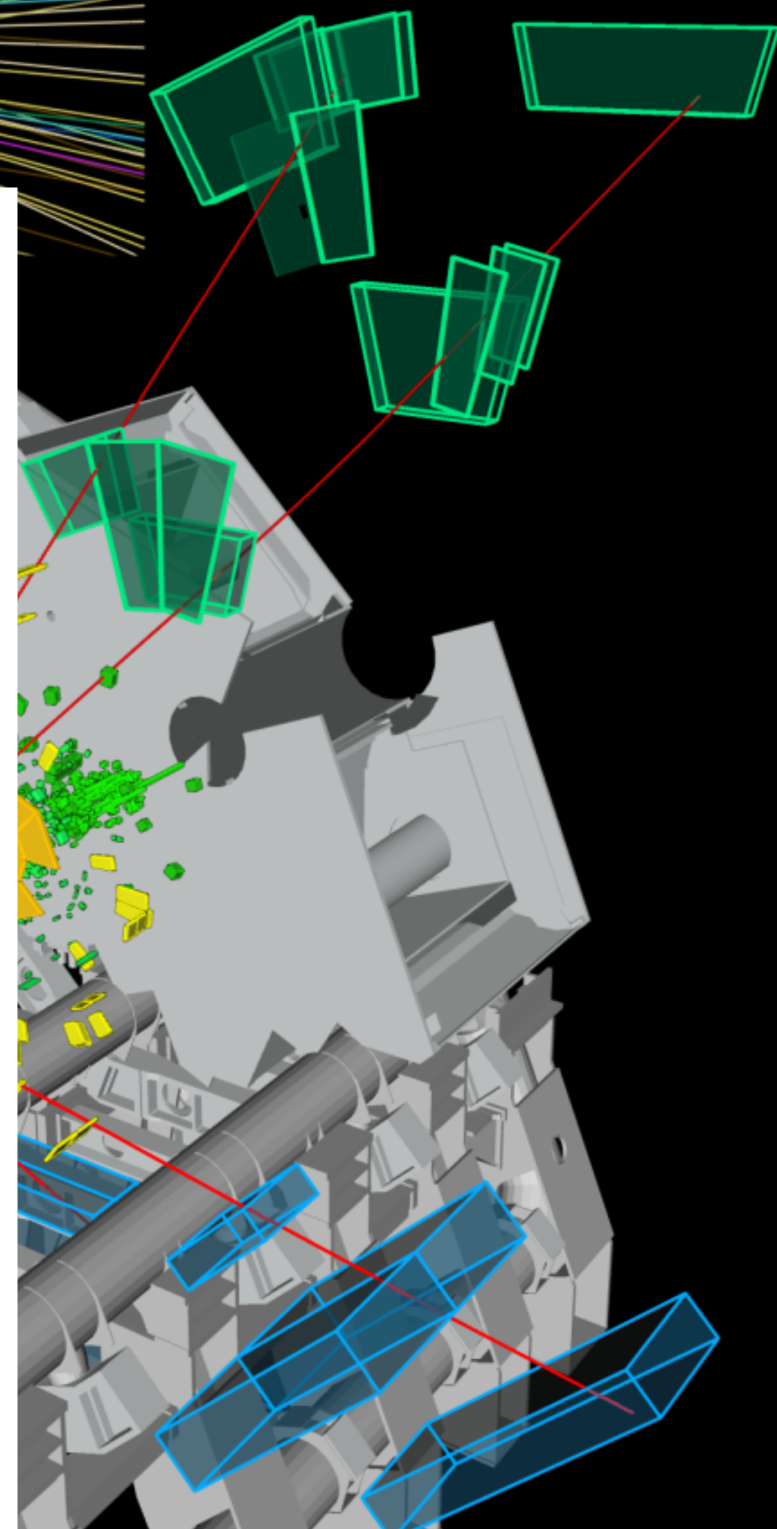

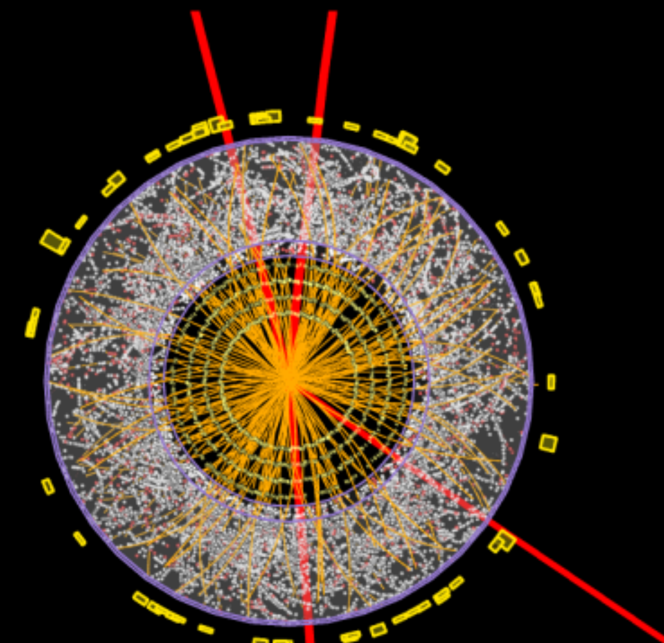

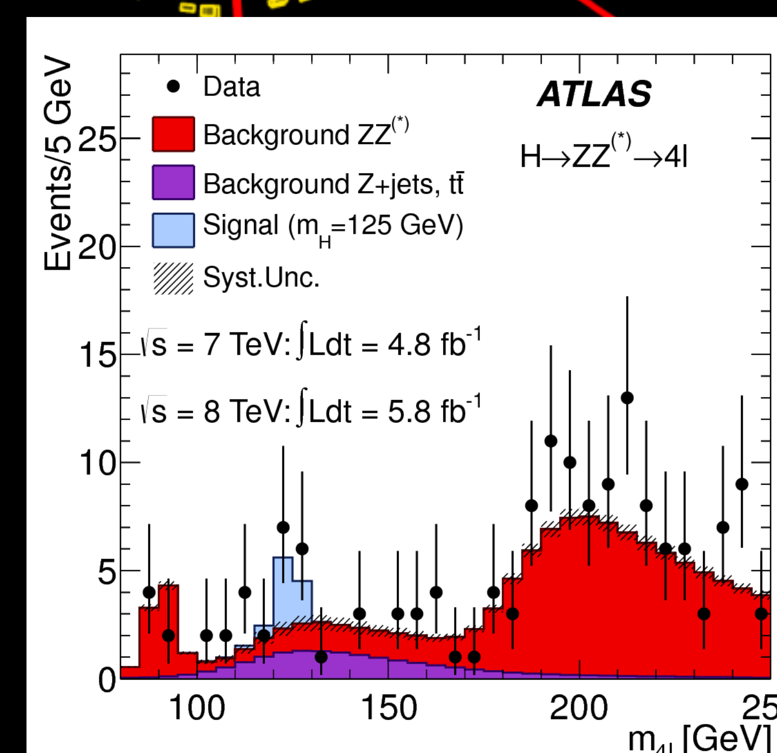

UNIVERSITY OF BIRMINGHAM

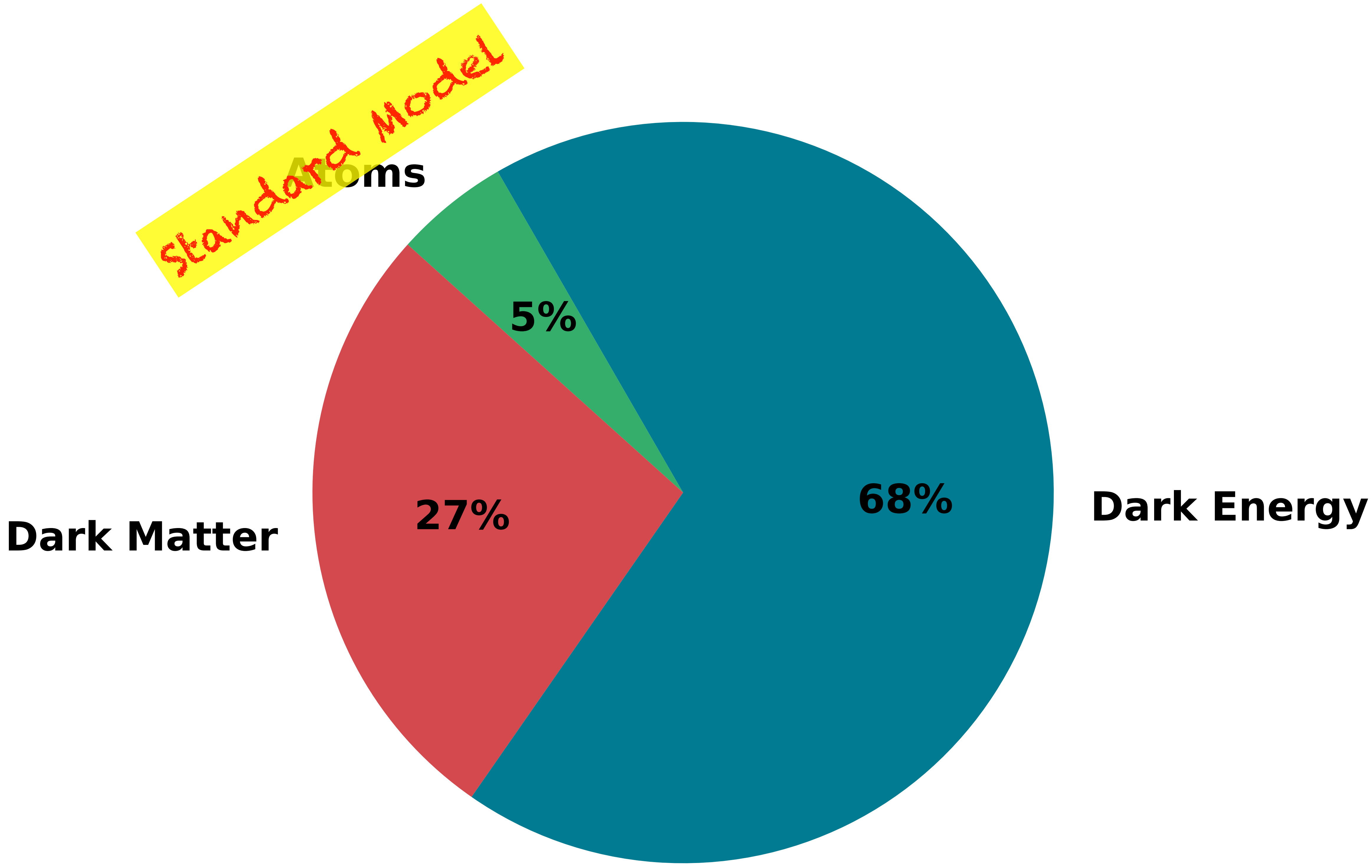
Standard Model
Atoms
5%
Dark Matter
27%
68%
Dark Energy

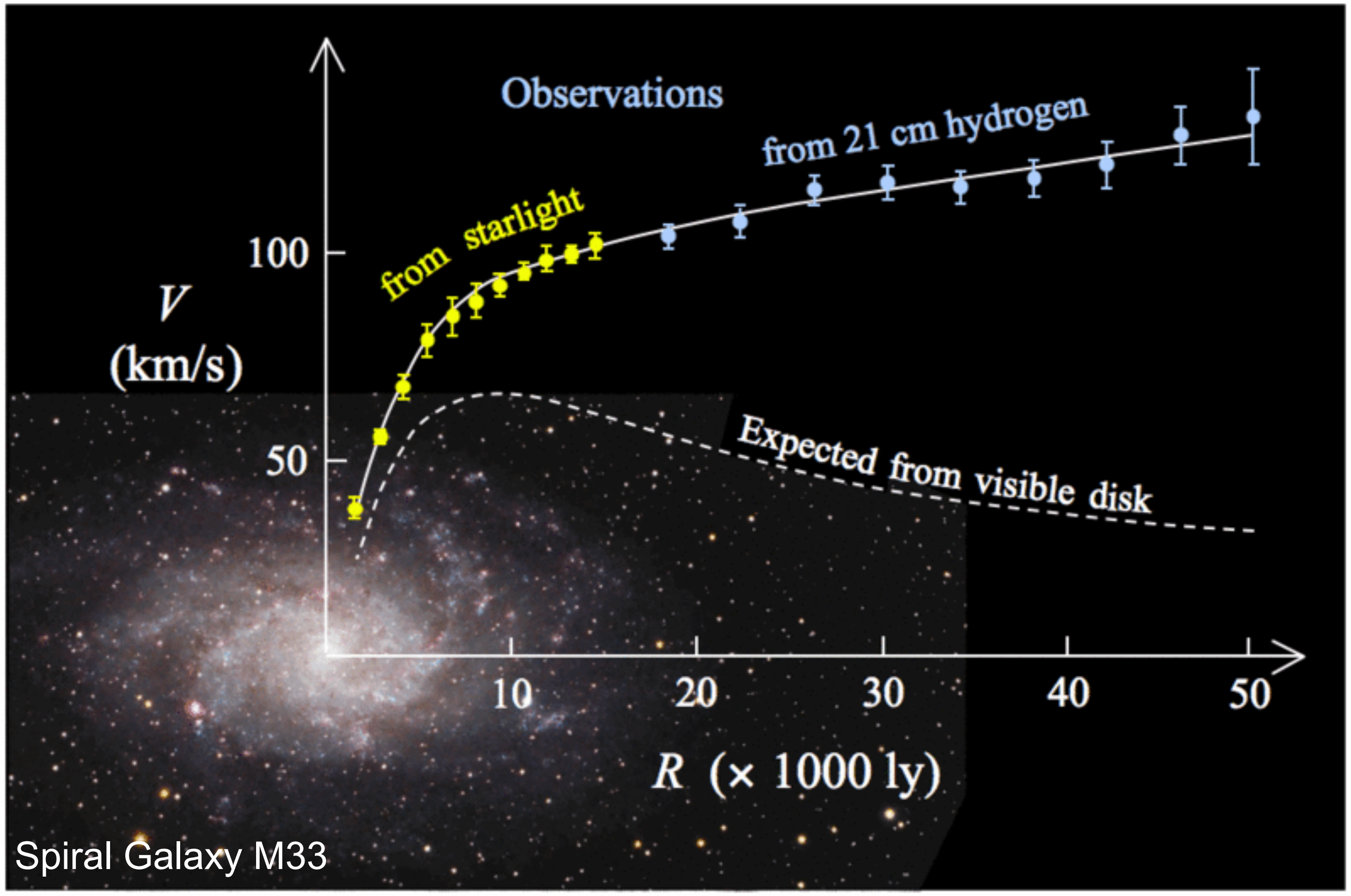

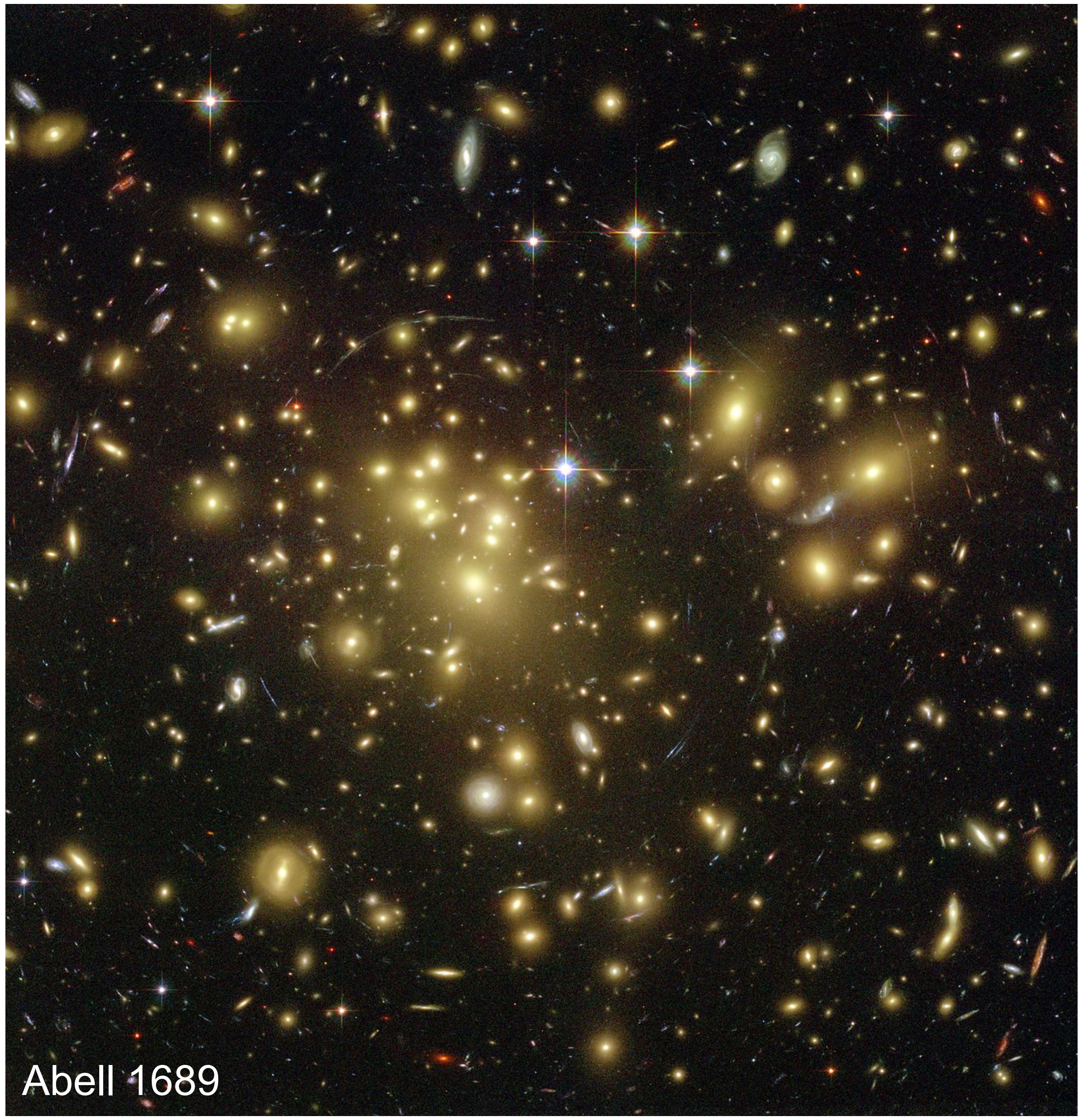

- **Evidence from gravitational interactions over many distance scales**
  - Rotational curves (galaxies and galaxy clusters)
  - Gravitational lensing
  - Cosmology
    - Cosmic microwave background
    - Large scale structure formation
  - Big Bang Nucleosynthesis

Dark matter characteristics

Dark Matter Particle (X^0)

X^0 mass: $m = ?$
X^0 spin: $J = ?$
X^0 parity: $P = ?$
X^0 lifetime: $\tau = ?$
X^0 scattering cross-section on nucleons: $?$
X^0 production cross-section in hadron colliders: $?$
X^0 self-annihilation cross-section: $?$

- **What we know about Dark Matter**
  - Non-Baryonic
  - Mostly "cold"
  - Electrically neutral (or milli-charged?)
  - "Weakly" interacting
  - $\Omega_{DM}h^2$=0.120±0.001
  - Stable or $\tau_{DM} \gg \tau_u$

Dark matter characteristics

Dark Matter Particle (X^0)

X^0 mass: $m = ?$
X^0 spin: $J = ?$
X^0 parity: $P = ?$
X^0 lifetime: $\tau = ?$
X^0 scattering cross-section on nucleons: ?
X^0 production cross-section in hadron colliders: ?
X^0 self-annihilation cross-section: ?

No known particle fits the bill!

- **What we know about Dark Matter**
  - Non-Baryonic
  - Mostly “cold”
  - Electrically neutral (or milli-charged?)
  - “Weakly” interacting
  - $\Omega_{DM}h^2=0.120\pm0.001$
  - Stable or $\tau_{DM} \gg \tau_U$

Dark matter characteristics

Dark Matter Particle (X^0)

No known particle fits the bill!

X^0 mass: $m = ?$
X^0 spin: $J = ?$
X^0 parity: $P = ?$
X^0 lifetime: $\tau = ?$
X^0 scattering cross-section on nucleons: ?
X^0 production cross-section in hadron colliders: ?
X^0 self-annihilation cross-section: ?

- **What we know about Dark Matter**
  - Non-Baryonic
  - Mostly “cold”
  - Electrically neutral (or milli-charged?)
  - “Weakly” interacting
  - $\Omega_{DM}h^2$=0.120±0.001
  - Stable or $\tau_{DM} \gg \tau_u$

- **Standard Halo Model**
  - Spherical
  - Isotropic
  - Maxwell velocity distribution
  - No substructure

Dark matter characteristics

Dark Matter Particle (X^0)

X^0 mass: $m = ?$
X^0 spin: $J = ?$
X^0 parity: $P = ?$
X^0 lifetime: $\tau = ?$
X^0 scattering cross-section on nucleons: ?
X^0 production cross-section in hadron colliders: ?
X^0 self-annihilation cross-section: ?

No known particle fits the bill!

What we know about Dark Matter

- Non-Baryonic
- Mostly "cold"
- Electrically neutral (or milli-charged?)
- "Weakly" interacting
- $\Omega_{DM}h^2 = 0.120 \pm 0.001$
- Stable or $\tau_{DM} \gg \tau_U$

Standard Halo Model

- Spherical
- Isotropic
- Maxwell velocity distribution
- No substructure

Phys.Rev.D 99 (2019) 2, 023012

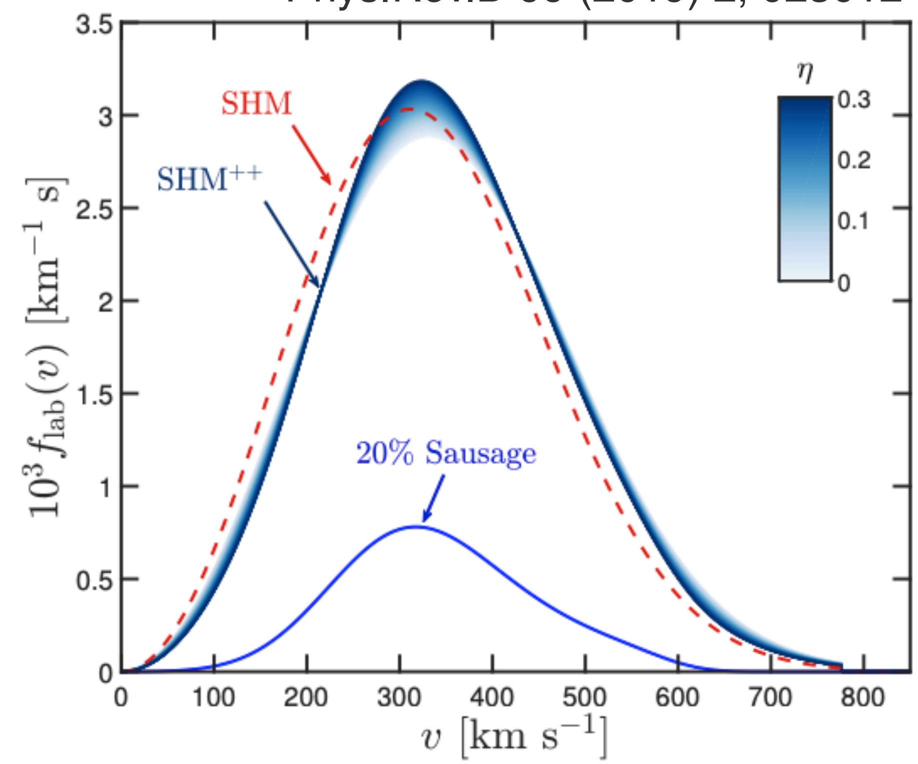

Wide field of possibilities!

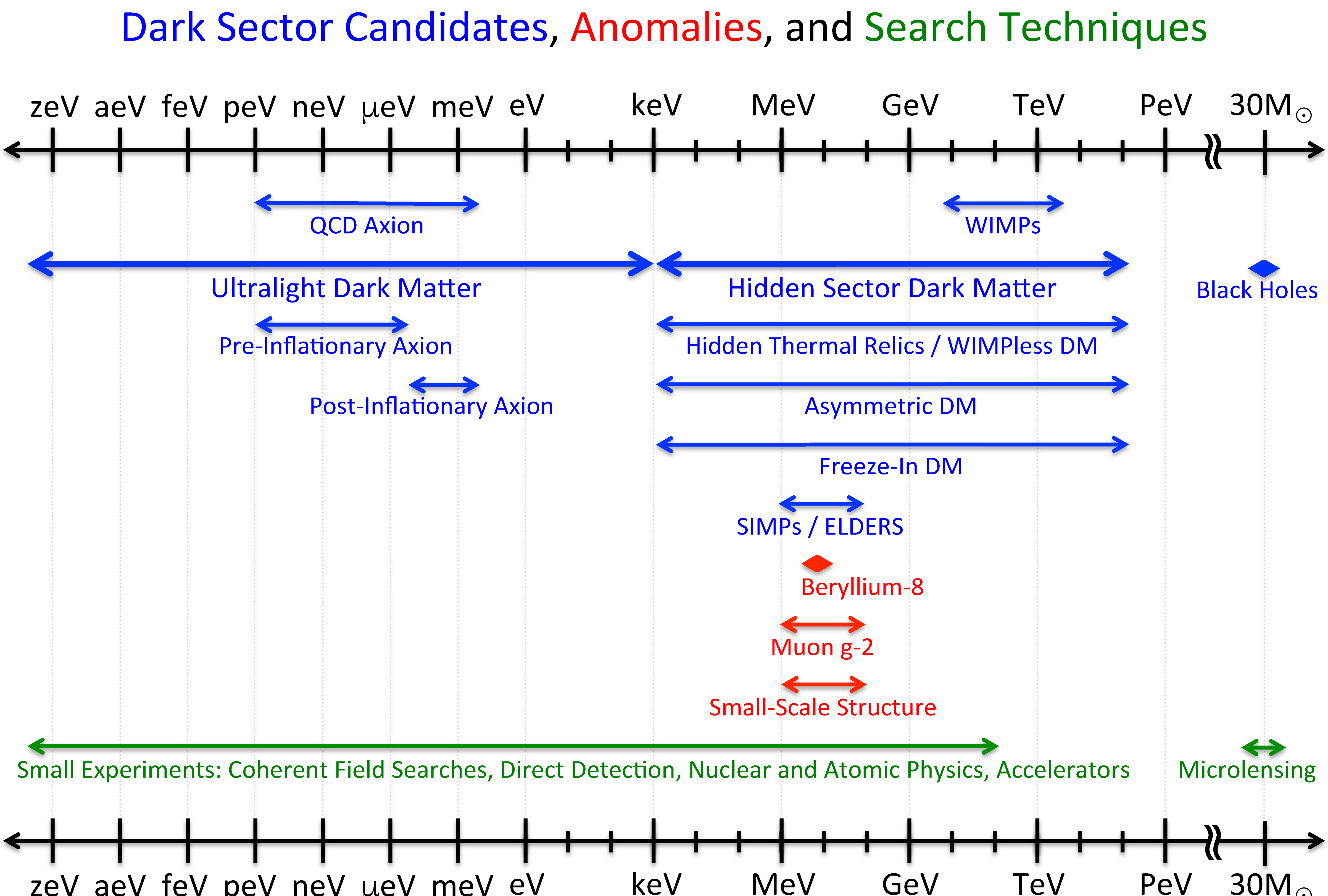

Cosmic visions
arXiv:1707.04591

Wide field of possibilities!

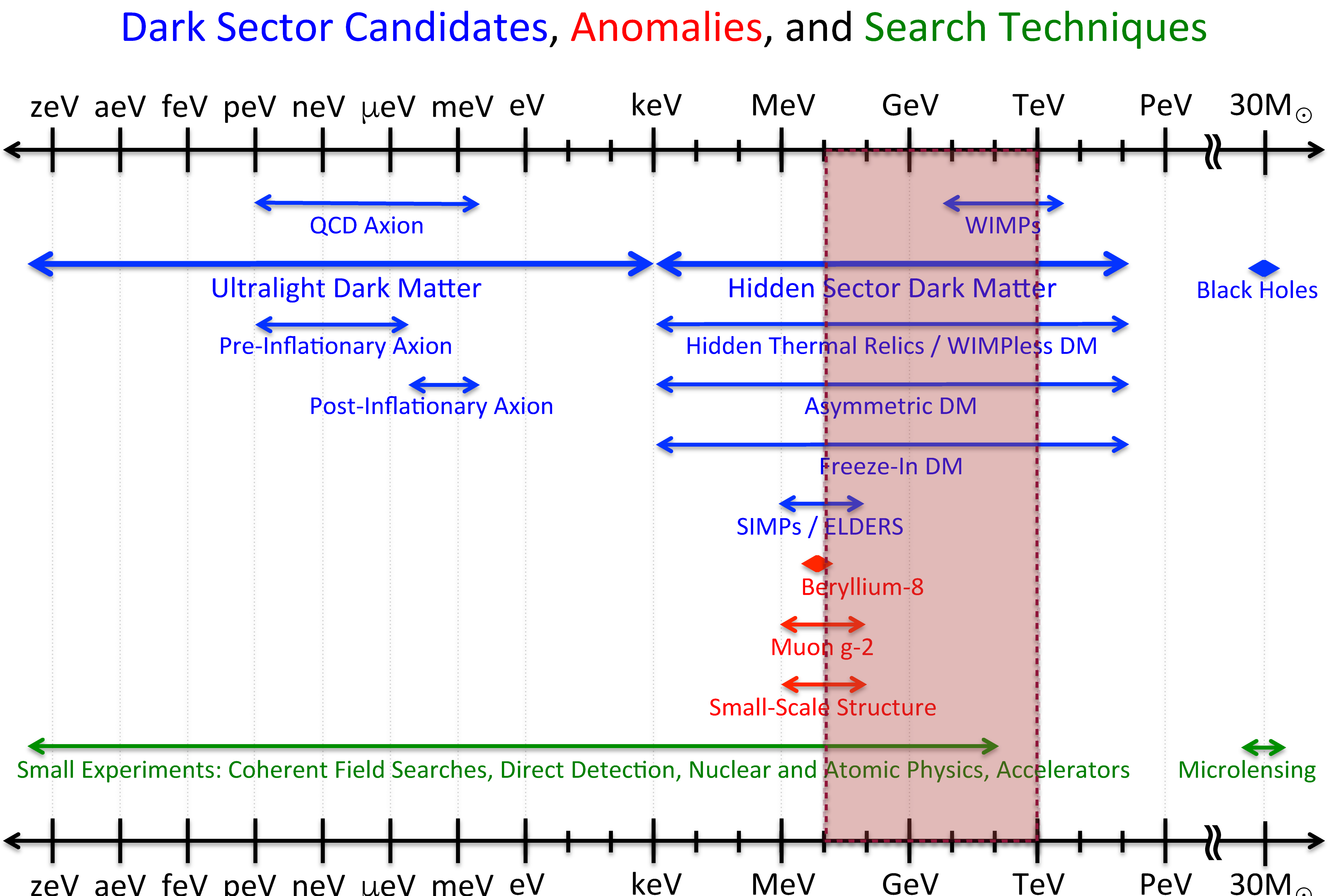

Cosmic visions
arXiv:1707.04591

Direct Dark Matter Detection

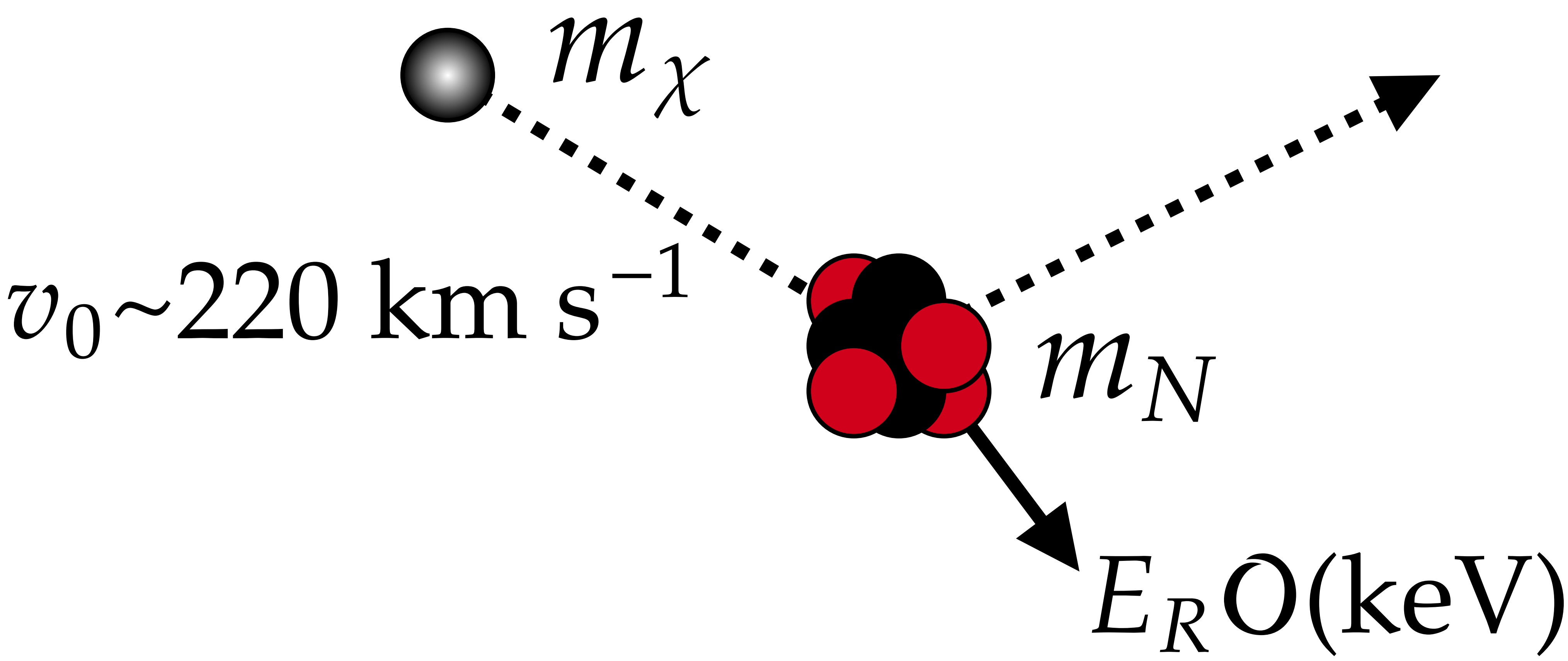

Direct Dark Matter Detection

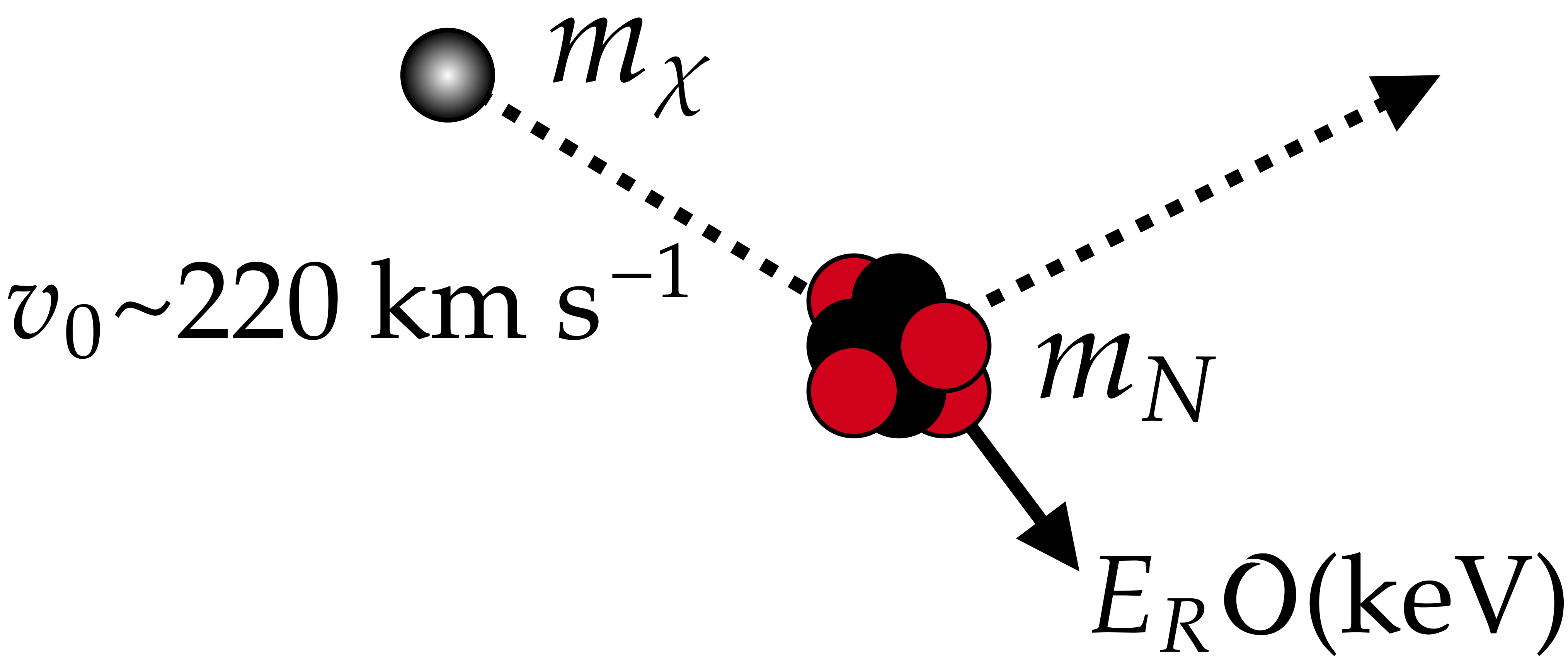

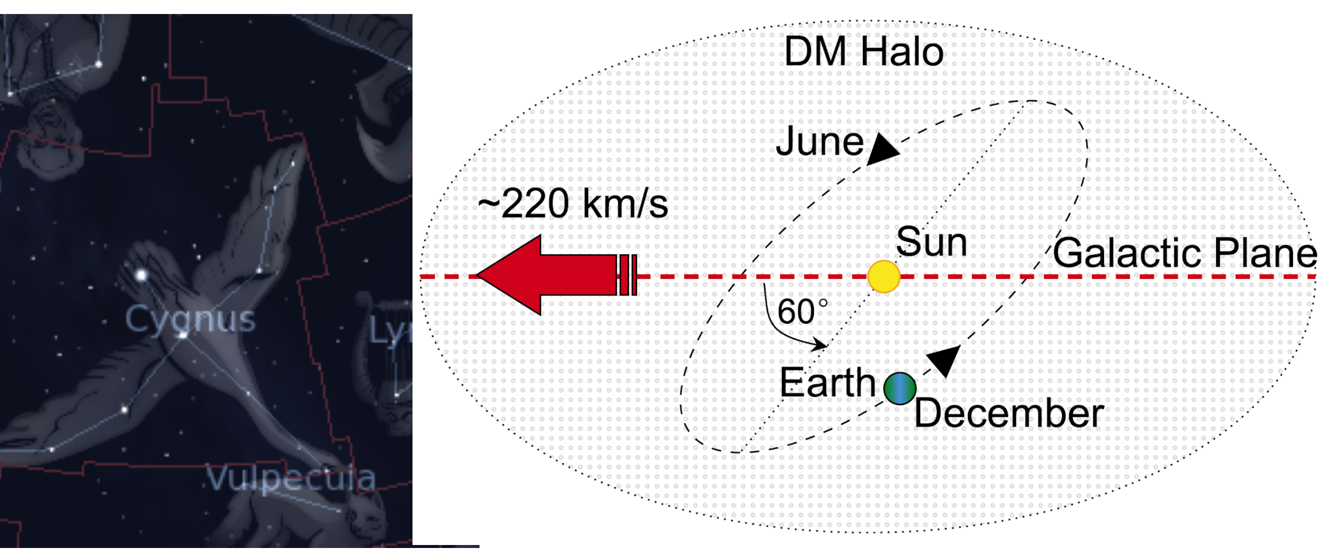

Handles to confirm possible signals

- Recoil energy distribution
- Seasonal flux variation
  - DM velocity is season dependent
- Directional detection
  - DM signal should point to Cygnus

Direct Detection Signals

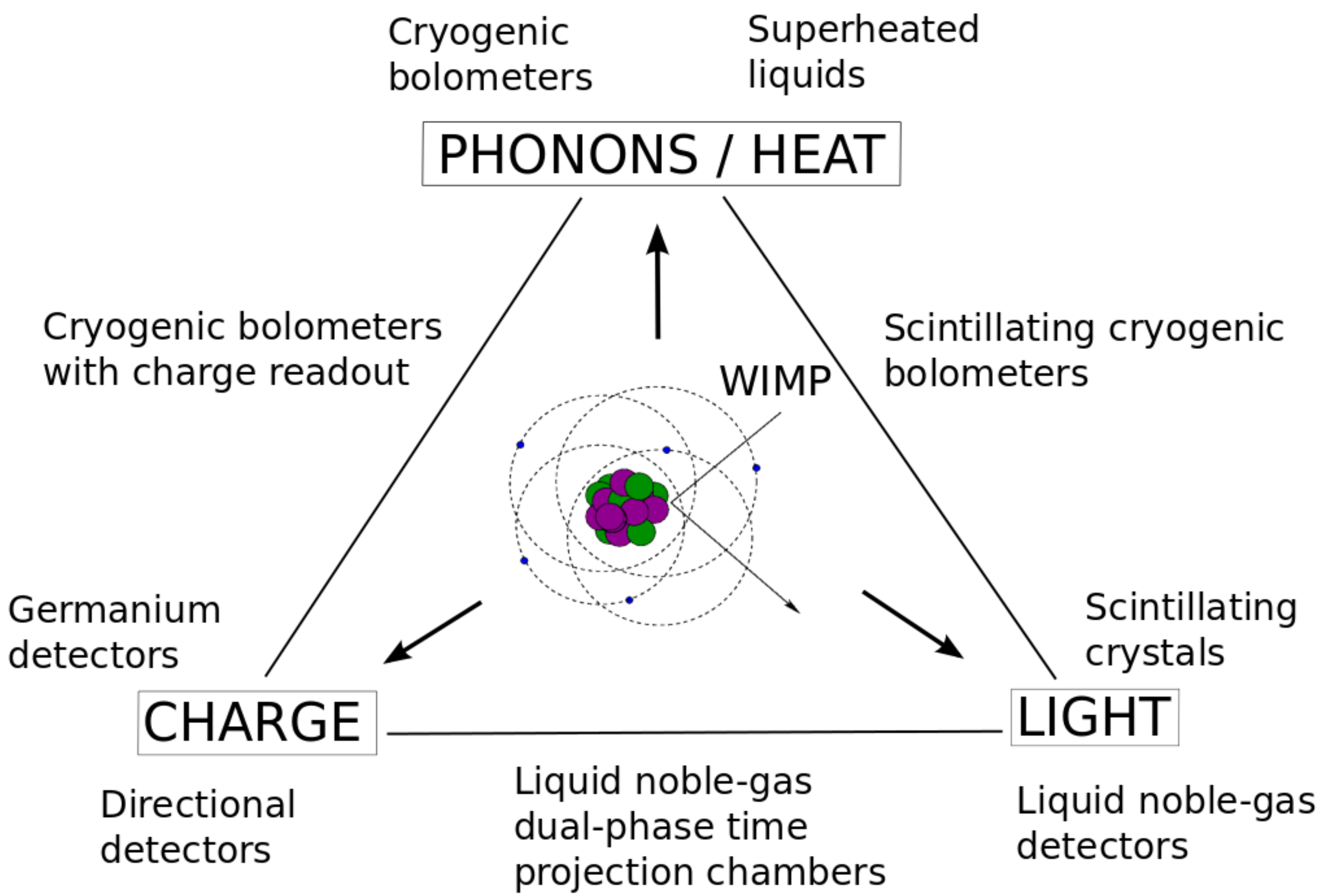

J.Phys. G43 (2016) 013001

- **Recoiling nucleus can deposit energy in several forms**
- **Experiments sensitive to one or more of these deposits**
  - Multiple signals can be used for background suppression

Direct Detection Signals

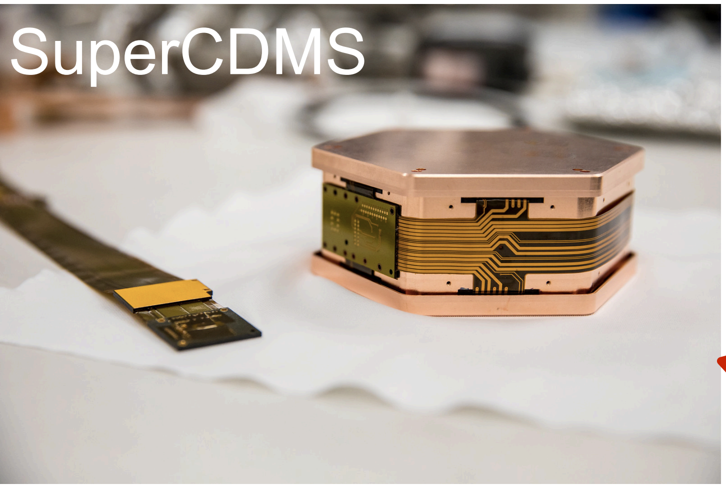

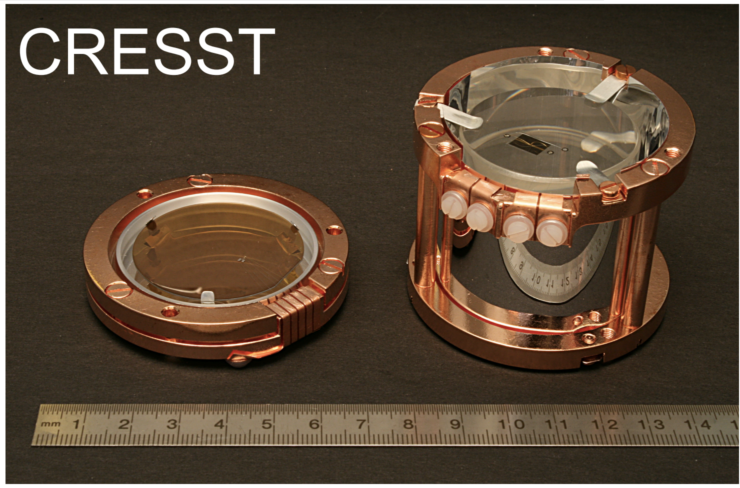

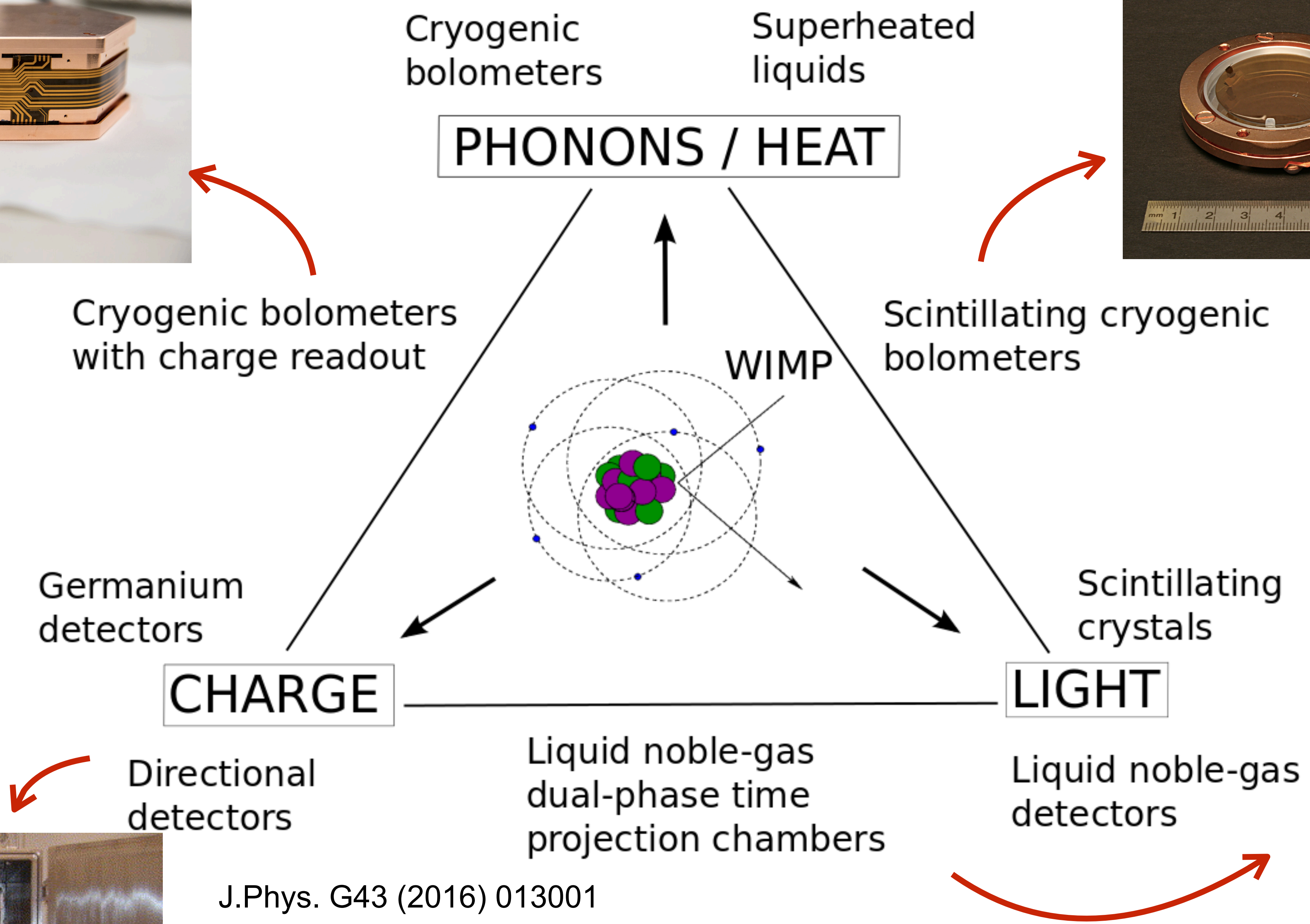

J.Phys. G43 (2016) 013001

XENON-1T

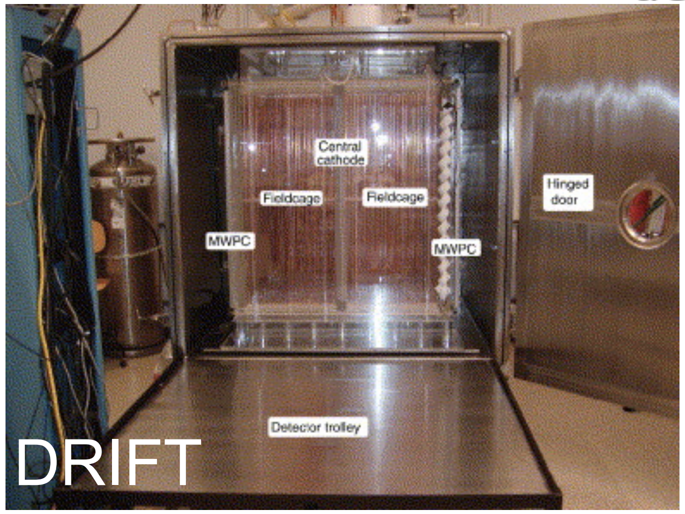

- **Recoiling nucleus can deposit energy in several forms**
- **Experiments sensitive to one or more of these deposits**
  - Multiple signals can be used for background suppression

Landscape of Direct Detection searches

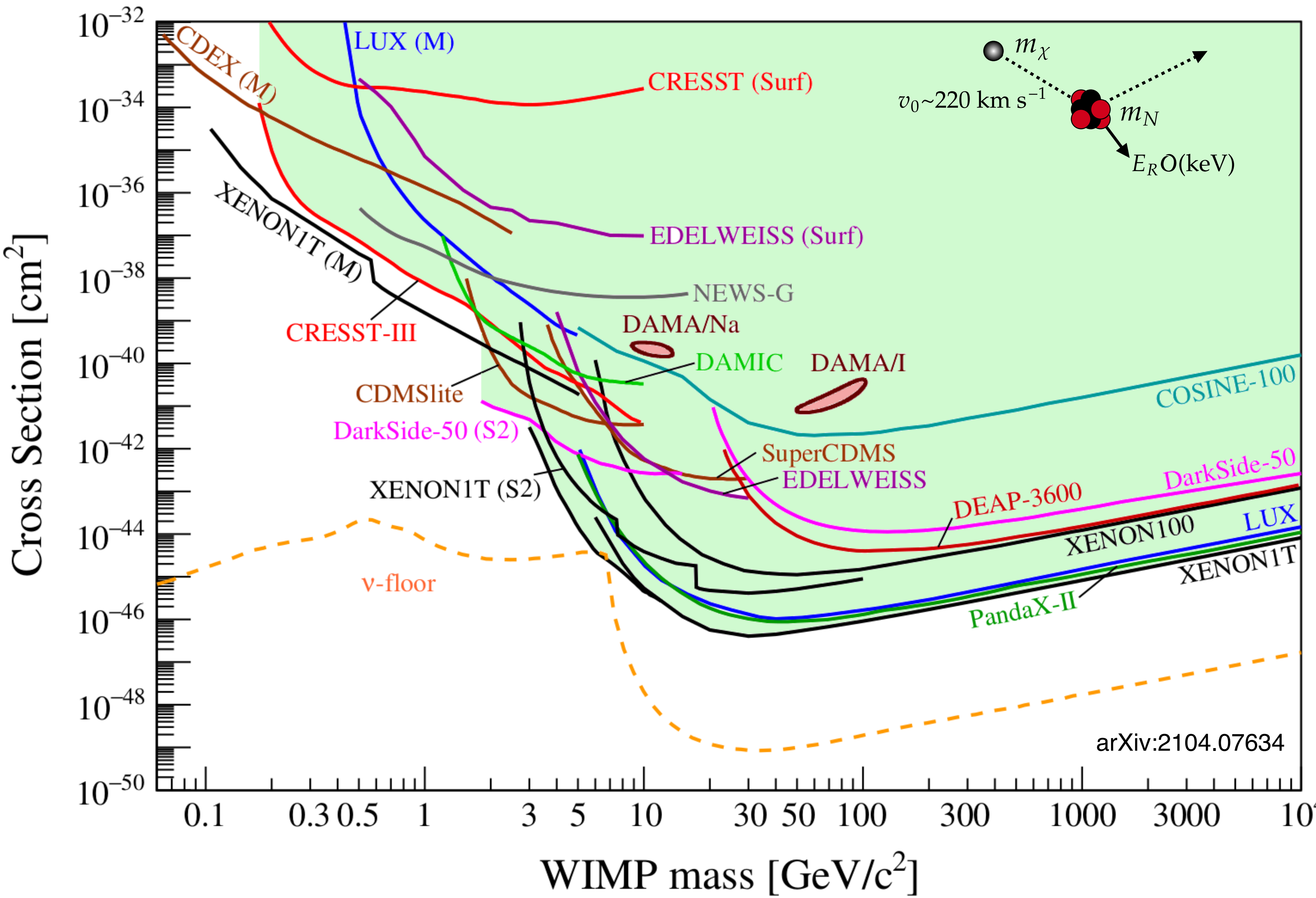

- Also constraints on spin-dependent proton/neutron-DM interactions

Landscape of Direct Detection searches

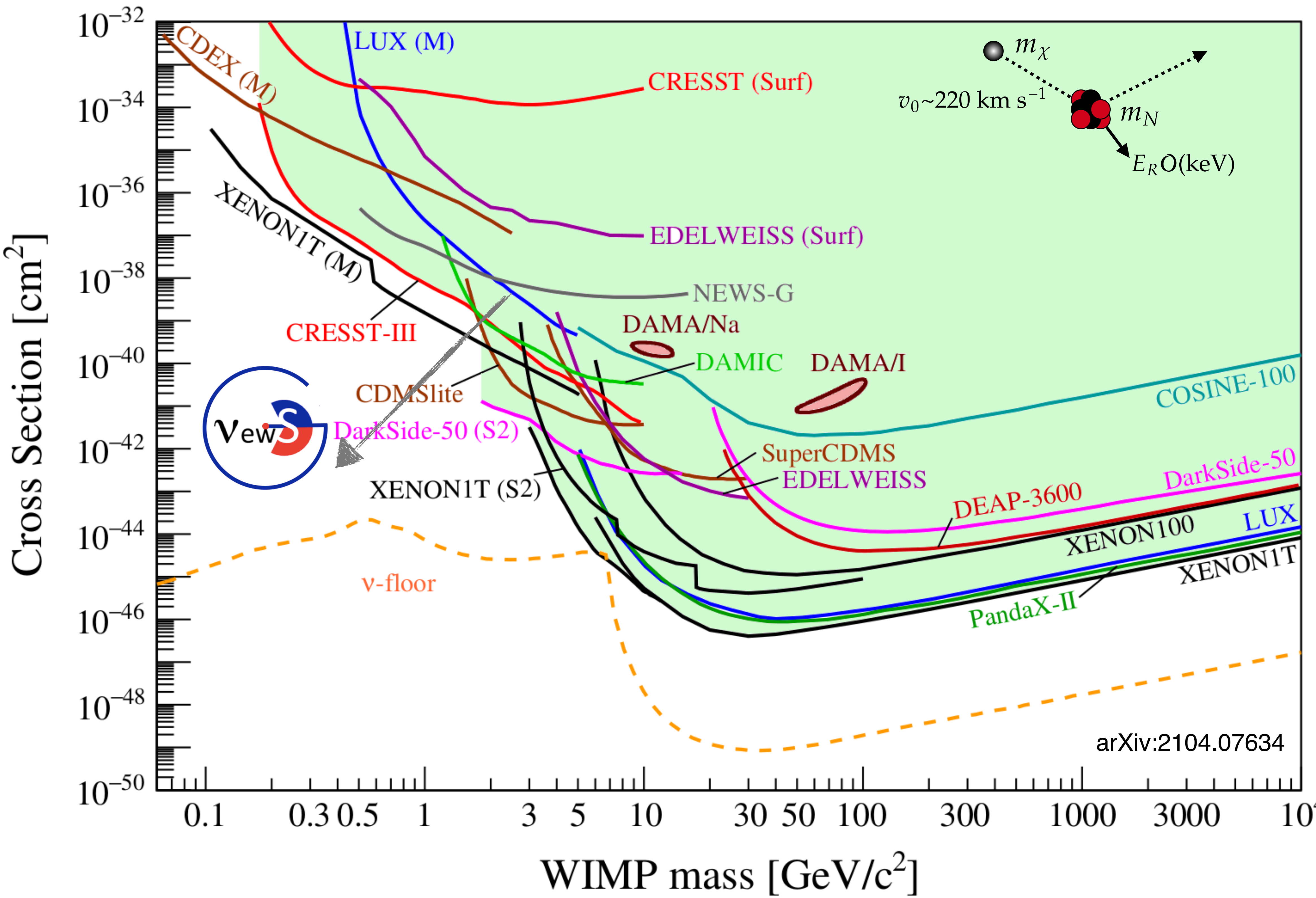

- Also constraints on spin-dependent proton/neutron-DM interactions

New Experiment With Spheres - Gas

11th collaboration meeting, August 2022

- NEWS-G Collaboration
  - 5 countries
  - 10 institutes
  - ~40 collaborators
- Three underground laboratories
  - SNOLAB
  - Laboratoire Souterrain de Modane
  - Boulby Underground Laboratory

Spherical Proportional Counter

Electric field scales as $1/r^2$, volume divided in: “drift” and “amplification” regions

Capacitance independent of size: low electronic noise

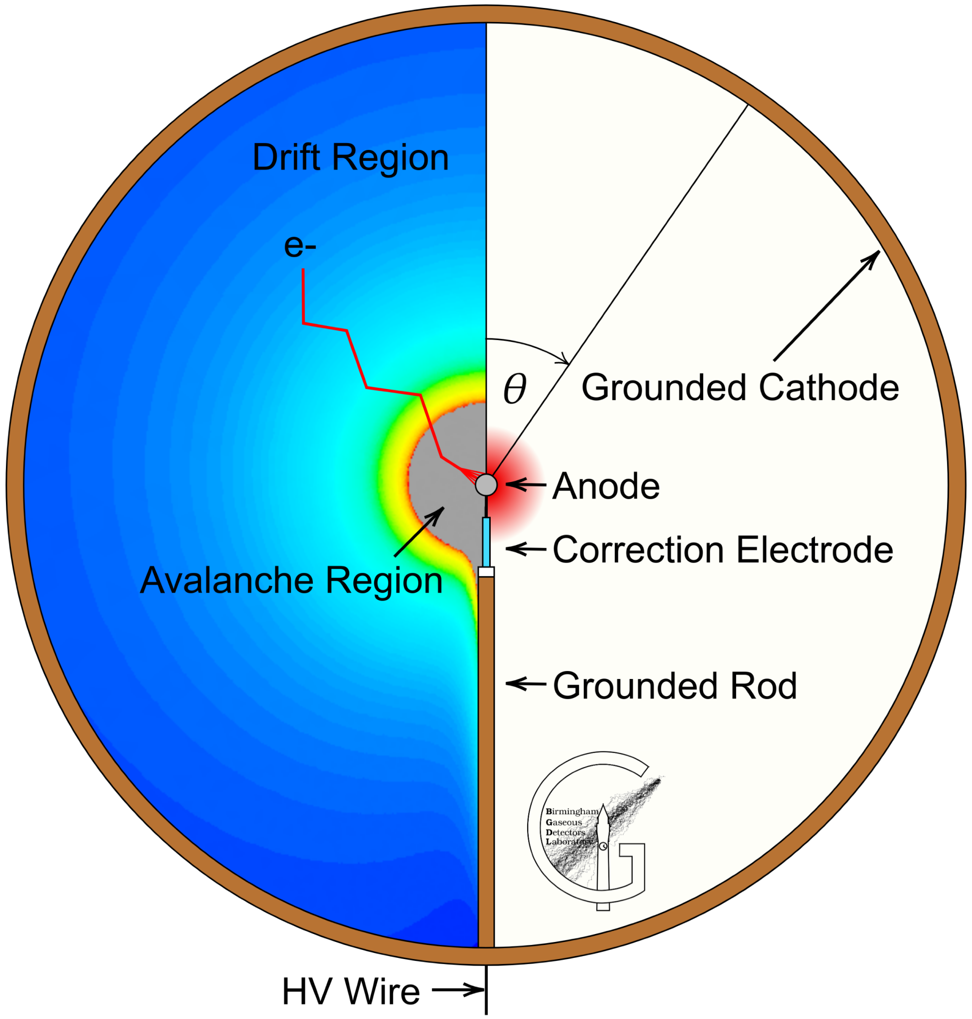

Spherical Proportional Counter

Electric field scales as $1/r^2$, volume divided in: “drift” and “amplification” regions

Capacitance independent of size: low electronic noise

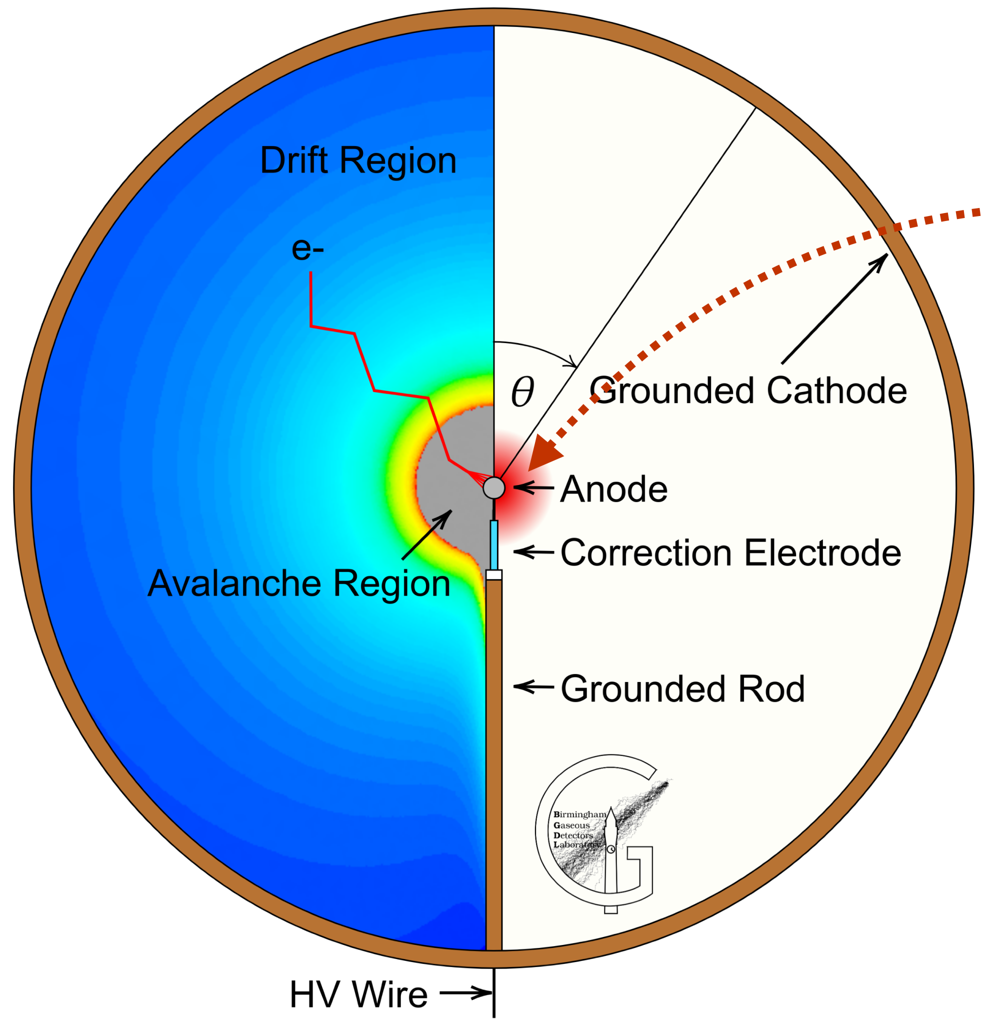

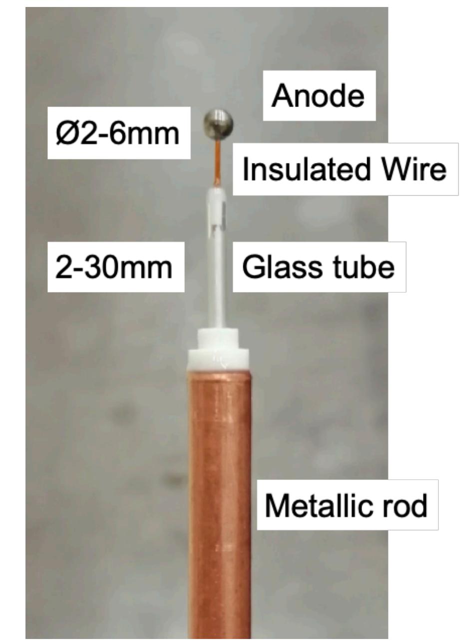

Spherical Proportional Counter

Electric field scales as $1/r^2$, volume divided in: “drift” and “amplification” regions
Capacitance independent of size: low electronic noise

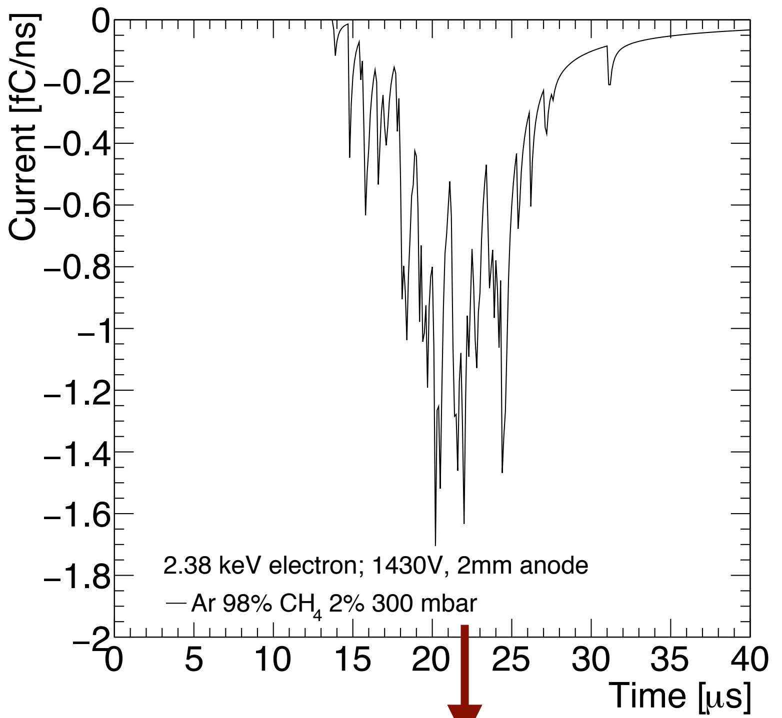

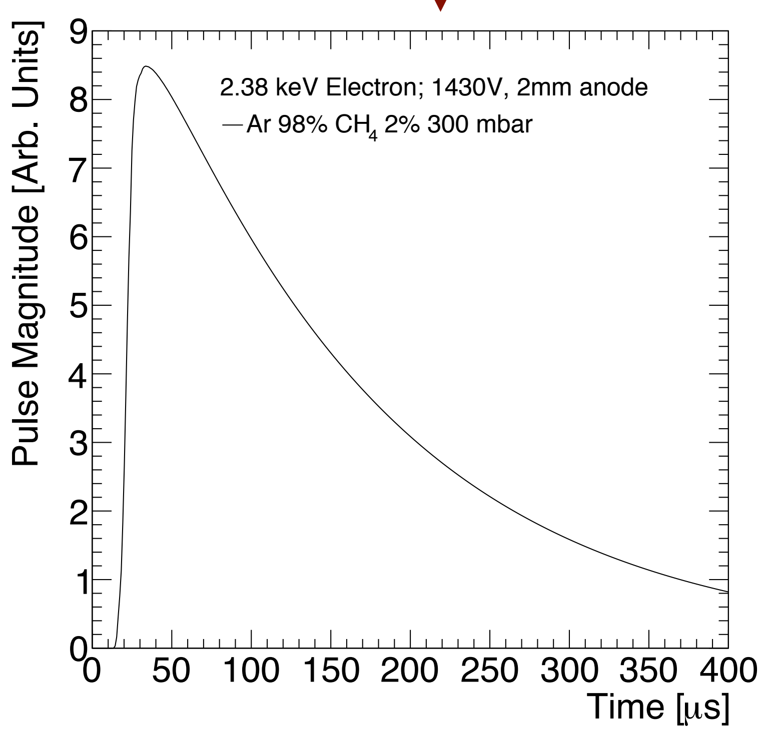

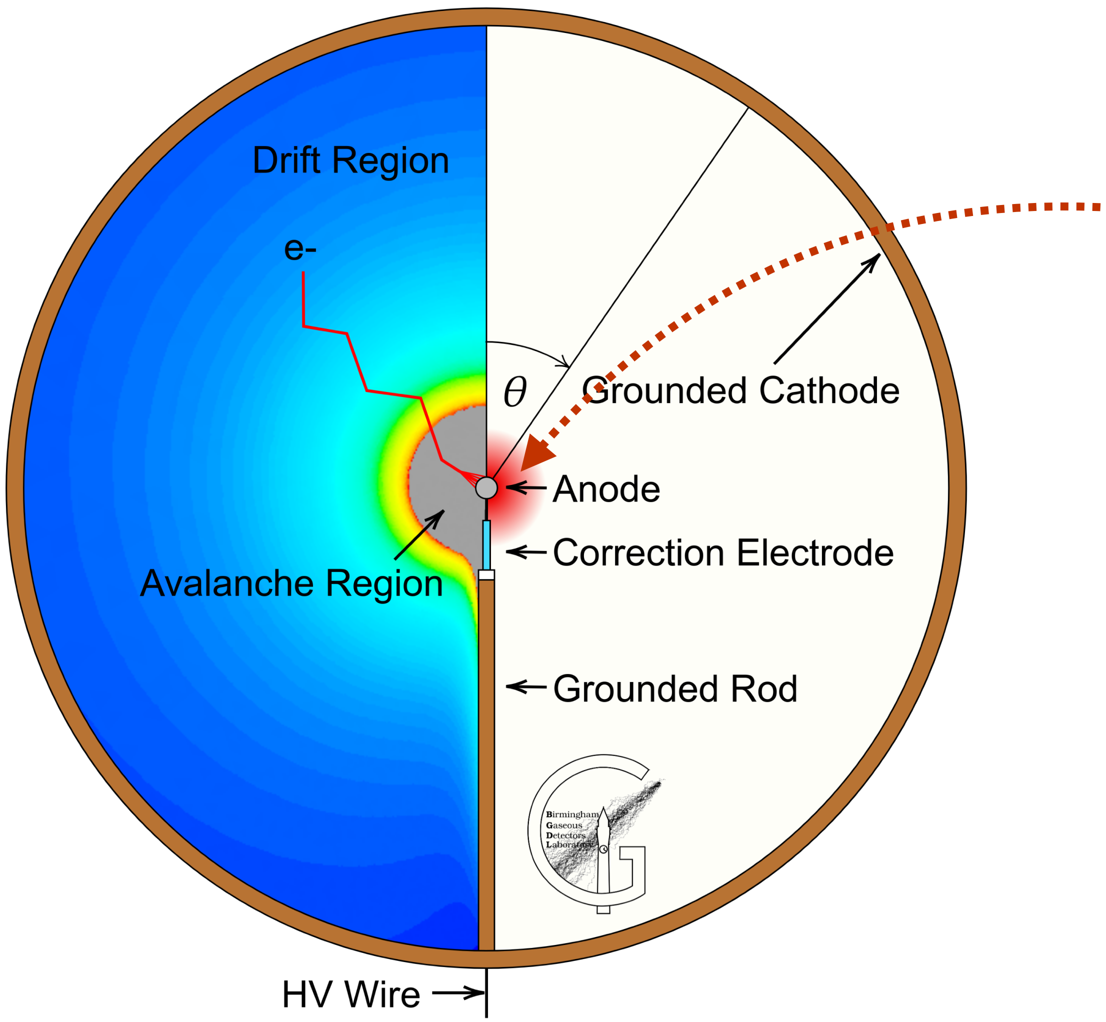

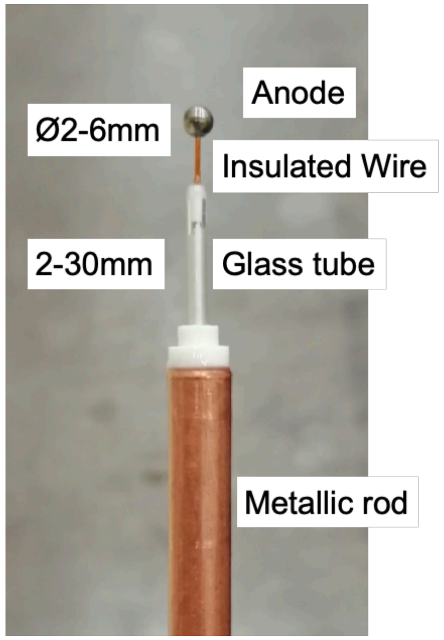

Spherical Proportional Counter

Electric field scales as $1/r^2$, volume divided in: "drift" and "amplification" regions
Capacitance independent of size: low electronic noise

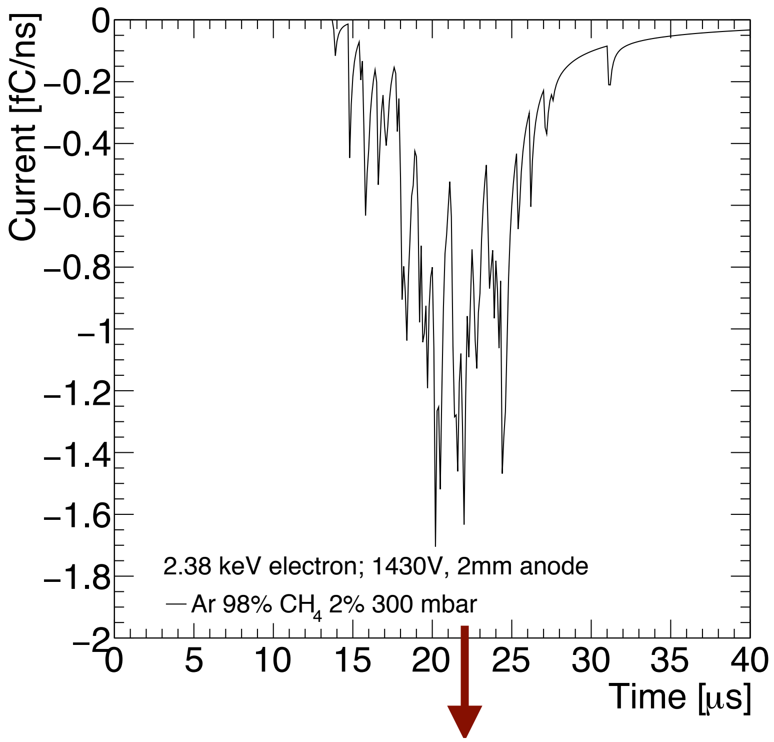

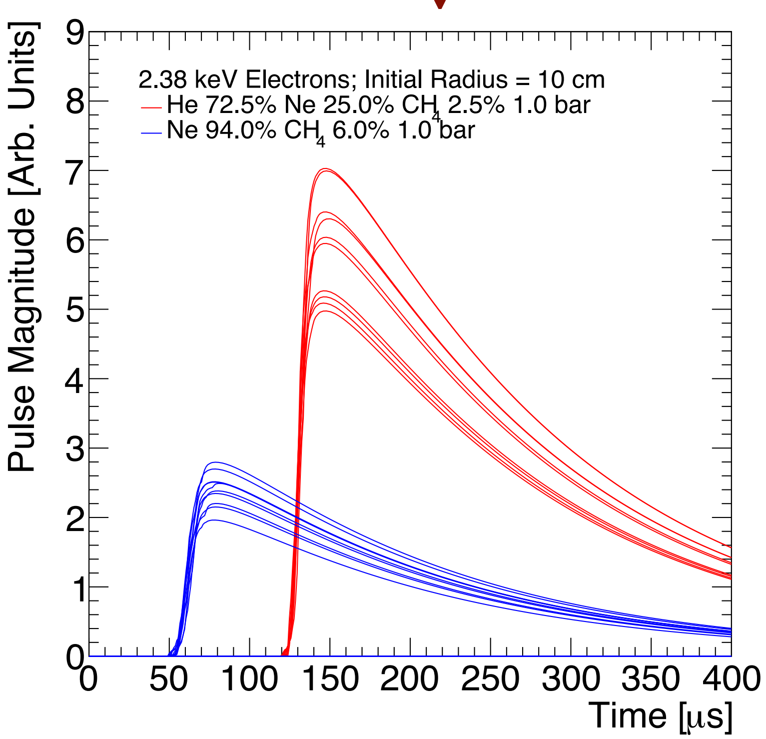

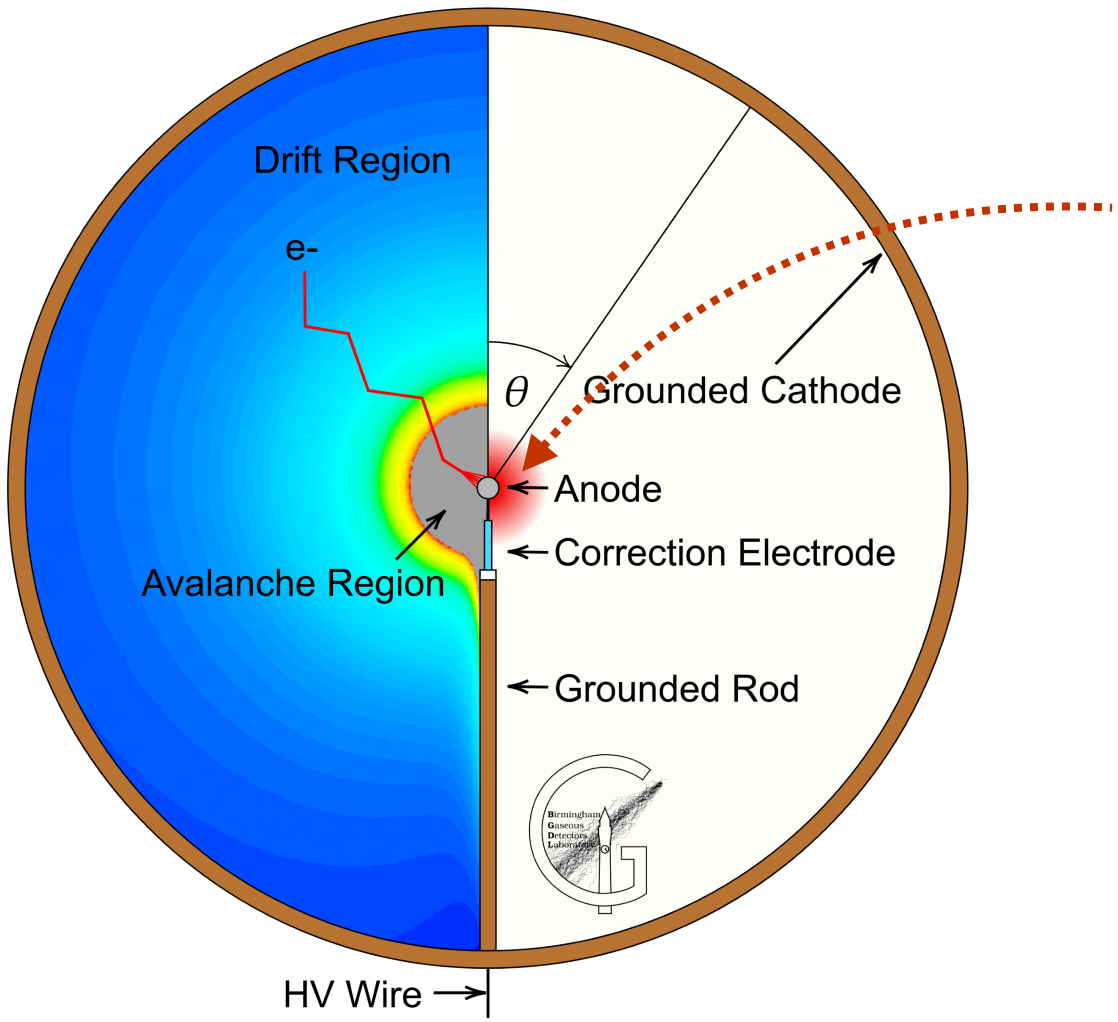

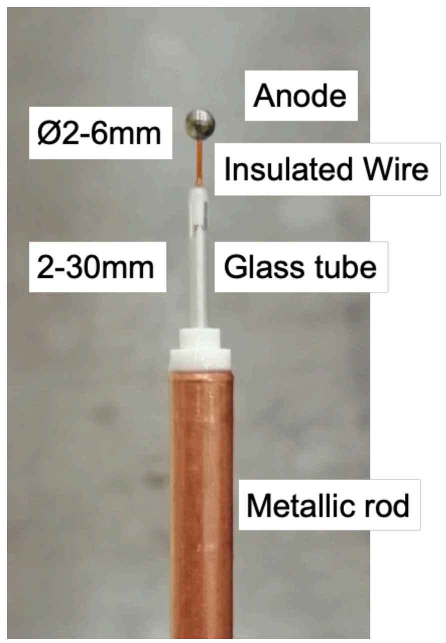

Spherical Proportional Counter

Electric field scales as $1/r^2$, volume divided in: "drift" and "amplification" regions

Capacitance independent of size: low electronic noise

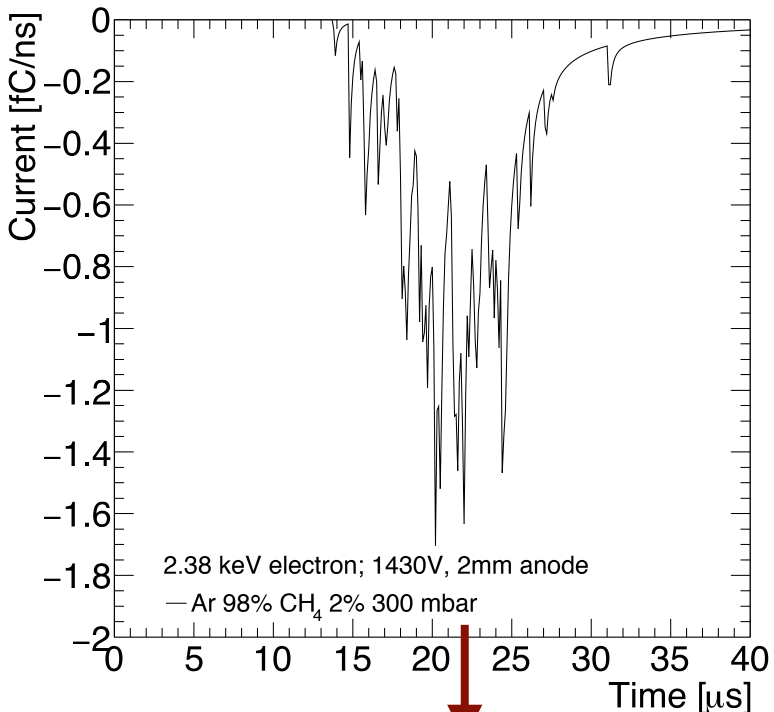

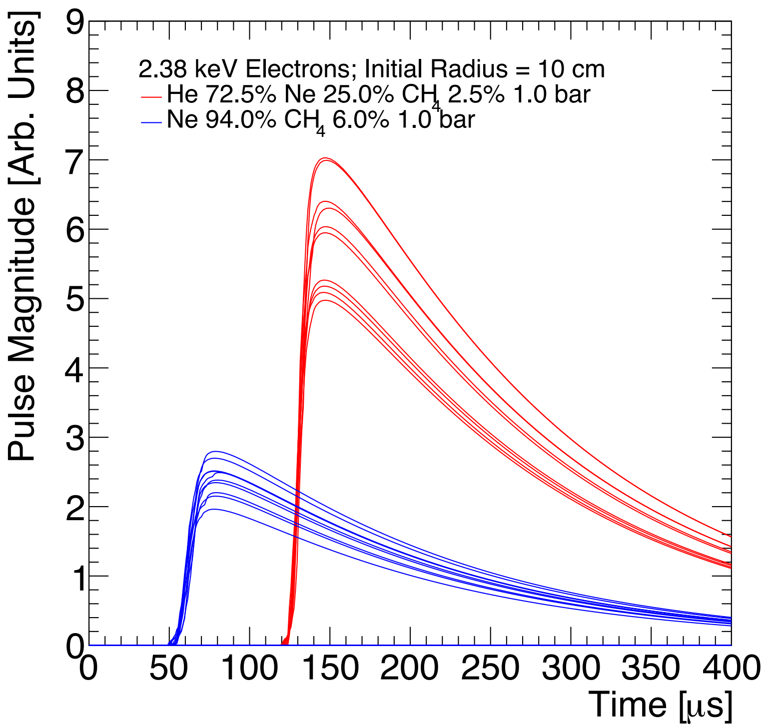

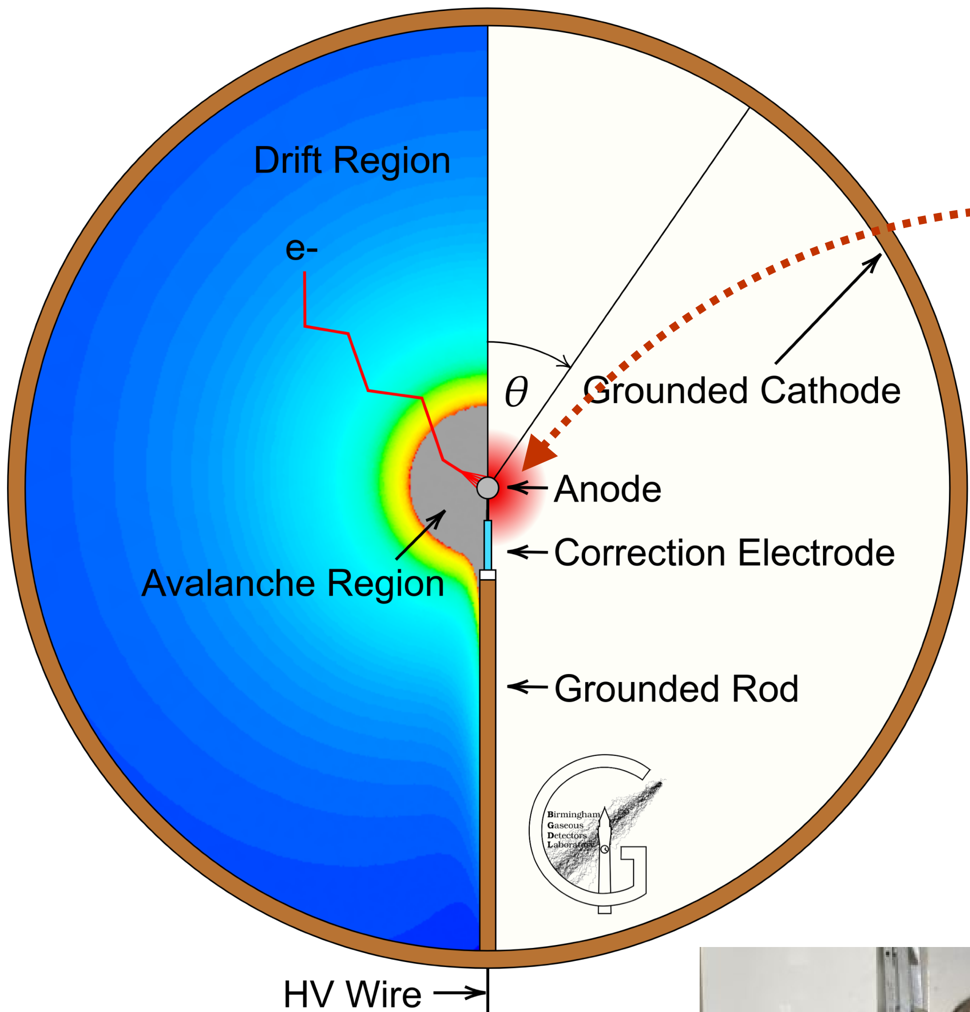

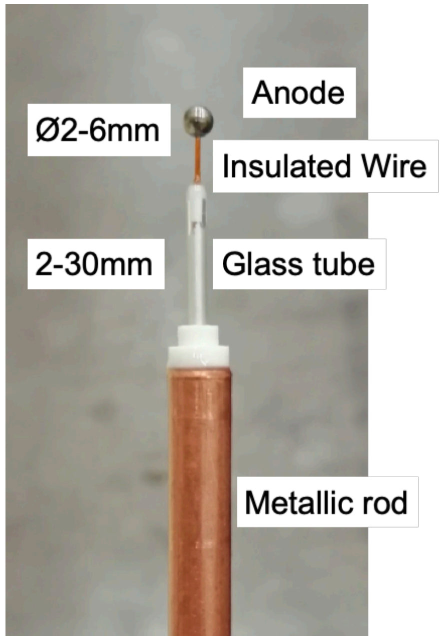

Direct Detection: Light Dark Matter

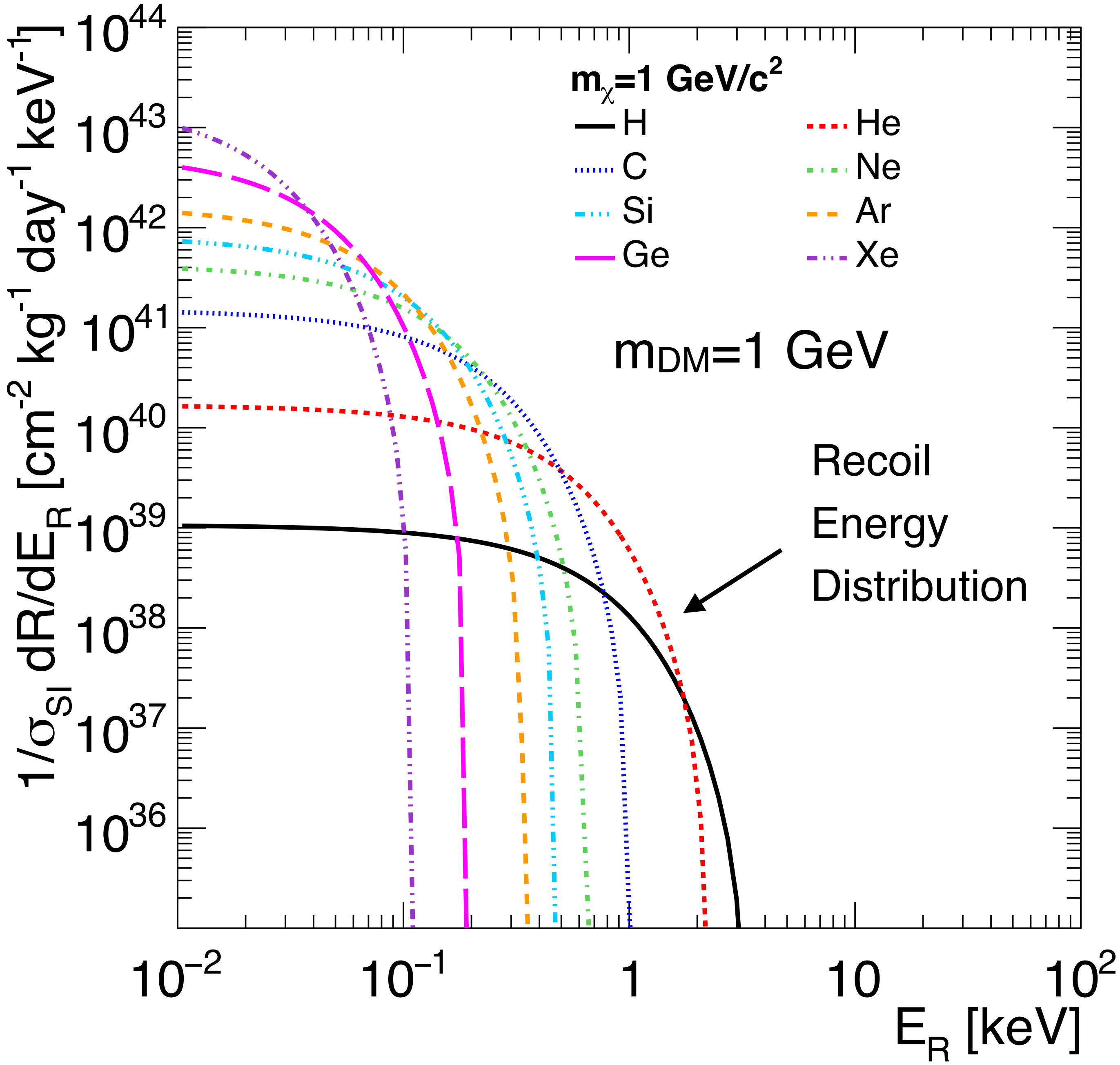

Favourable recoil energy distribution for lighter targets

Direct Detection: Light Dark Matter

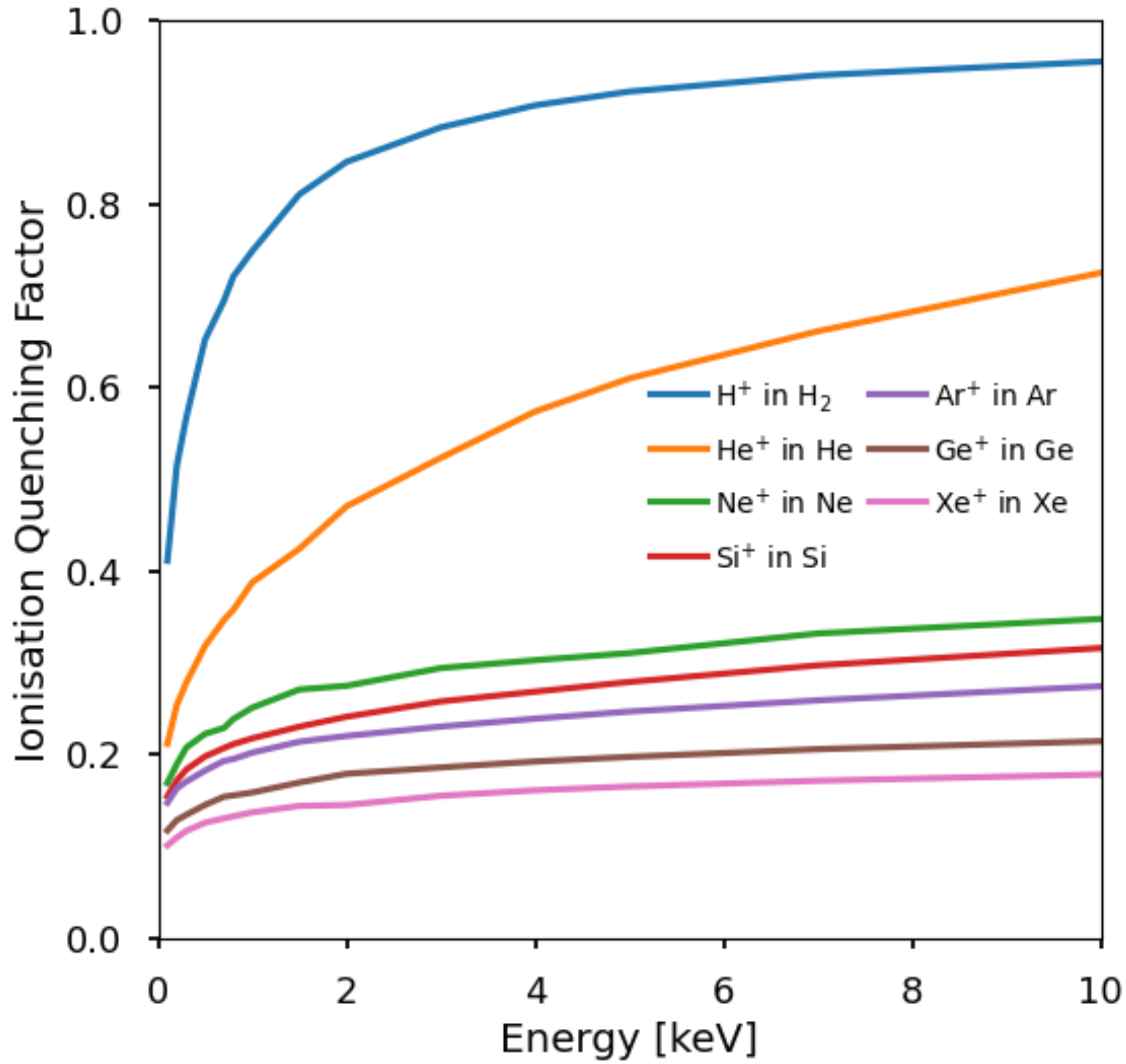

- Fraction of energy dissipated as ionisation quantified by quenching factor
  - Several definitions of quenching factor in the literature
- For lighter elements more of the recoil energy turns into detectable signal
  - Larger fraction of energy deposited by recoil nucleus is visible to detector

Pulse Shape Discrimination

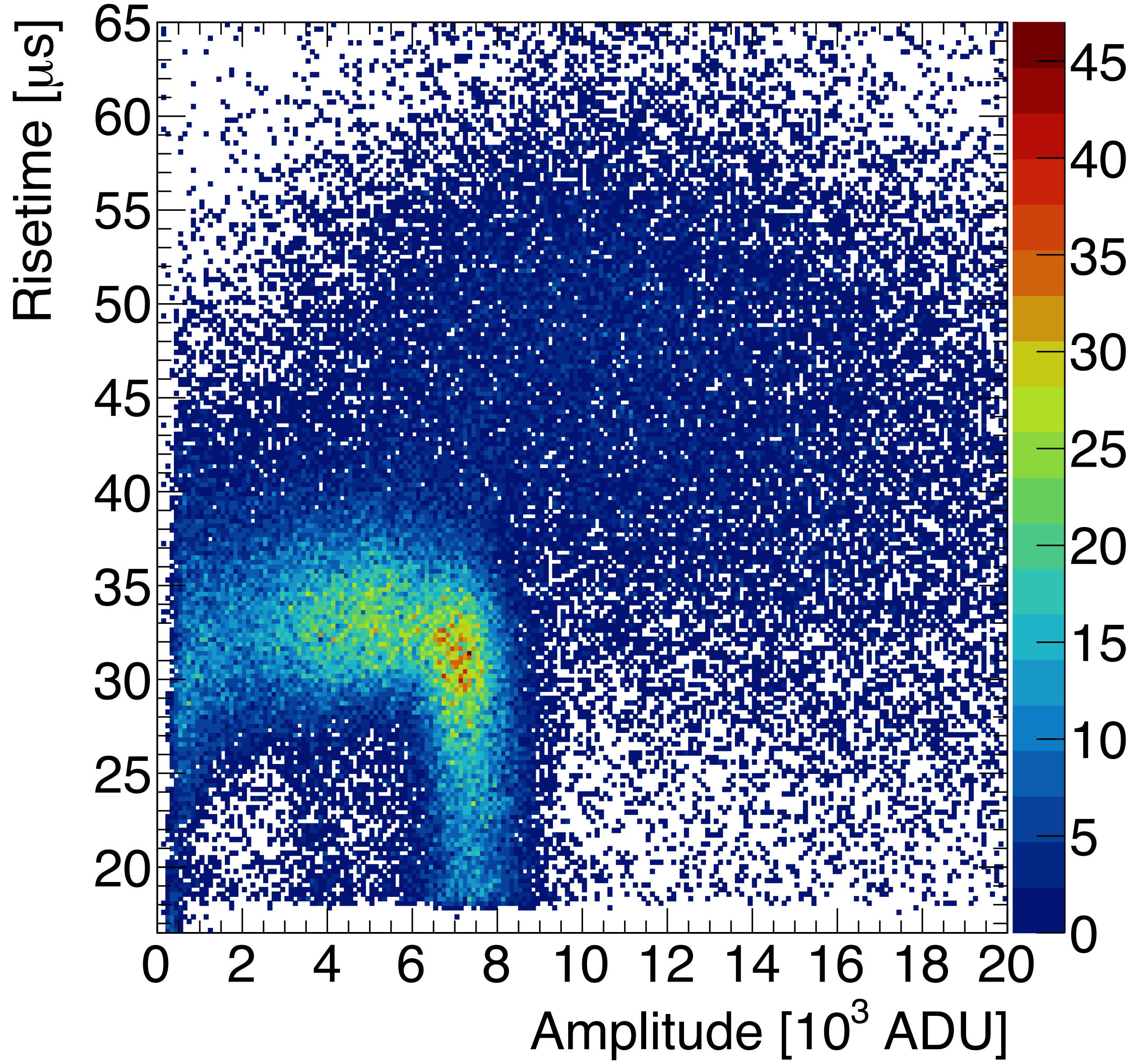

Pulse Shape Discrimination

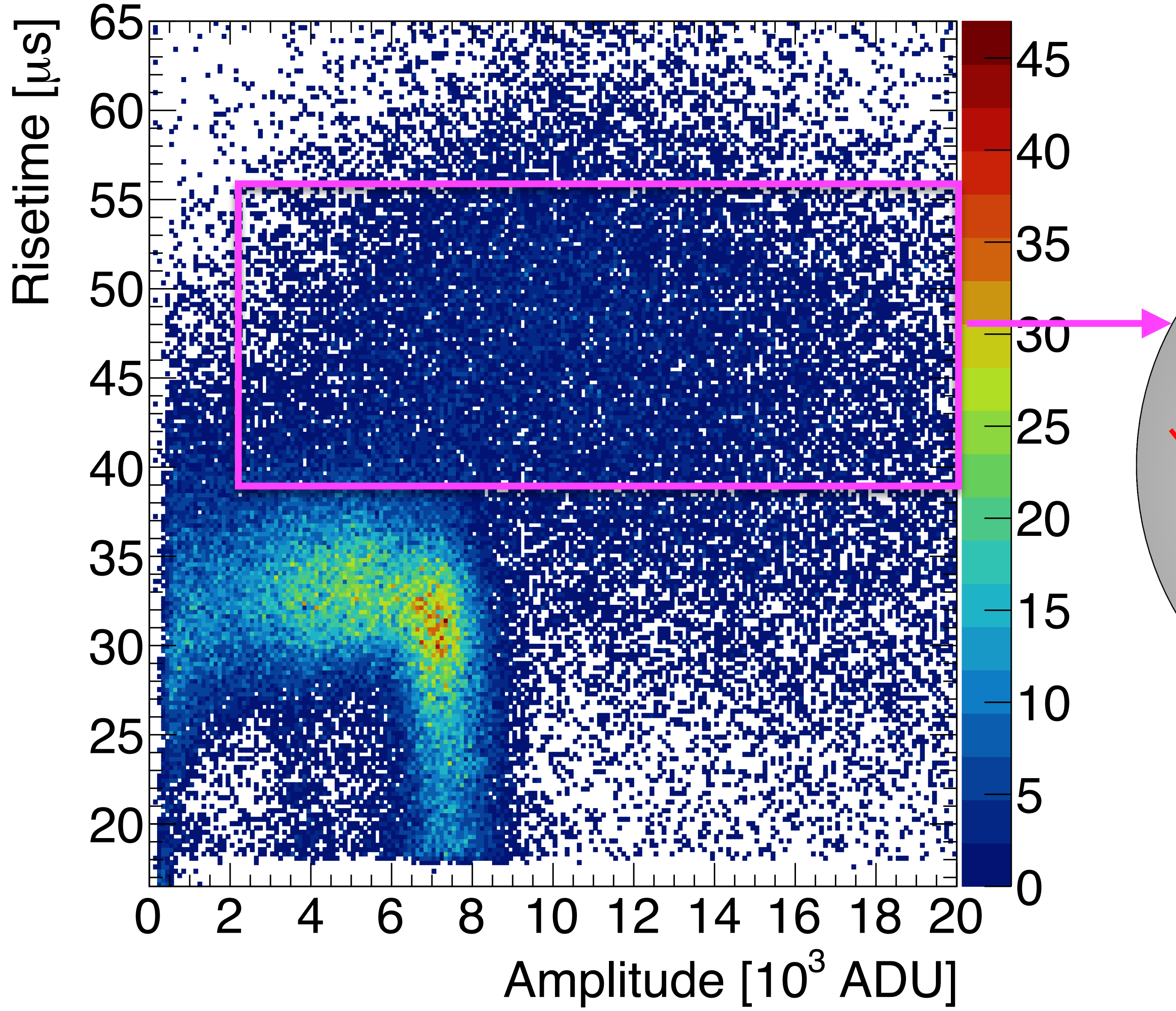

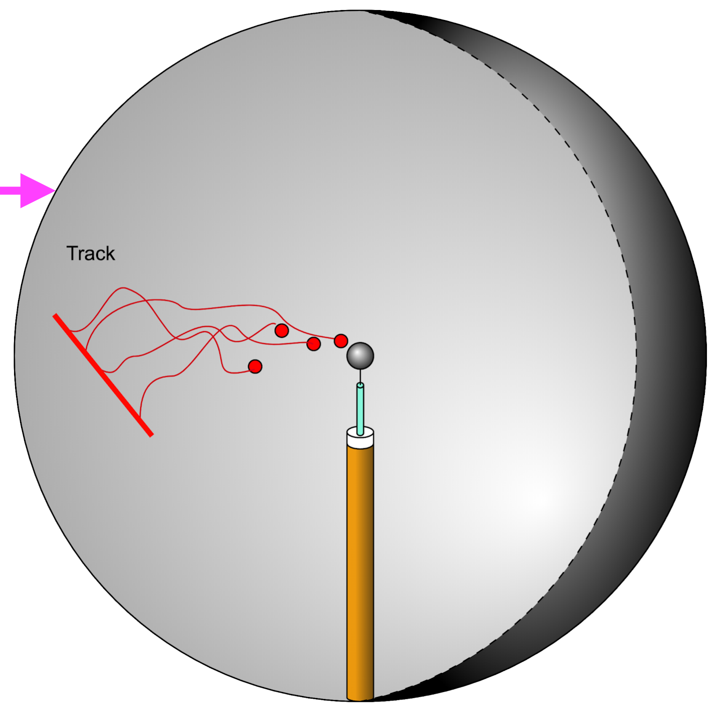

“Muon”-like events

Pulse Shape Discrimination

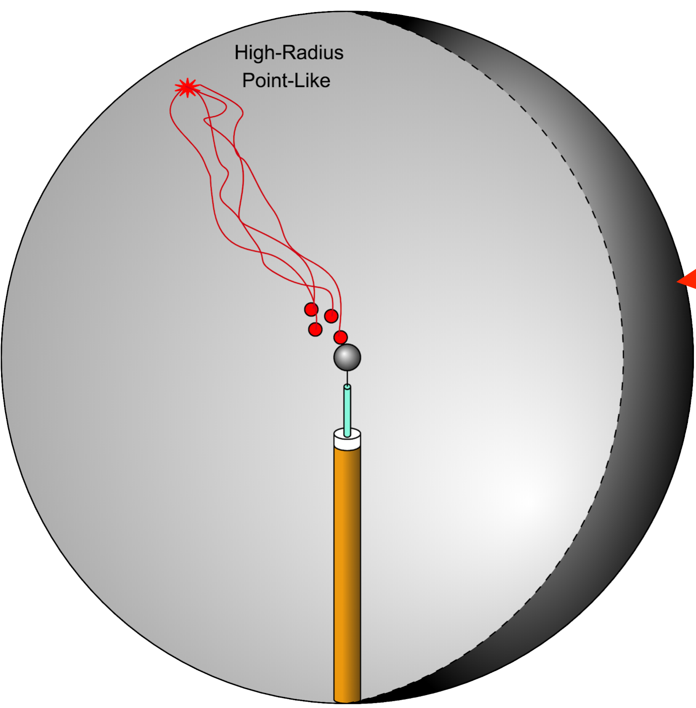

"Surface"-like events

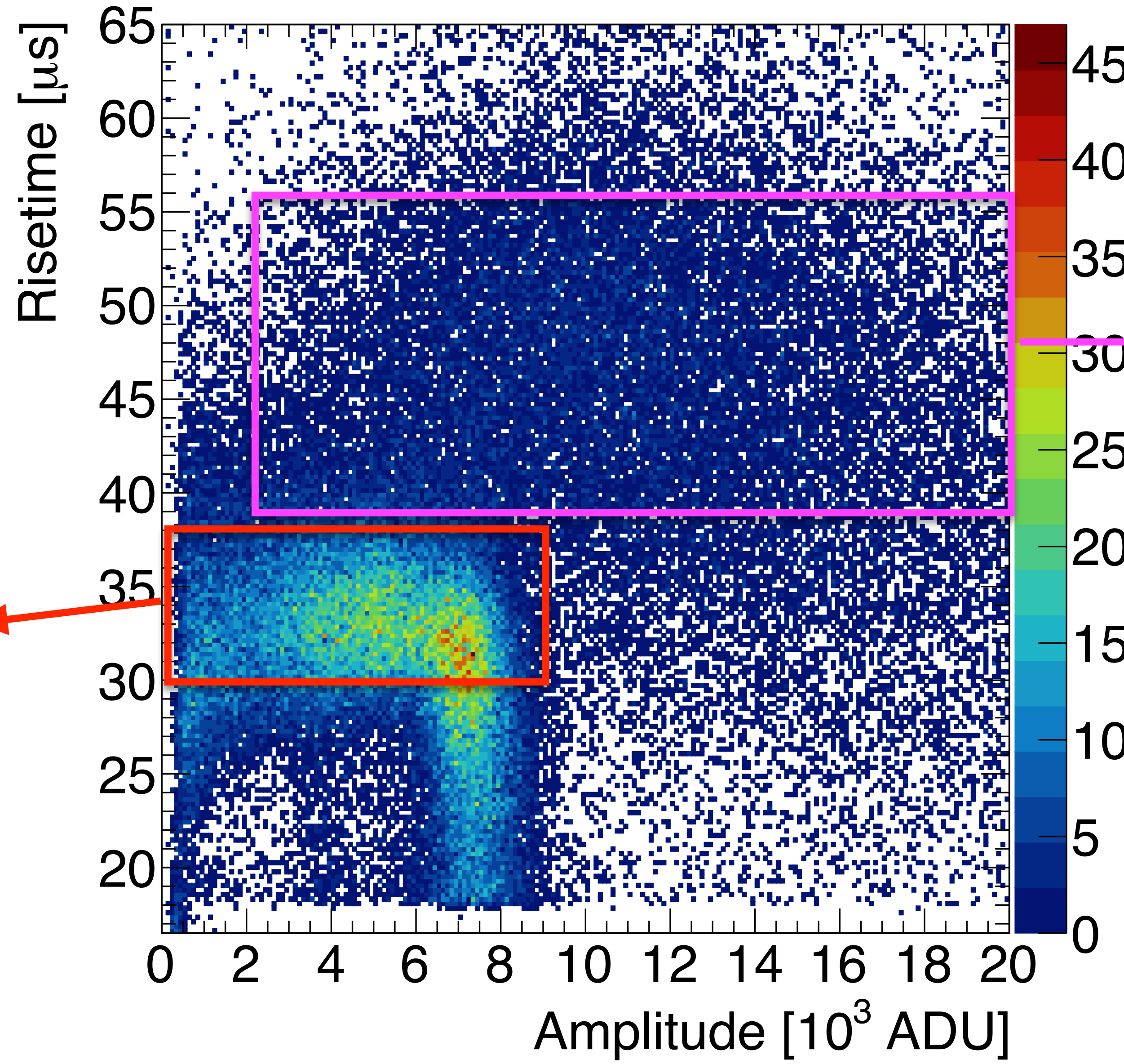

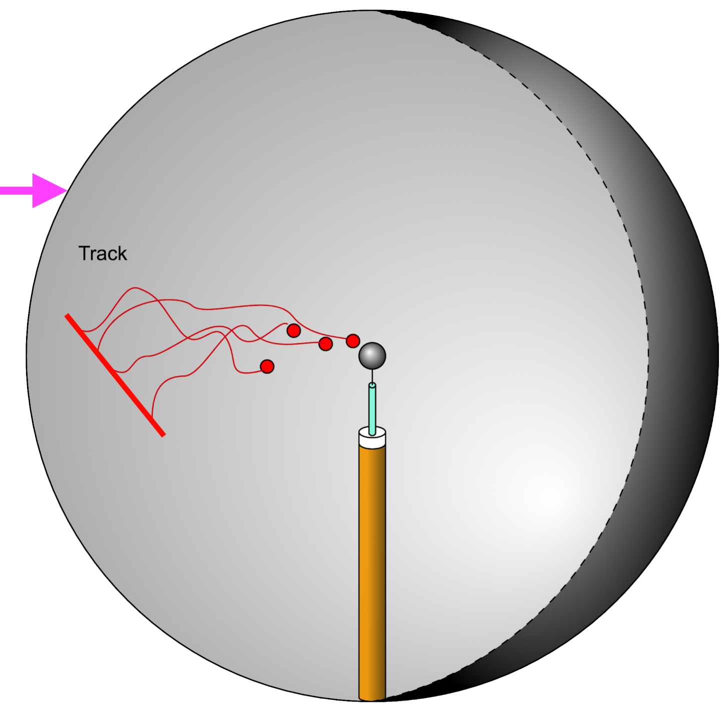

"Muon"-like events

Pulse Shape Discrimination

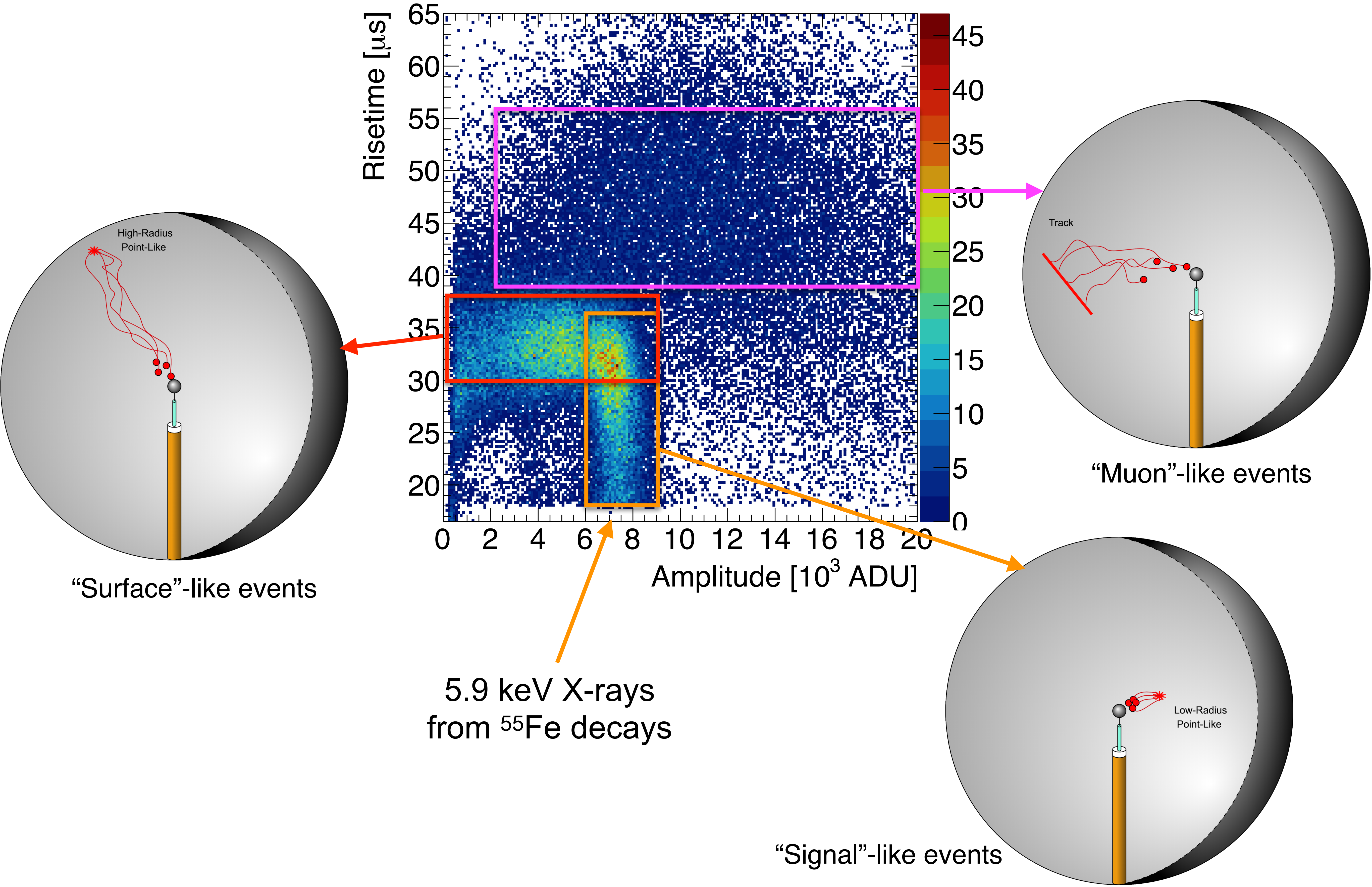

NEWS-G: Prototype at Modane

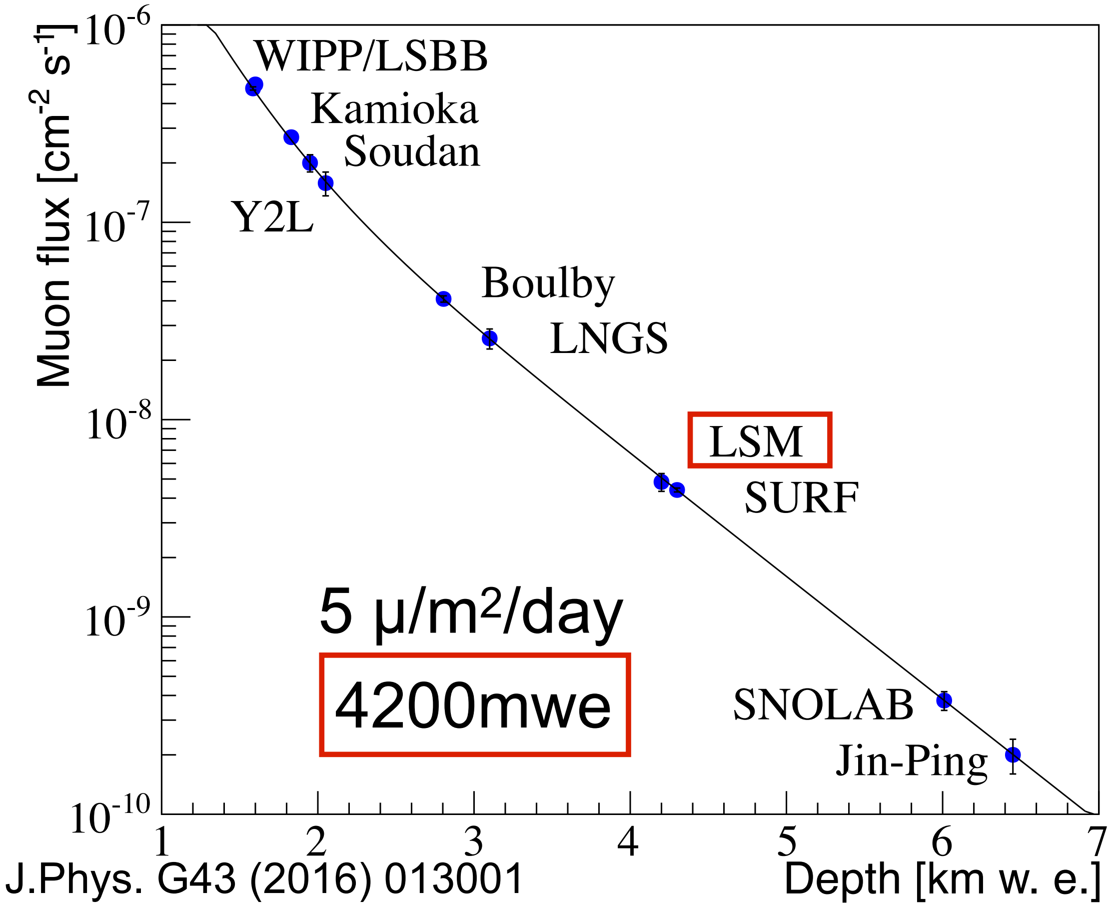

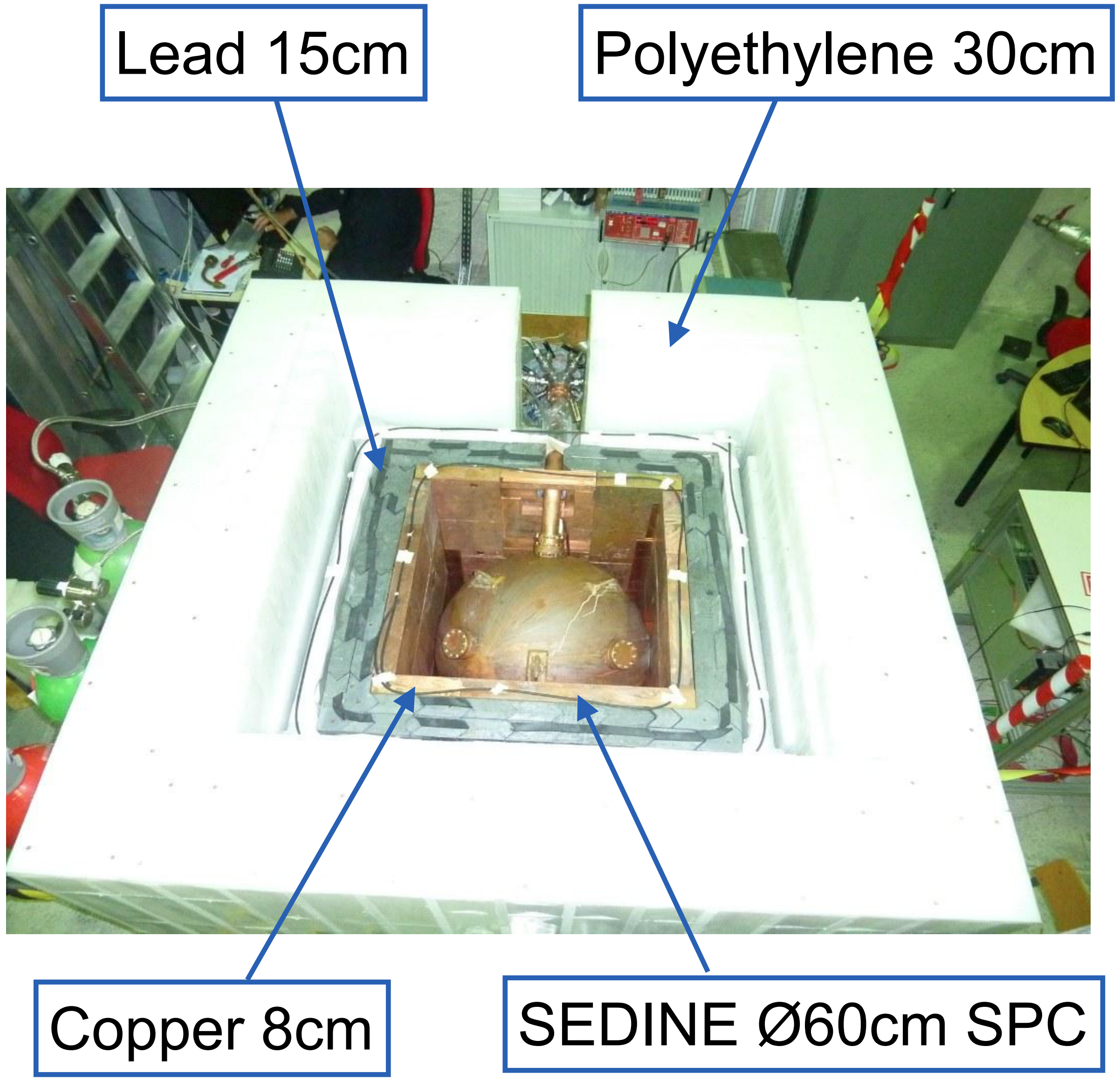

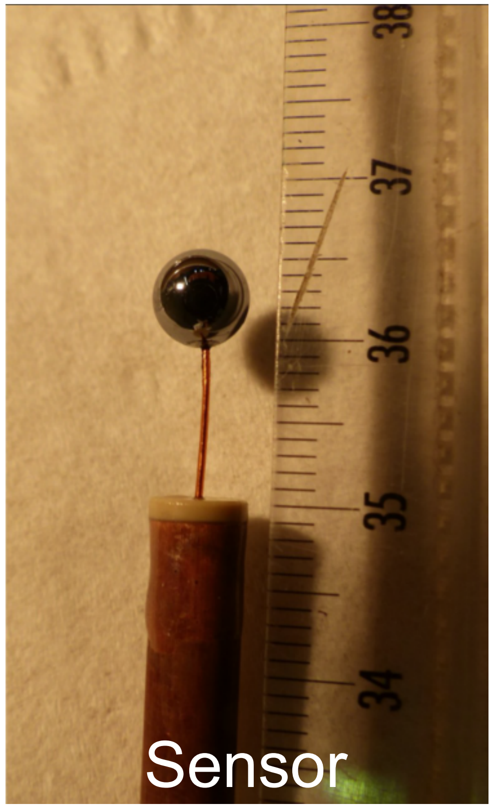

- NOSV Copper vessel (Ø60 cm)
- Equipped with a Ø6.3 mm sensor
- Chemically cleaned several times for Rn deposit removal

NEWS-G: First results

NEWS-G collaboration, Astropart. Phys. 97, 54 (2018)

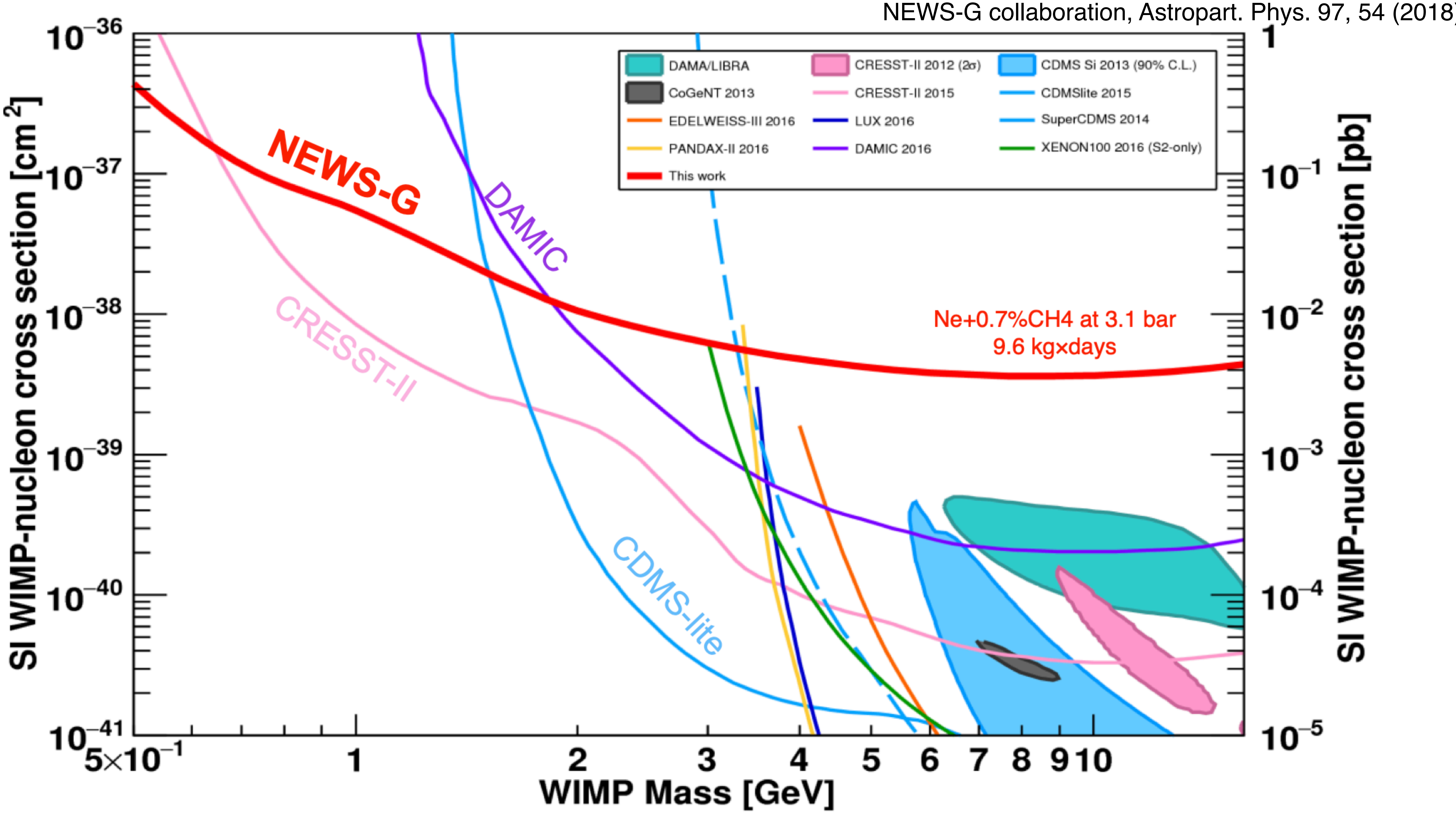

NEWS-G: First results

NEWS-G collaboration, Astropart. Phys. 97, 54 (2018)

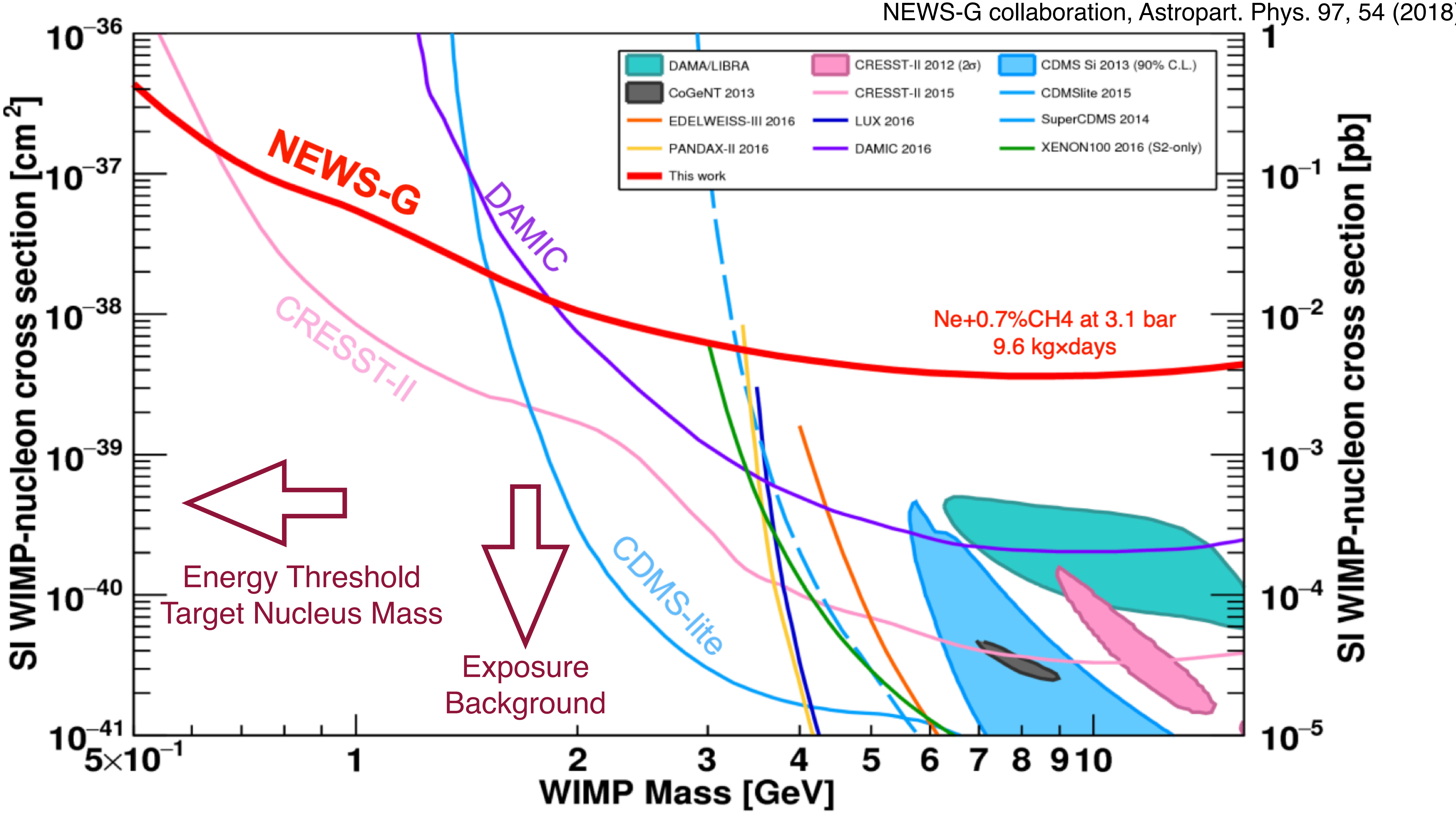

Exposure: Larger volume and higher operating pressure

Backgrounds: Higher purity materials

NEWS-G at SNOLAB

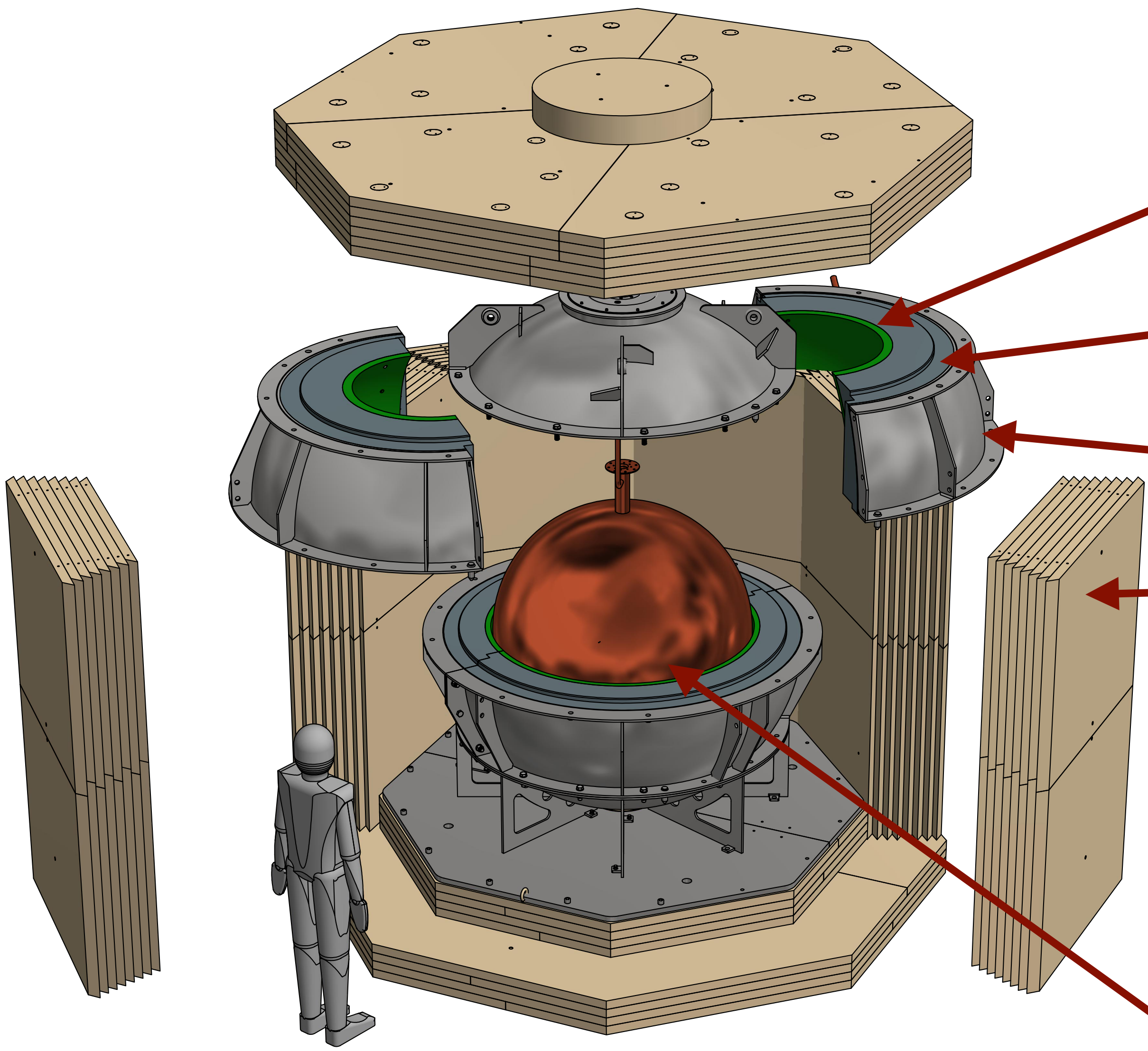

3 cm archaeological lead

22 cm of Very Low Activity lead

Stainless steel skin

40 cm high density polyethylene

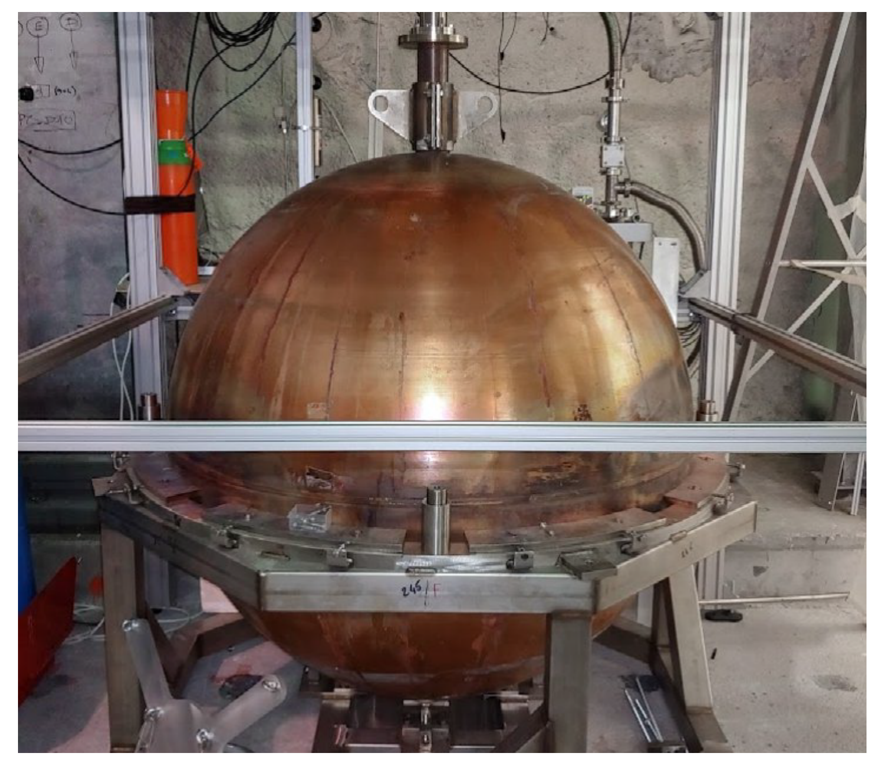

Ø140 cm
4N Copper (99.99% pure)
Assembled at LSM

Increasing Target Mass

Increasing Target Mass

Single anode: Drift and Amplification fields are connected $E = \frac{V_a}{r^2} \frac{r_a r_c}{r_c - r_a} \approx \frac{V_a r_a}{r^2}$

Increasing Target Mass

Single anode: Drift and Amplification fields are connected $E = \frac{V_a}{r^2}\frac{r_a r_c}{r_c - r_a} \approx \frac{V_a r_a}{r^2}$

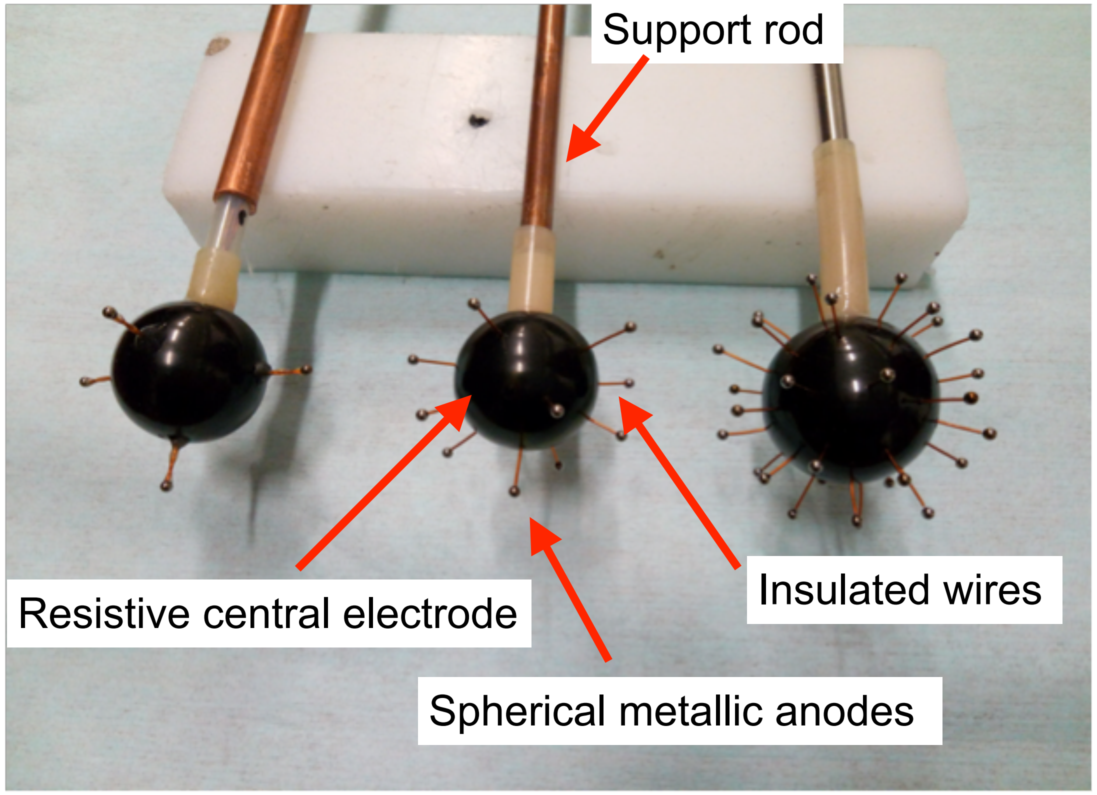

- ACHINOS: Multi-anode sensor JINST 12 (2017) 12, P12031
  - Multiple anodes placed at equal radii
    - Sensors with 5, 11, 33 anodes operated
  - Decoupling drift and amplification fields
  - Opportunity: individual anode read-out
    - TPC-like capabilities

Increasing Target Mass

Single anode: Drift and Amplification fields are connected $E = \frac{V_a}{r^2}\frac{r_a r_c}{r_c - r_a} \approx \frac{V_a r_a}{r^2}$

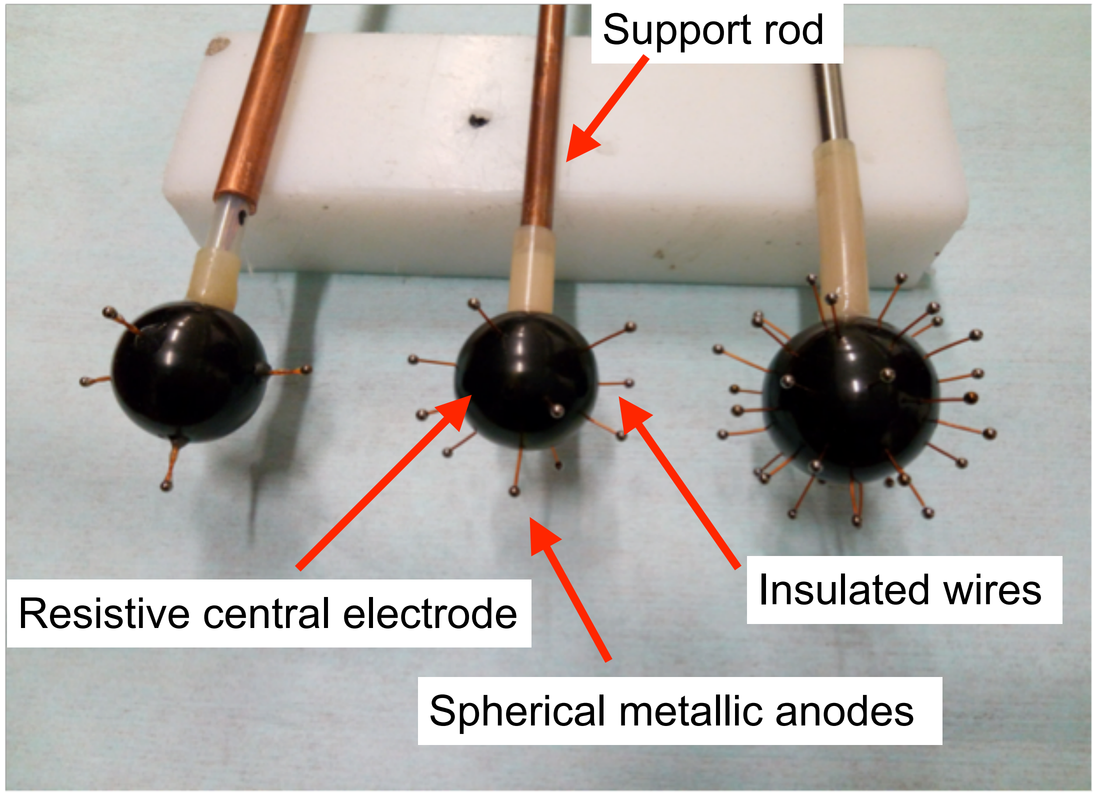

- ACHINOS: Multi-anode sensor JINST 12 (2017) 12, P12031
  - Multiple anodes placed at equal radii
    - Sensors with 5, 11, 33 anodes operated
  - Decoupling drift and amplification fields
  - Opportunity: individual anode read-out
    - TPC-like capabilities

Αχινός (greek. sea urchin)

Increasing Target Mass

Single anode: Drift and Amplification fields are connected $E = \frac{V_a}{r^2}\frac{r_a r_c}{r_c - r_a} \approx \frac{V_a r_a}{r^2}$

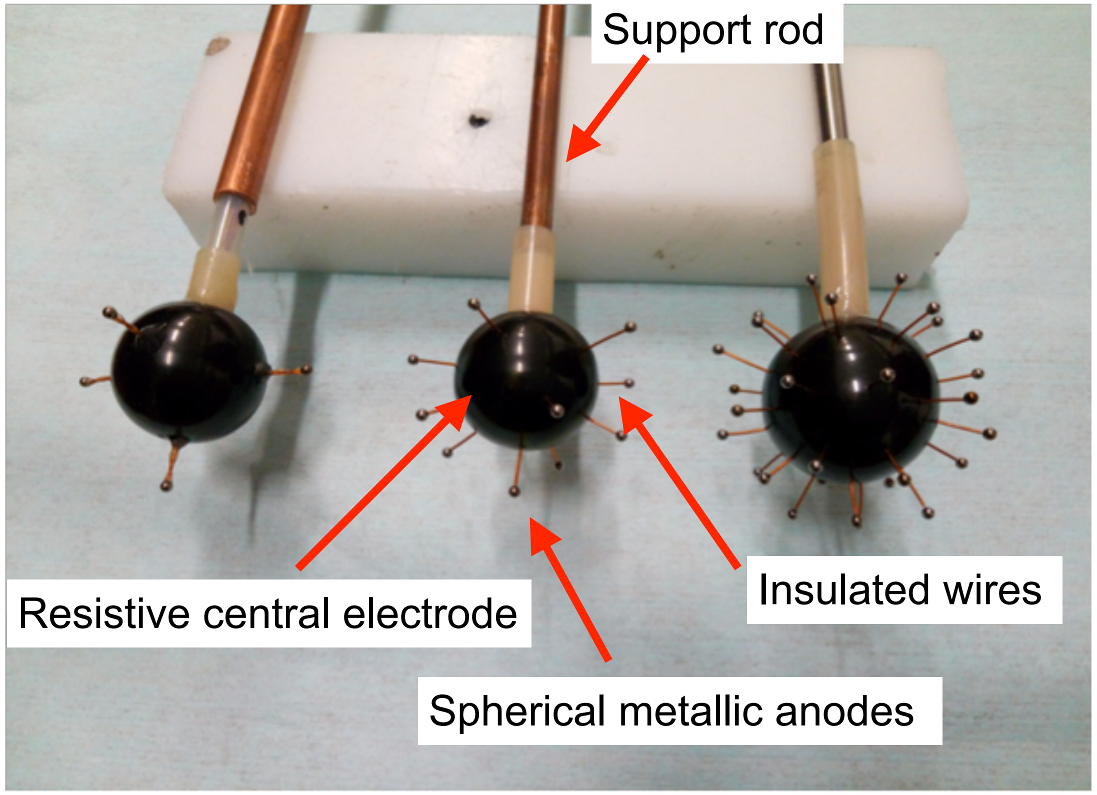

- ACHINOS: Multi-anode sensor JINST 12 (2017) 12, P12031
  - Multiple anodes placed at equal radii
    - Sensors with 5, 11, 33 anodes operated
  - Decoupling drift and amplification fields
  - Opportunity: individual anode read-out
    - TPC-like capabilities

Αχινός (greek. sea urchin)

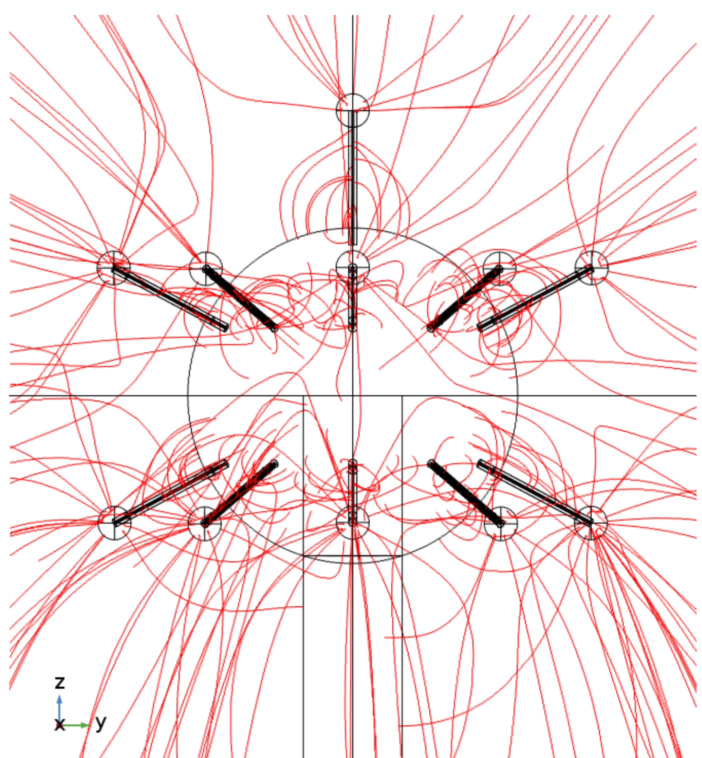

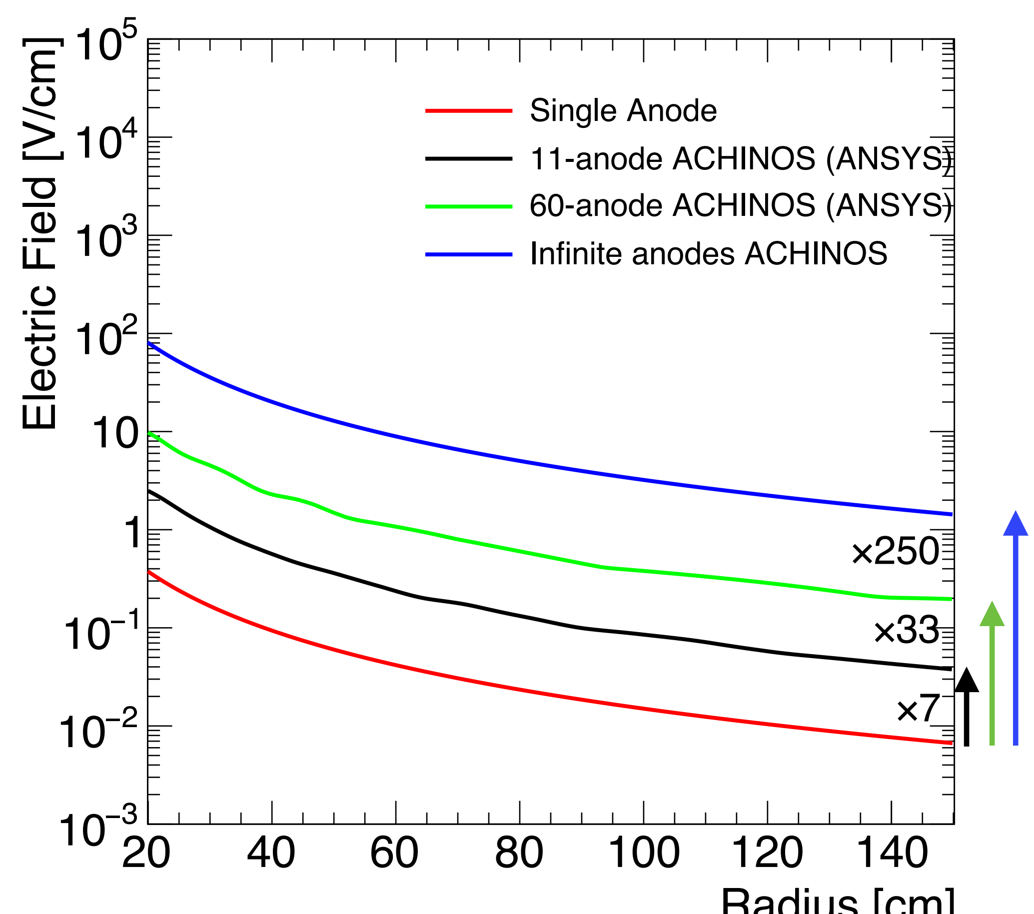

ACHINOS performance with DLC coating

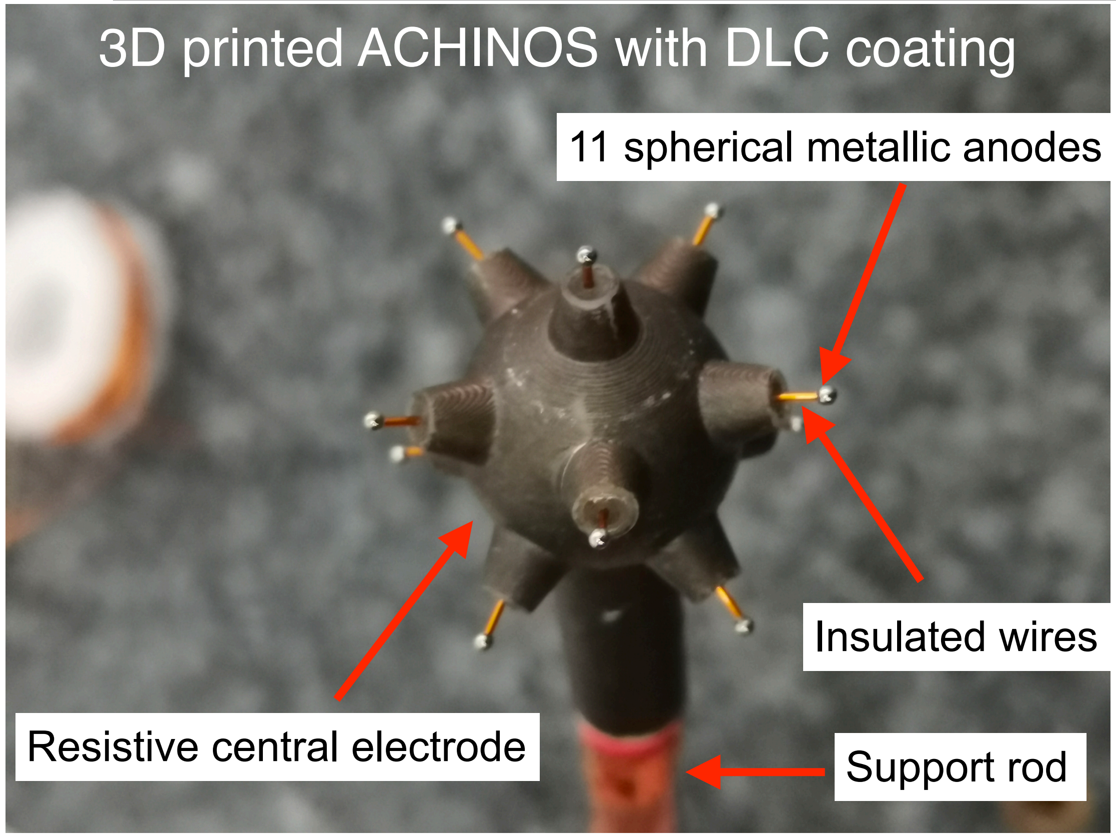

JINST 15 (2020) 11, 11

ACHINOS performance with DLC coating

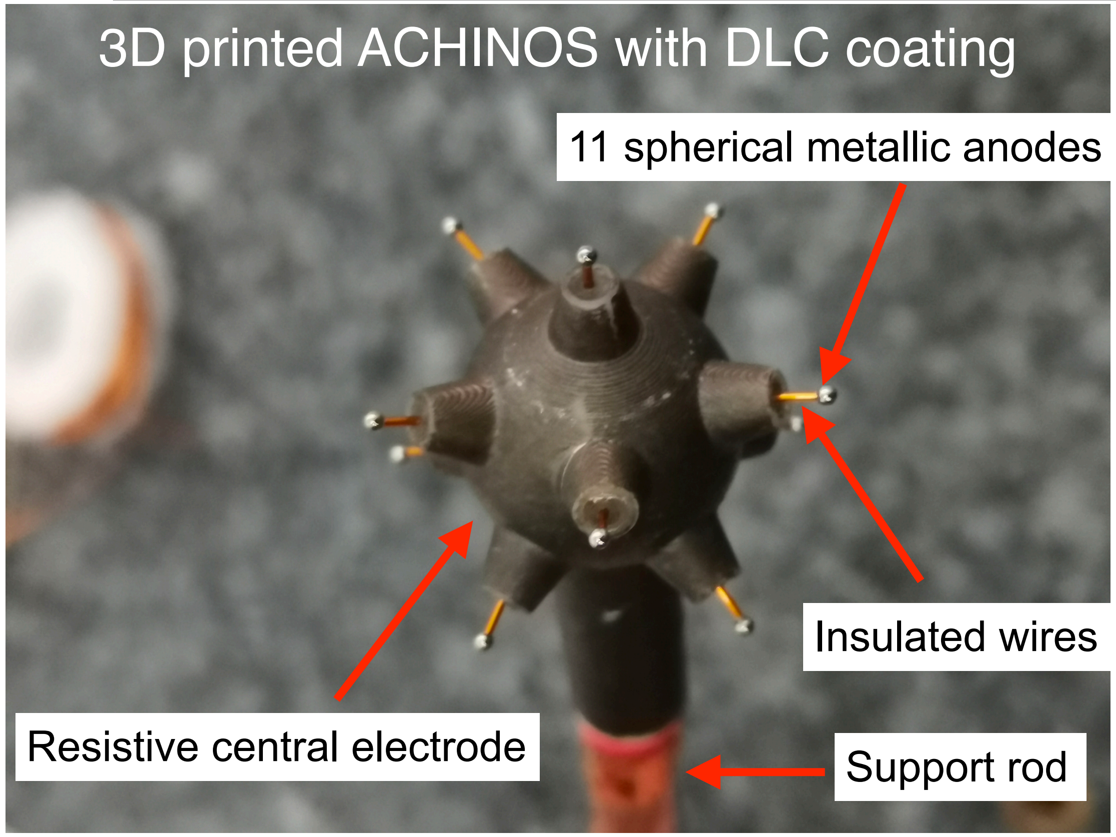

Measurement of the 5.9 keV ^{55}Fe X-ray line

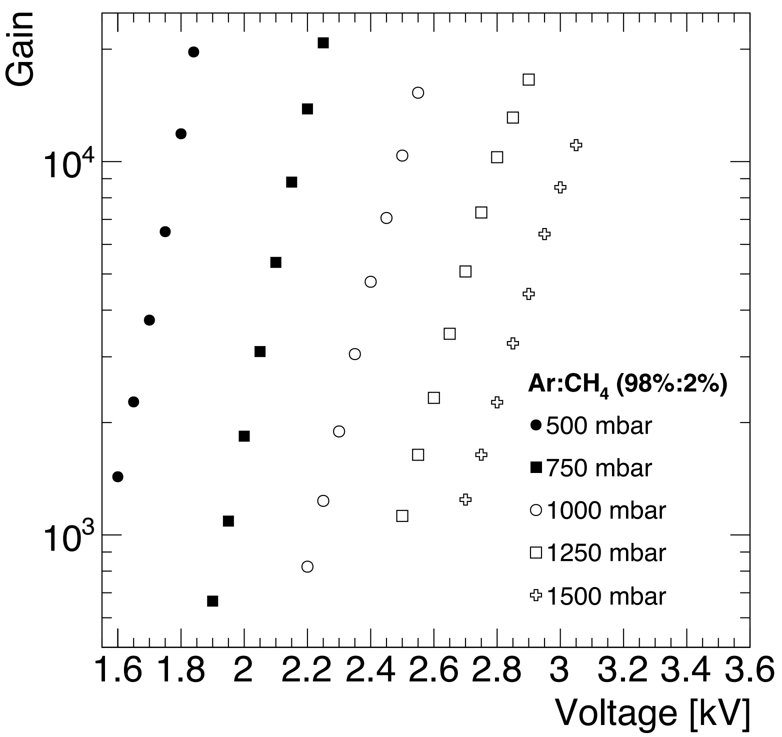

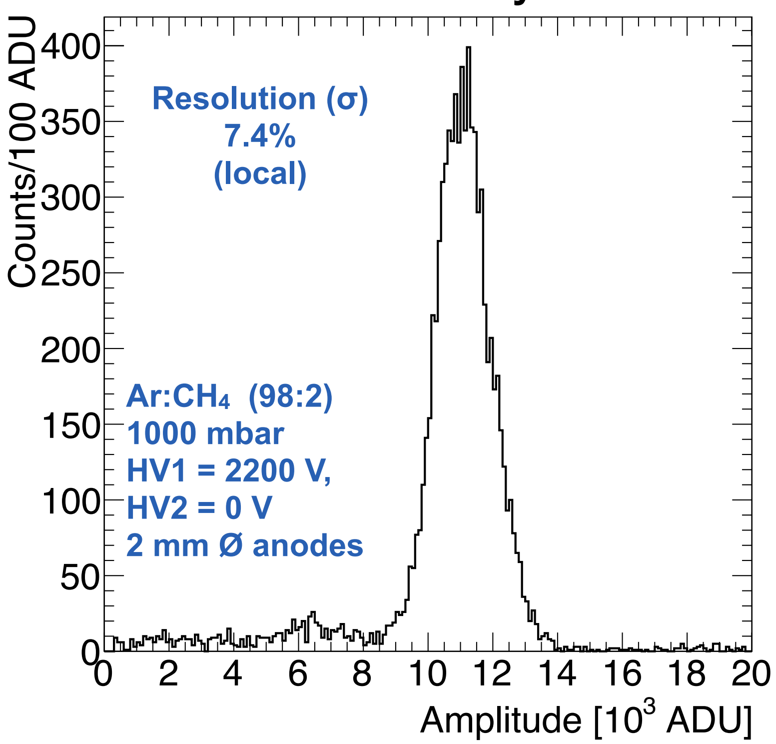

- Performance
  - Good energy resolution
  - High gain/pressure operation
  - Stable operation

JINST 15 (2020) 11, 11

ACHINOS performance with DLC coating

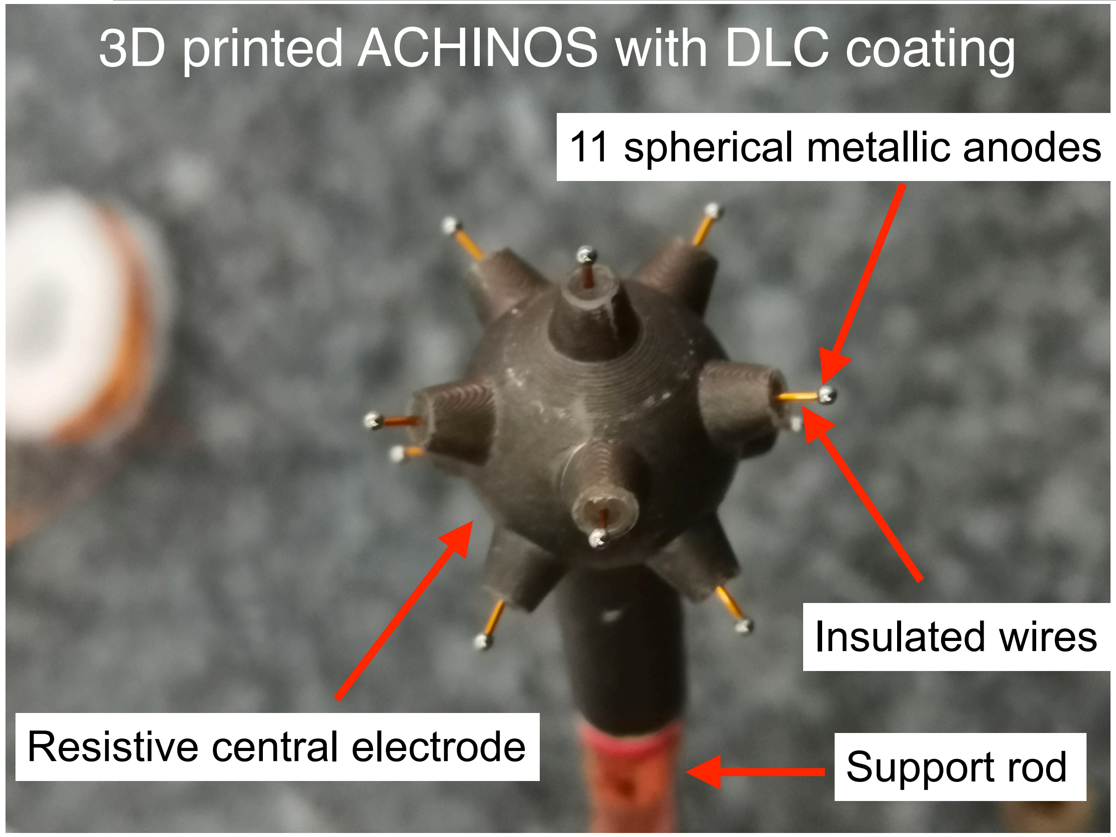

Measurement of the 5.9 keV ^{55}Fe X-ray line

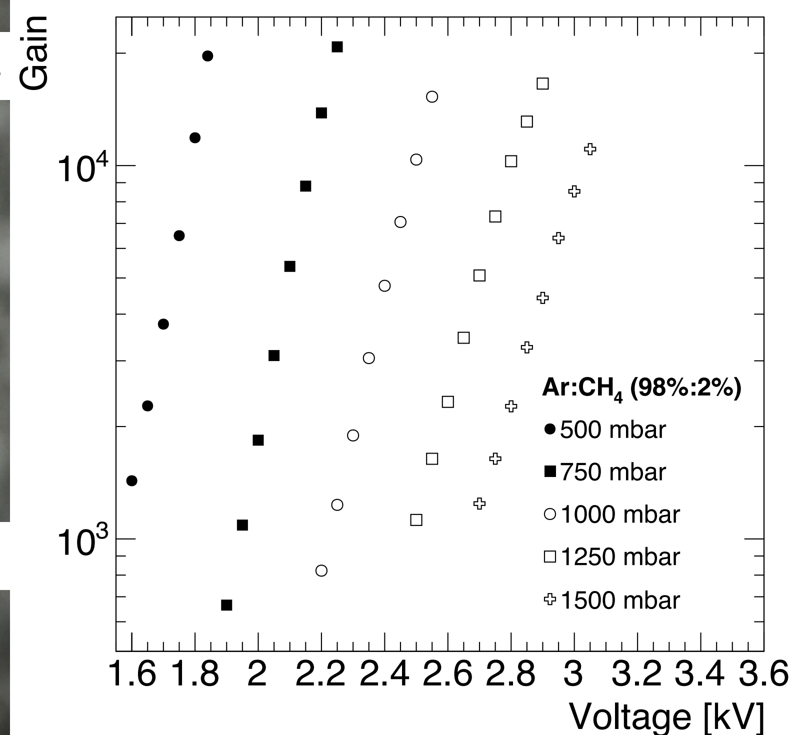

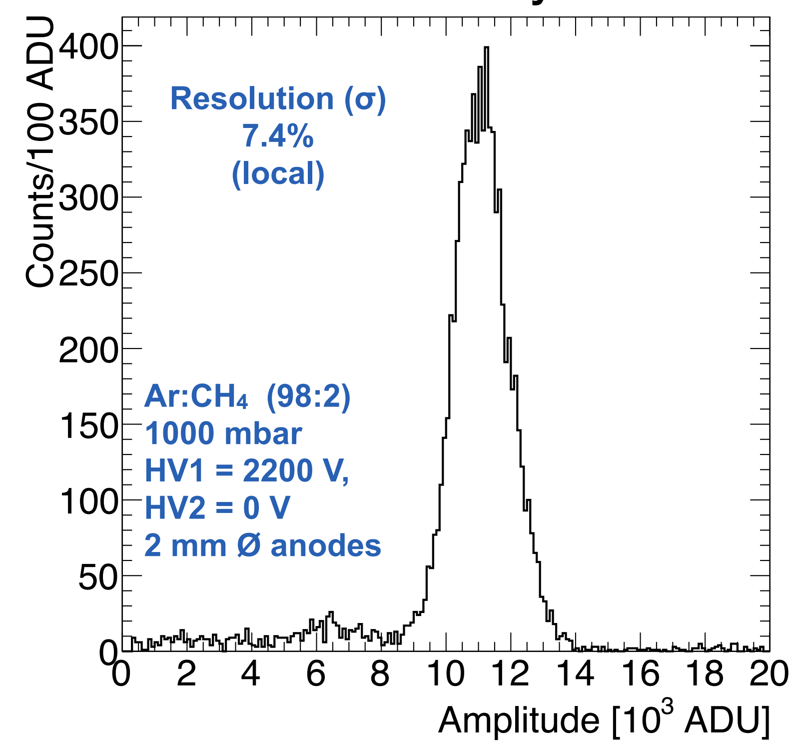

- Performance
  - Good energy resolution
  - High gain/pressure operation
  - Stable operation

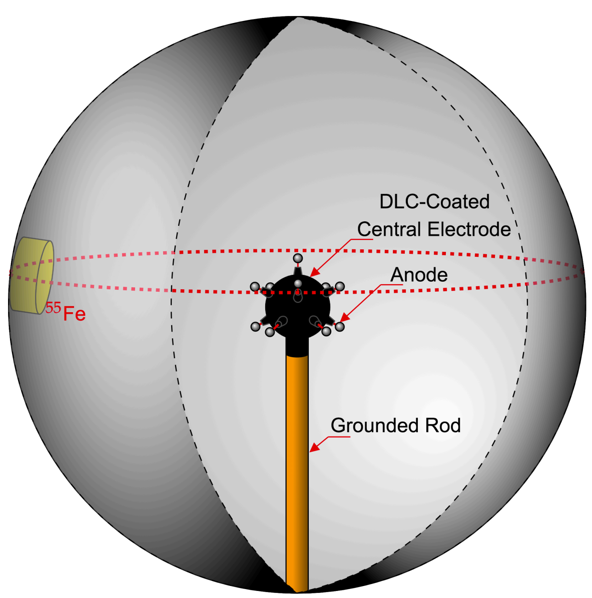

Simulations

Group anodes into two electrodes: Near and Far from the rod

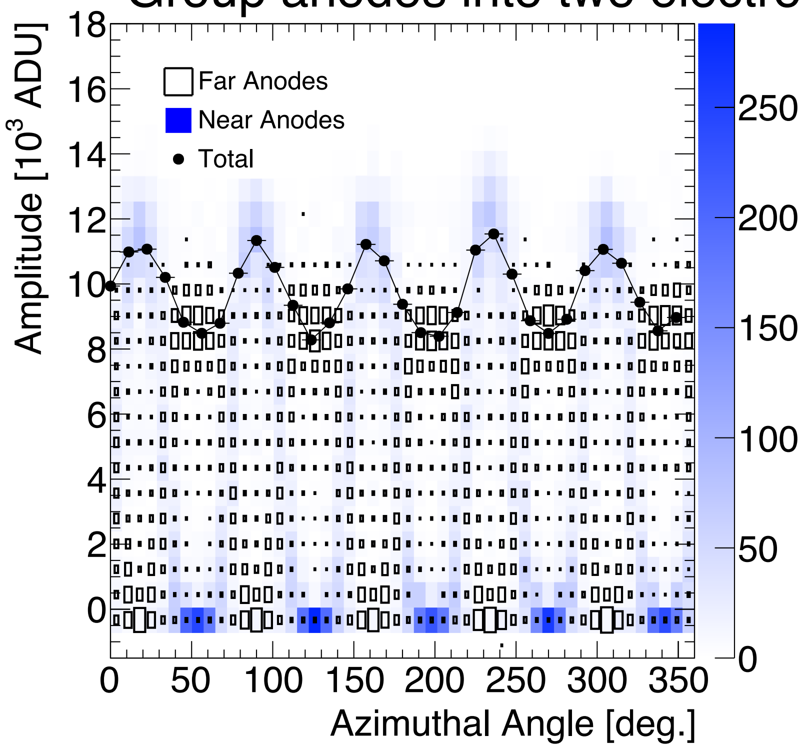

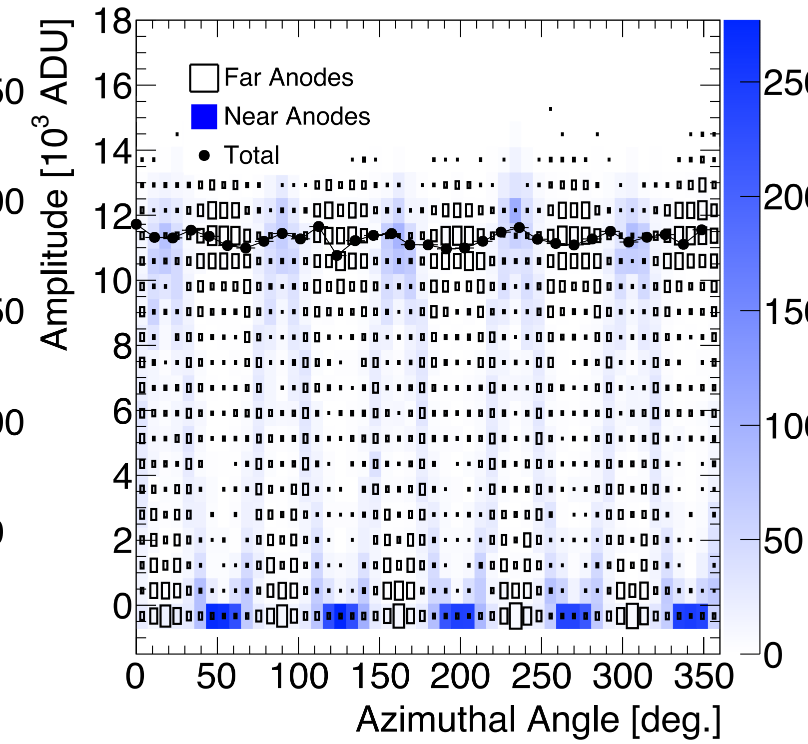

JINST 15 (2020) 11, 11

Fiducialisation

Birmingham simulation framework, combining strengths of Geant4 and Garfield++

JINST 15 (2020) 06, C06013

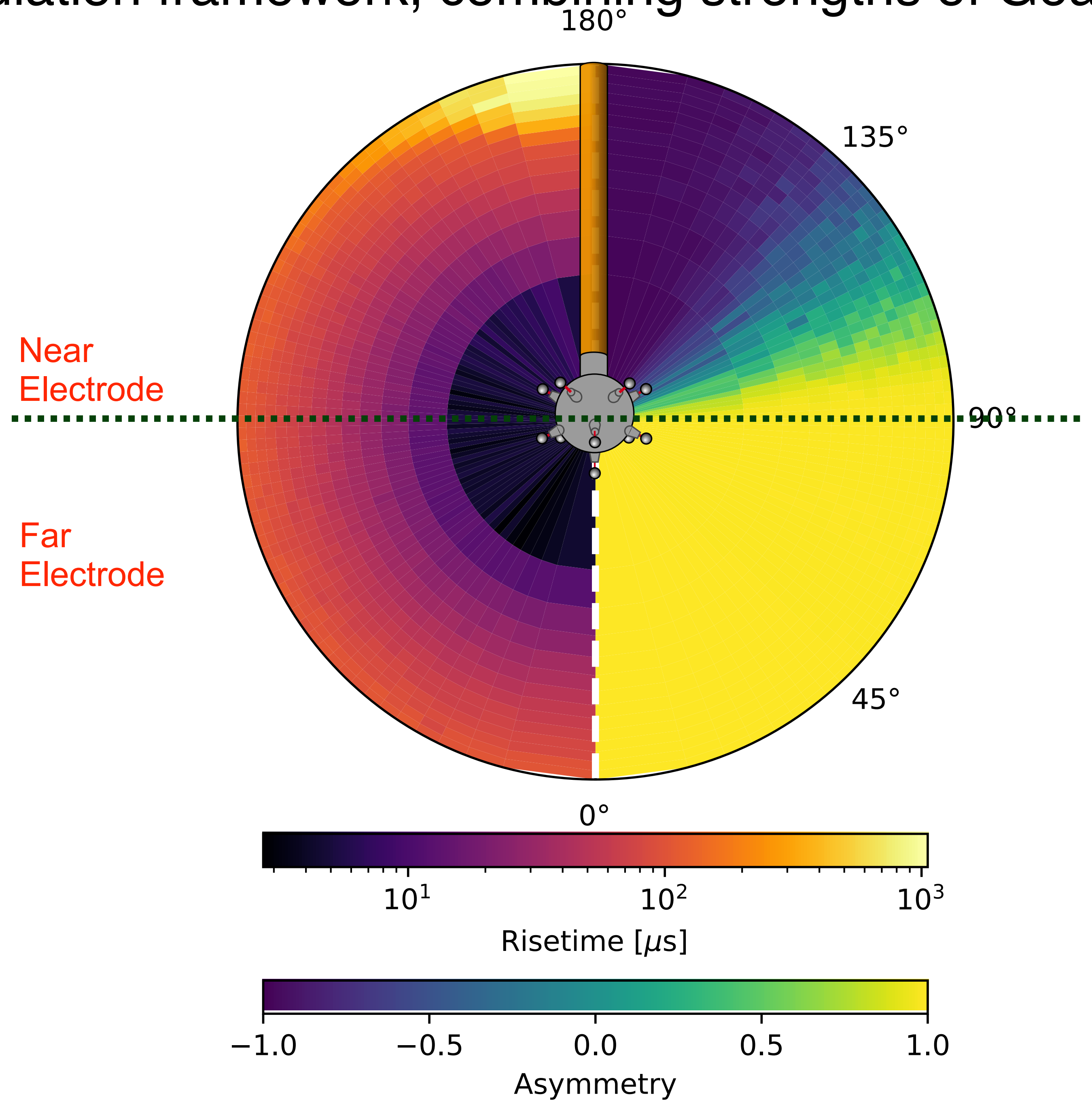

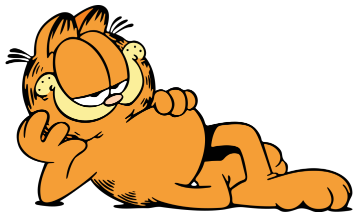

- Reading out individual ACHINOS anodes: position of interaction can be reconstructed
- First tests: Separate the anodes in two electrodes "Near" and "Far" (from the rod)
  - Asymmetry of pulse amplitudes: zenith angle
  - Pulse rise-time: radius

Fiducialisation

Birmingham simulation framework, combining strengths of Geant4 and Garfield++

) 06, C06013

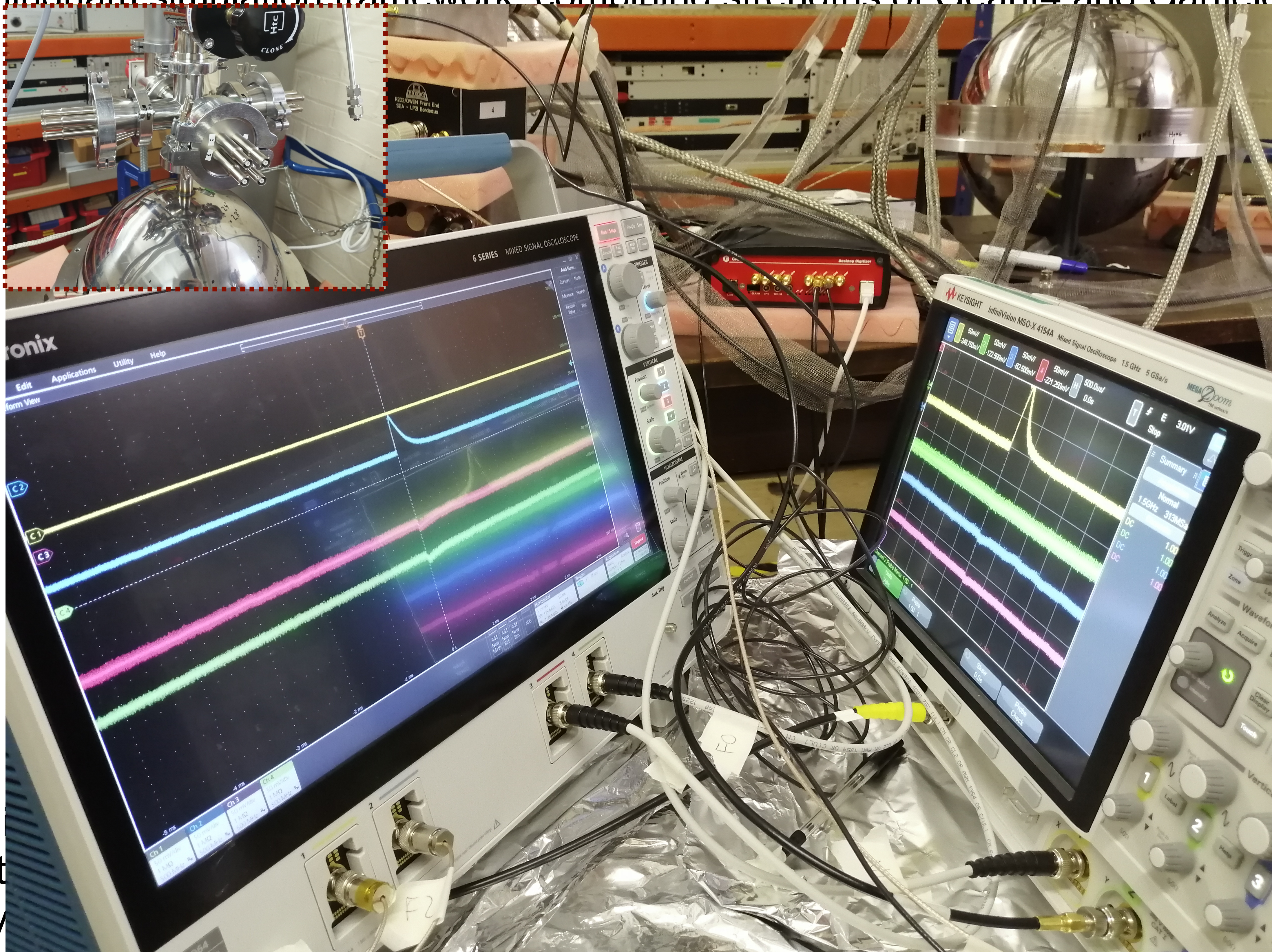

- Read… structured
- First t… rod)
  - Asy…
  - Pulse rise-time: radius

Event reconstruction

Birmingham simulation framework, combining strengths of Geant4 and Garfield++

JINST 15 (2020) 06, C06013

Many anodes with individual read-out: track reconstruction

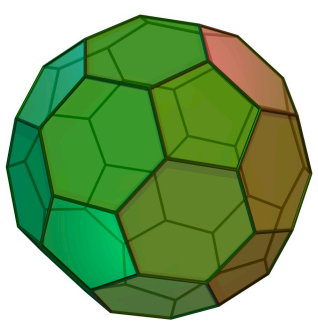

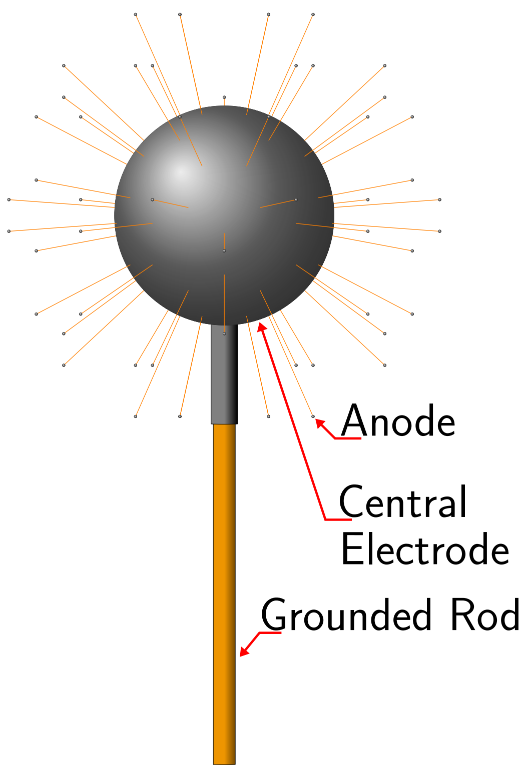

60-anodes (truncated icosahedron)

Event reconstruction

Birmingham simulation framework, combining strengths of Geant4 and Garfield++

JINST 15 (2020) 06, C06013

Many anodes with individual read-out: track reconstruction

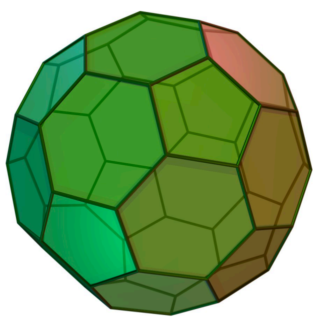

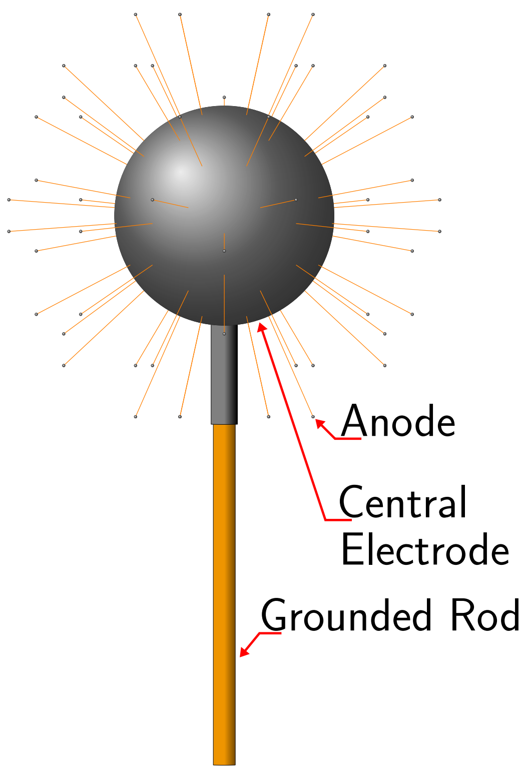

60-anodes (truncated icosahedron)

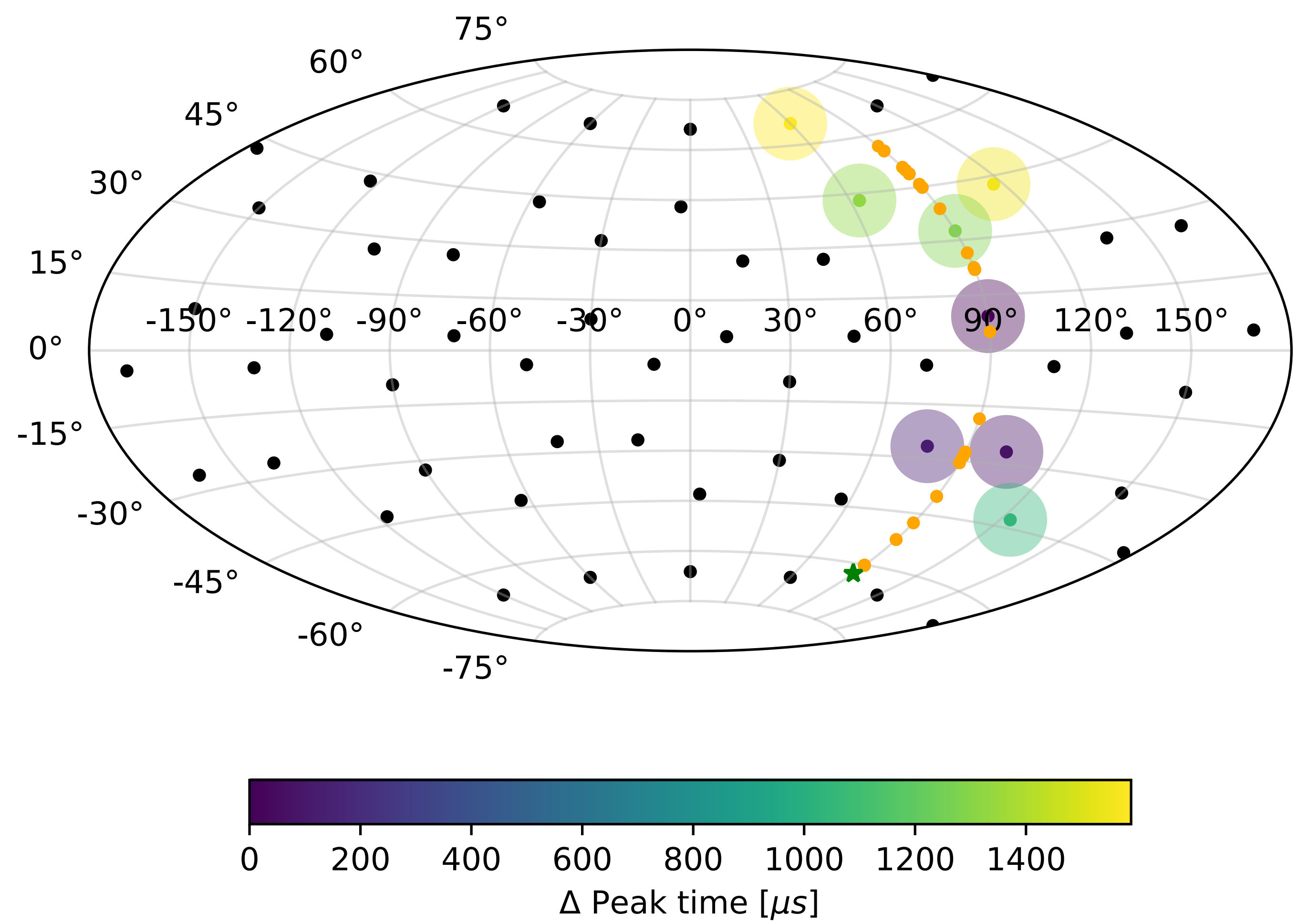

Event reconstruction

Birmingham simulation framework, combining strengths of Geant4 and Garfield++

JINST 15 (2020) 06, C06013

Many a

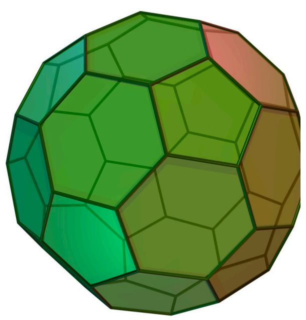

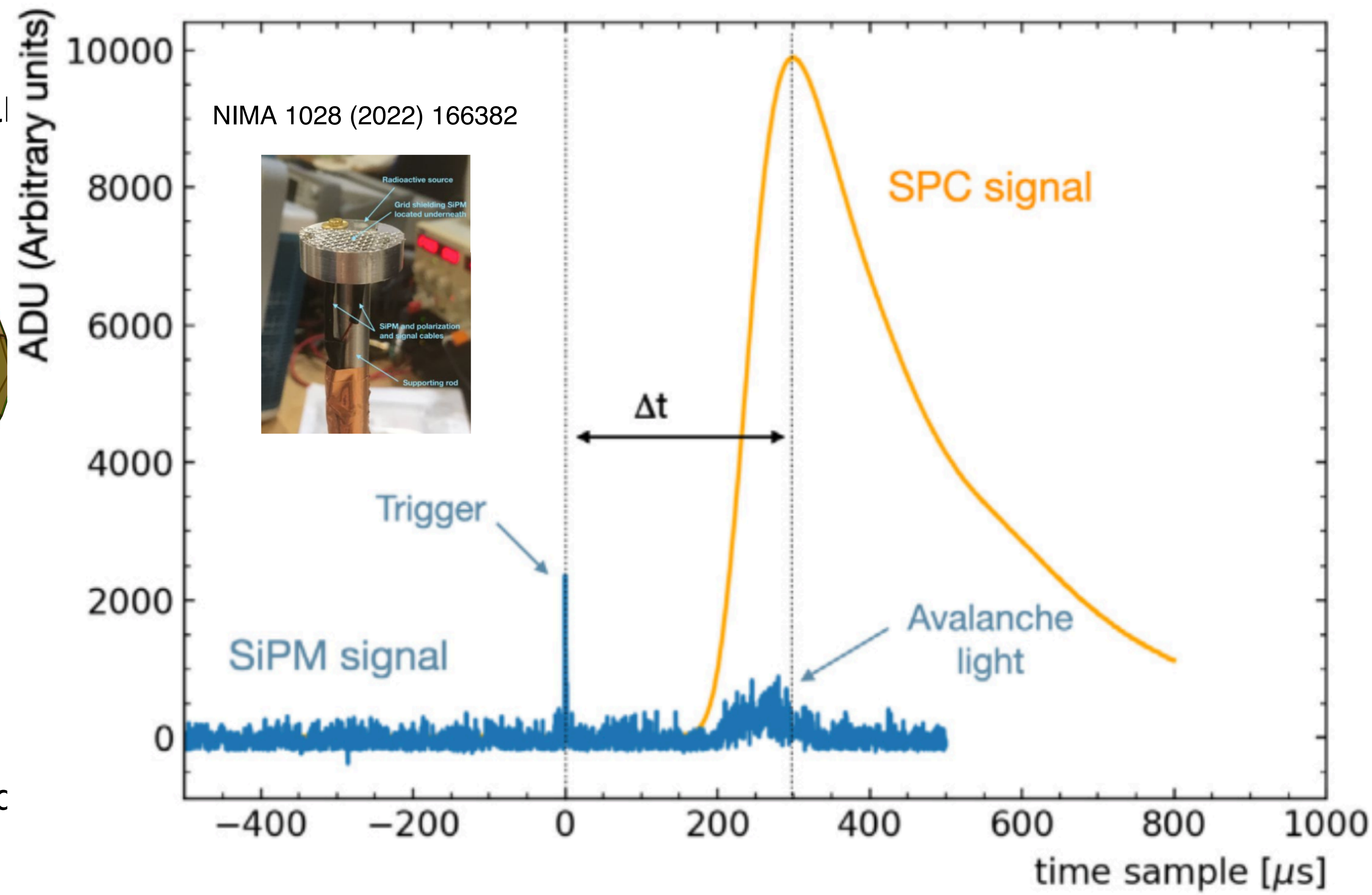

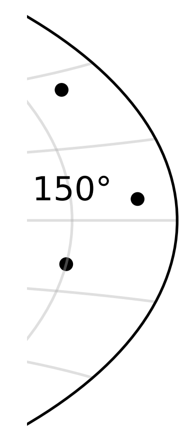

60-anoc

Estimating the expected response

Quenching factor measurements: TUNL

- TANDEM Van de Graaff accelerator at TUNL (USA)
- Pulsed 20 MeV proton beam on $^{7}\mathrm{Li}$
  - (Quasi-)Mono-energetic neutrons at a given angle
  - Neutron energy at $0°$: 545 ± 20 keV
- Detector: ⌀15 cm stainless-steel SPC
  - Calibration using an $^{55}\mathrm{Fe}$ source

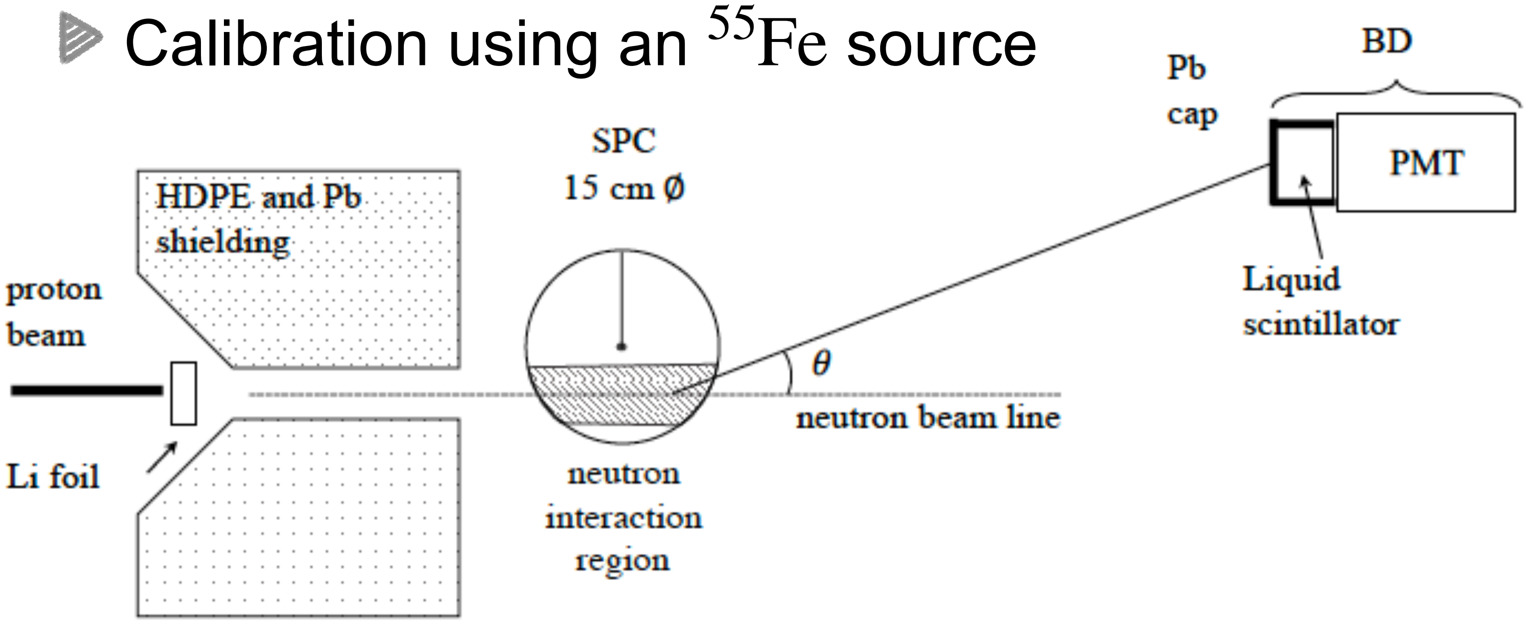

Phys.Rev.D 105 (2022) 5, 052004

Quenching factor measurements: TUNL

- TANDEM Van de Graaff accelerator at TUNL (USA)
- Pulsed 20 MeV proton beam on $^{7}\mathrm{Li}$
  - (Quasi-)Mono-energetic neutrons at a given angle
  - Neutron energy at $0°$: 545 ± 20 keV
- Detector: ⌀15 cm stainless-steel SPC
  - Calibration using an $^{55}\mathrm{Fe}$ source

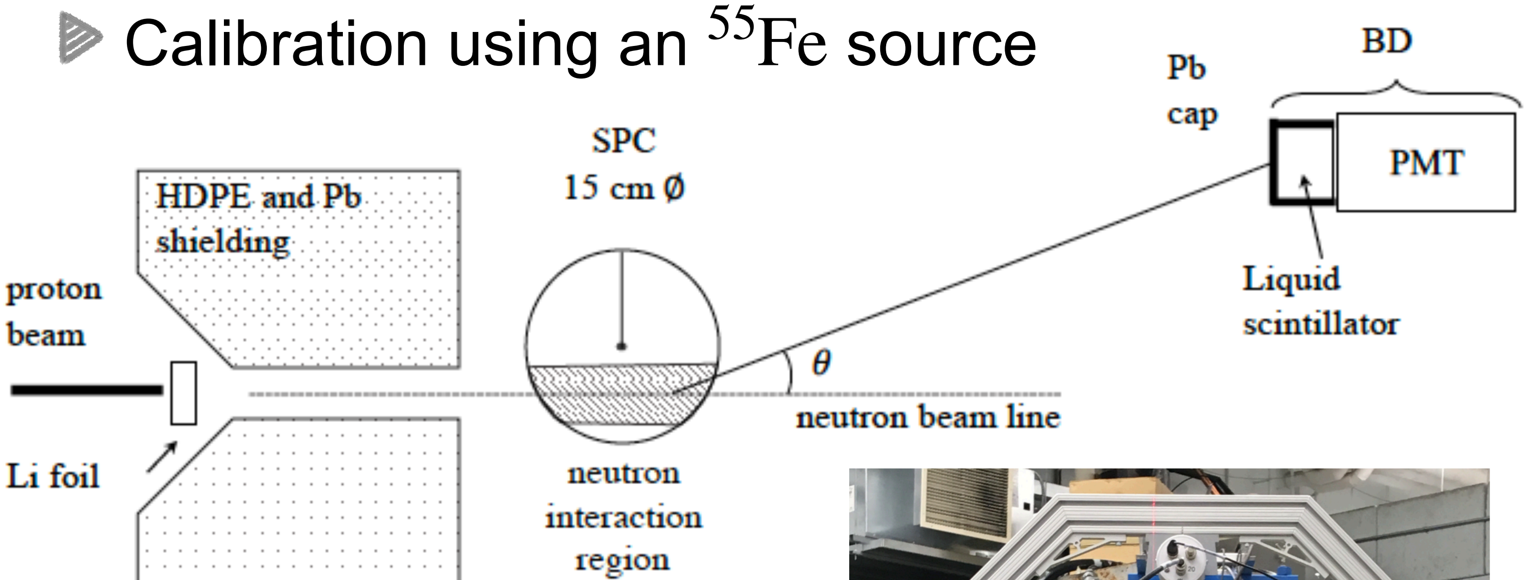

liquid-scintillator/PMT backing detectors

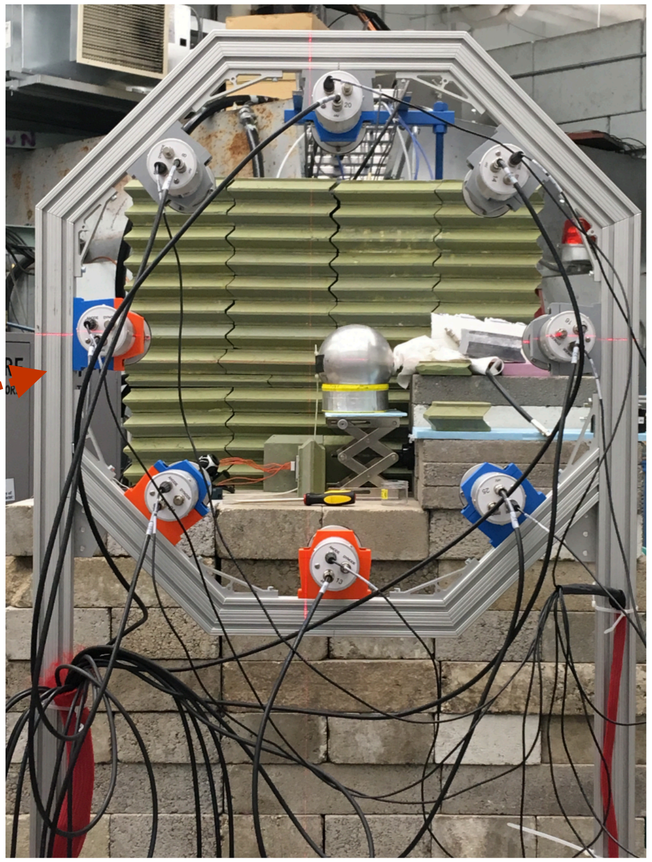

Phys.Rev.D 105 (2022) 5, 052004

Quenching factor measurements: TUNL

- TANDEM Van de Graaff accelerator at TUNL (USA)
- Pulsed 20 MeV proton beam on $^{7}\mathrm{Li}$
  - (Quasi-)Mono-energetic neutrons at a given angle
  - Neutron energy at $0°$: $545 \pm 20\ \mathrm{keV}$
- Detector: ∅15 cm stainless-steel SPC
  - Calibration using an $^{55}\mathrm{Fe}$ source

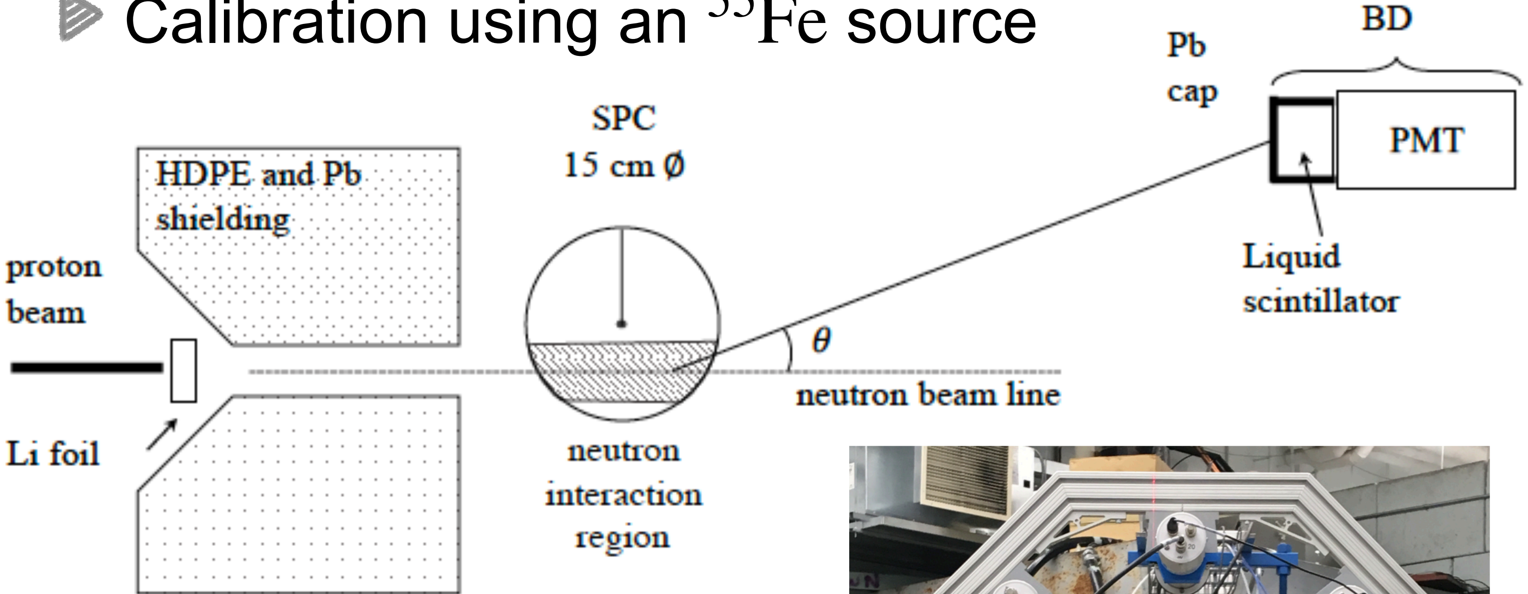

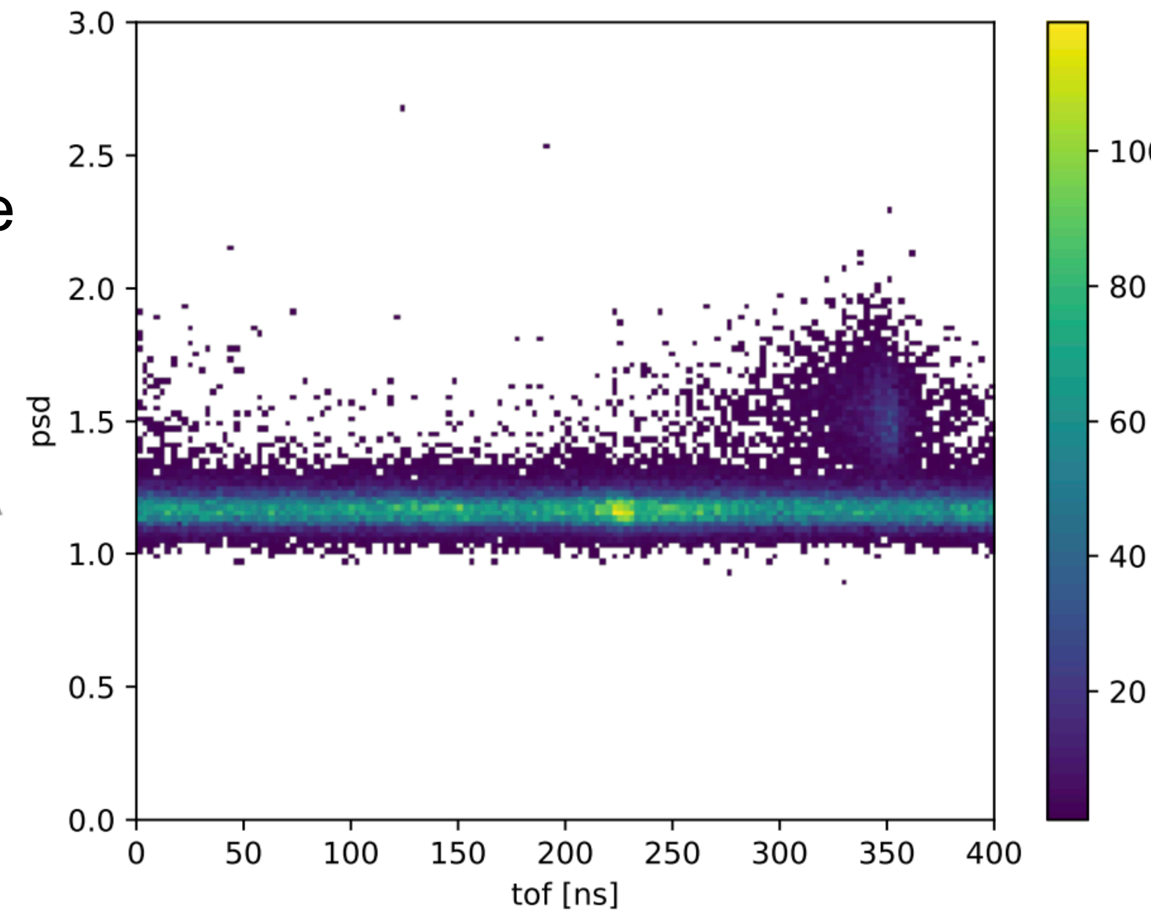

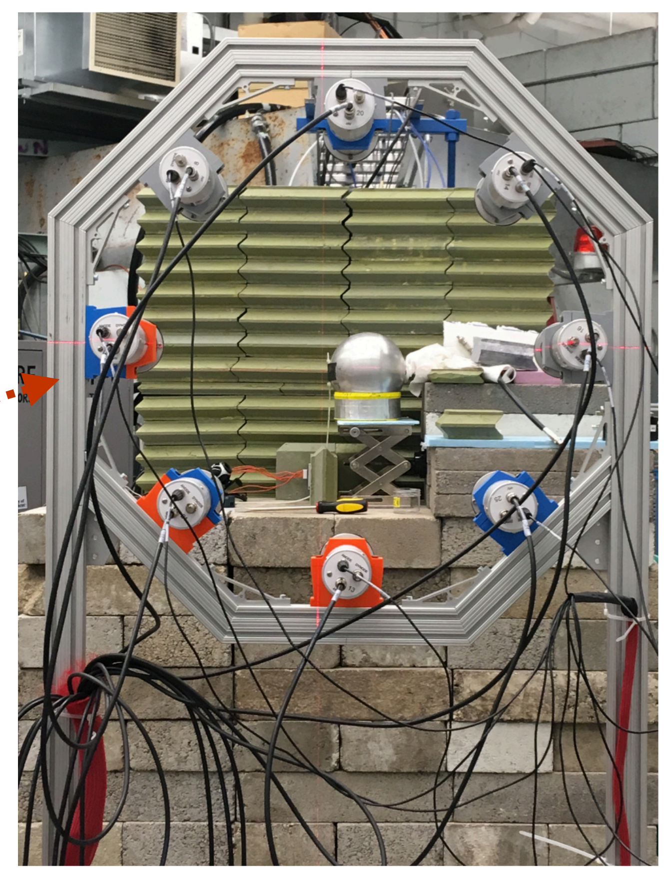

liquid-scintillator/PMT backing detectors

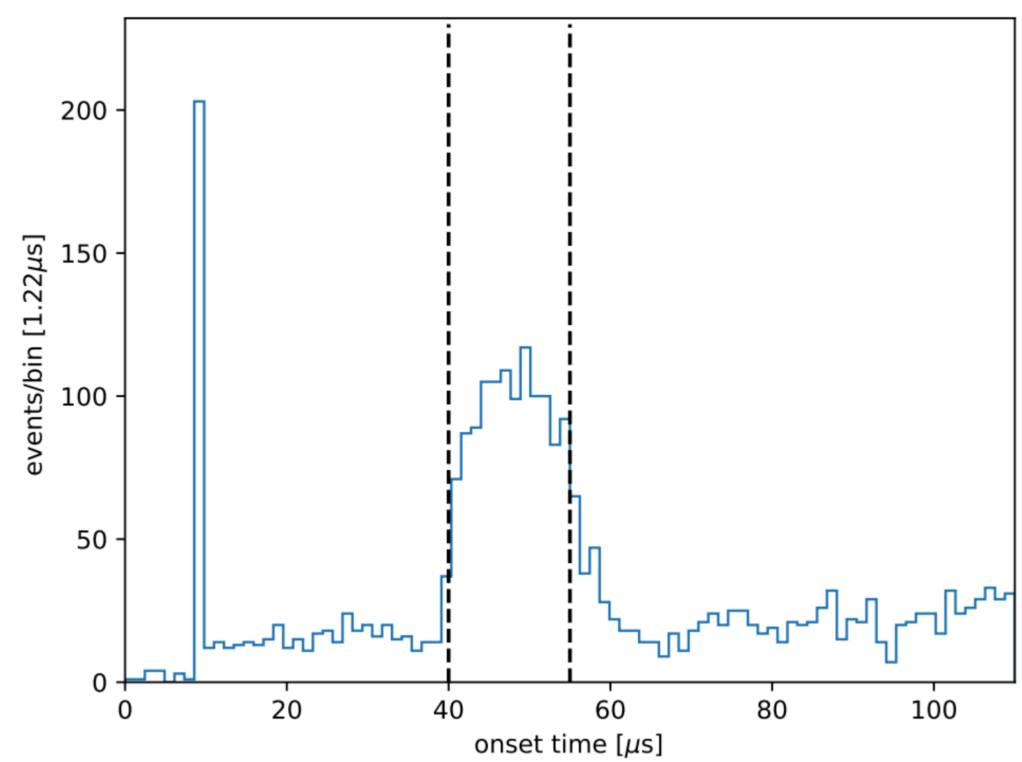

Phys.Rev.D 105 (2022) 5, 052004

Quenching factor measurements: TUNL

Run	E_{nr} [keV_{nr}]	$\sigma_{E_{nr}}$ [keV_{nr}]	θ [°]	σ_θ [°]
8	6.80	1.15	29.02 ± 0.4	2.45
7	2.93	0.46	18.84 ± 0.1	1.47
14	2.02	0.29	15.63 ± 0.3	1.12
9	1.70	0.26	14.33 ± 0.06	1.1
10	1.30	0.2	12.48 ± 0.05	0.94
14	1.03	0.2	11.13 ± 0.3	1.1
11	0.74	0.11	9.4 ± 0.03	0.69
14	0.34	0.11	6.33 ± 0.26	1.1

Estimated Recoil Energy

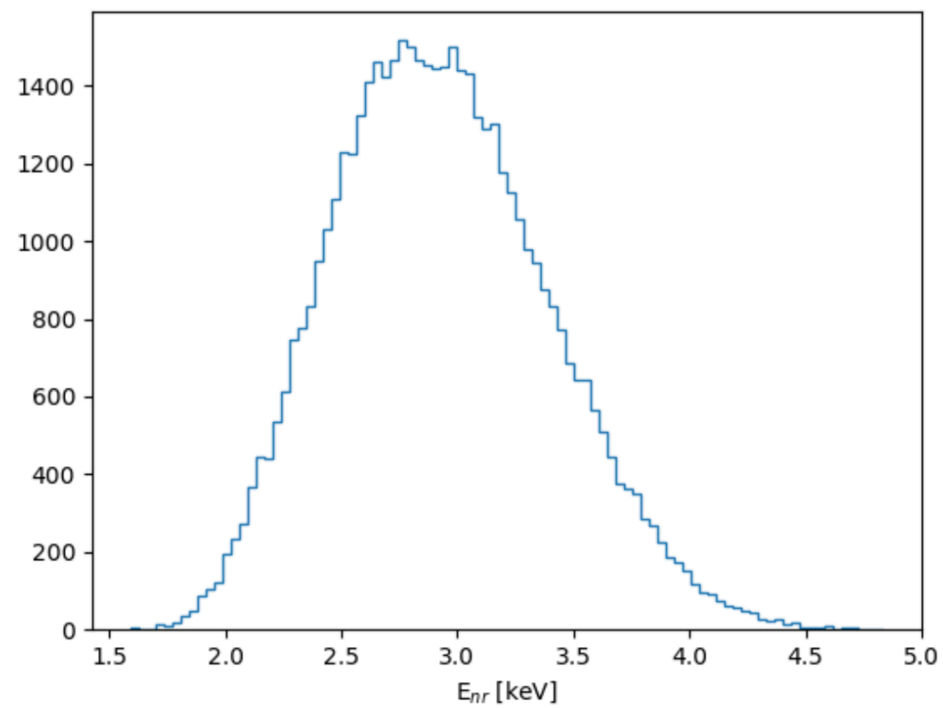

Measured Energy

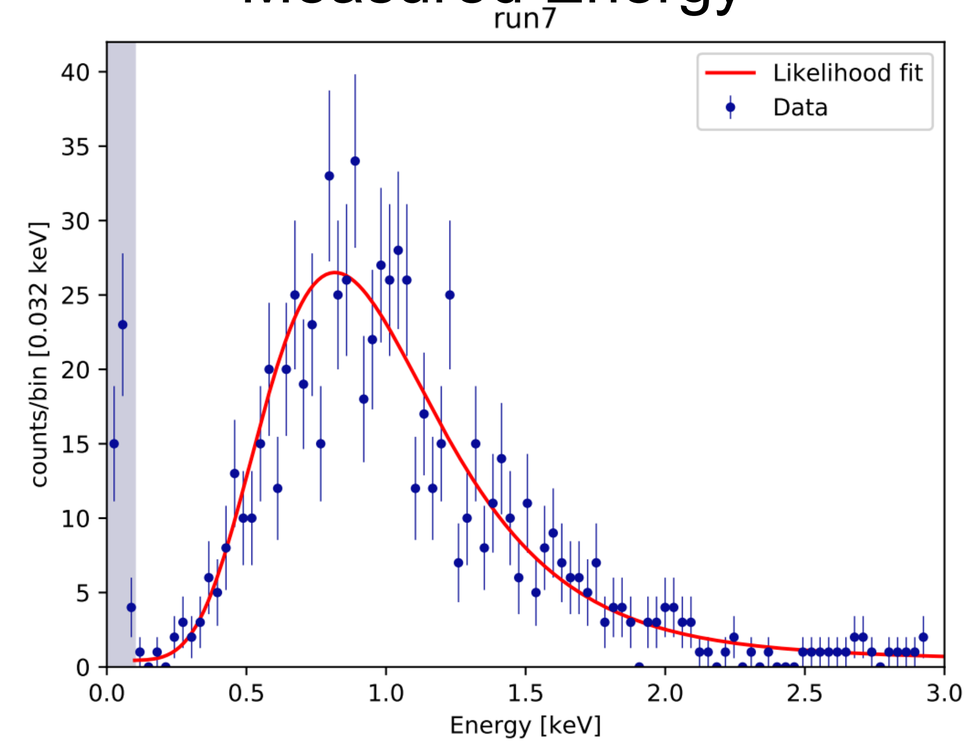

Phys.Rev.D 105 (2022) 5, 052004

Quenching factor measurements: TUNL

Run	E_{nr} [keV_{nr}]	$\sigma_{E_{nr}}$ [keV_{nr}]	θ [°]	σ_θ [°]
8	6.80	1.15	29.02 ± 0.4	2.45
7	2.93	0.46	18.84 ± 0.1	1.47
14	2.02	0.29	15.63 ± 0.3	1.12
9	1.70	0.26	14.33 ± 0.06	1.1
10	1.30	0.2	12.48 ± 0.05	0.94
14	1.03	0.2	11.13 ± 0.3	1.1
11	0.74	0.11	9.4 ± 0.03	0.69
14	0.34	0.11	6.33 ± 0.26	1.1

Estimated Recoil Energy

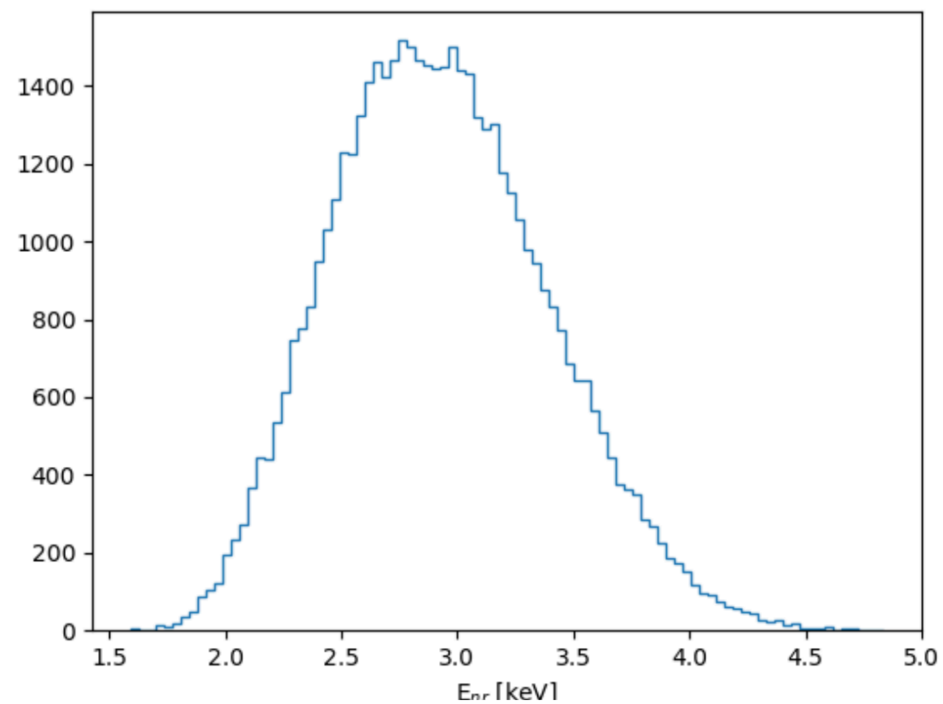

Measured Energy

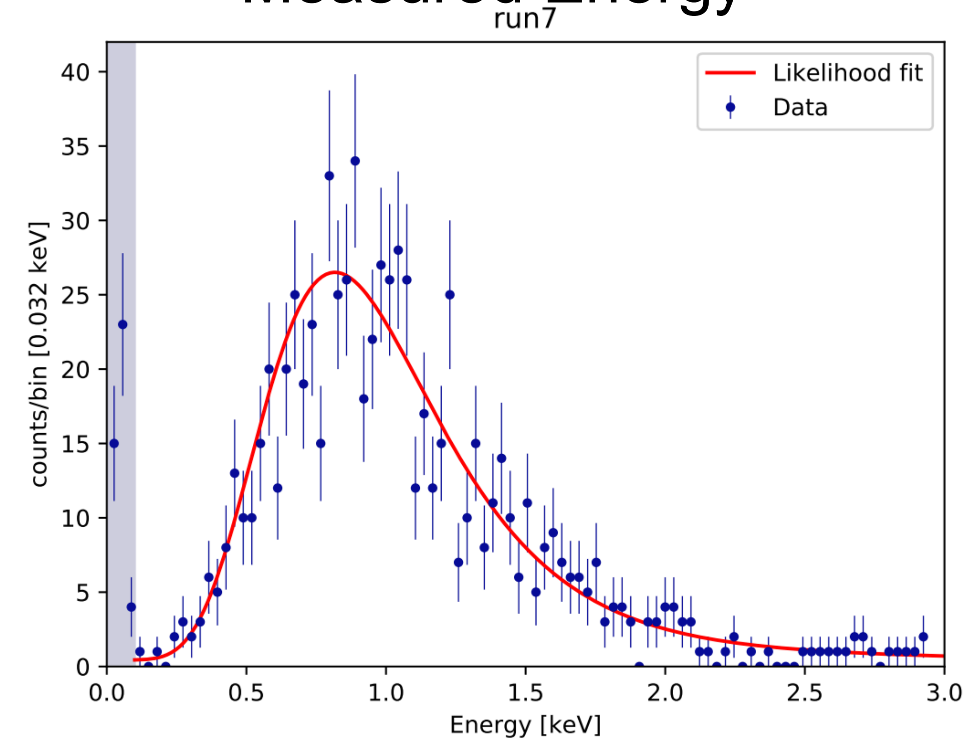

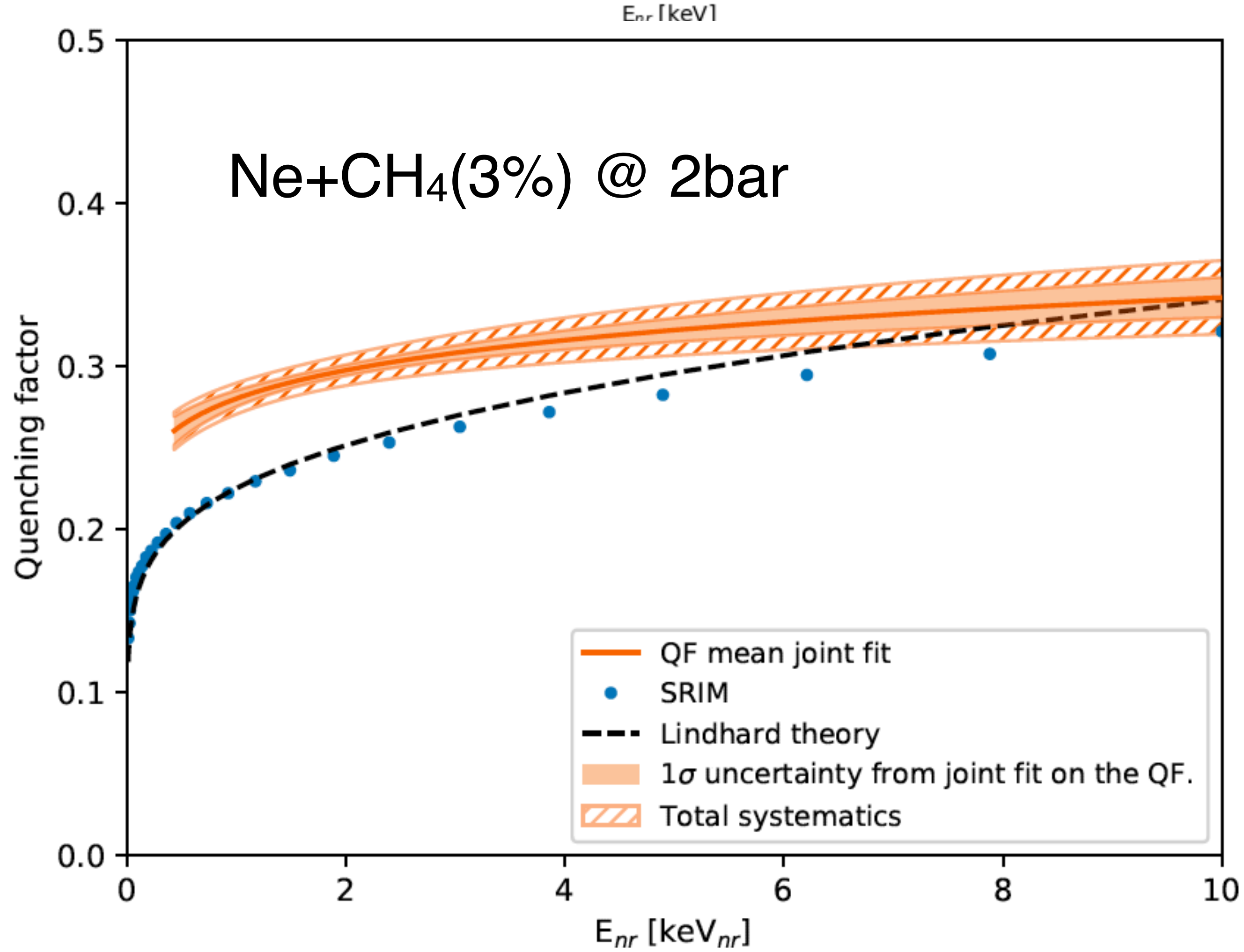

Phys.Rev.D 105 (2022) 5, 052004

Quenching factor measurements: COMIMAC

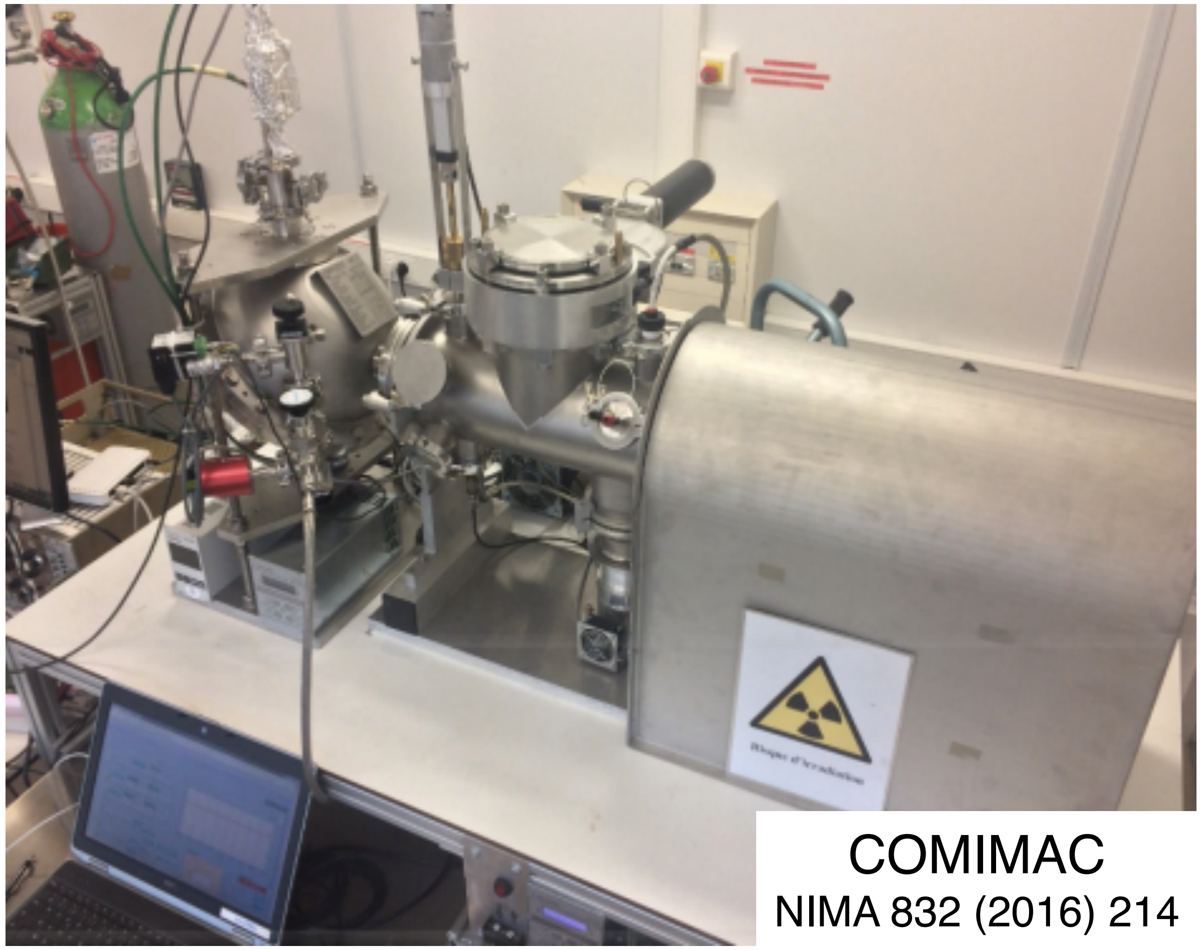

COMIMAC
NIMA 832 (2016) 214

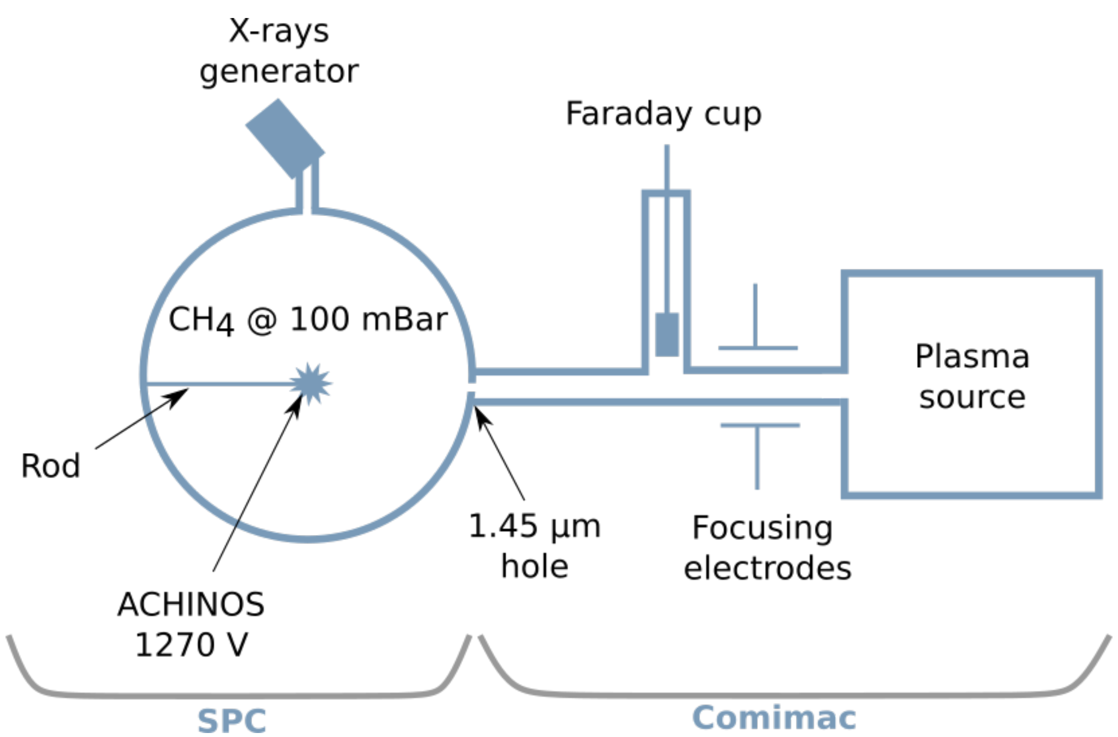

arXiv:2201.09566

- COMIMAC Facility at Grenoble
  - Electrons and ions directed into detector
  - Directly compare response
  - Ion energies studied: 2 - 13 keV
  - Electron energies studied: 1.5 - 13 keV

Quenching factor measurements: COMIMAC

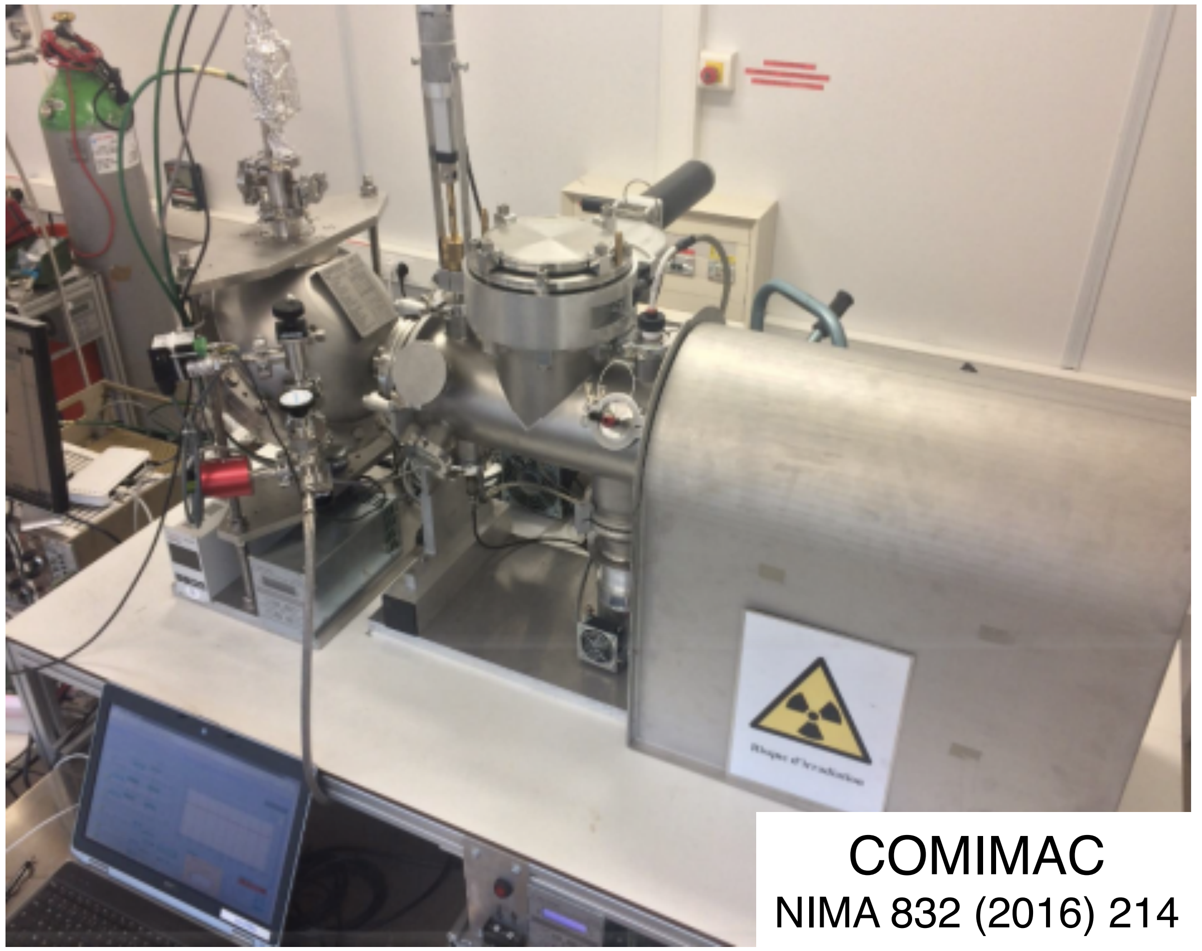

COMIMAC
NIMA 832 (2016) 214

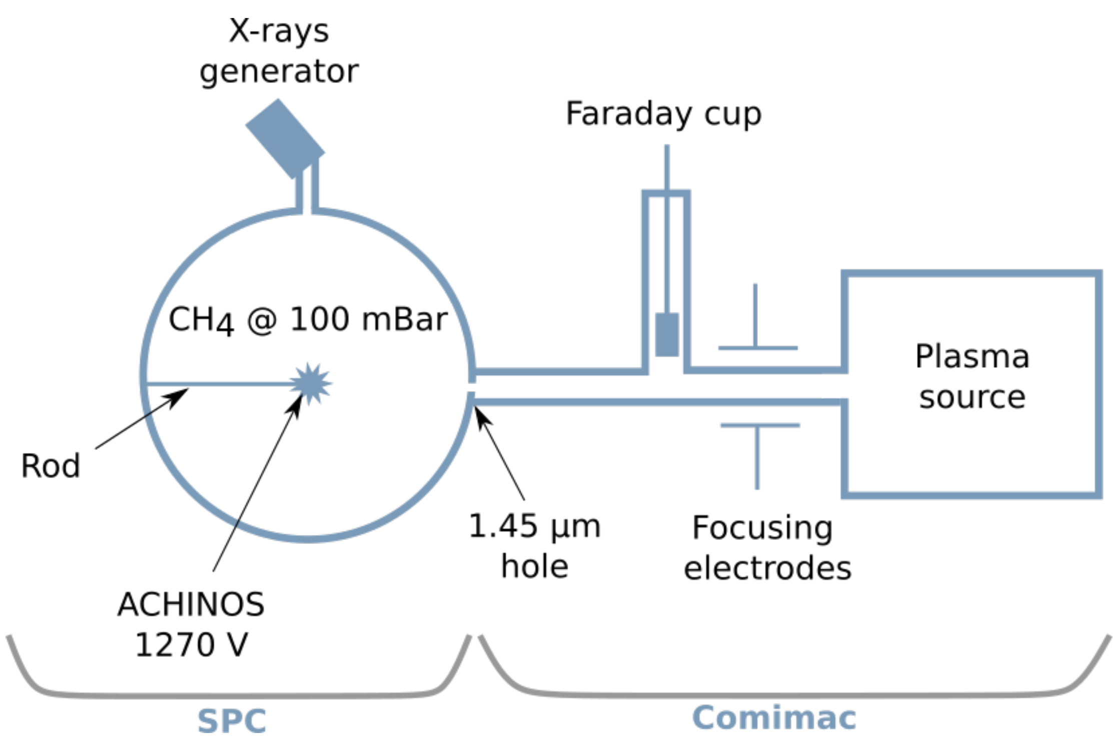

arXiv:2201.09566

- COMIMAC Facility at Grenoble
  - Electrons and ions directed into detector
  - Directly compare response
  - Ion energies studied: 2 - 13 keV
  - Electron energies studied: 1.5 - 13 keV

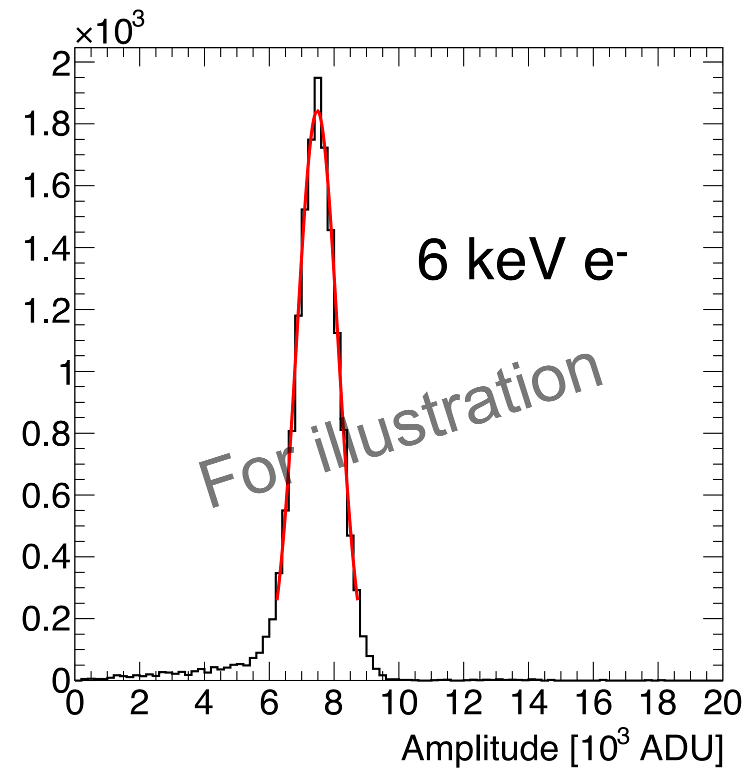

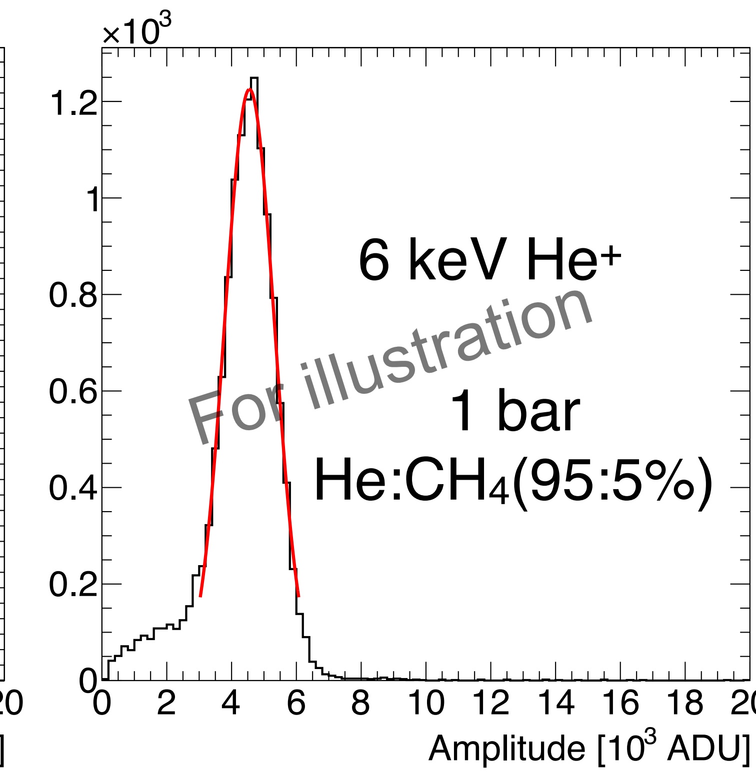

Quenching factor measurements: COMIMAC

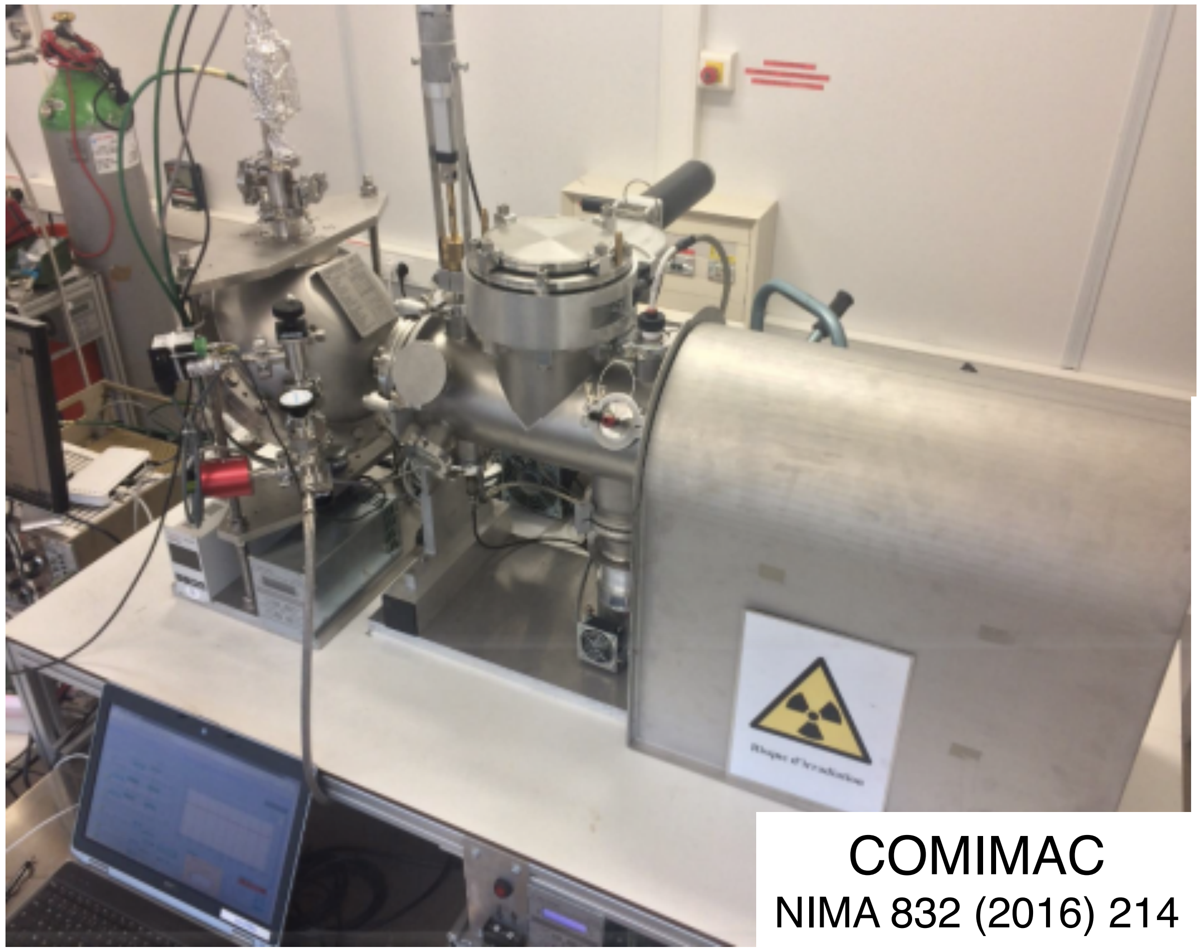

COMIMAC
NIMA 832 (2016) 214

- COMIMAC Facility at Grenoble
  - Electrons and ions directed into detector
  - Directly compare response
  - Ion energies studied: 2 - 13 keV
  - Electron energies studied: 1.5 - 13 keV

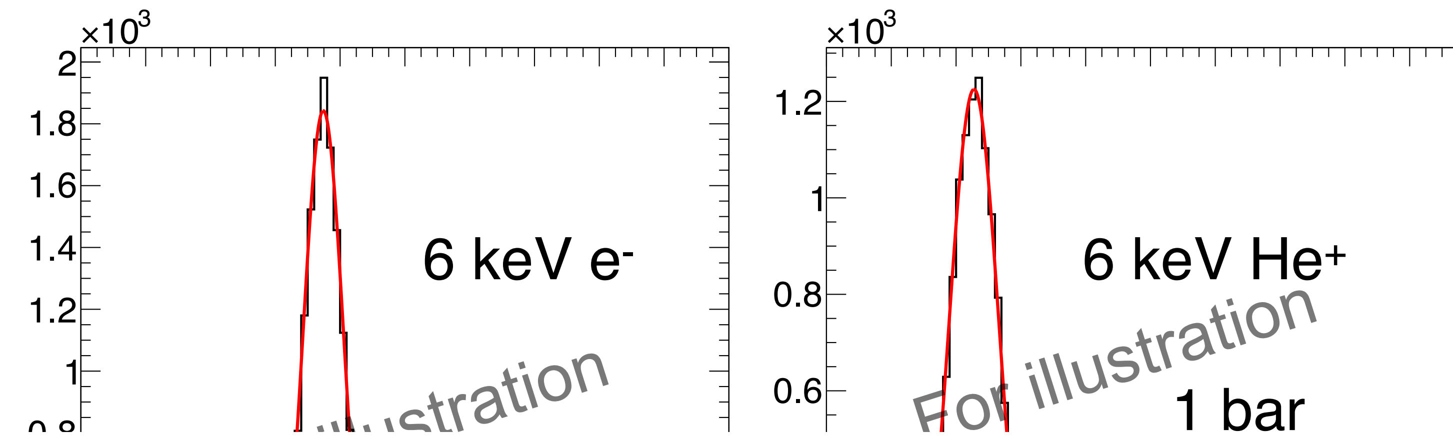

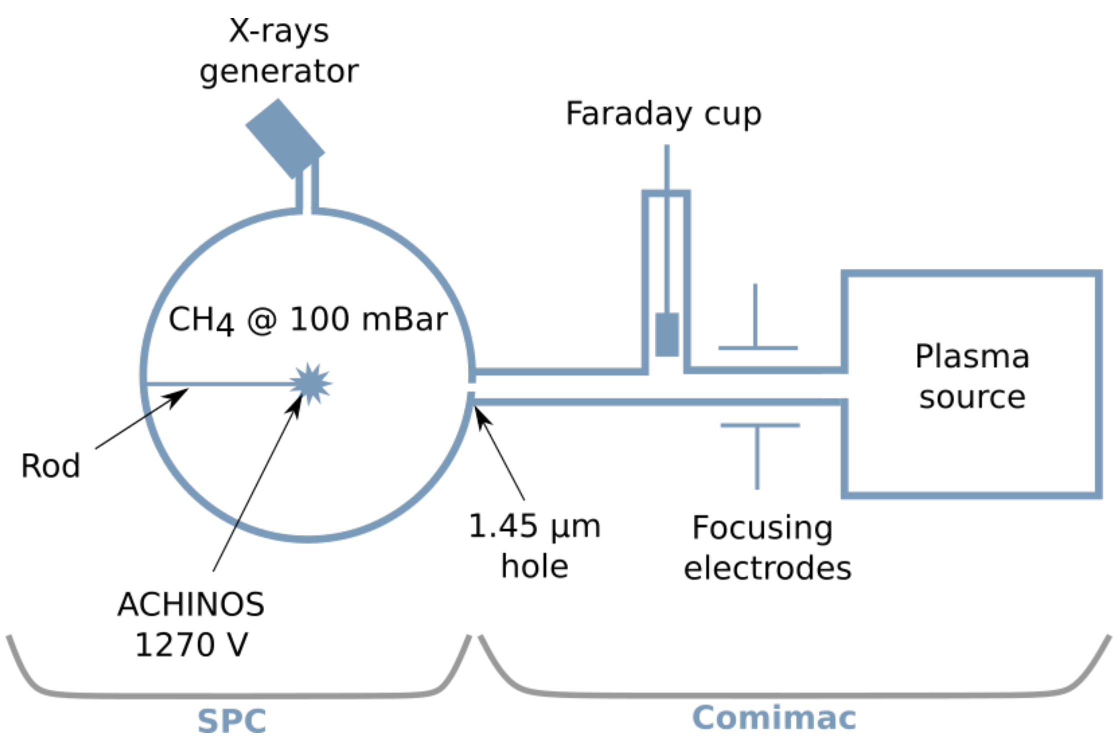

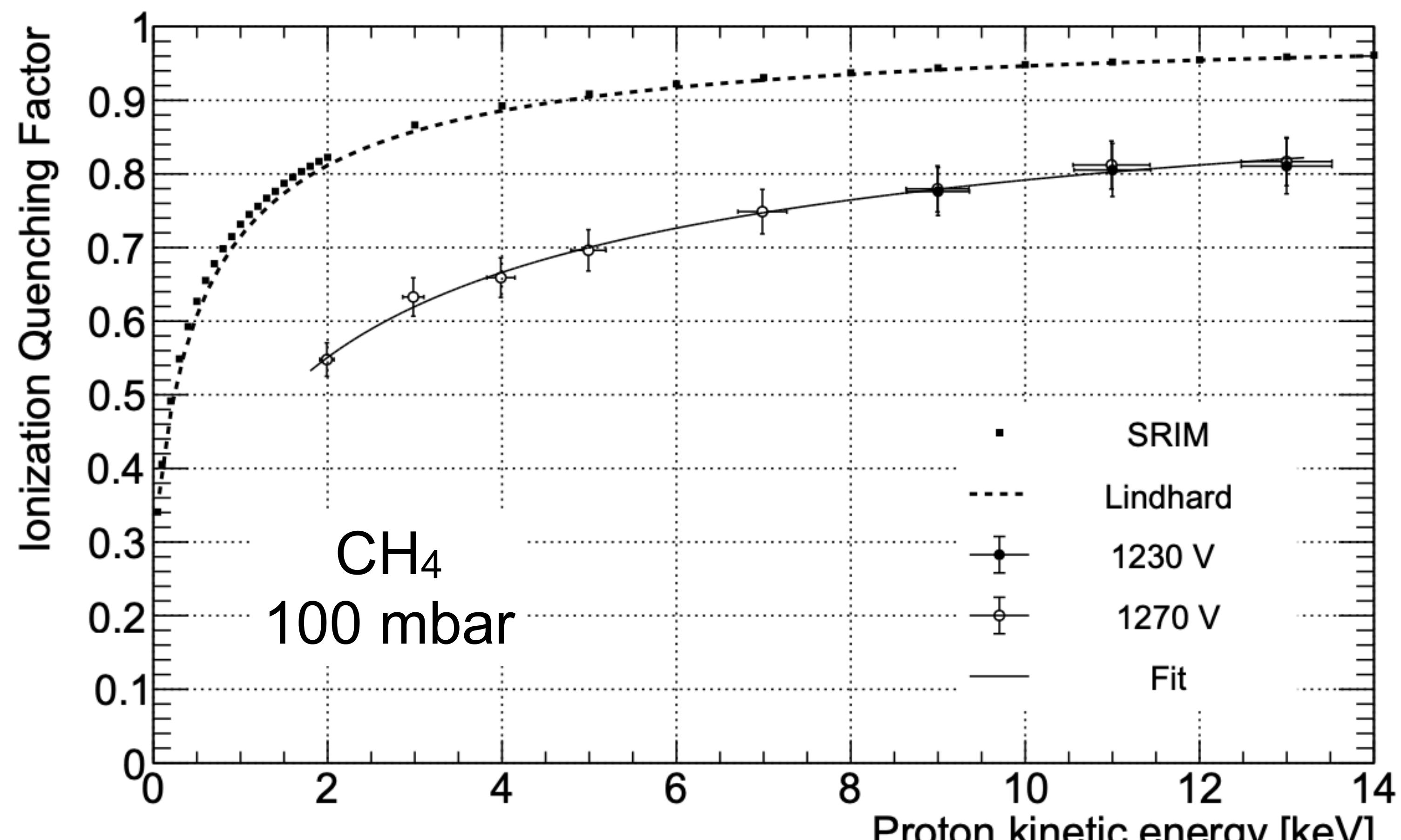

arXiv:2201.09566

Quenching factor: W-value measurements

- Quenching factor intimately connected to W-value
  - W-value is the average energy required to liberate an e-ion pair
  - Typically, detector response calibrated with electrons of known energy

$$q_f(E) = \frac{E_{ee}}{E} = \frac{N_i^i \cdot W_e(E)}{E} = \frac{W_e(E)}{W_i(E)}$$

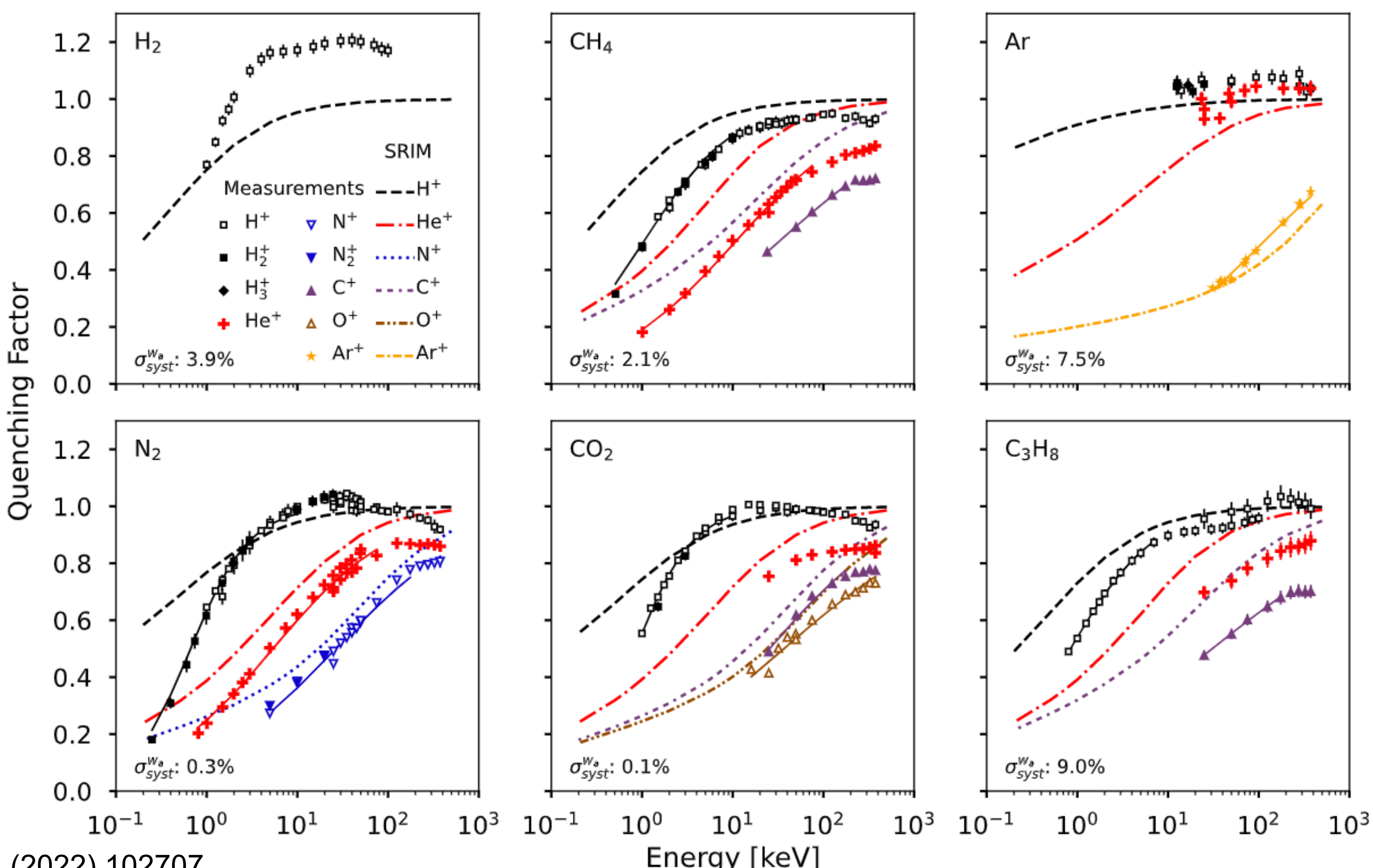

Astropart.Phys. 141 (2022) 102707

In-situ background measurements

Background measurements: neutrons

- **Neutrons: background in DM searches**
  - Identical signature to signal events
  - Few measurements at underground laboratories
    - ^{3}He-based detectors extremely expensive

Background measurements: neutrons

- **Neutrons: background in DM searches**
  - Identical signature to signal events
  - Few measurements at underground laboratories
    - ^{3}He-based detectors extremely expensive
- Nitrogen-filled Spherical Proportional Counter
  - $^{14}N+n \rightarrow ^{14}C+p$ **+** 625 keV
  - $^{14}N+n \rightarrow ^{11}B+\alpha$ **-** 159 keV

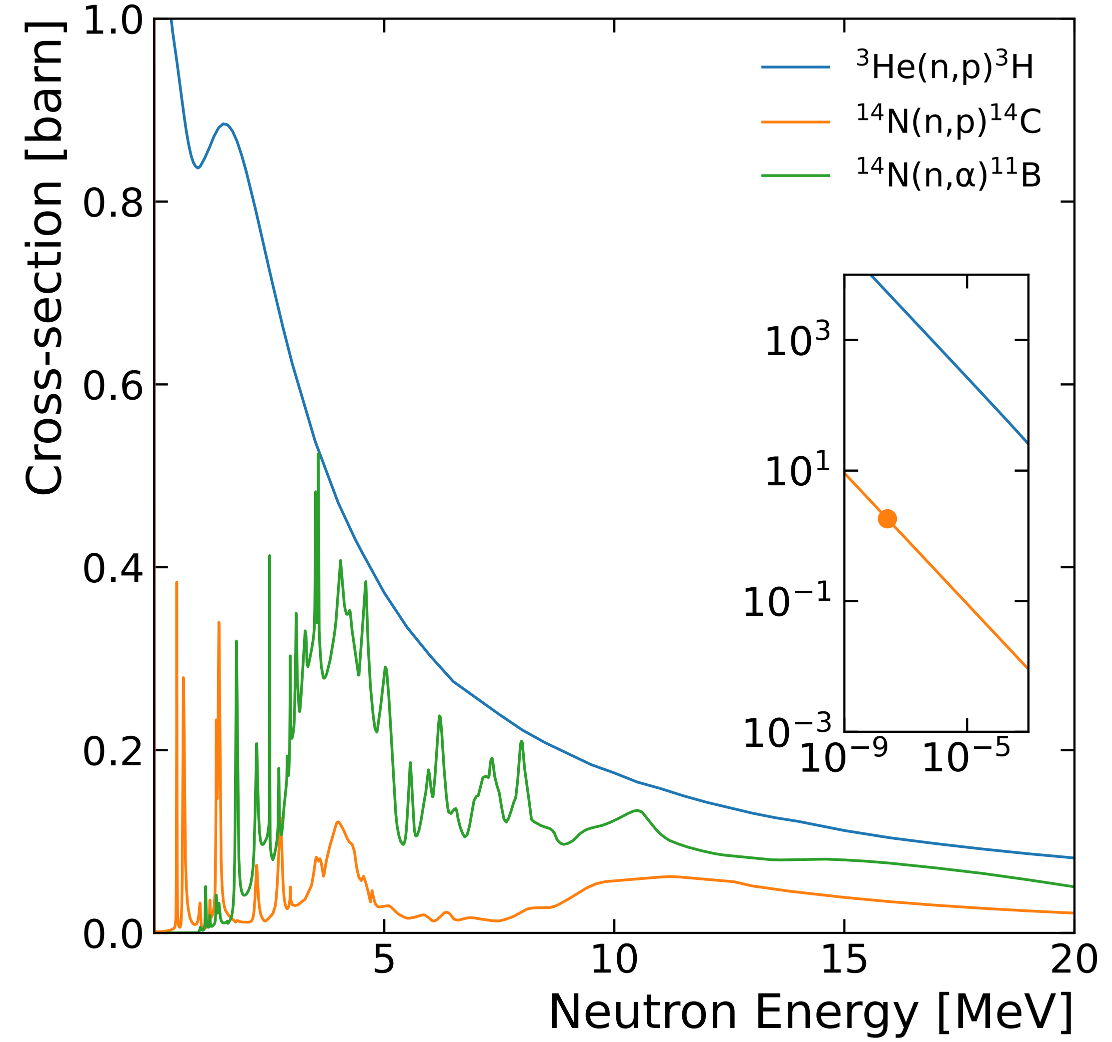

Background measurements: neutrons

- **Neutrons: background in DM searches**
  - Identical signature to signal events
  - Few measurements at underground laboratories
    - ^{3}He-based detectors extremely expensive
- Nitrogen-filled Spherical Proportional Counter
  - $^{14}N + n \rightarrow {}^{14}C + p$ + 625 keV
  - $^{14}N + n \rightarrow {}^{11}B + \alpha$ - 159 keV
- Initial demonstration: NIM A847 (2017) 10
  - ^{252}Cf, ^{241}Am^{9}Be, ambient fast neutrons
  - Thermal neutrons
  - Operation at 0.2-0.5 bar → HV at 6 kV

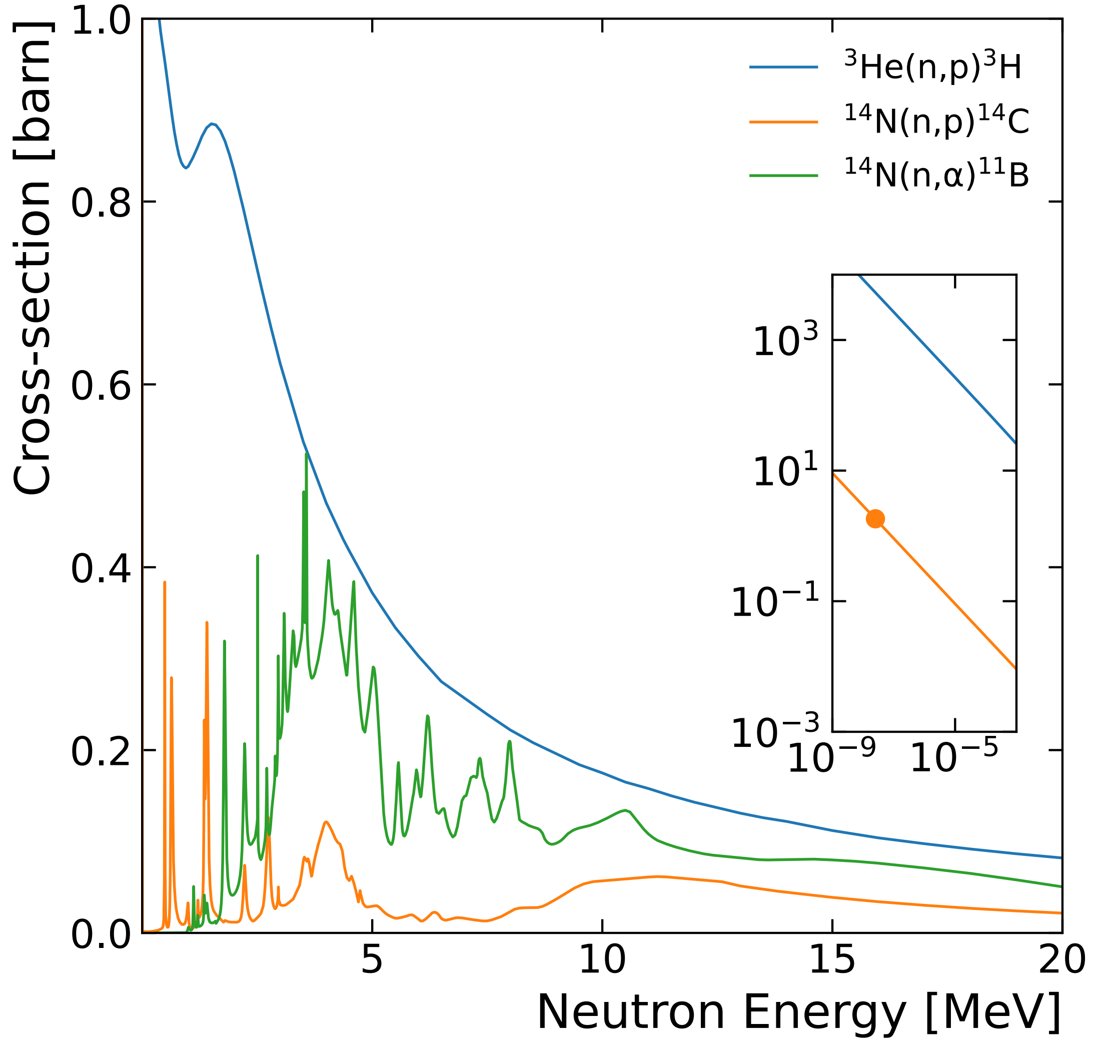

Background measurements: neutrons

- **Neutrons: background in DM searches**
  - Identical signature to signal events
  - Few measurements at underground laboratories
    - ^{3}He-based detectors extremely expensive
- Nitrogen-filled Spherical Proportional Counter
  - $^{14}N+n \rightarrow {}^{14}C+p$ **+** 625 keV
  - $^{14}N+n \rightarrow {}^{11}B+\alpha$ **-** 159 keV
- Initial demonstration: NIM A847 (2017) 10
  - ^{252}Cf, $^{241}Am^{9}Be$, ambient fast neutrons
  - Thermal neutrons
  - Operation at 0.2-0.5 bar → HV at 6 kV

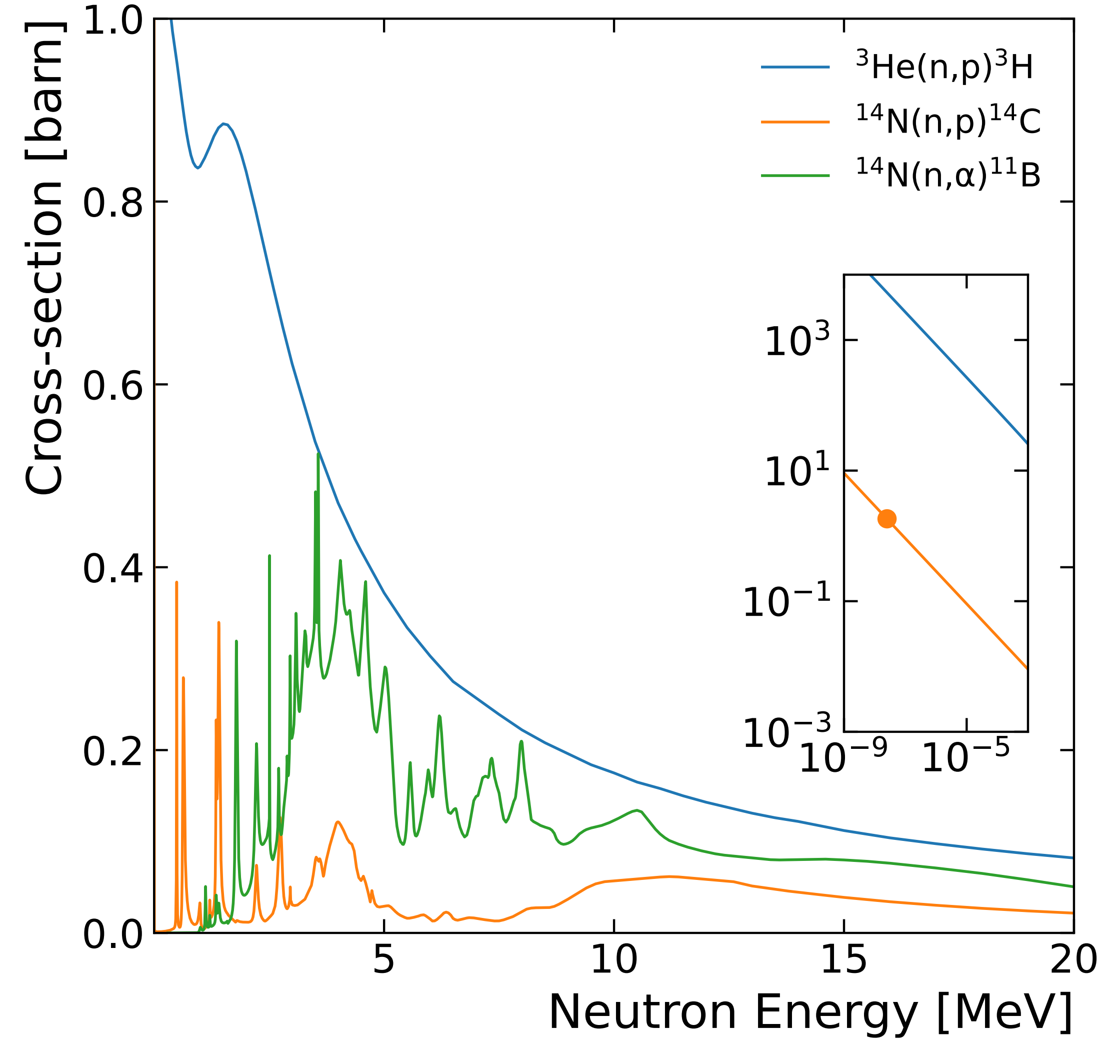

- **Limiting Factors:**
  - Low pressure operation → Wall effect
  - Sparking/Stability → Gas gain
  - Impurities
  - Charge collection efficiency

Progress in all fronts!

Background measurements: neutrons

- **Neutrons: background in DM searches**
  - Identical signature to signal events
  - Few measurements at underground laboratories
    - ^{3}He-based detectors extremely expensive
- Nitrogen-filled Spherical Proportional Counter
  - $^{14}N+n \rightarrow {}^{14}C+p$ + 625 keV
  - $^{14}N+n \rightarrow {}^{11}B+\alpha$ - 159 keV
- Initial demonstration: NIM A847 (2017) 10
  - ^{252}Cf, ^{241}Am^{9}Be, ambient fast neutrons
  - Thermal neutrons
  - Operation at 0.2-0.5 bar → HV at 6 kV

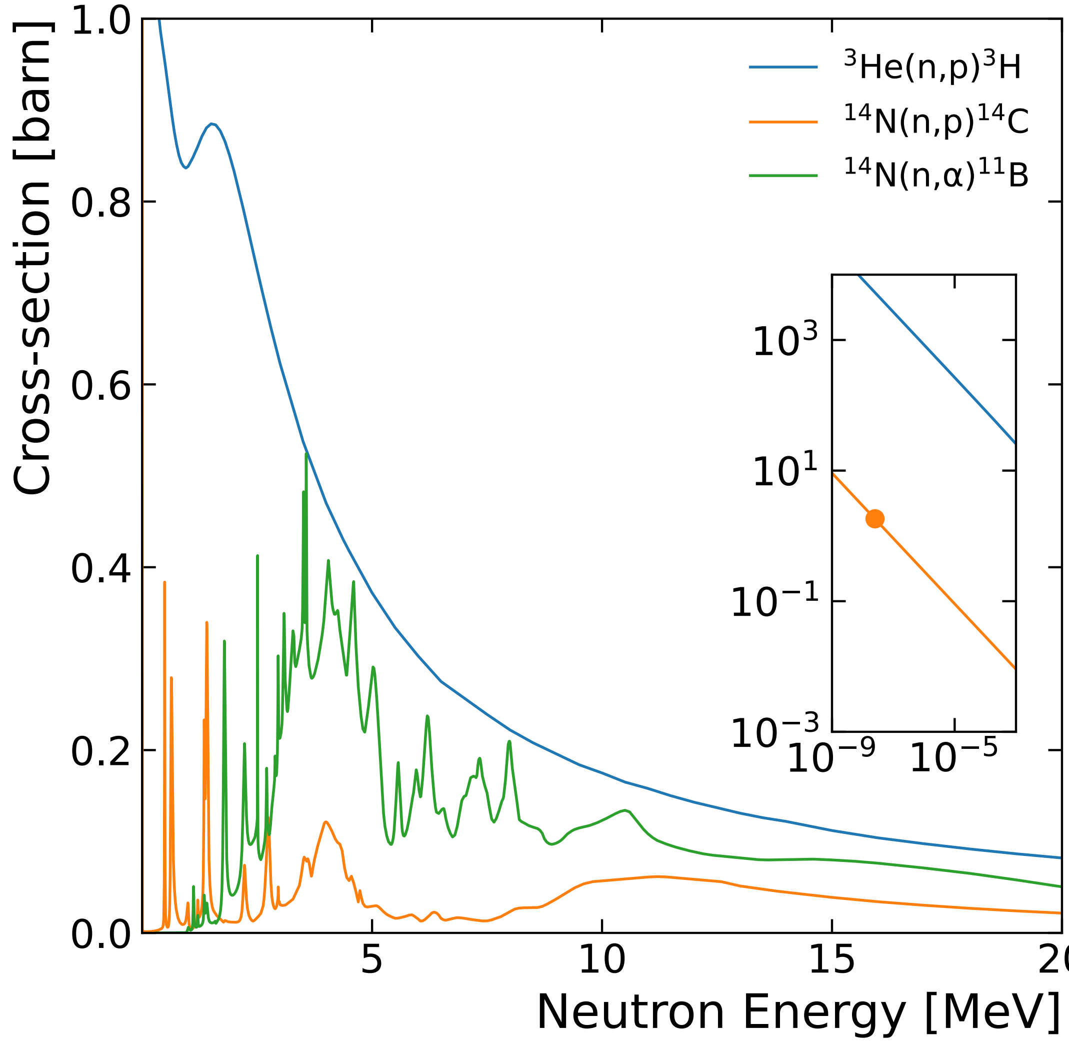

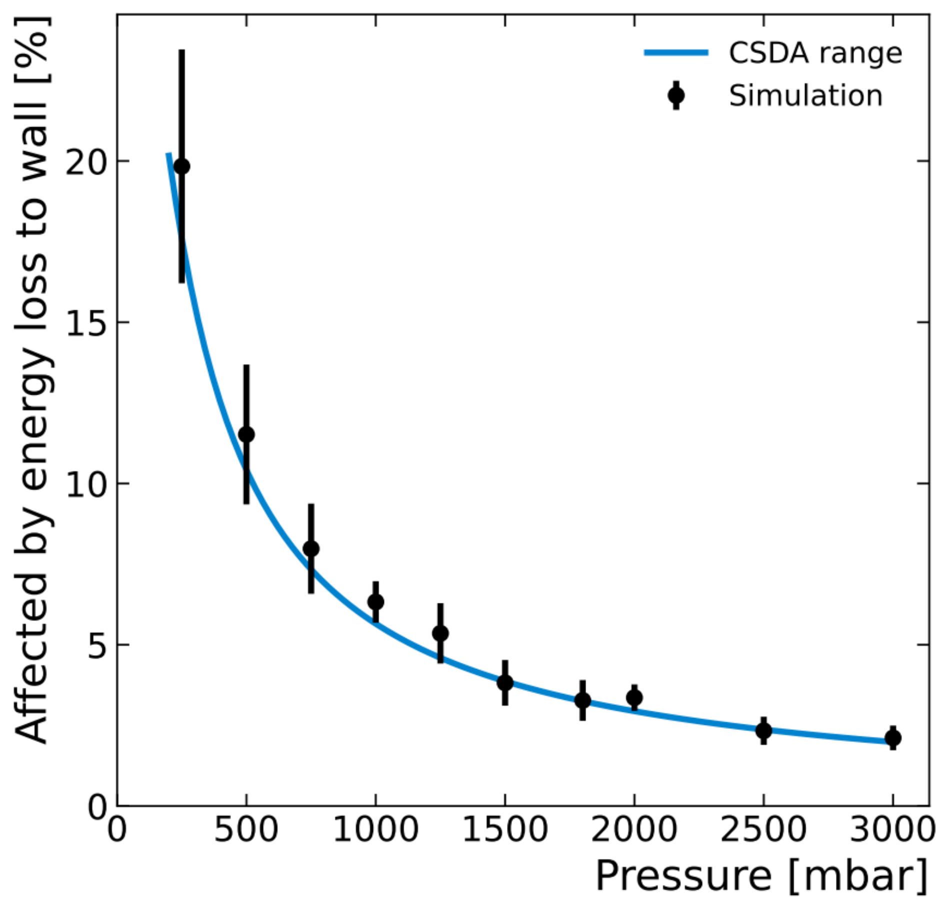

- **Limiting Factors:**
  - Low pressure operation ⟶ Wall effect
  - Sparking/Stability ⟶ Gas gain
  - Impurities
  - Charge collection efficiency

Progress in all fronts!

Simulation of neutron transport

Neutron Beam
0.025 eV

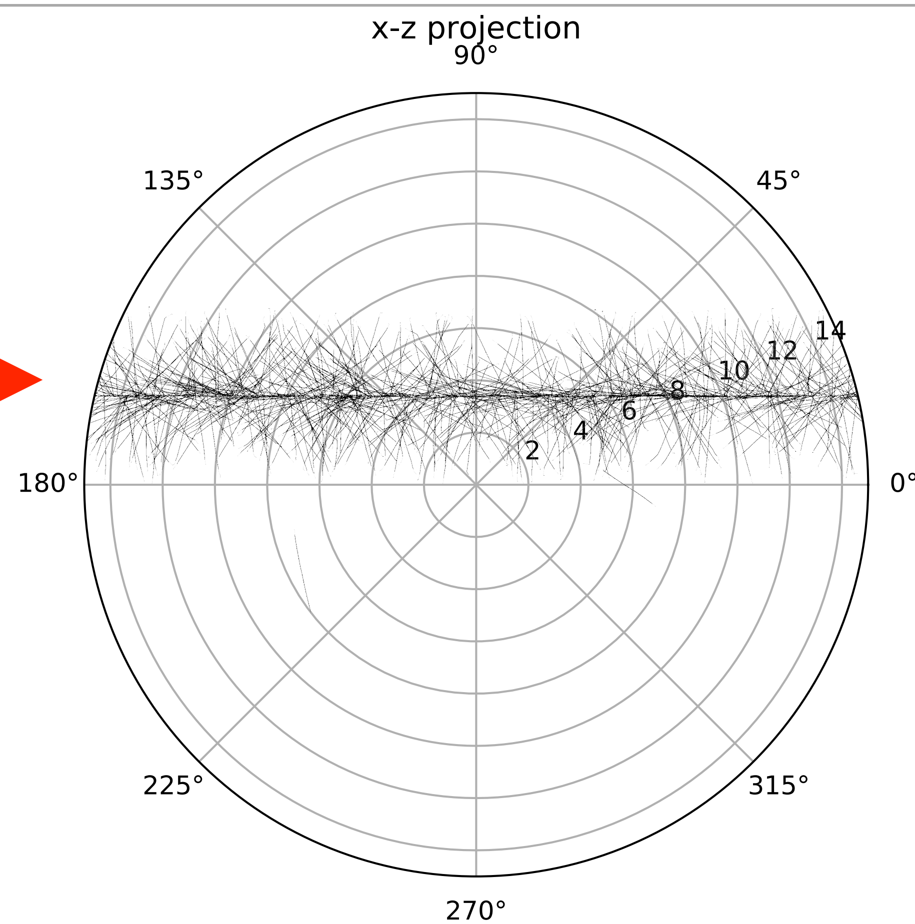

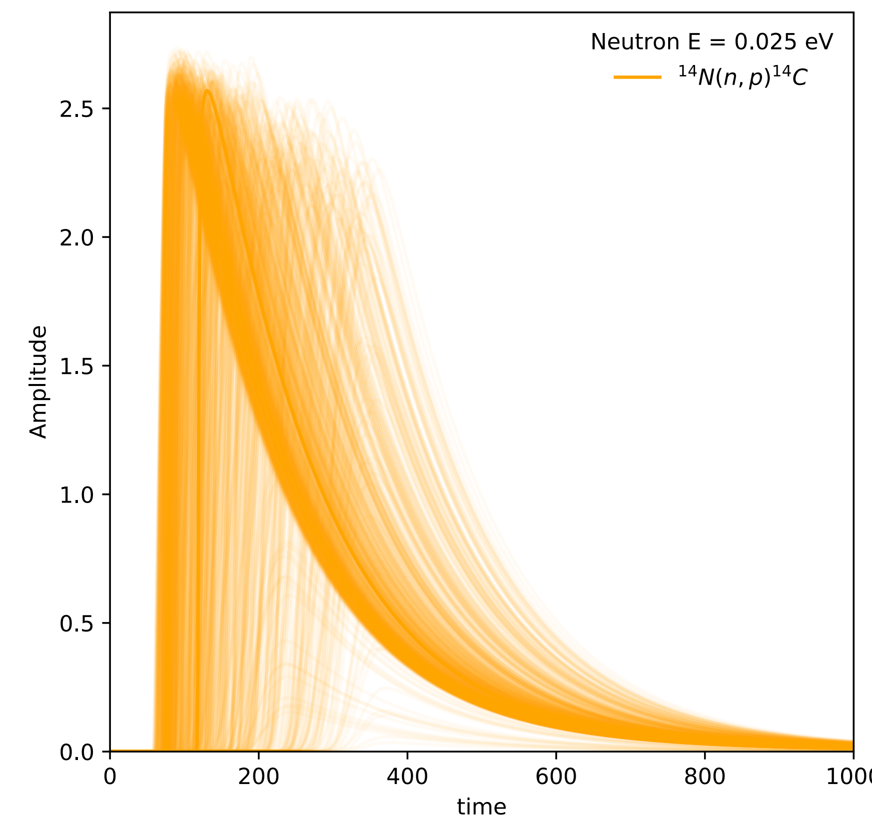

Parameters

Ø30cm vessel

N_2 at 300mbar

Ø2mm anode

Neutron Beam
4 MeV

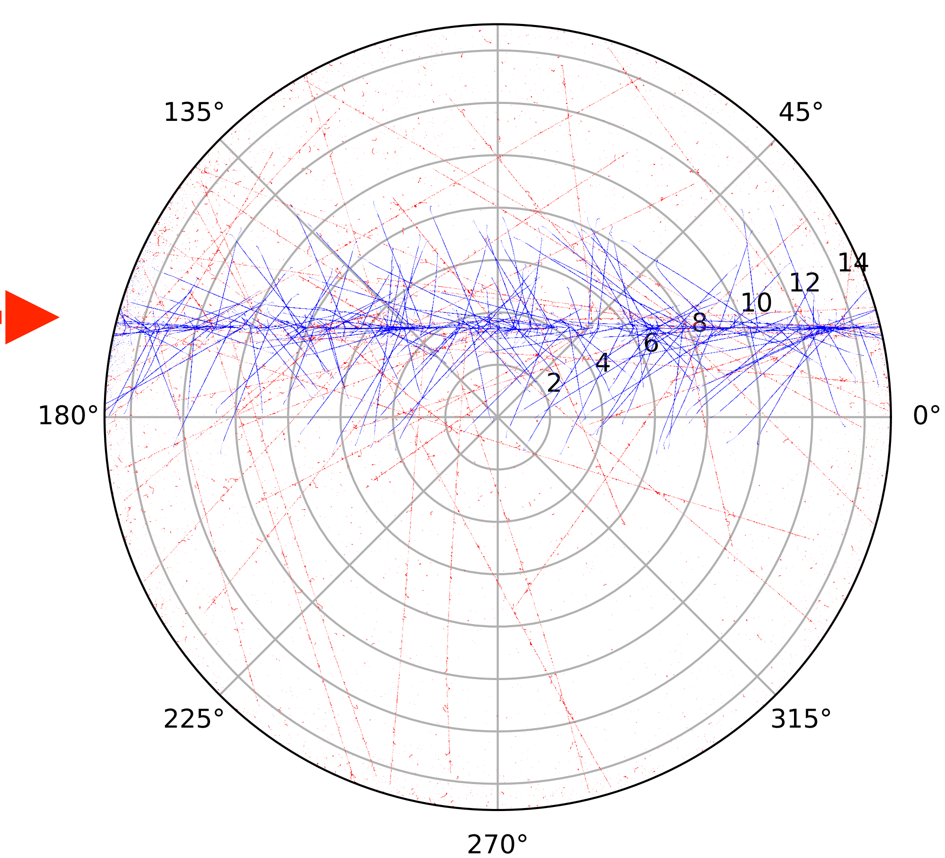

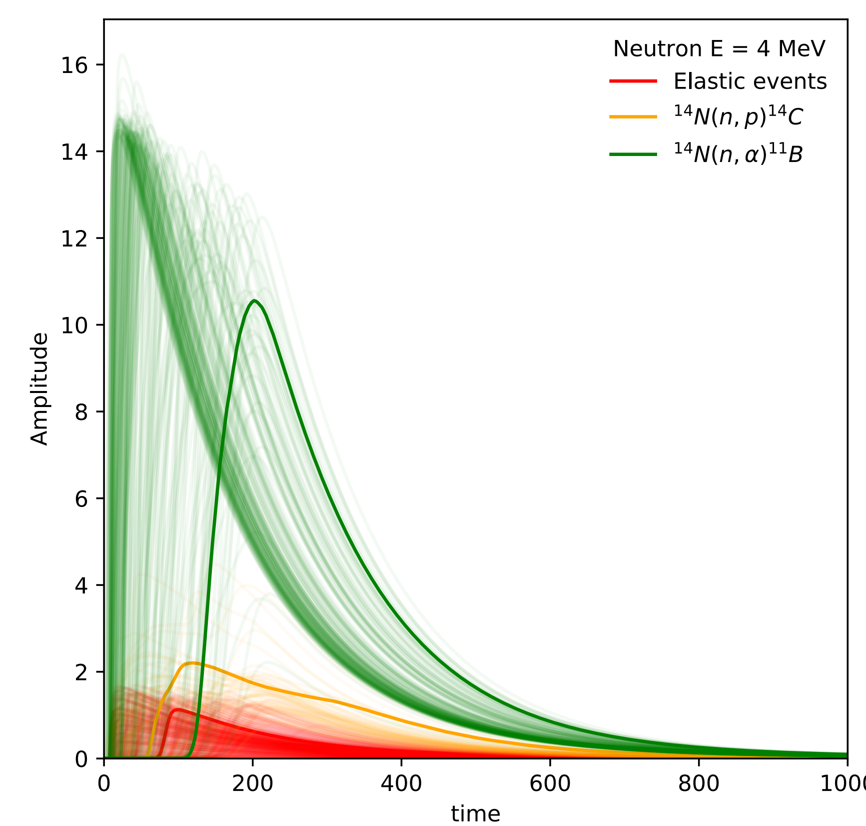

In-situ neutron measurements

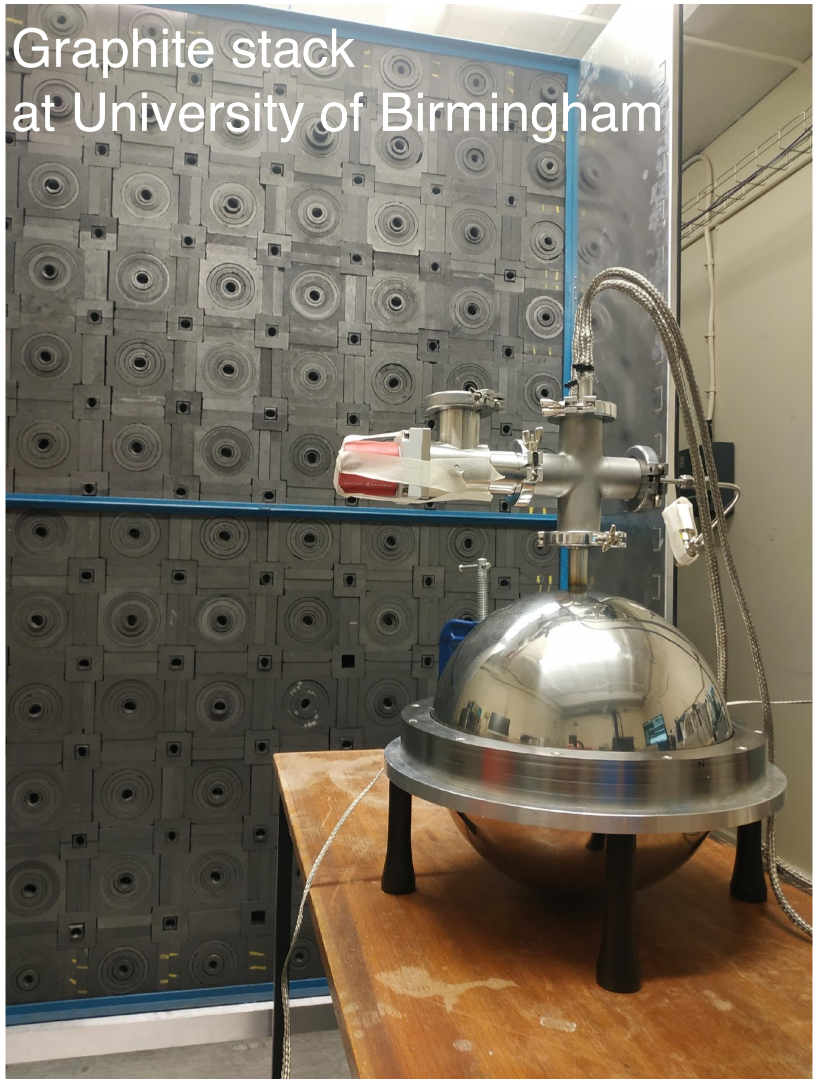

- Nitrogen-filled SPC
  - ∅ 30 cm
- Multi-anode sensor
  - 11 anodes, ∅ 1mm
  - “Near” - “Far” read-out

In-situ neutron measurements

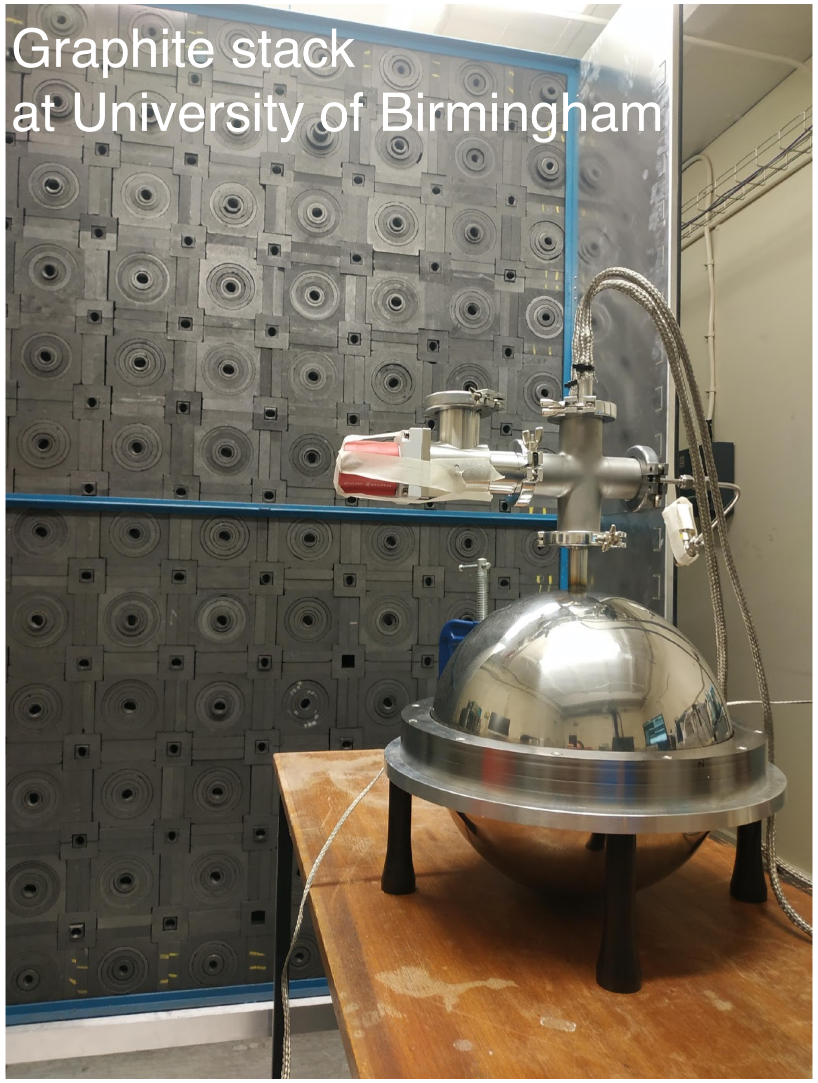

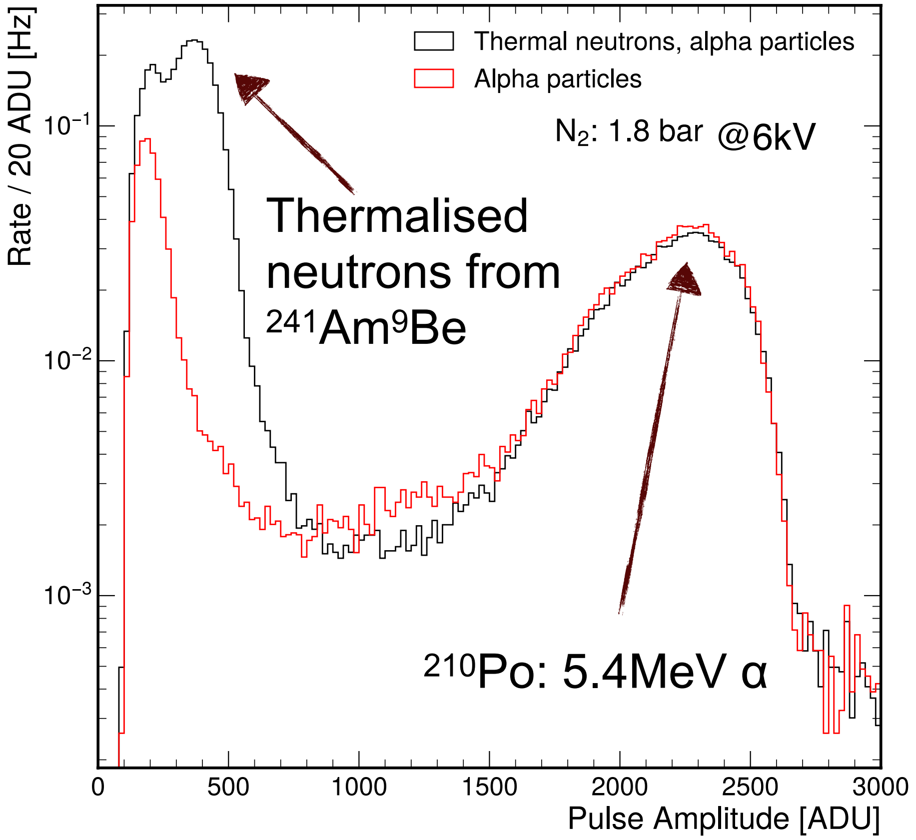

- Nitrogen-filled SPC
  - ∅ 30 cm
- Multi-anode sensor
  - 11 anodes, ∅ 1mm
  - “Near” - “Far” read-out

In-situ neutron measurements

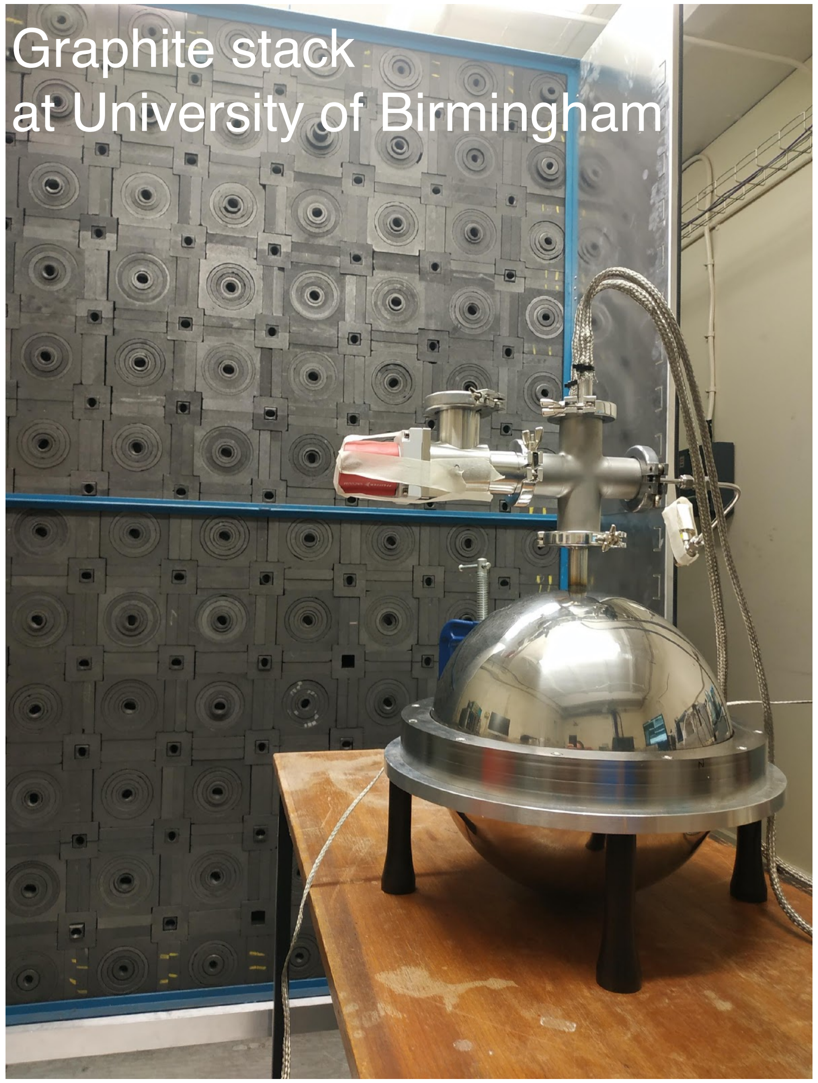

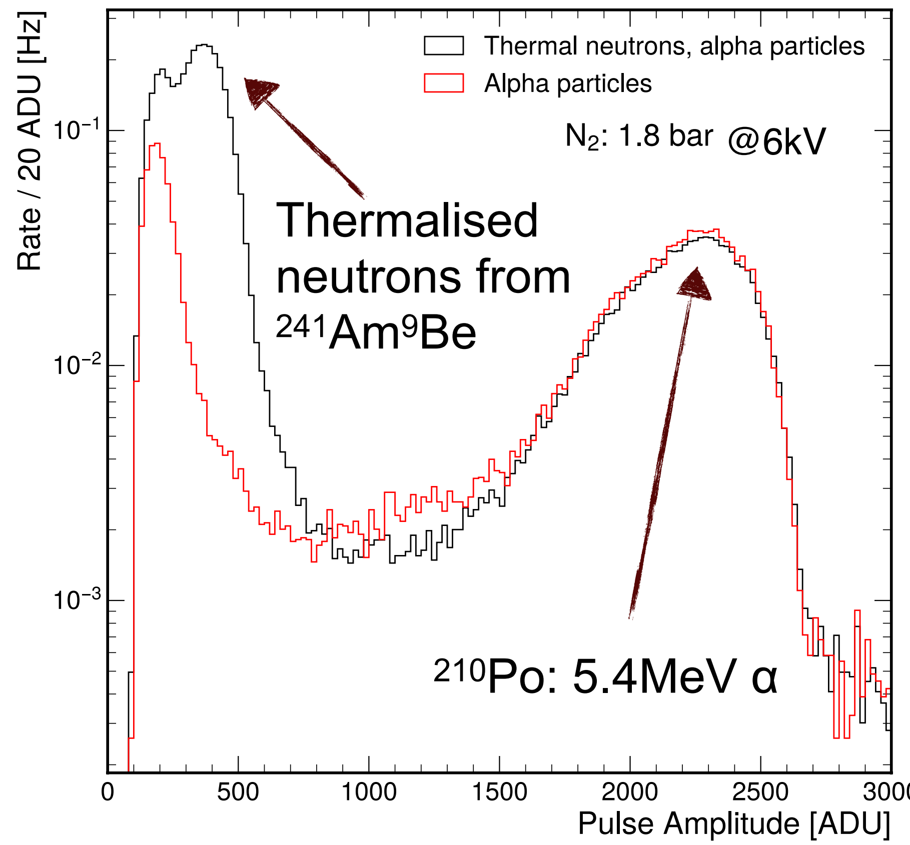

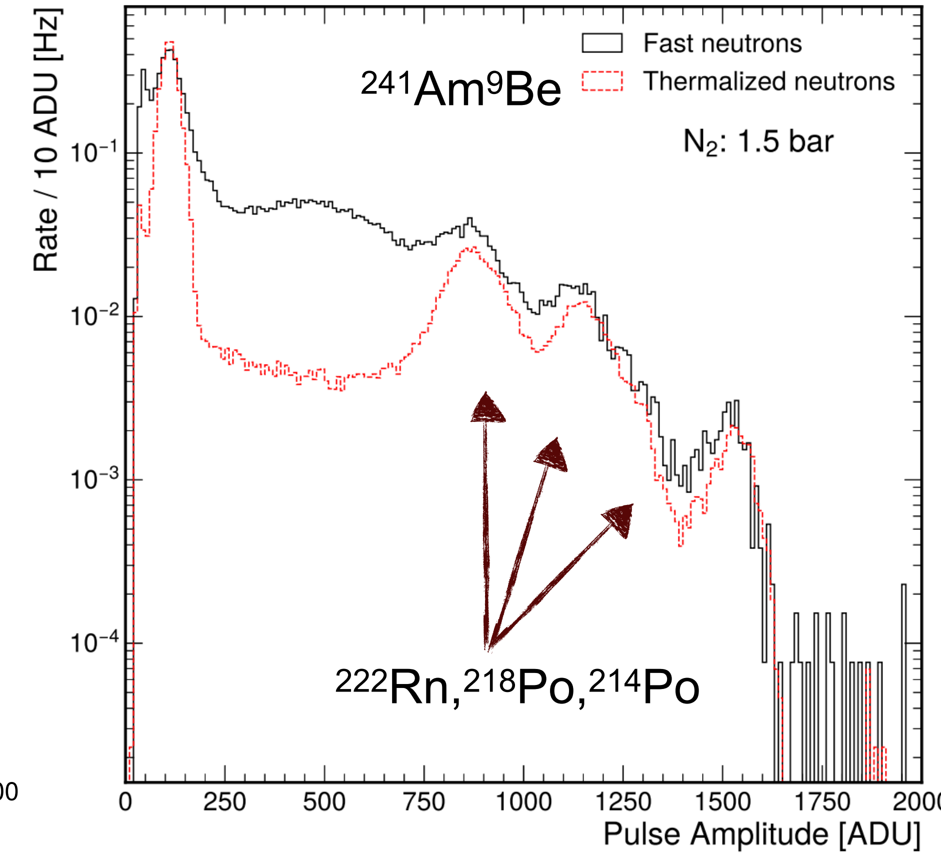

- Nitrogen-filled SPC
  - ∅ 30 cm
- Multi-anode sensor
  - 11 anodes, ∅ 1mm
  - “Near” - “Far” read-out

In-situ neutron measurements

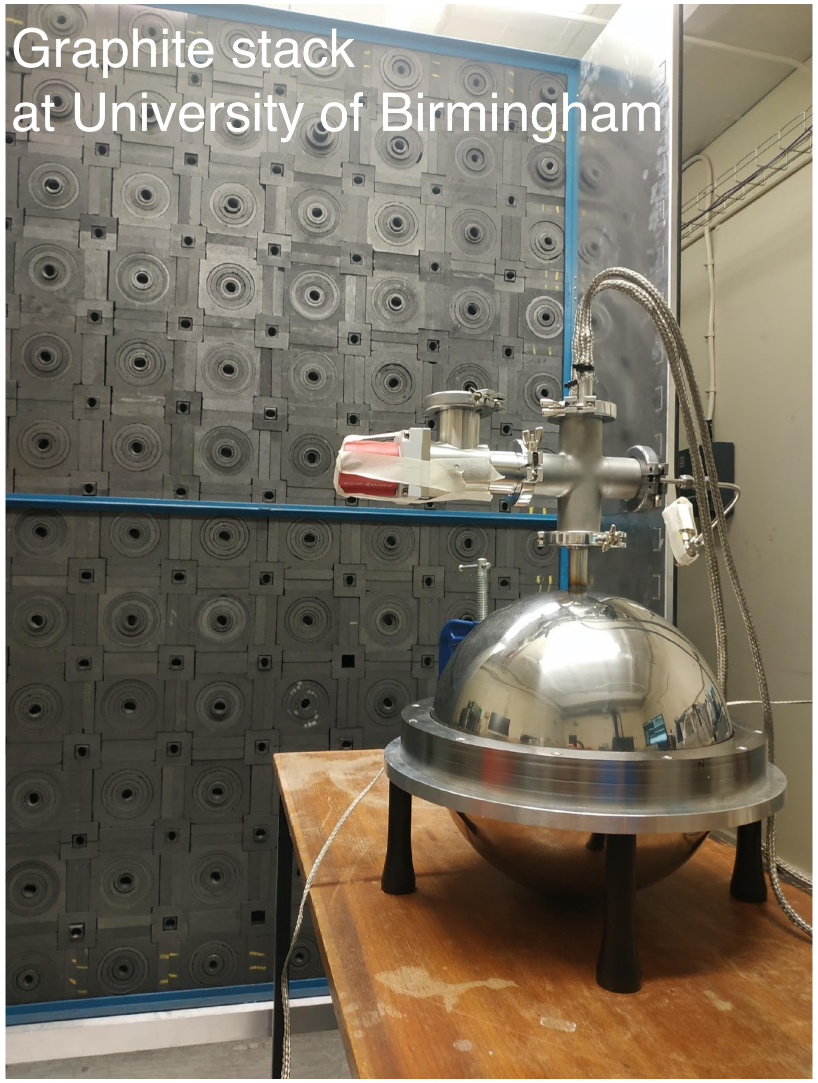

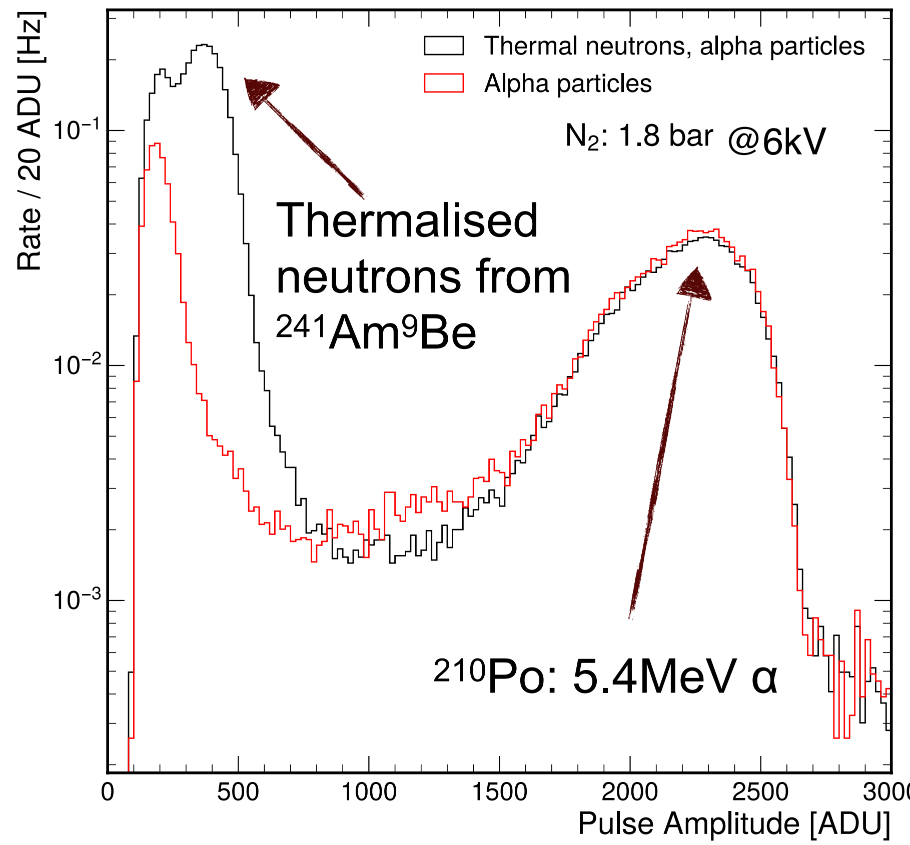

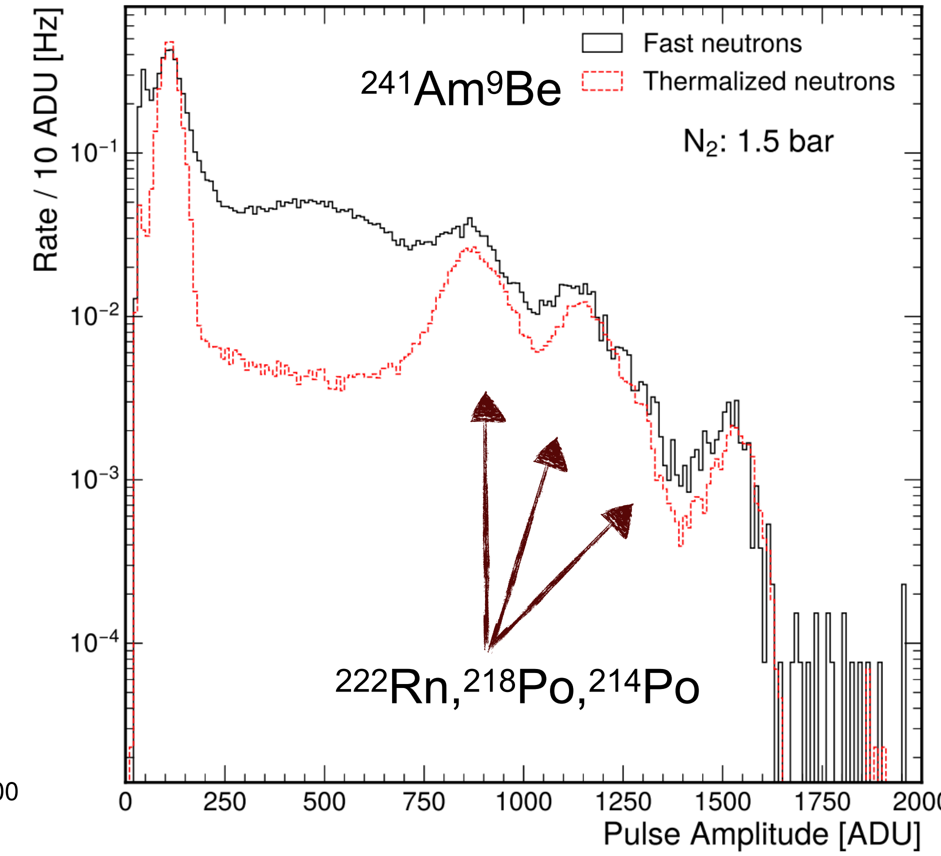

- Nitrogen-filled SPC
  - ∅ 30 cm
- Multi-anode sensor
  - 11 anodes, ∅ 1mm
  - “Near” - “Far” read-out

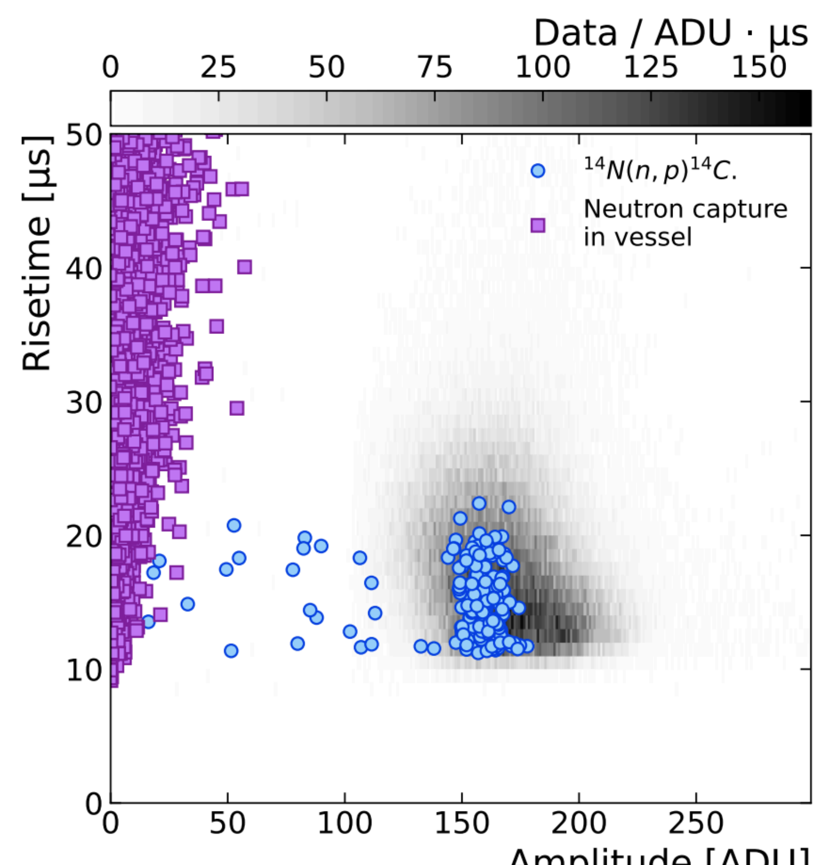

In-situ neutron measurements

UNIVERSITY OF BIRMINGHAM | CYCLOTRON FACILITY

- Deuterium beam on ^{9}Be
  - 5.90±0.08 MeV deuterons
  - $^{9}Be(d,n)^{10}B$ reaction
  - Moderators used to study neutron detection

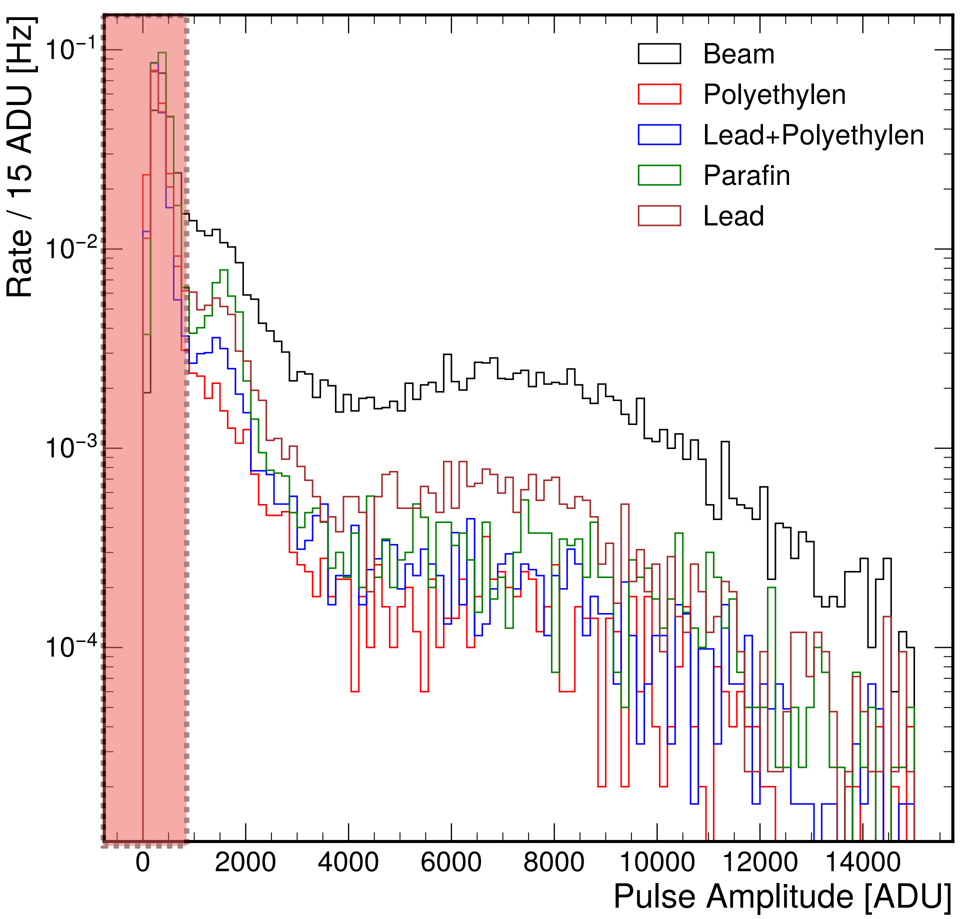

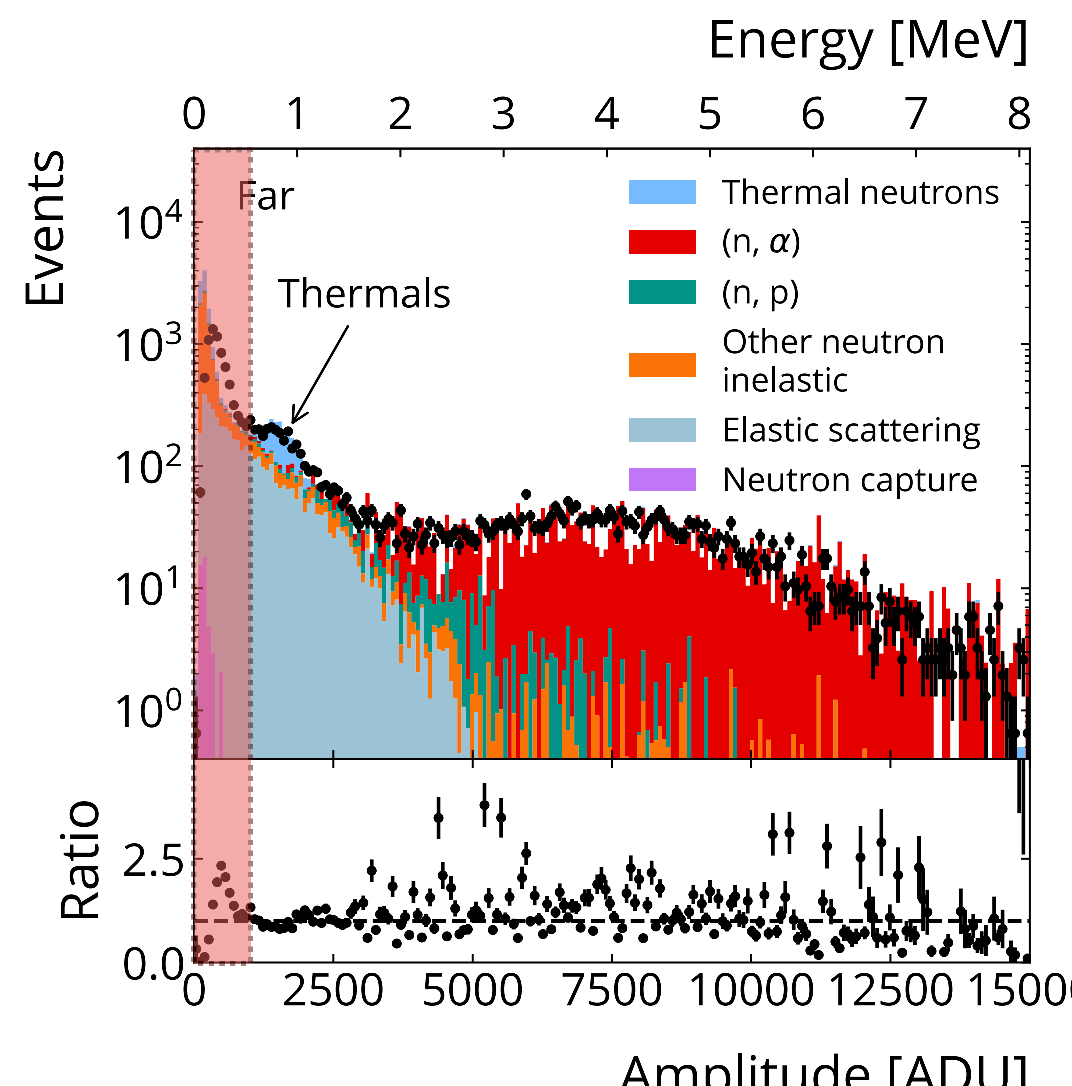

Reducing Backgrounds

Higher purity materials

- **Copper common material for rare event experiments**
  - Strong enough to build gas vessels
  - No long-lived isotopes (^{67}Cu $t_{1/2}$=62h)
  - Low cost/commercially available at high purity
- **Backgrounds**
  - Cosmogenic: ^{63}Cu(n,α)^{60}Co from fast neutrons
  - Contaminants: ^{238}U/^{232}Th decay chains

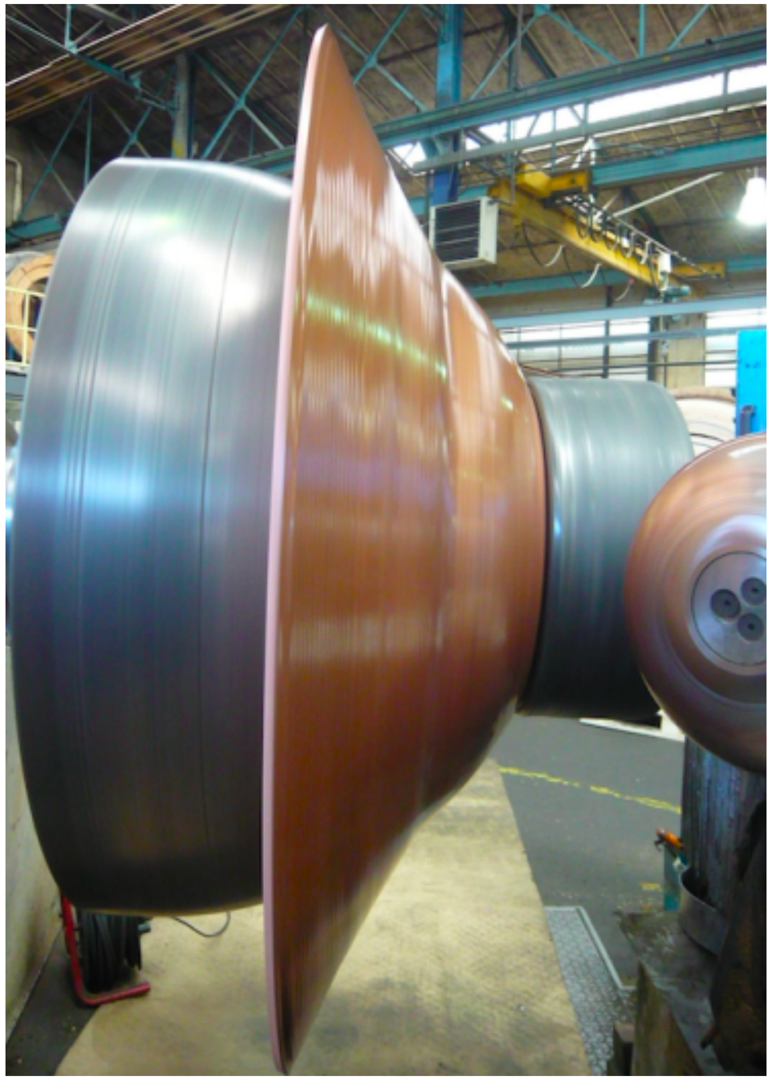

4N Aurubis AG Oxygen Free Copper (99.99% pure)

- Spun into two hemispheres
- Electron-beam welded together

Higher purity materials

- **Copper common material for rare event experiments**
  - Strong enough to build gas vessels
  - No long-lived isotopes (^{67}Cu $t_{1/2}$=62h)
  - Low cost/commercially available at high purity
- **Backgrounds**
  - Cosmogenic: ^{63}Cu(n,α)^{60}Co from fast neutrons
  - Contaminants: ^{238}U/^{232}Th decay chains

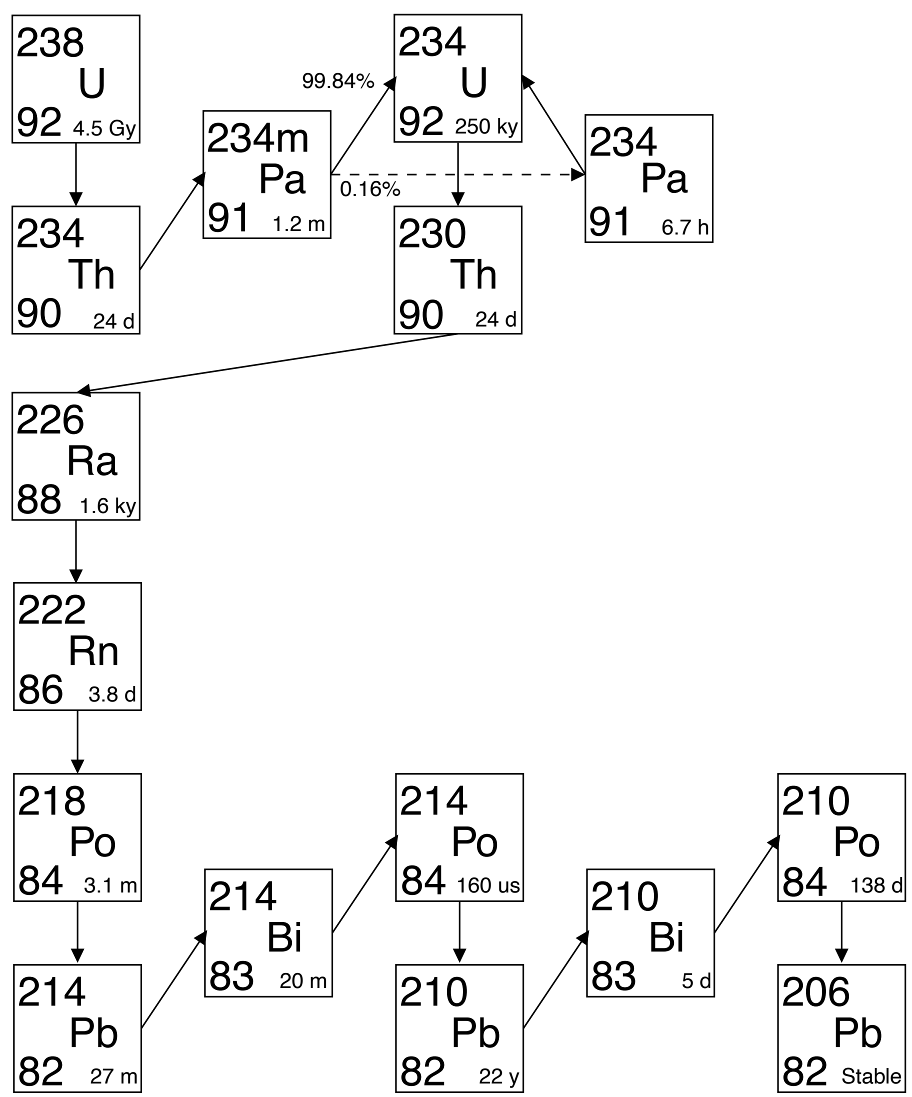

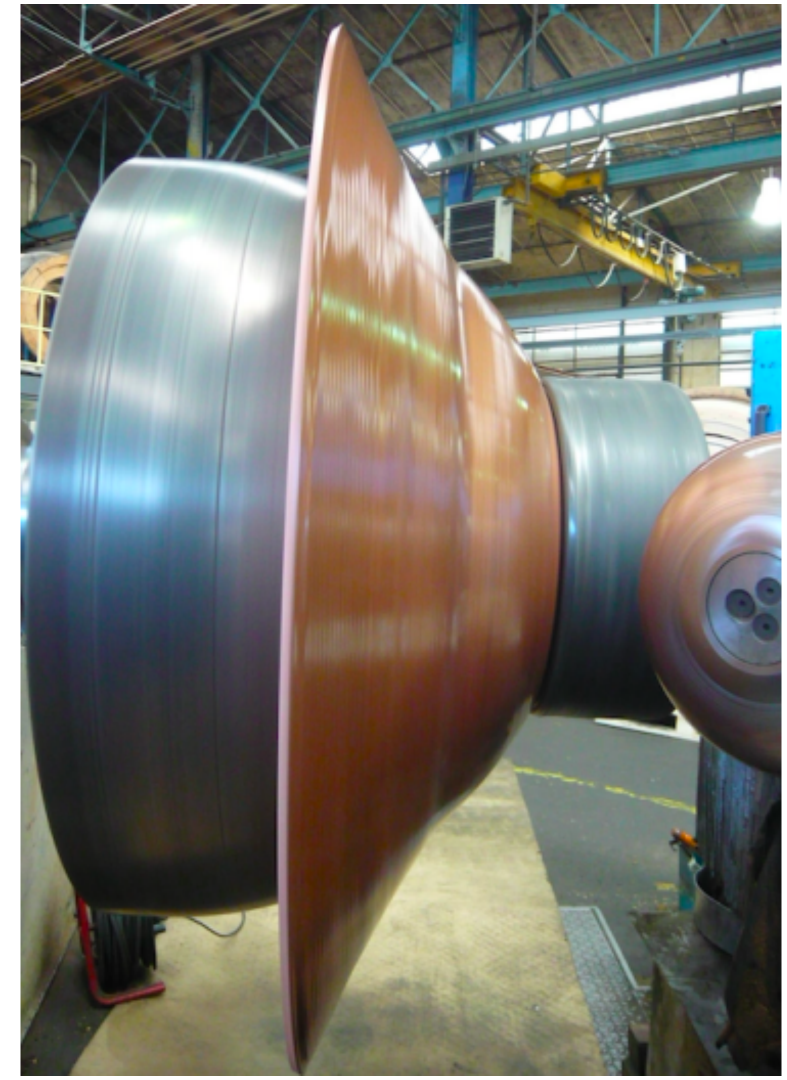

4N Aurubis AG Oxygen Free Copper (99.99% pure)

- Spun into two hemispheres
- Electron-beam welded together

Higher purity materials

- **Copper common material for rare event experiments**
  - Strong enough to build gas vessels
  - No long-lived isotopes (^{67}Cu $t_{1/2}$=62h)
  - Low cost/commercially available at high purity
- **Backgrounds**
  - Cosmogenic: $^{63}Cu(n,\alpha)^{60}Co$ from fast neutrons
  - Contaminants: $^{238}U/^{232}Th$ decay chains

directly measured with mass spectrometers ~10 μBq/kg

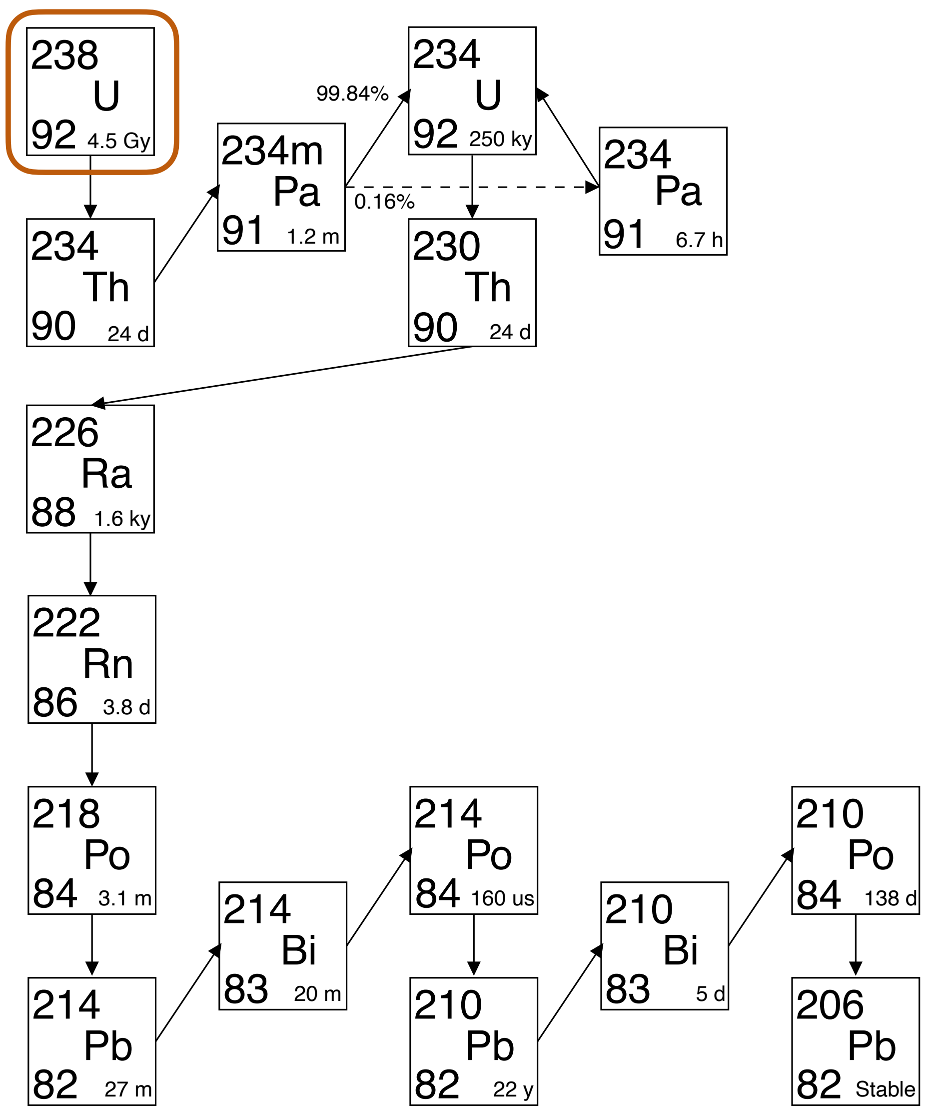

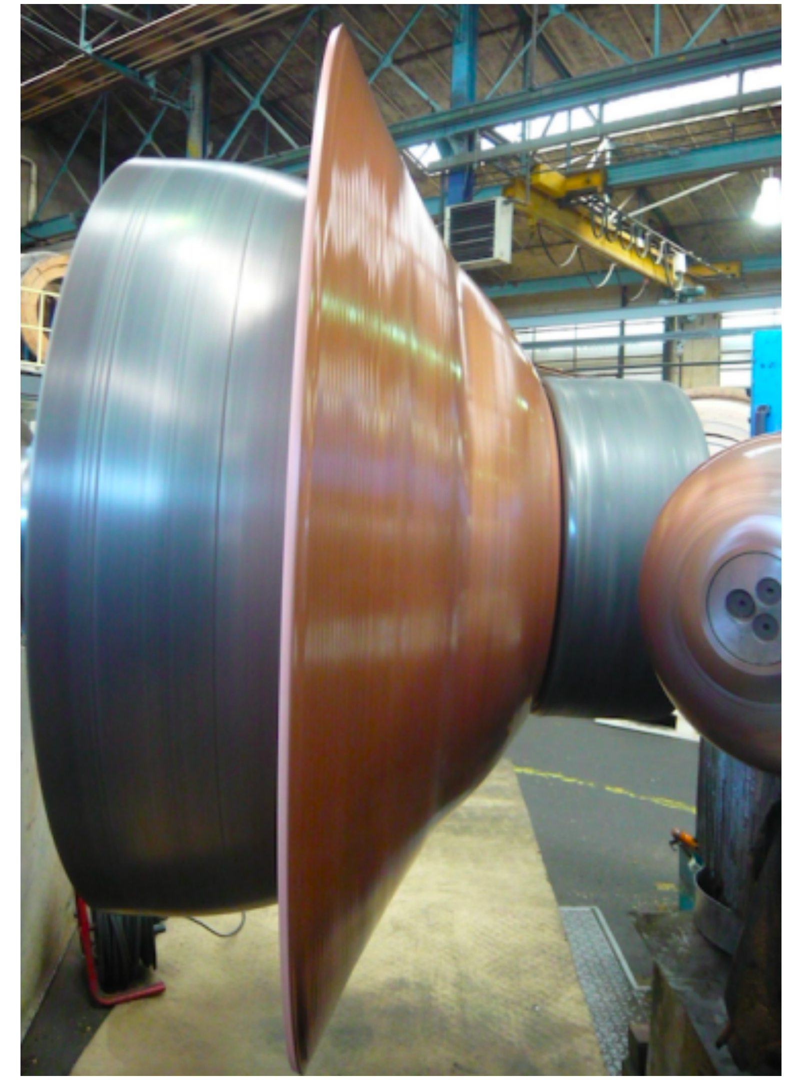

4N Aurubis AG Oxygen Free Copper (99.99% pure)

- Spun into two hemispheres
- Electron-beam welded together

Higher purity materials

- **Copper common material for rare event experiments**
  - Strong enough to build gas vessels
  - No long-lived isotopes (^{67}Cu $t_{1/2}$=62h)
  - Low cost/commercially available at high purity
- **Backgrounds**
  - Cosmogenic: $^{63}Cu(n,\alpha)^{60}Co$ from fast neutrons
  - Contaminants: $^{238}U/^{232}Th$ decay chains

directly measured with mass spectrometers ~10 µBq/kg

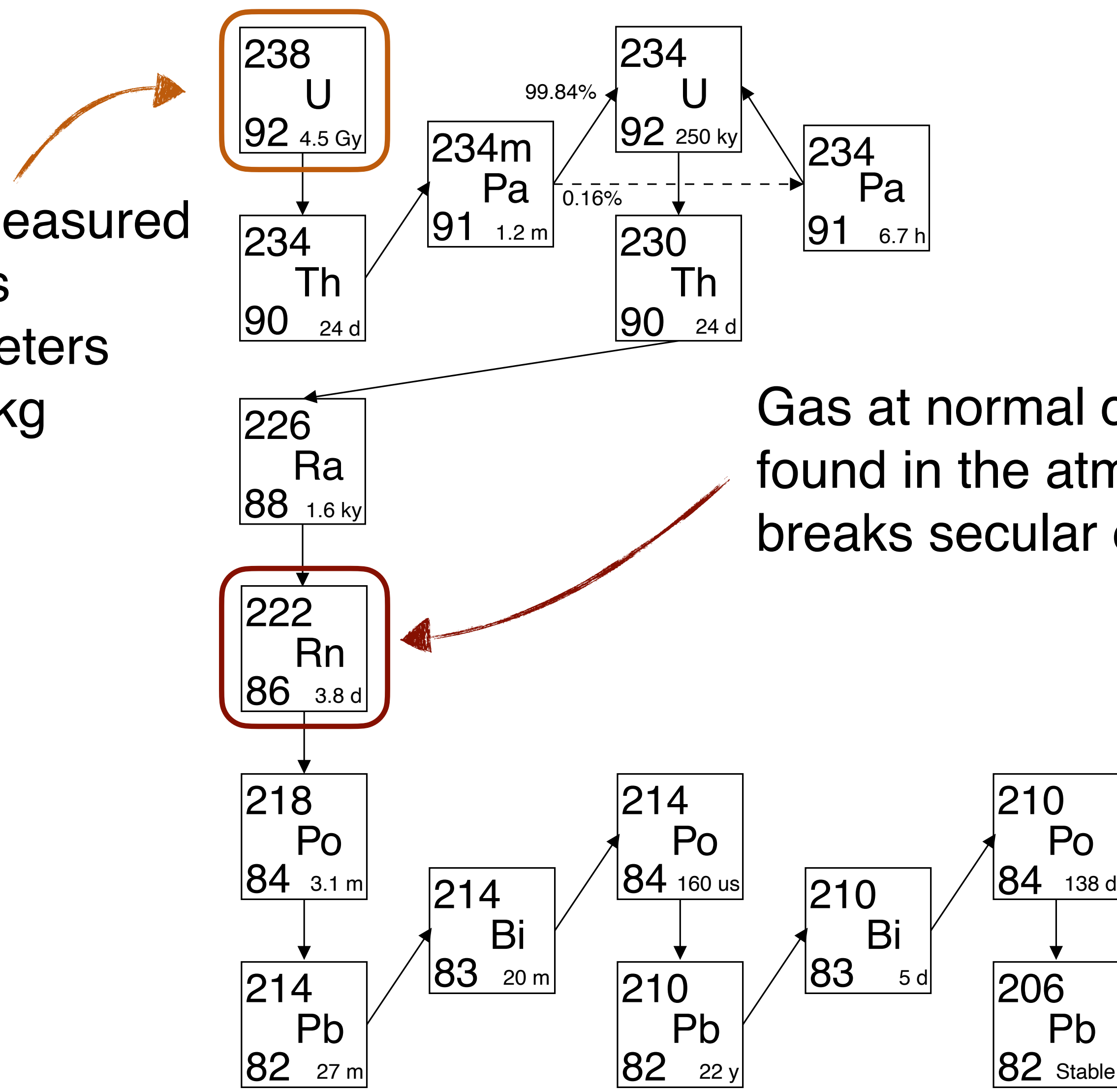

Gas at normal conditions: found in the atmosphere breaks secular equilibrium

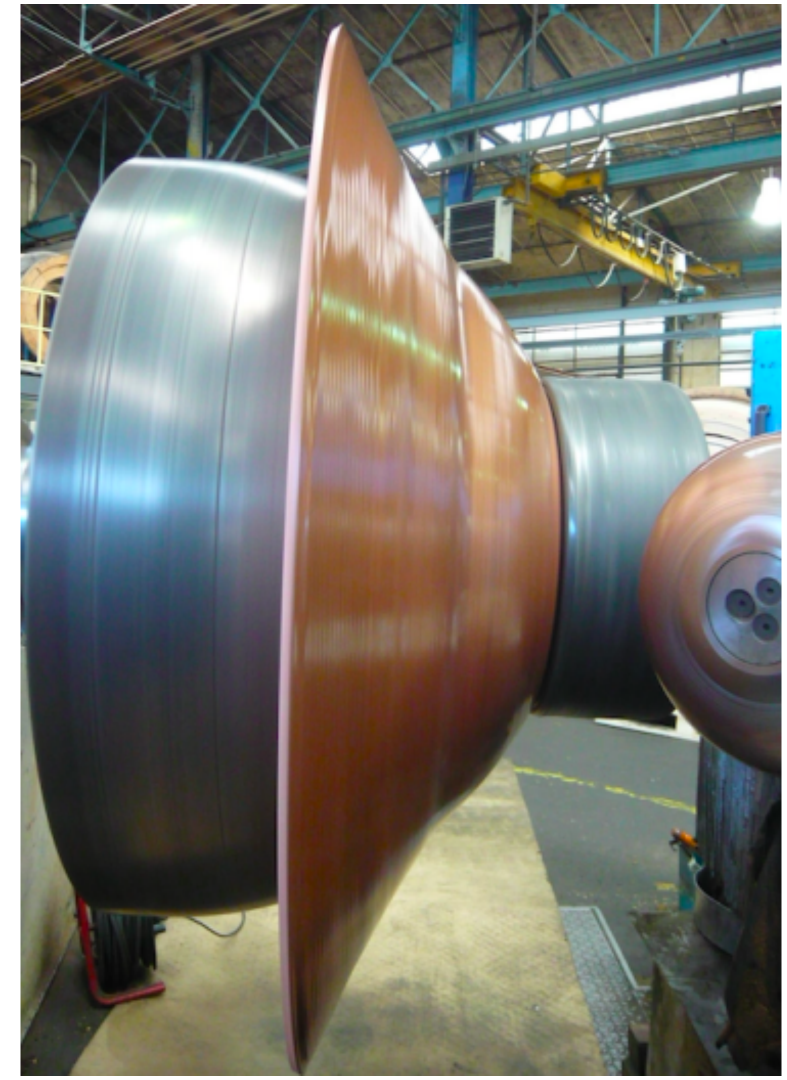

4N Aurubis AG Oxygen Free Copper (99.99% pure)

- Spun into two hemispheres
- Electron-beam welded together

Higher purity materials

- **Copper common material for rare event experiments**
  - Strong enough to build gas vessels
  - No long-lived isotopes (^{67}Cu $t_{1/2}$=62h)
  - Low cost/commercially available at high purity
- **Backgrounds**
  - Cosmogenic: ^{63}Cu(n,α)^{60}Co from fast neutrons
  - Contaminants: ^{238}U/^{232}Th decay chains

directly measured with mass spectrometers ~10 µBq/kg

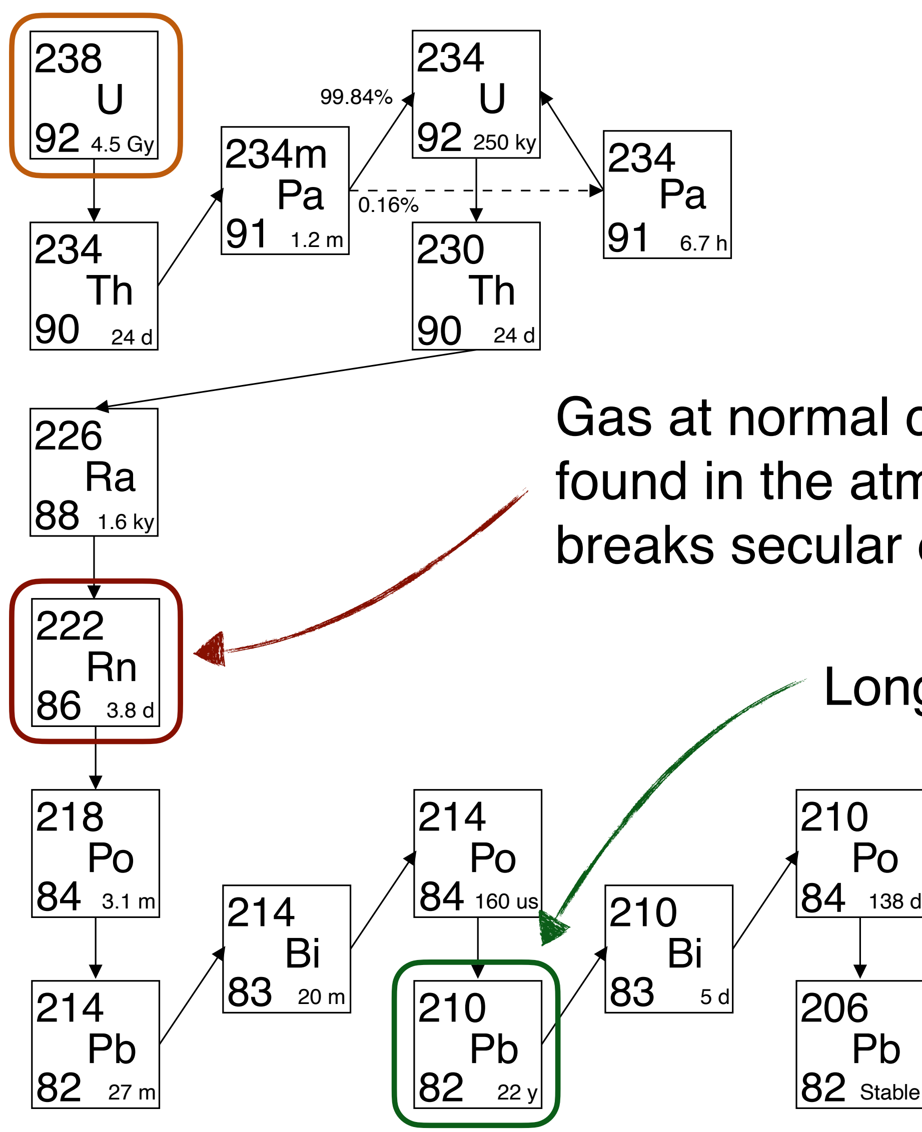

Gas at normal conditions: found in the atmosphere breaks secular equilibrium

Long-lived!

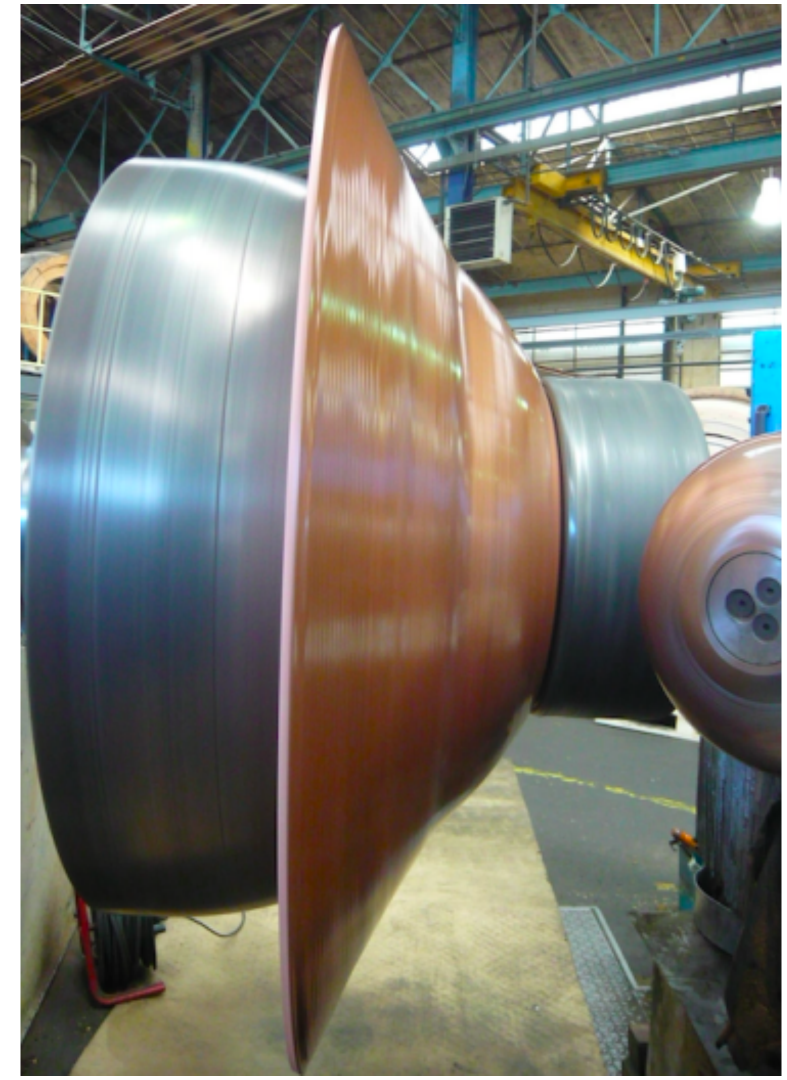

4N Aurubis AG Oxygen Free Copper (99.99% pure)
- Spun into two hemispheres
- Electron-beam welded together

^{210}Pb contamination

Recent development: low background α-particle counting

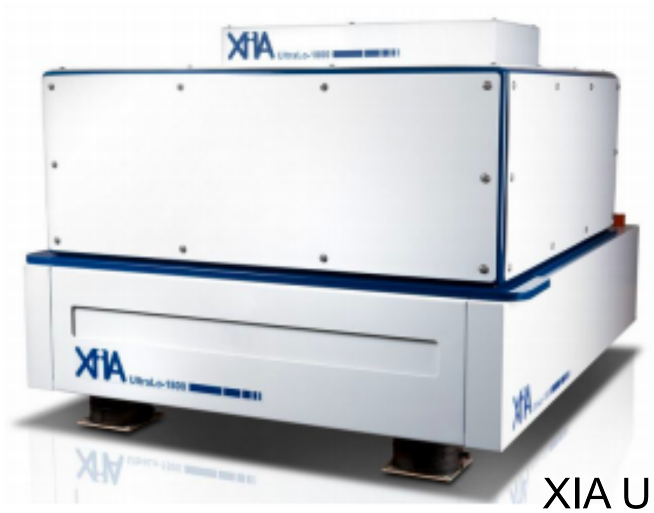

XIA UltraLo-1800
https://www.xia.com/ultralo-theory.html

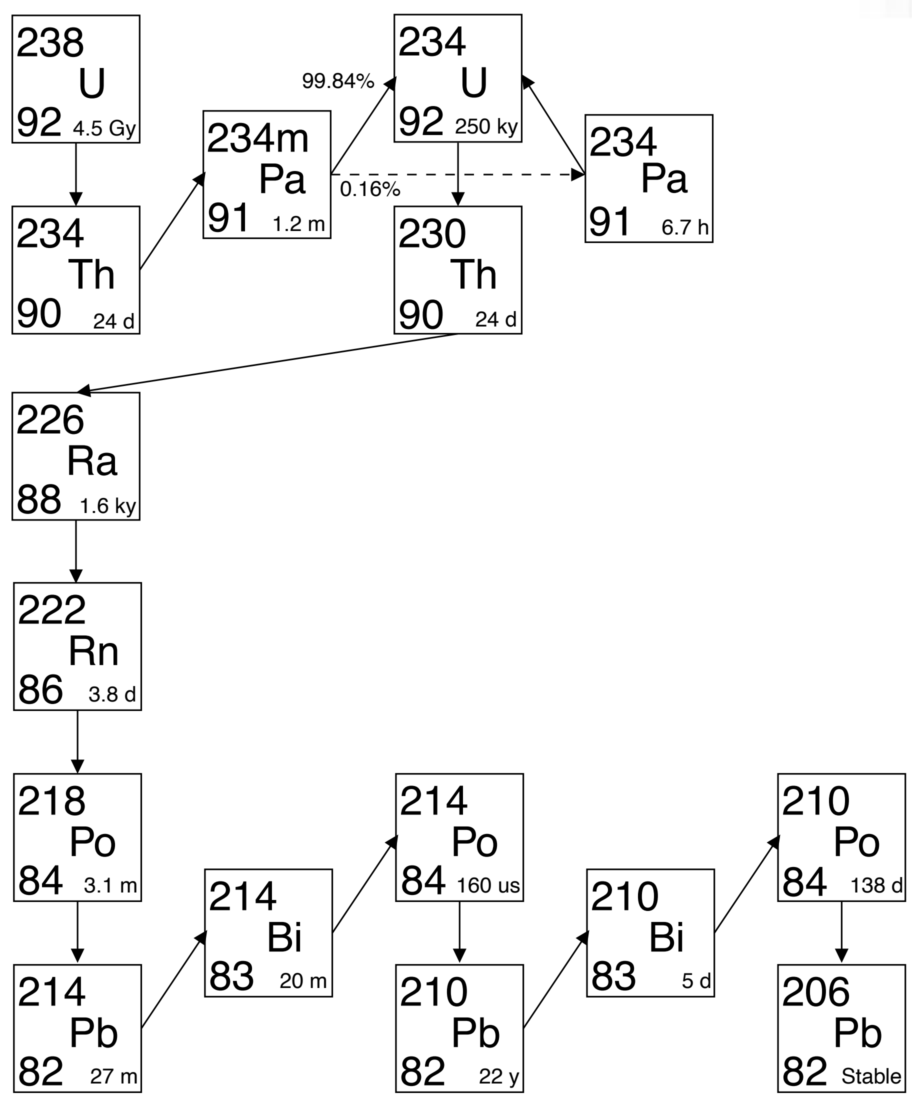

^{210}Pb contamination

Recent development: low background α-particle counting

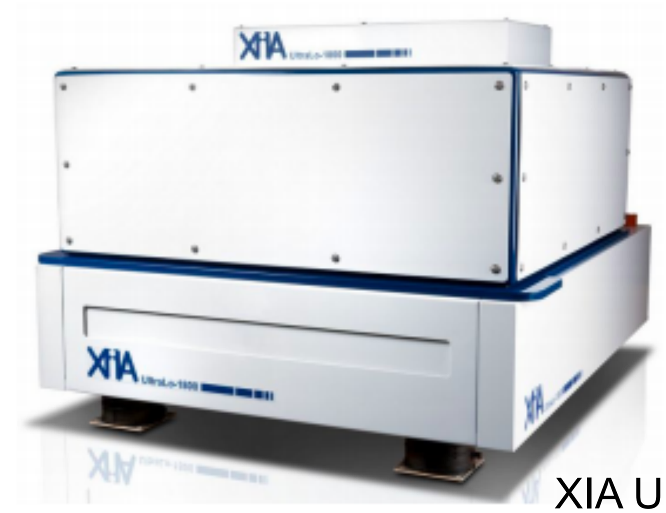

XIA UltraLo-1800
https://www.xia.com/ultralo-theory.html

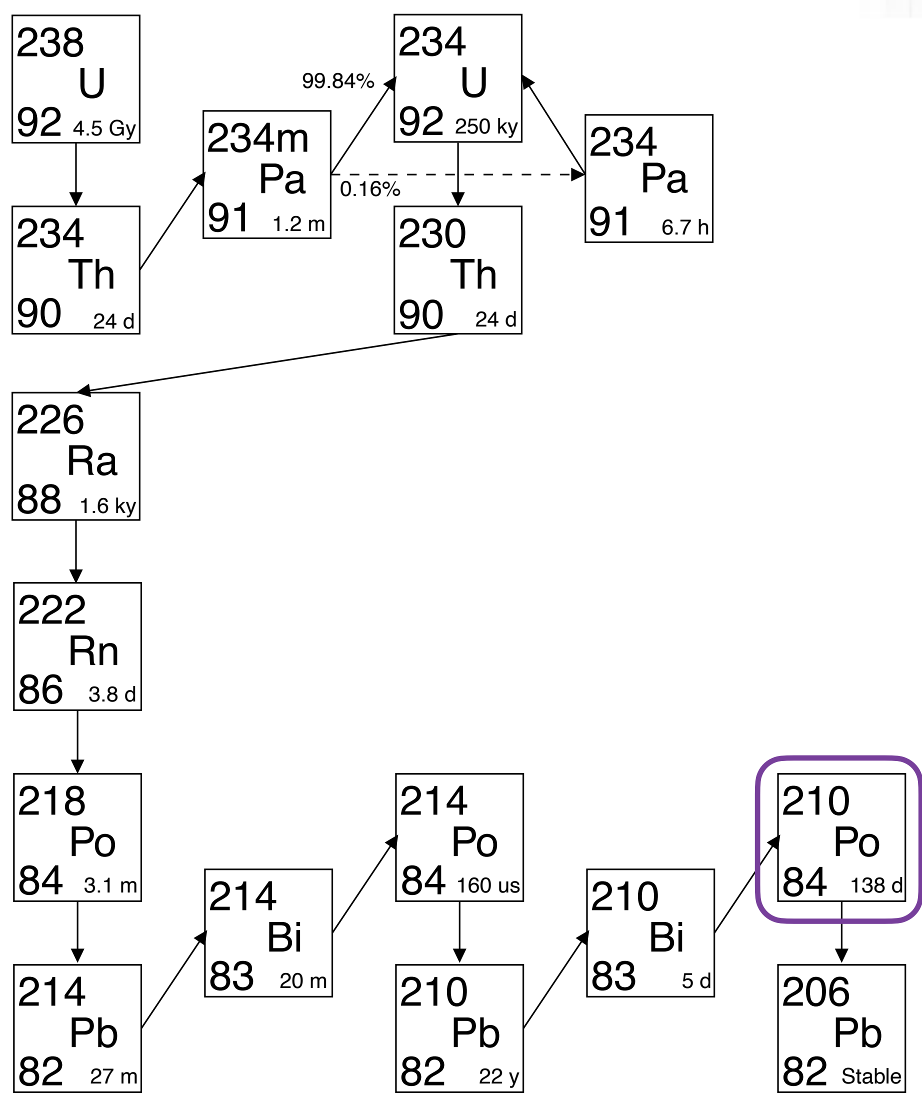

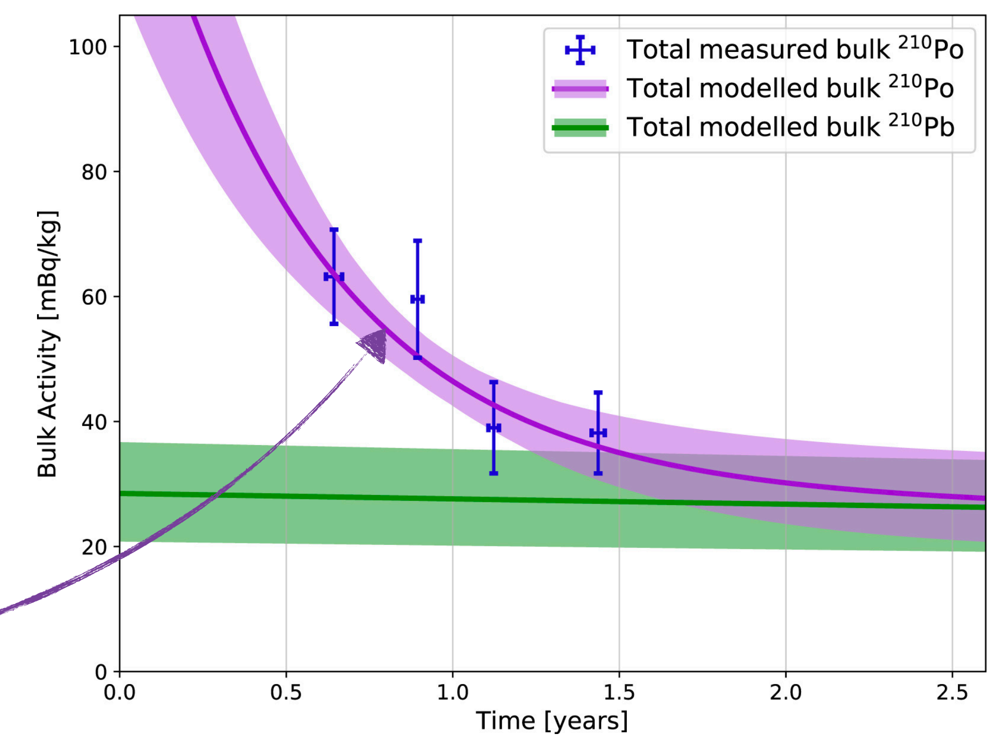

^{210}Pb contamination

Recent development: low background α-particle counting

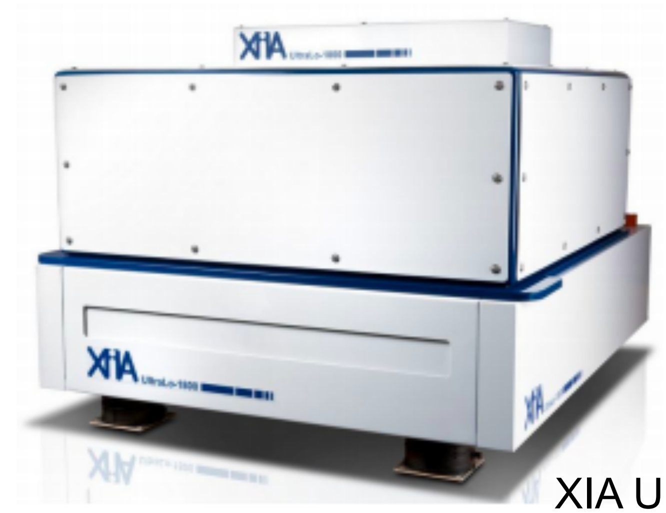

XIA UltraLo-1800
https://www.xia.com/ultralo-theory.html

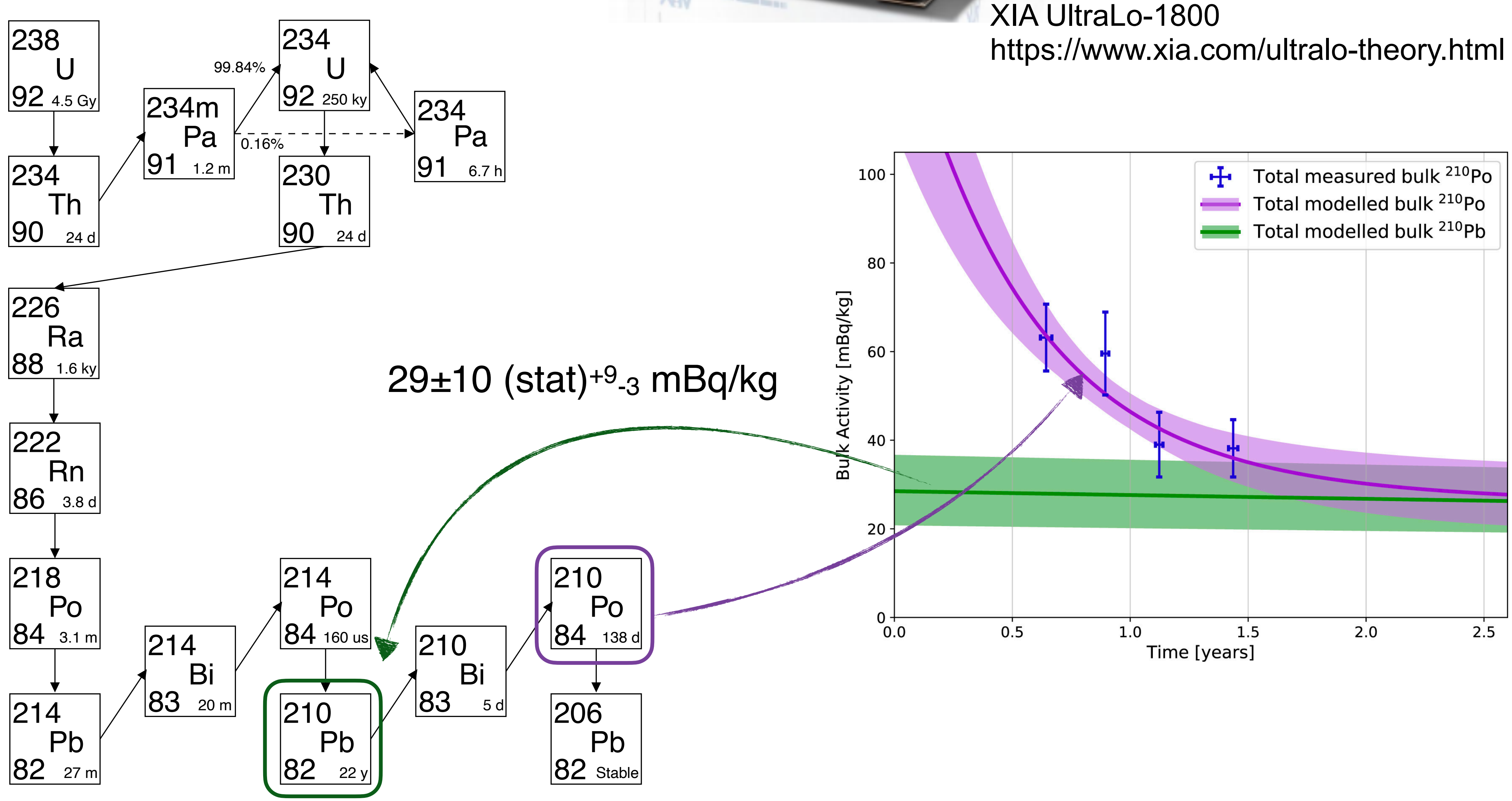

Copper Electroplating

SNOLAB detector: 4N Aurubis AG Oxygen Free Cu (99.99% pure)

- Out-of-equilibrium ^{210}Pb contamination: 29±10 (stat)$^{+9}_{-3}$ mBq/kg

Copper Electroplating

SNOLAB detector: 4N Aurubis AG Oxygen Free Cu (99.99% pure)

- Out-of-equilibrium ^{210}Pb contamination: 29±10 (stat)$^{+9}_{-3}$ mBq/kg

Background

- Bremsstrahlung X-rays from ^{210}Pb and ^{210}Bi β-decays in Cu

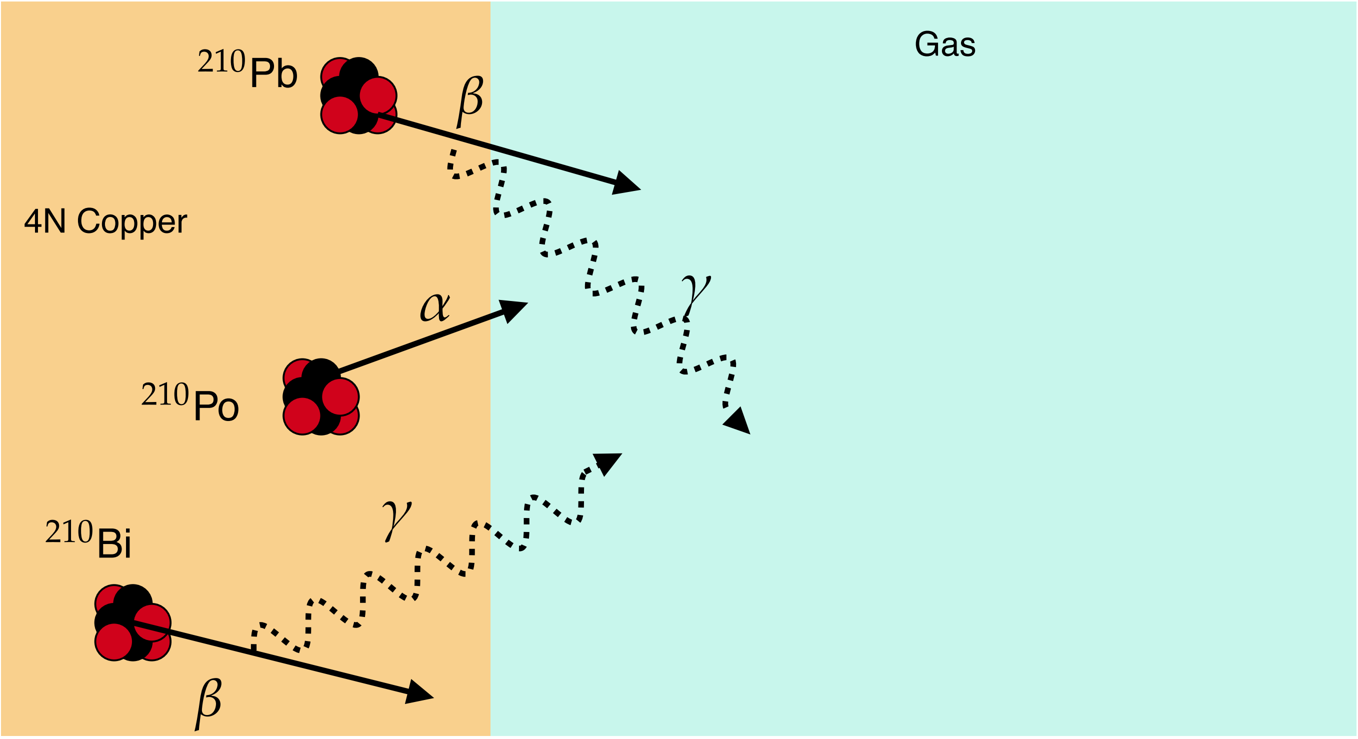

Copper Electroplating

SNOLAB detector: 4N Aurubis AG Oxygen Free Cu (99.99% pure)

- Out-of-equilibrium ^{210}Pb contamination: 29±10 (stat)$^{+9}_{-3}$ mBq/kg

Background

- Bremsstrahlung X-rays from ^{210}Pb and ^{210}Bi β-decays in Cu

Internal shield

- Ultra-pure Cu layer on detector inner surface
- Suppresses ^{210}Pb and ^{210}Bi backgrounds by factor 2.6 under 1 keV

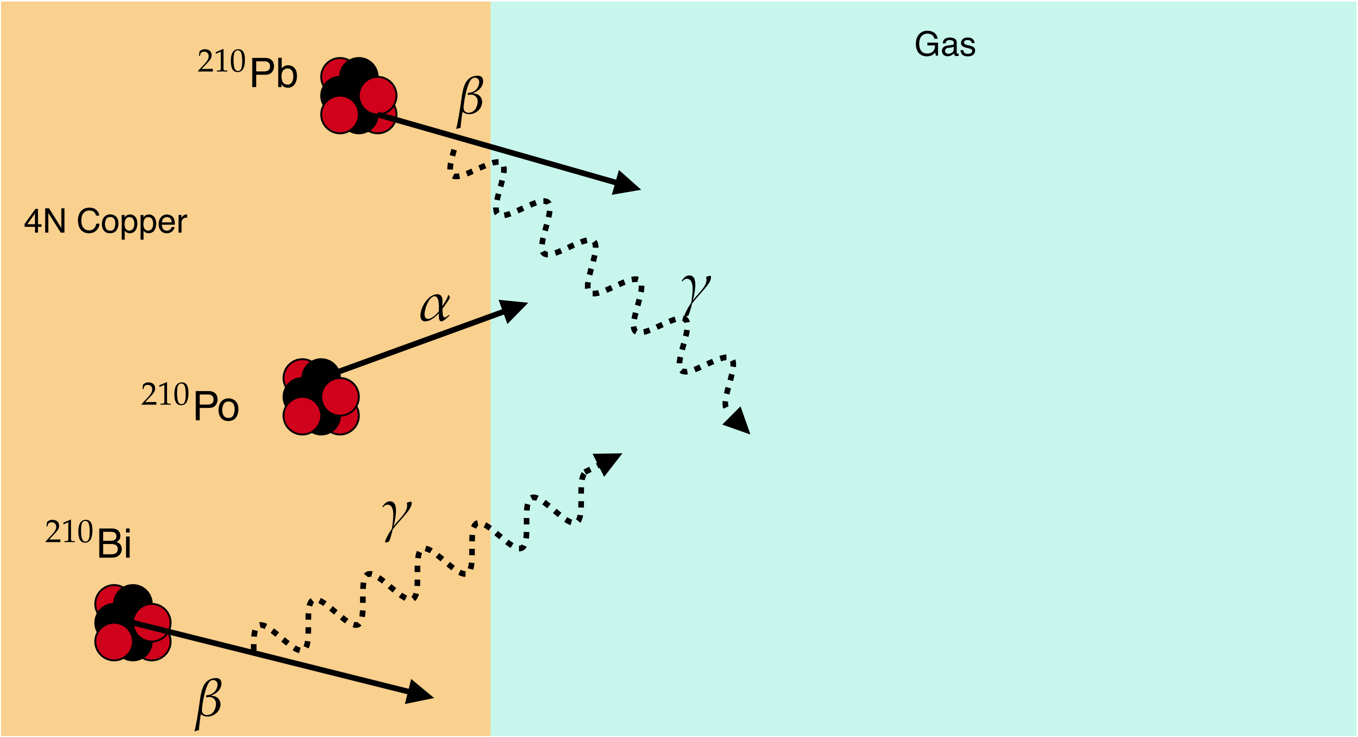

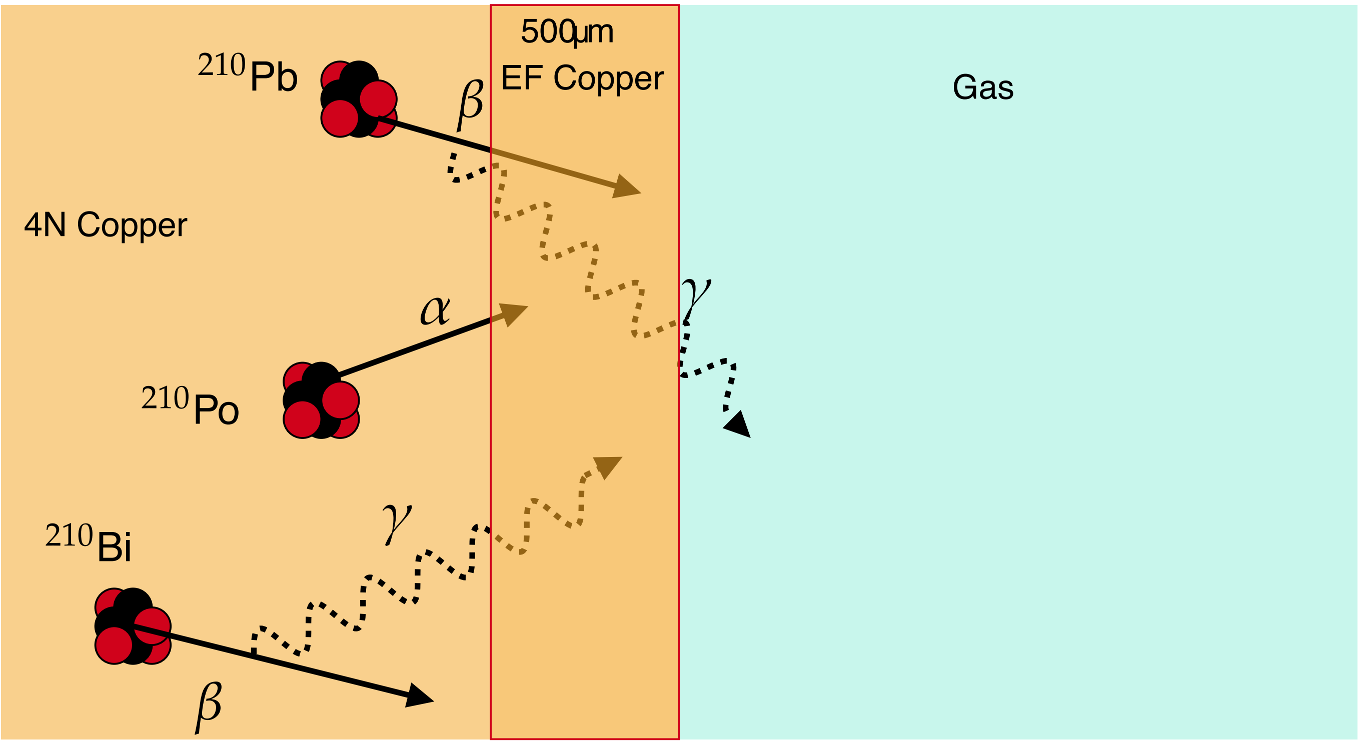

Copper Electroplating

Internal shield: add a layer of extremely radio-pure copper

NIM A 988 (2021) 164844

Copper Electroplating

Internal shield: add a layer of extremely radio-pure copper

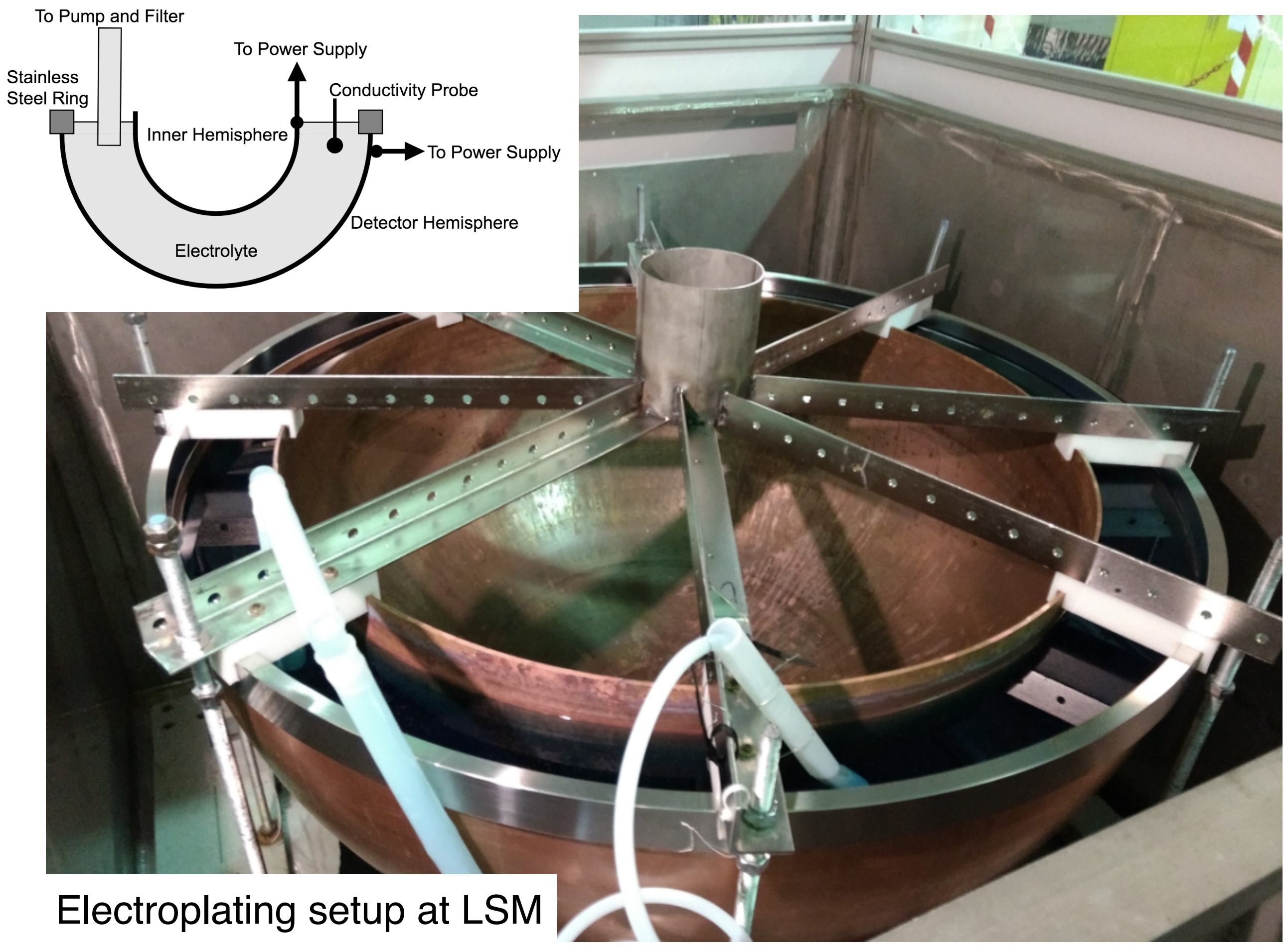

Electroplating setup at LSM

NIM A 988 (2021) 164844

Copper Electroplating

Internal shield: add a layer of extremely radio-pure copper

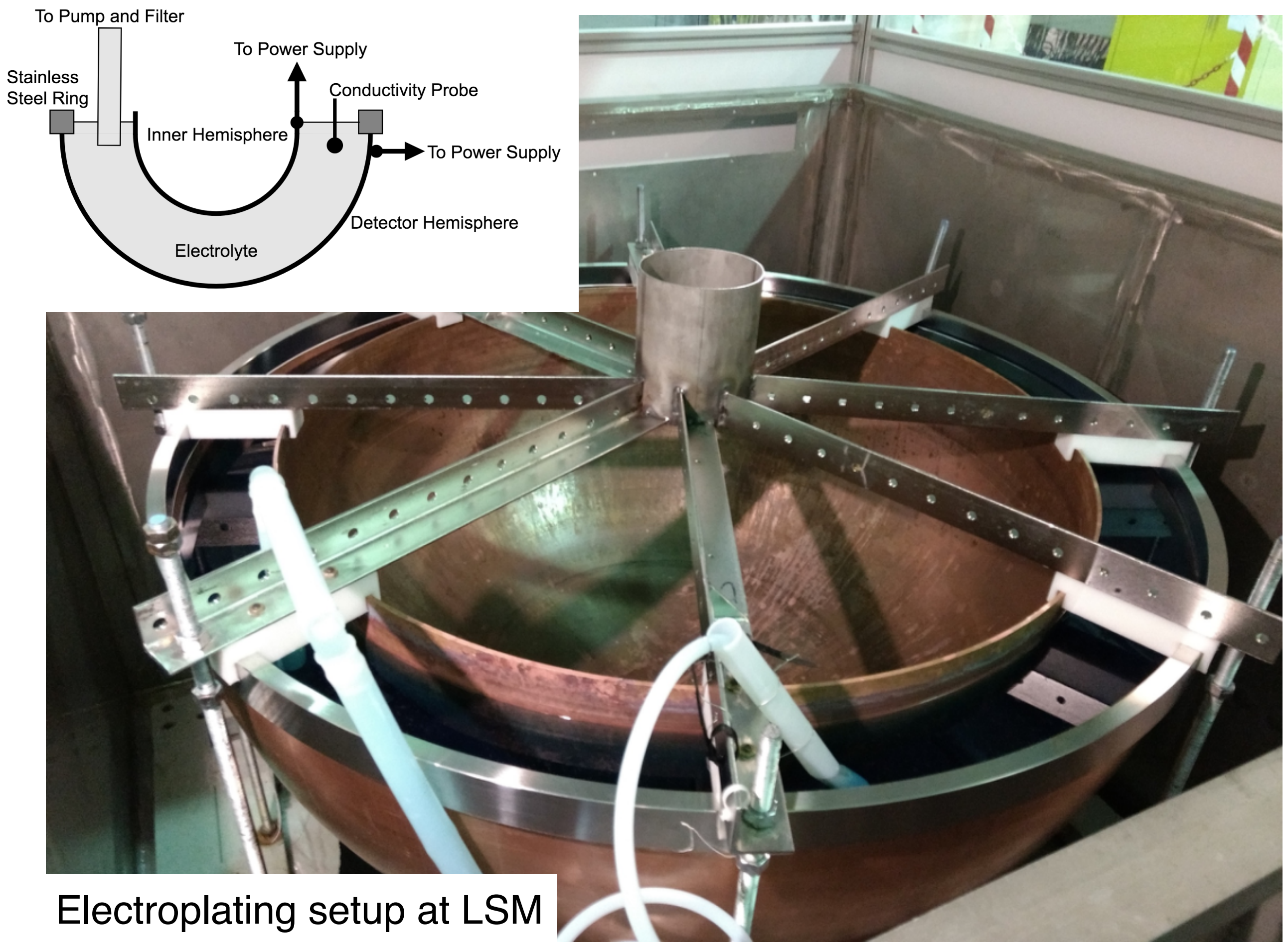

Electroplating setup at LSM

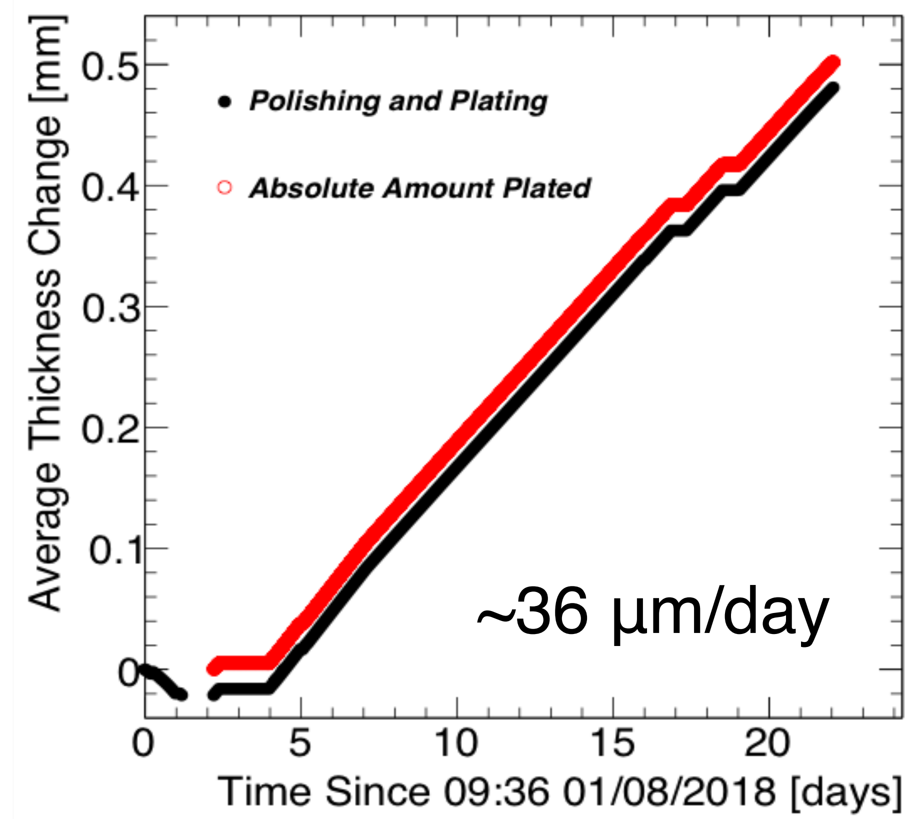

NIM A 988 (2021) 164844

Copper Electroplating

Internal shield: add a layer of extremely radio-pure copper

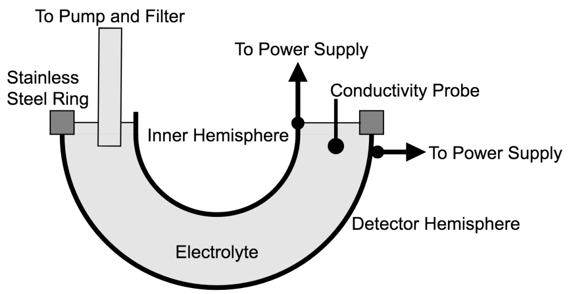

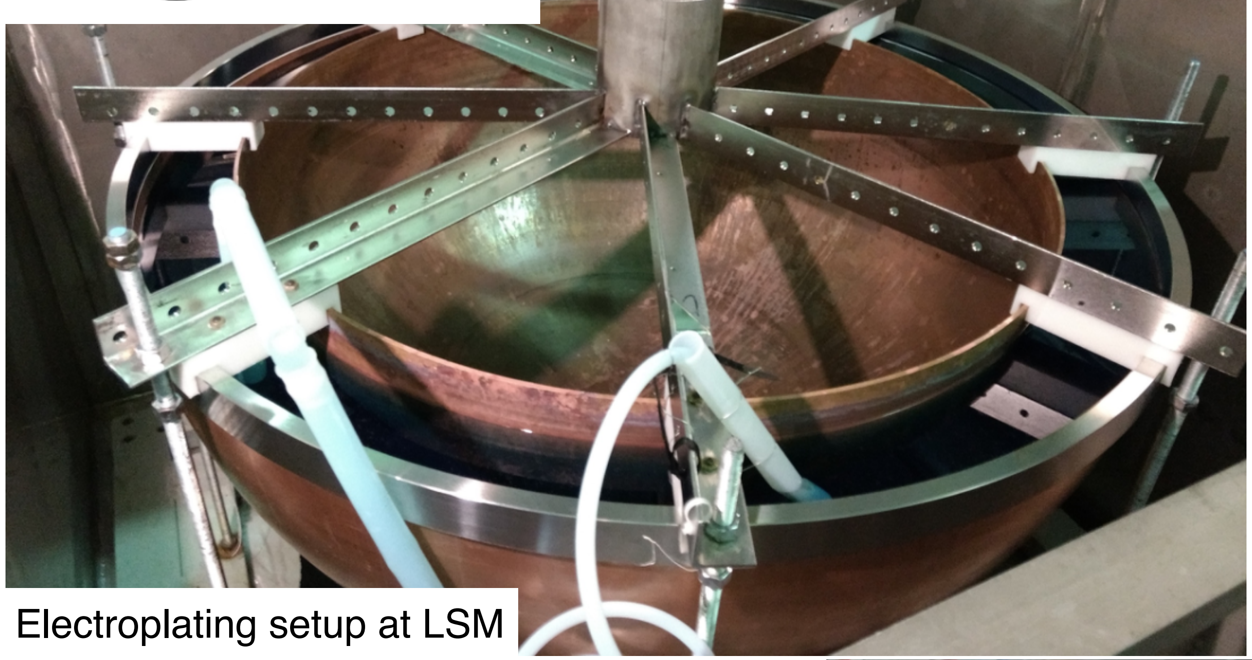

Electroplating setup at LSM

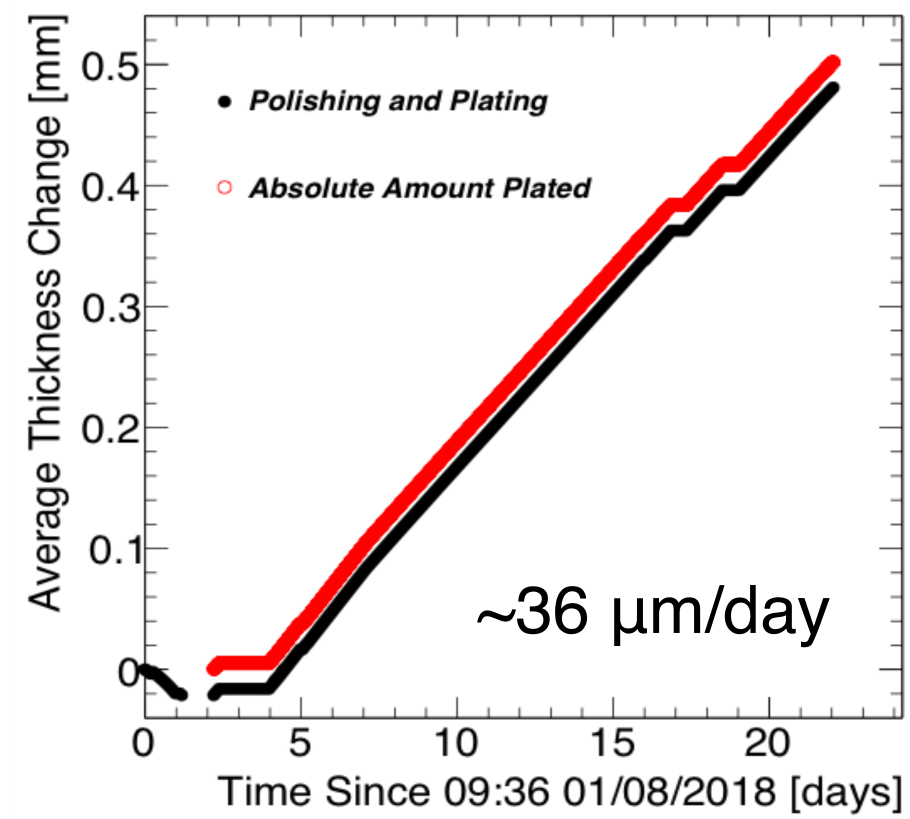

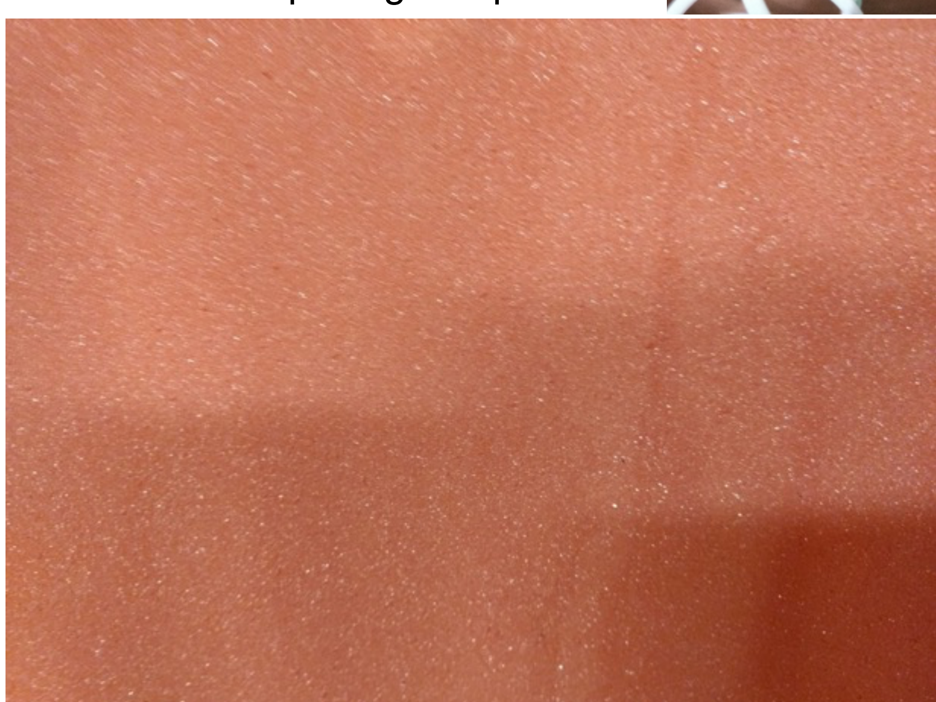

Sample	Weight [g]	^{232}Th [µBq/kg]	^{238}U [µBq/kg]
C10100 Cu (Machined)	-	8.7 ± 1.6	27.9 ± 1.9
Cu Electroformed	-	< 0.119	< 0.099
Hemisphere 1	0.256	< 0.58	< 0.26
Hemisphere 2	0.614	< 0.24	< 0.11

NIM A 988 (2021) 164844

SNOGLOBE at LSM

- 2019: detector assembly in France
  - Hemispheres e-beam welded
  - 500 μm electroformed inner layer
- April 2019: initial commissioning at LSM
  - UV laser and ^{37}Ar calibration
  - Multi-anode sensor
- July 2019: Pb and H_2O shield installed
  - ~10 days of physics data
  - 135 mbar of CH_4 (~100g)

Electron Counting

- Pulse treatment (deconvolution)
  - Resolve individual electrons
- Diffusion O(100μs)
  - Obtain time separation of peaks
  - Surface vs volume discrimination
- Signal and background model
  - Derived from simulations
  - Validated with calibration data

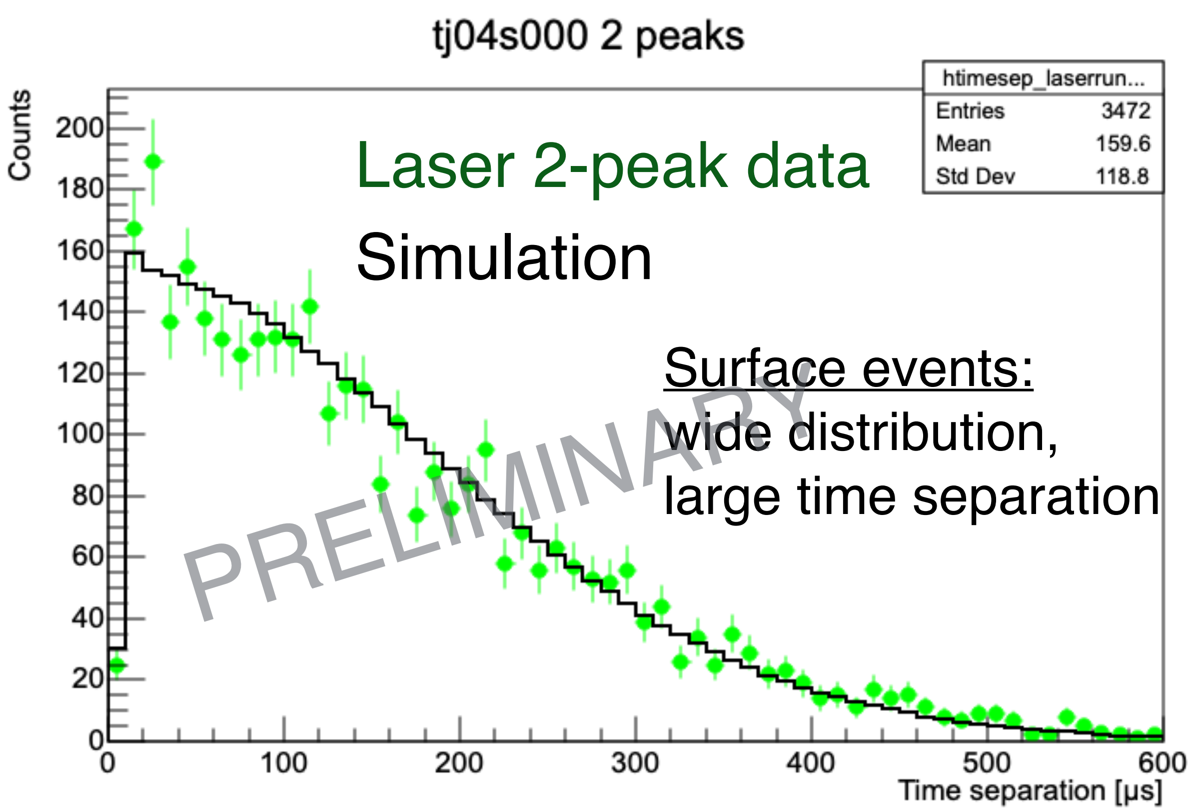

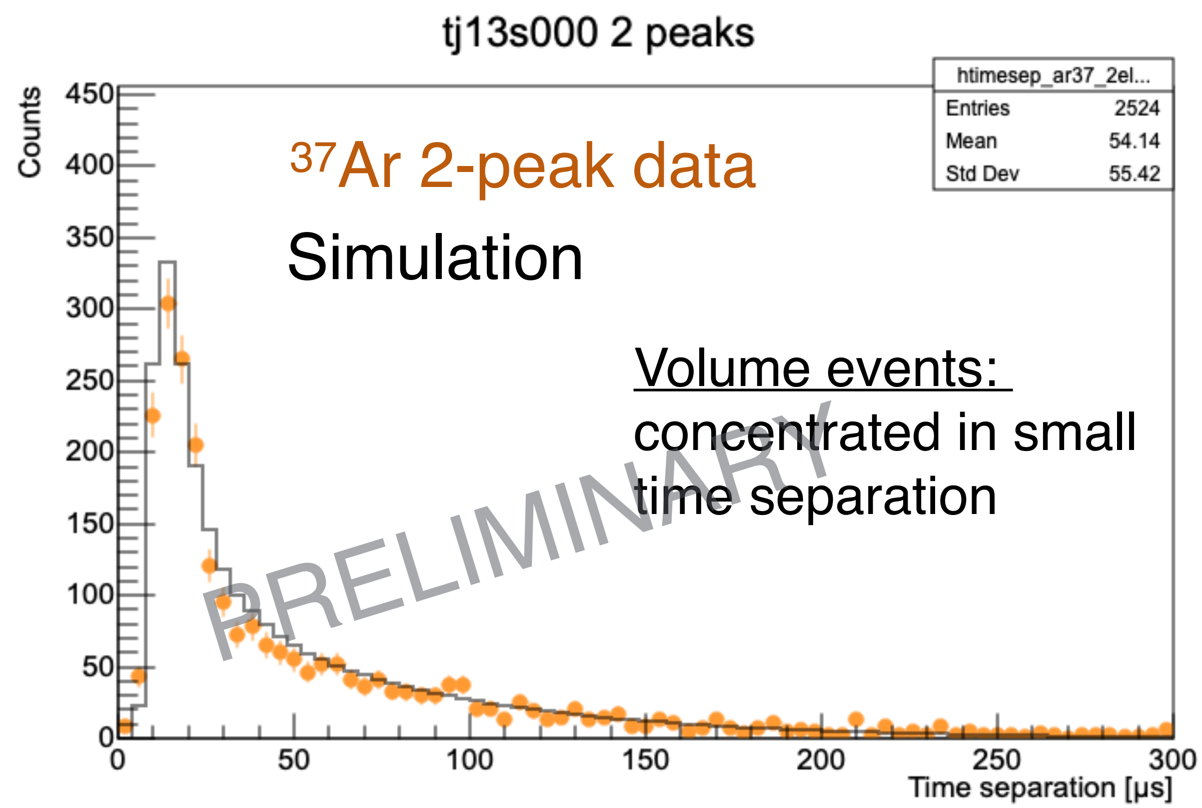

Results with LSM data

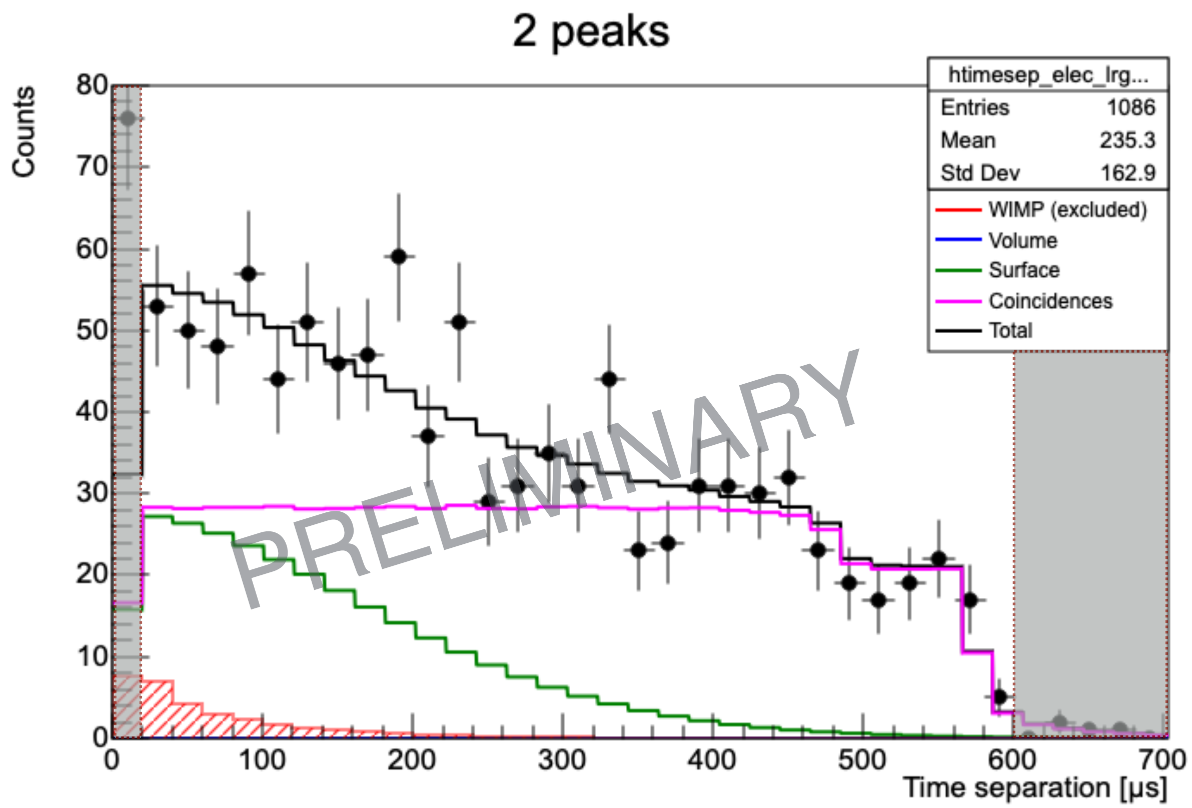

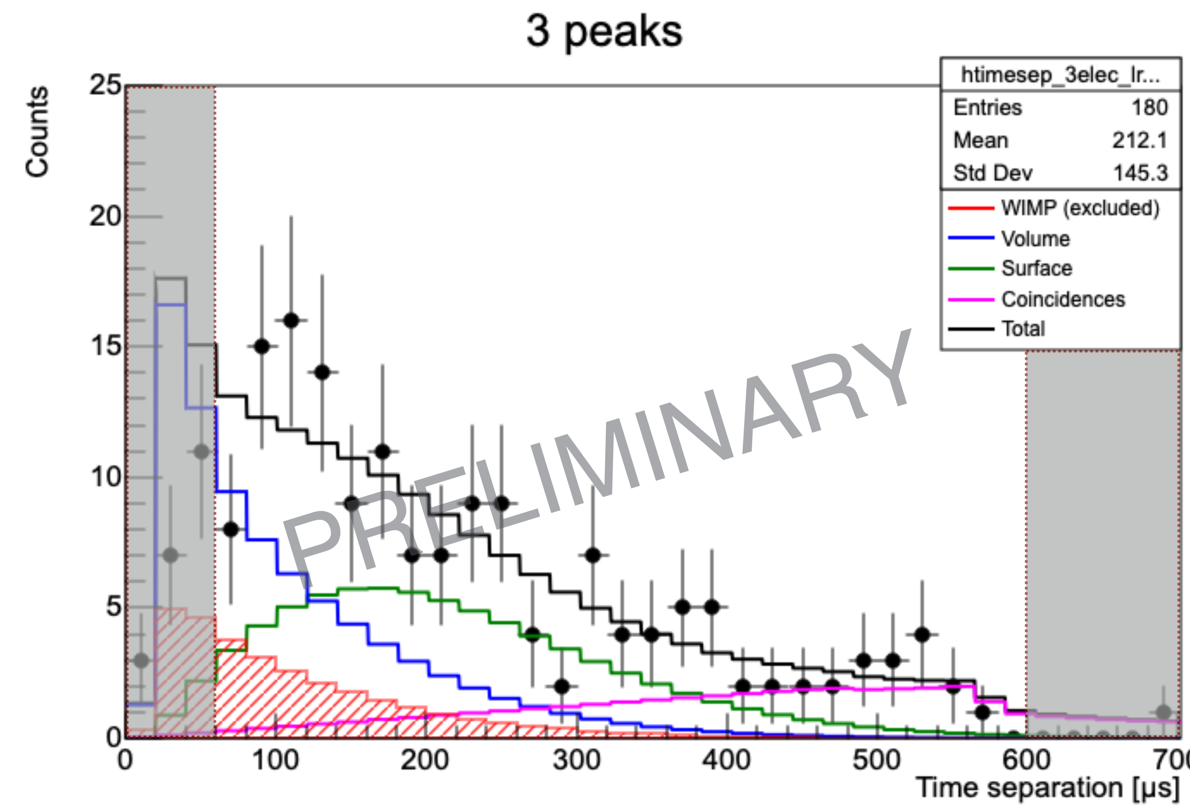

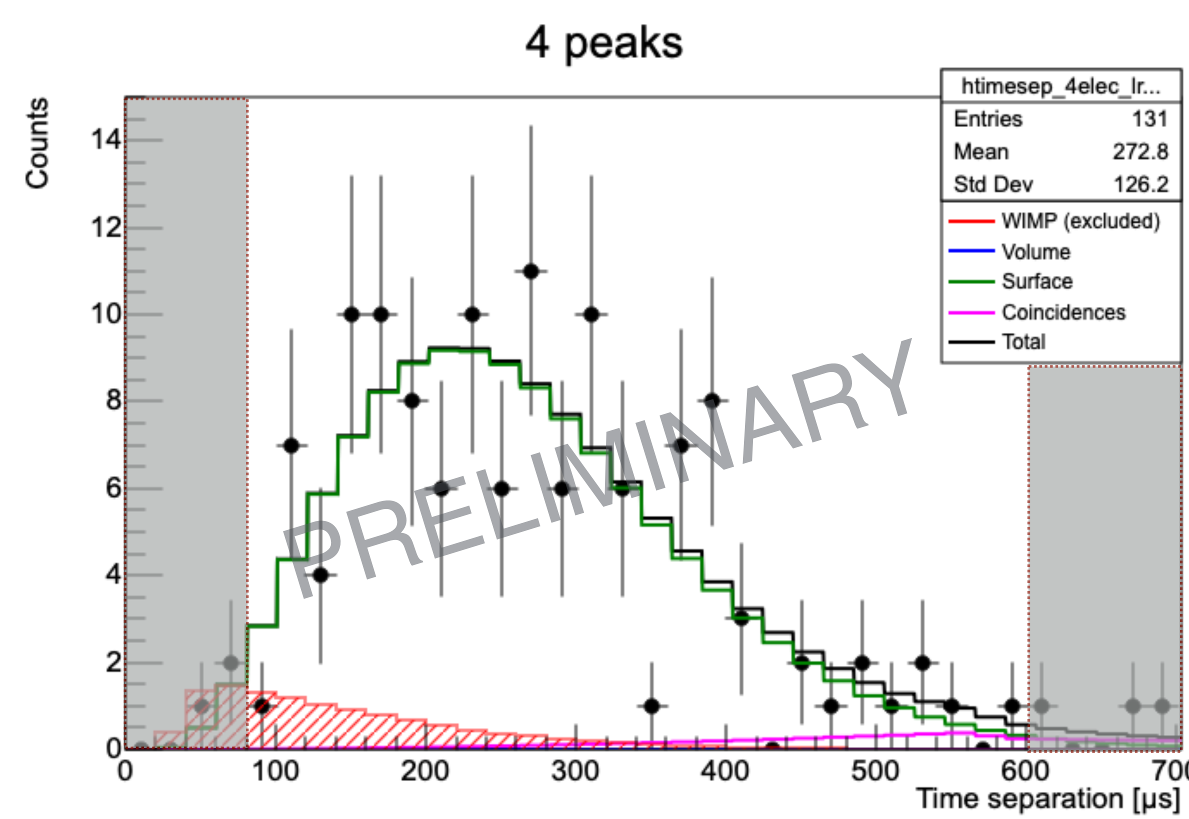

- Data divided into 2/3/4 peak
- Maximum likelihood fit to time separation
- Only test data analysed so far: ~30% data
  - Remaining data is blinded

LSM Physics Result

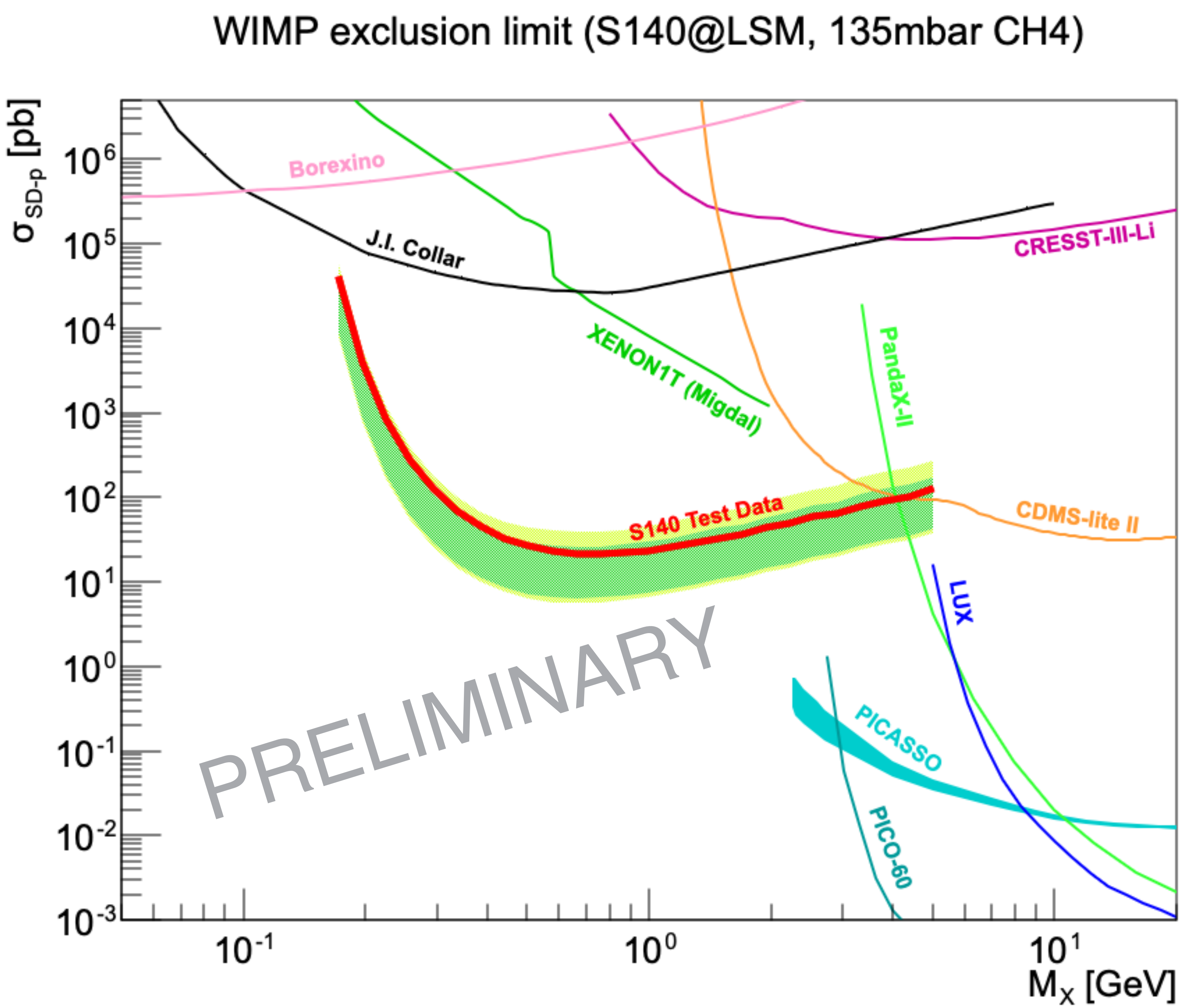

- 90% upper limits set with profile likelihood ratio
- Exposure 0.12 kg·days

NEWS-G at SNOLAB

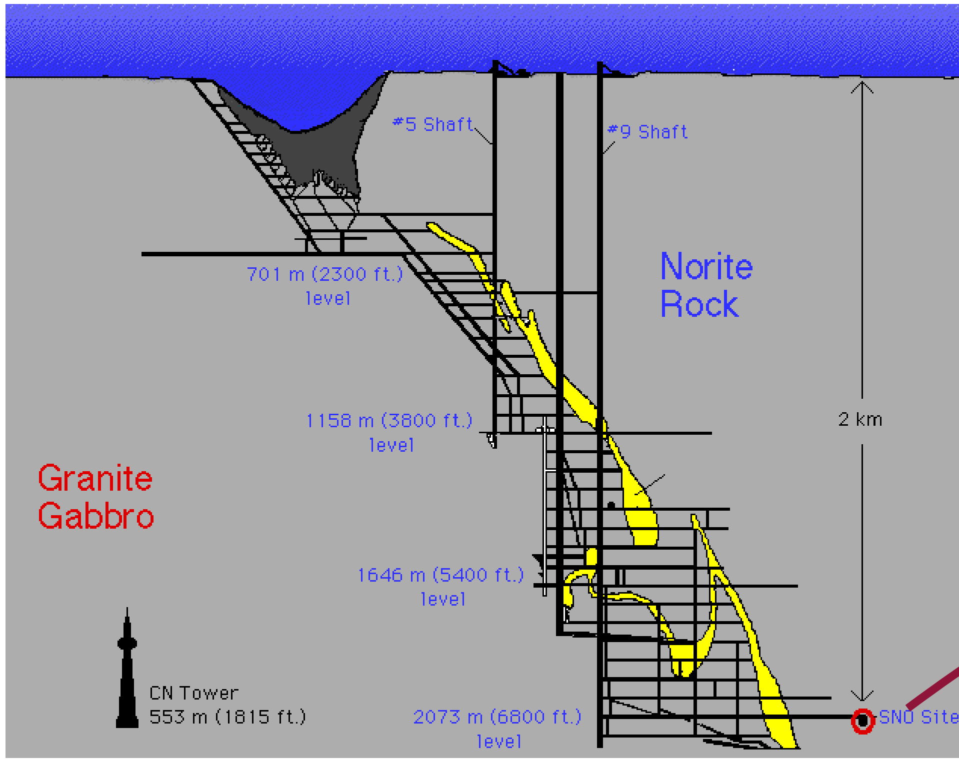

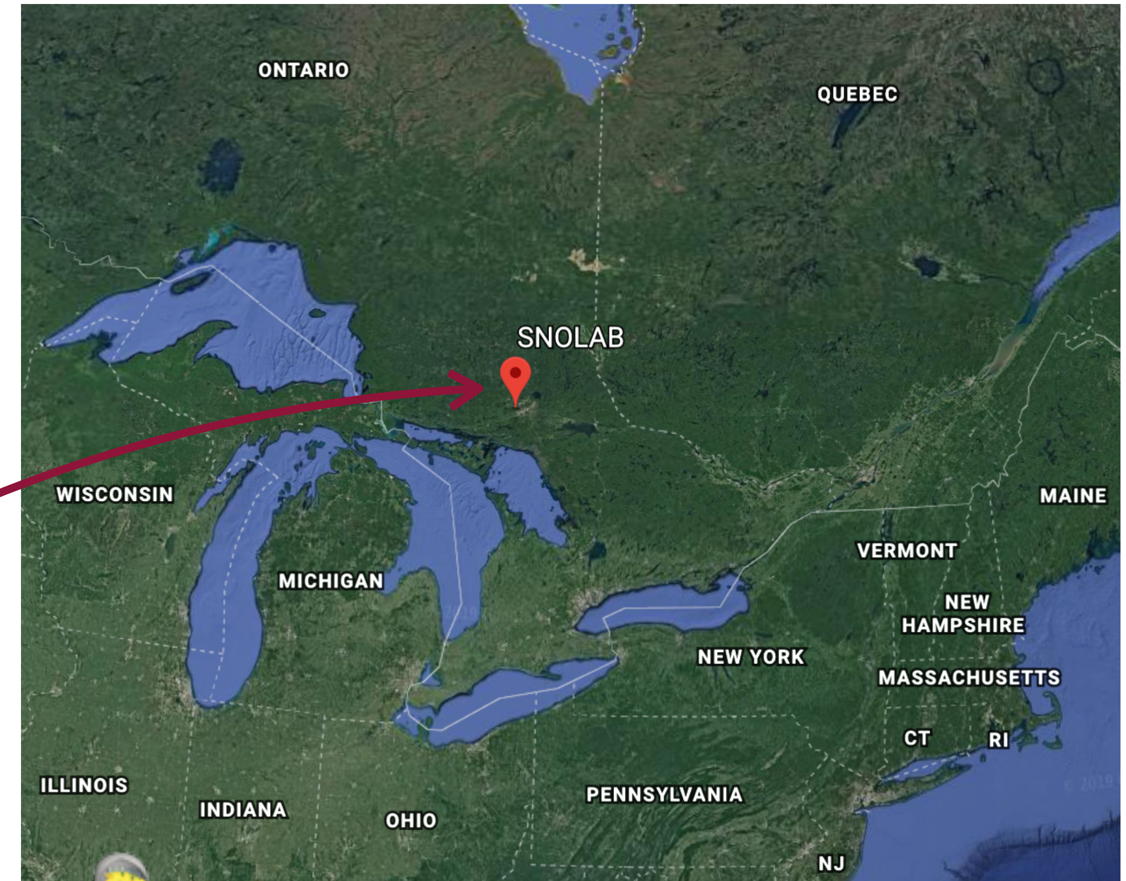

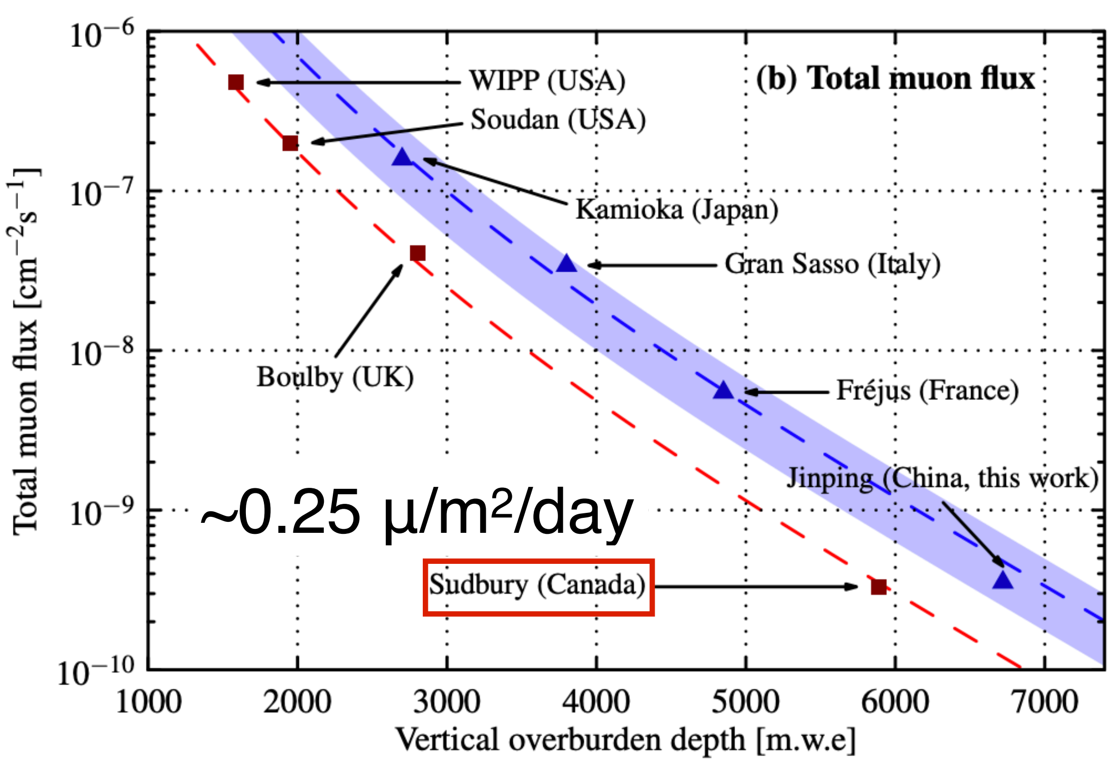

Chin.Phys.C 45 (2021) 2, 025001

Installation at SNOLAB

Arrival at SNOLab (Dec ’19)

Unwrapped and baked (Sep ’20)

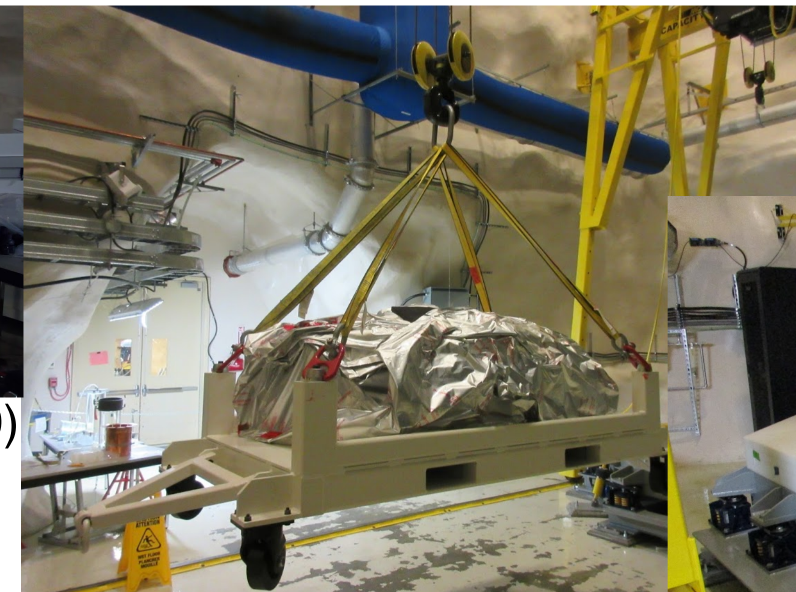

Pb shielding arrival

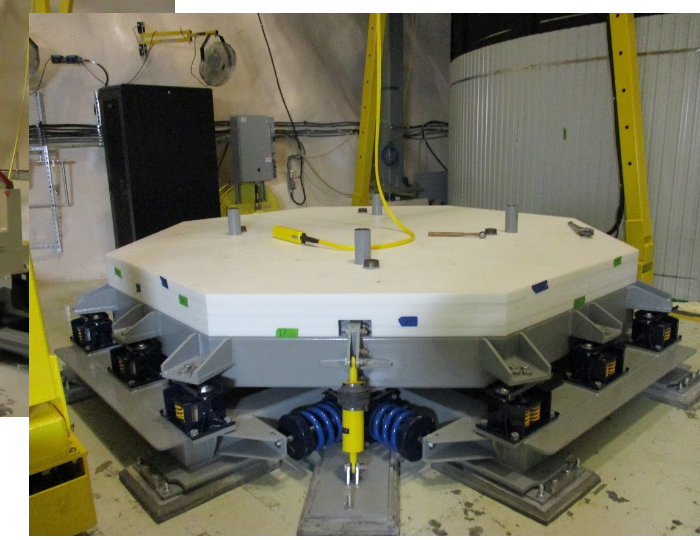

Seismic platform installation

Detector Installation

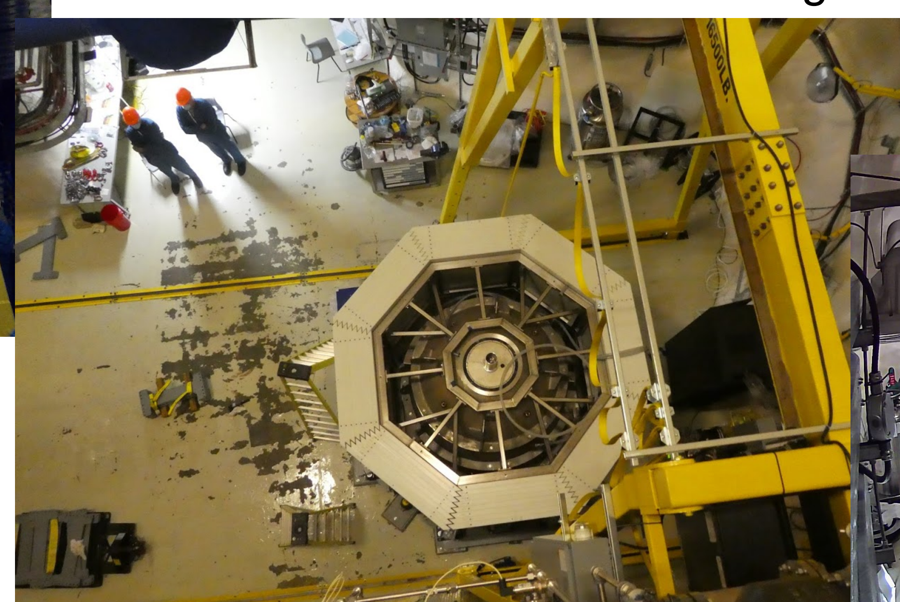

PE shielding installation

SNOGLOBE complete (Dec ’20)

Installation at SNOLAB

Arrival at SNOLab (Dec '19)

Unwra

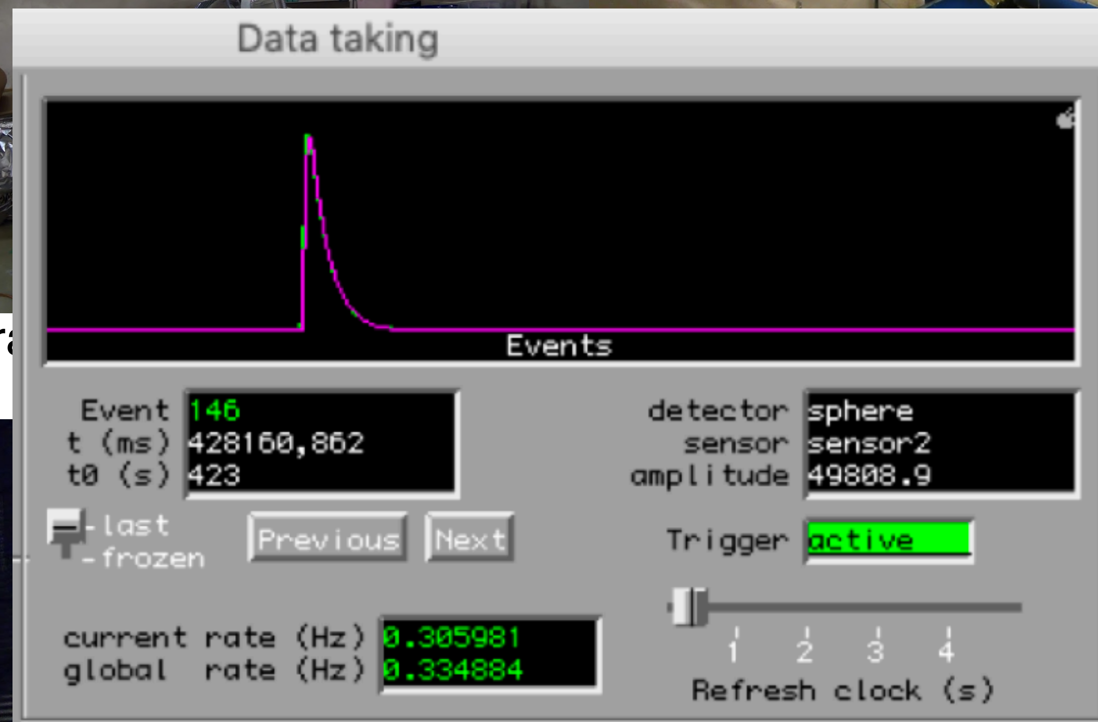

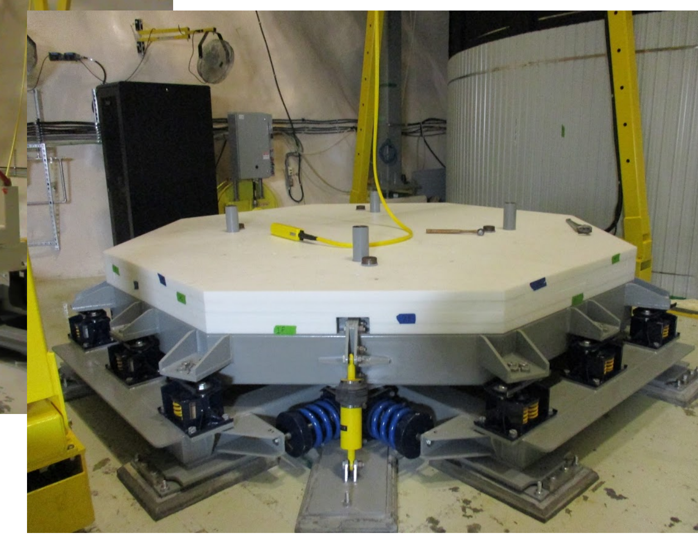

Seismic platform installation

Detector Installation

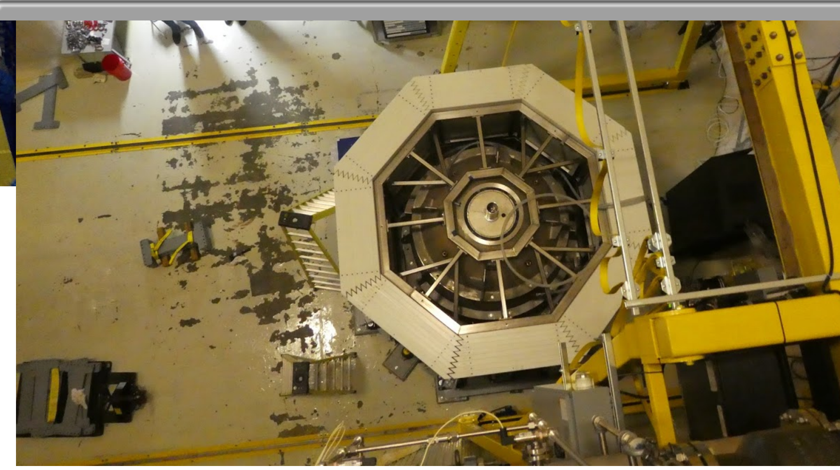

PE shielding installation

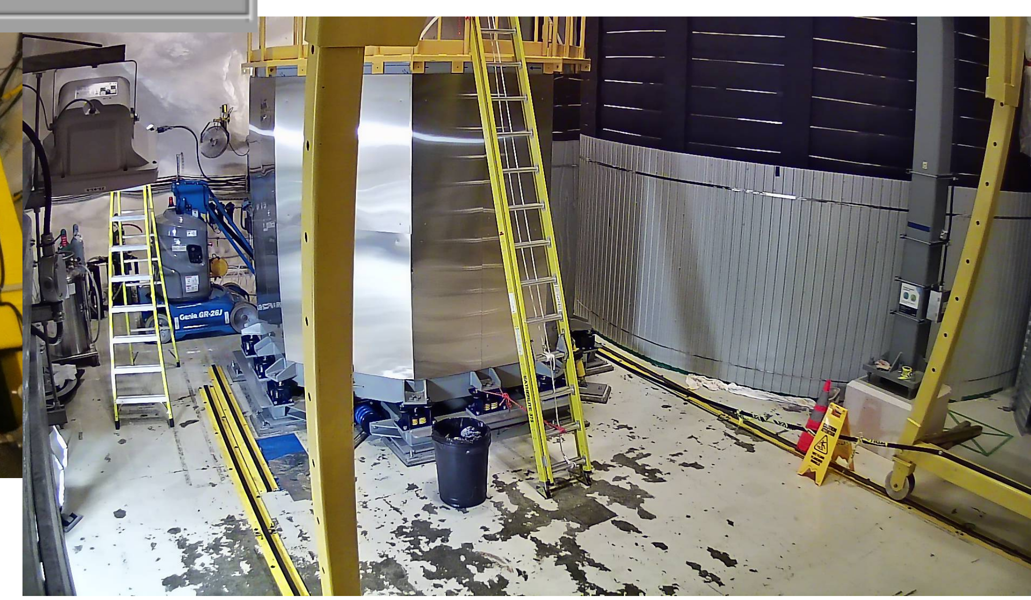

SNOGLOBE complete (Dec '20)

Installation at SNOLAB

Arrival at SNOLab (Dec ’19)

Detector Installation

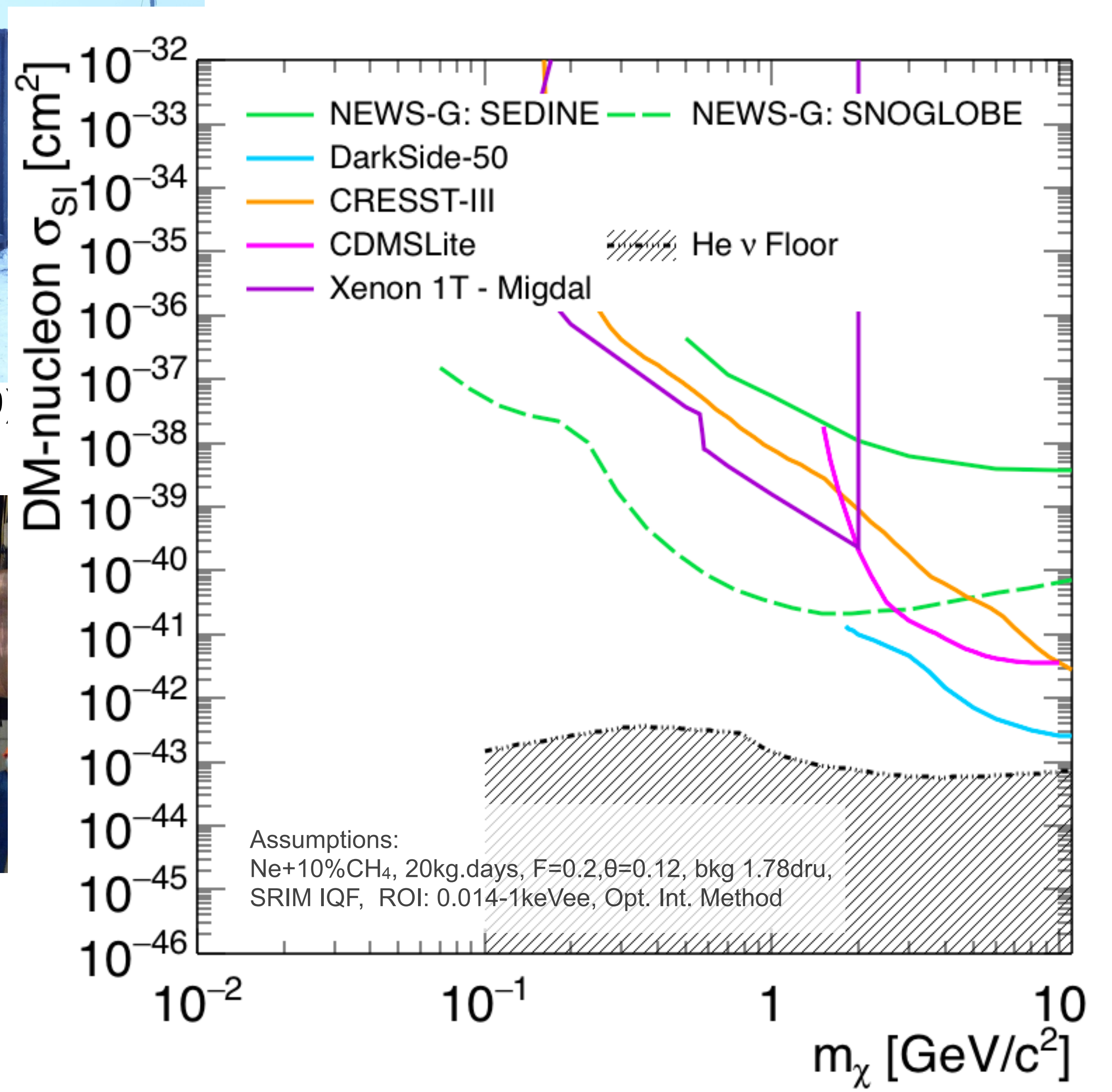

PE shielding installation

Seismic platform installation

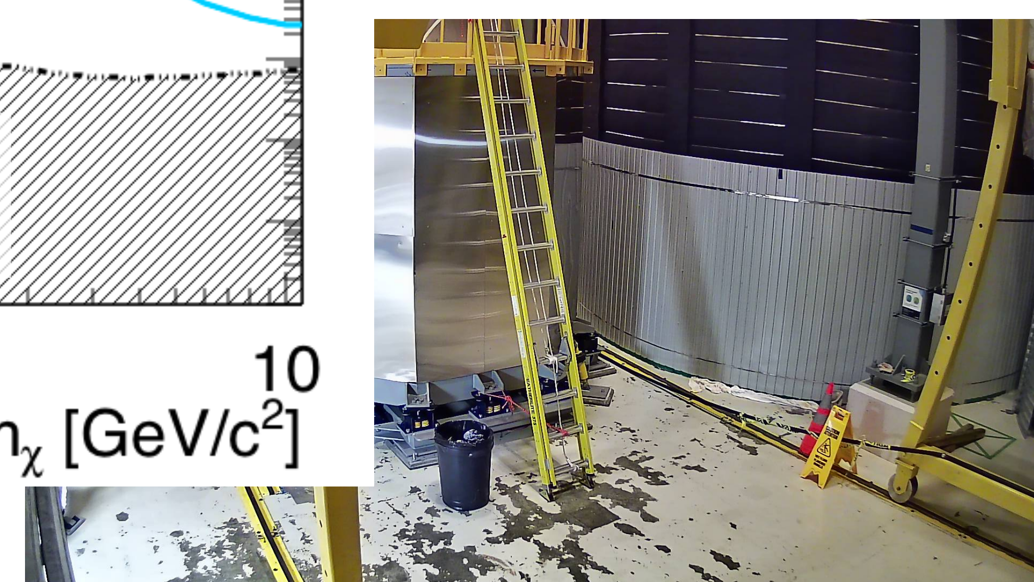

SNOGLOBE complete (Dec ’20)

Electroformed Cuprum Manufacturing Experiment

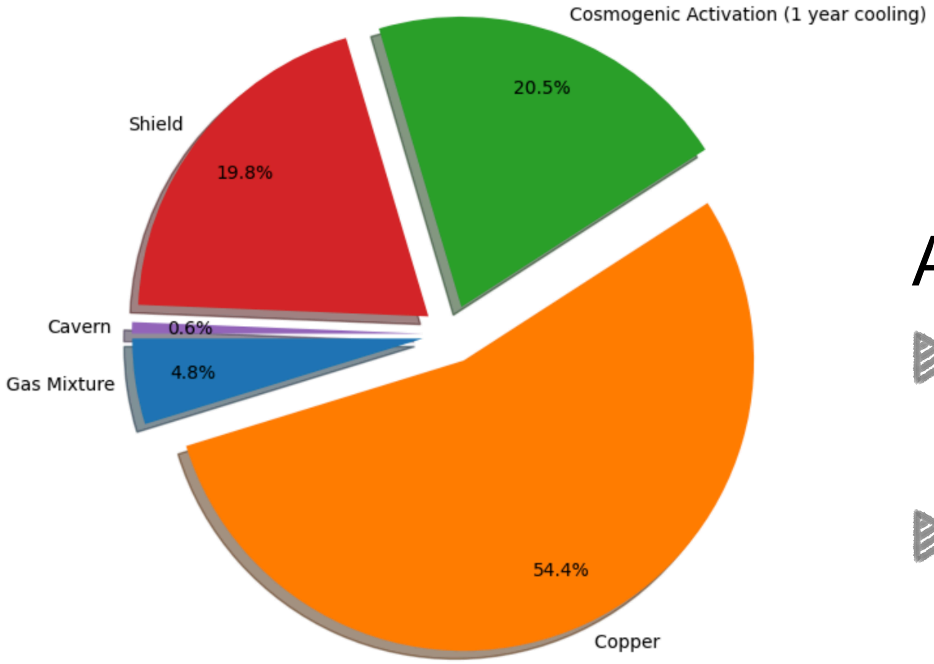

ECuME

A ⌀140 cm sphere electroformed underground in SNOLAB

- Builds on achievements of NEWS-G electroplating
  - 36 μm/day → ~1 mm/month
- No machining or welding - grow sphere directly

Electroformed Cuprum Manufacturing Experiment

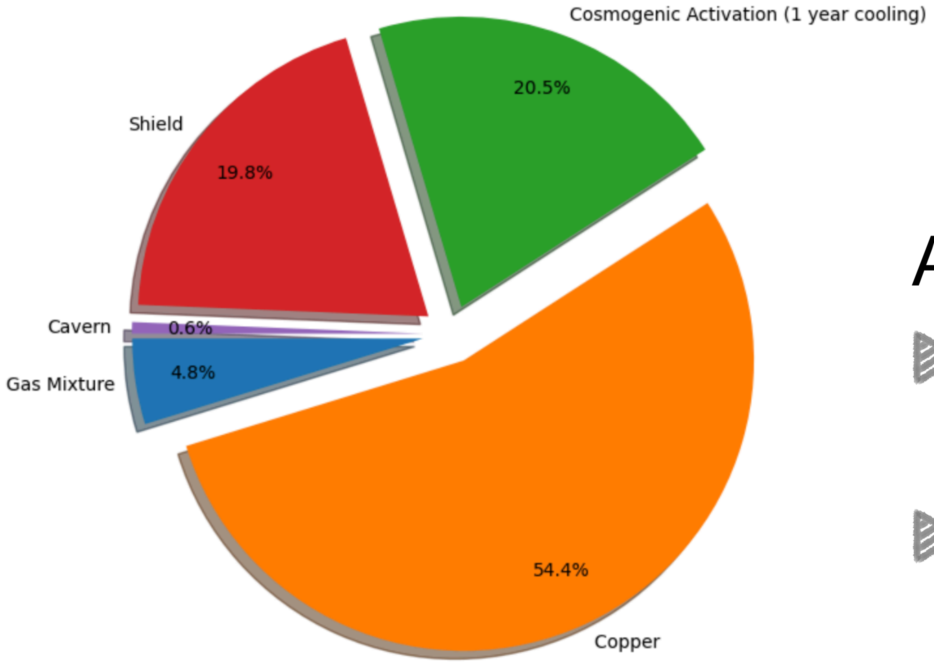

ECuME

A ⌀140 cm sphere electroformed underground in SNOLAB

- Builds on achievements of NEWS-G electroplating
  - 36 μm/day → ~1 mm/month
- No machining or welding - grow sphere directly

Current Status

- ⌀30 cm scale prototype to be produced at PNNL
  - Bath designed and assembled
  - Initial electroformation tests undertaken
  - Potential to undertake similar efforts at Boulby
- ⌀140 cm detector to follow shortly after
  - Use existing shielding for physics exploitation
- R&D on EF CuCr allows through PureAlloys project

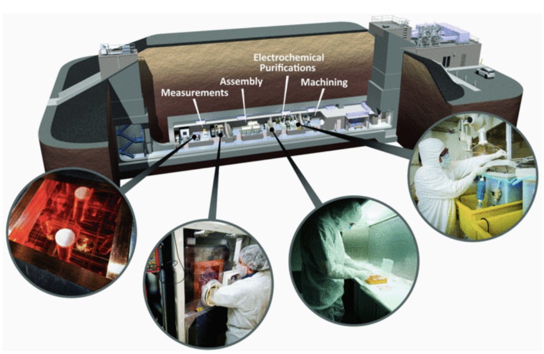

PNNL Shallow Underground Laboratory

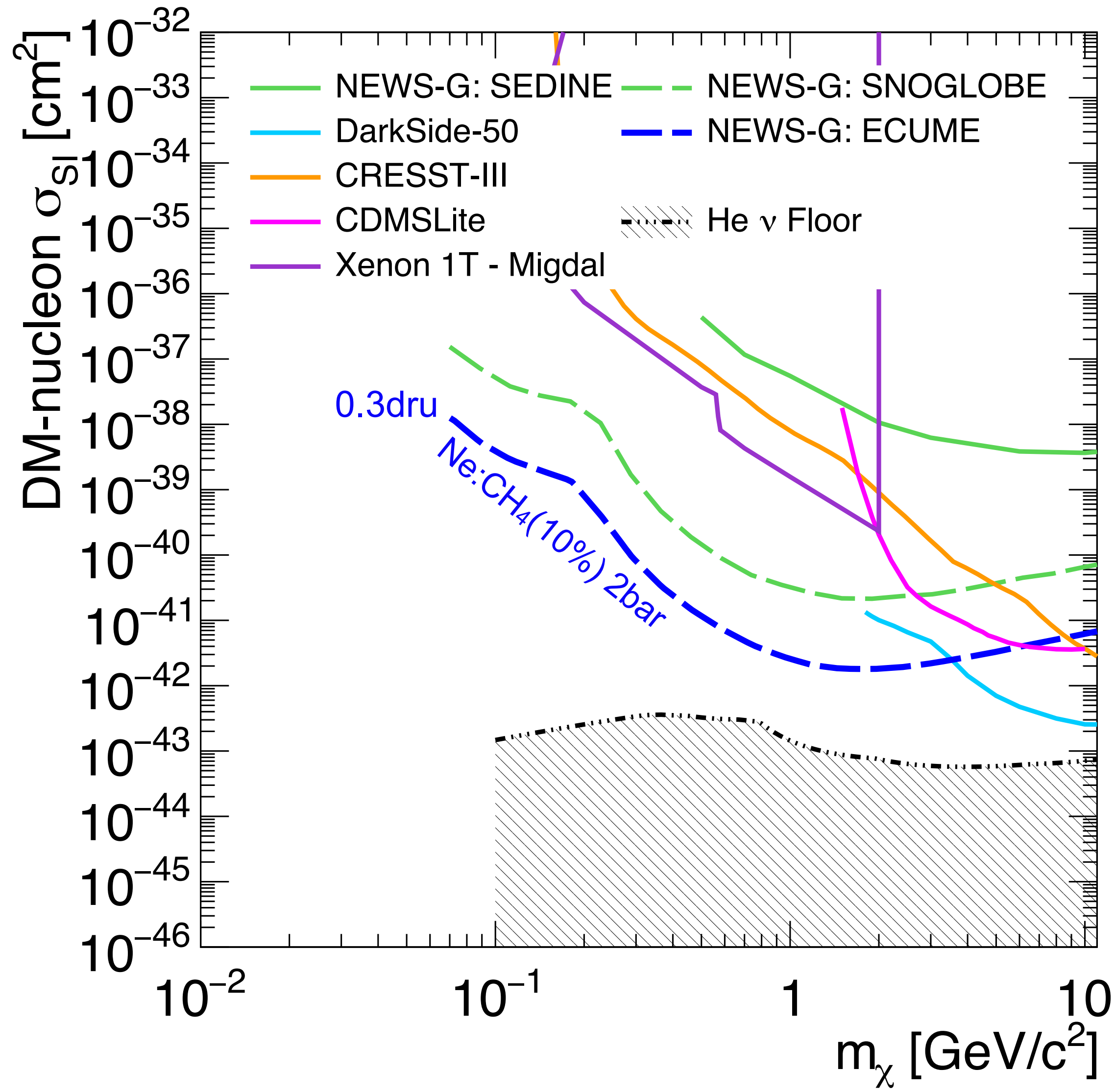

Reaching the neutrino floor

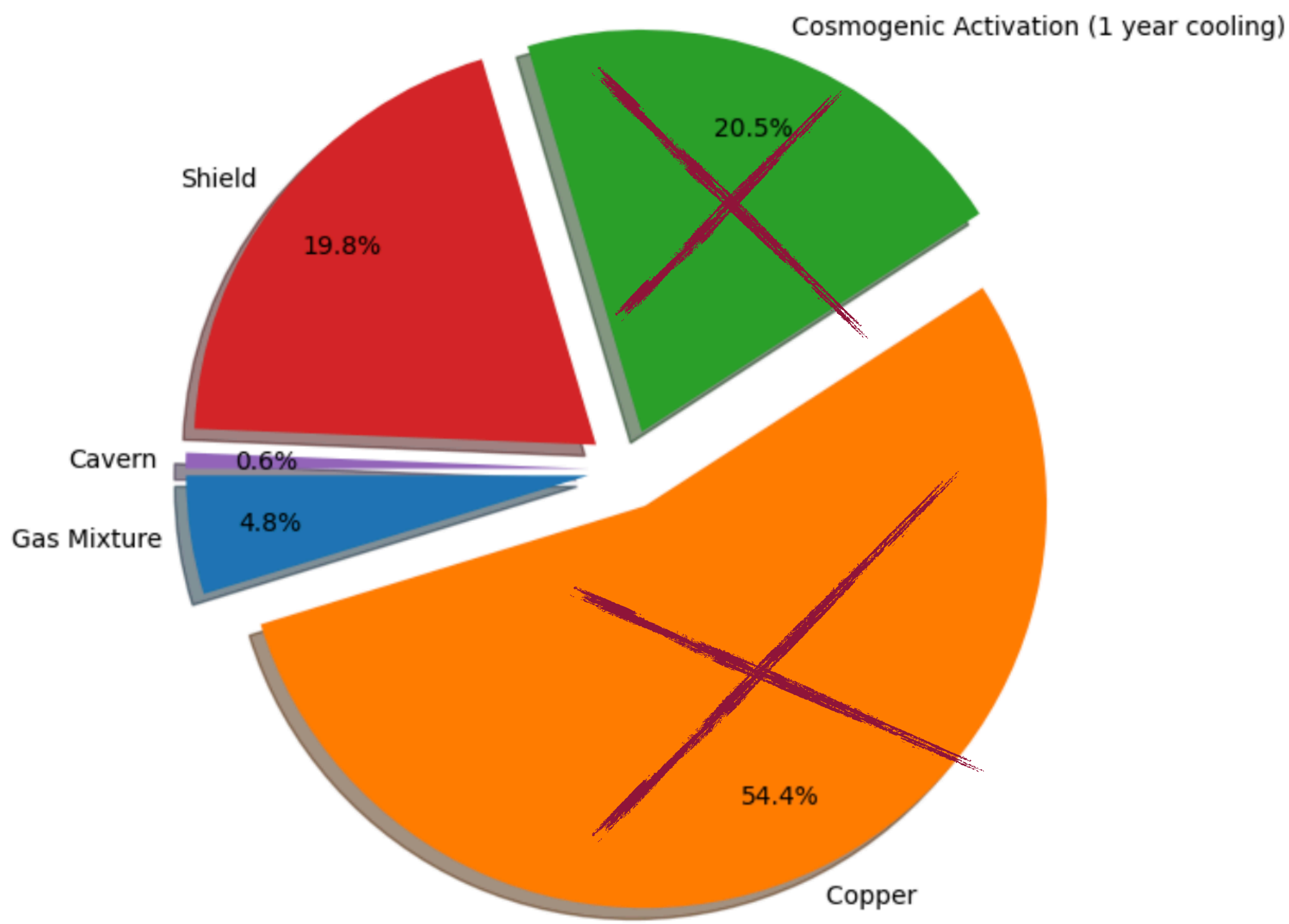

Reaching the neutrino floor

Scale volume and improve shielding

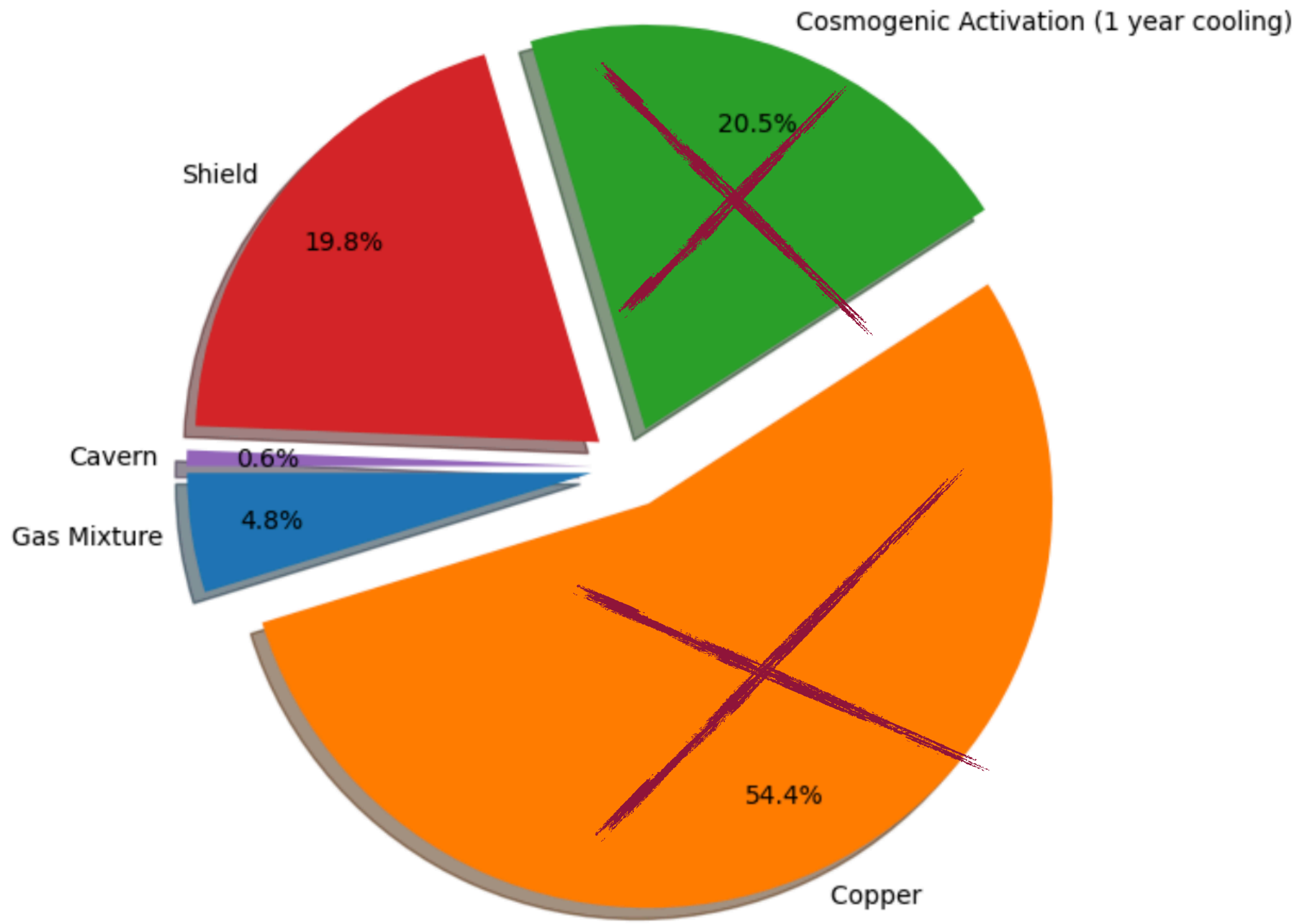

DarkSPHERE

Volume ×10: ⌀300cm intact underground electroformed spherical proportional counter with water-based shield

UKRI Science and Technology Facilities Counc

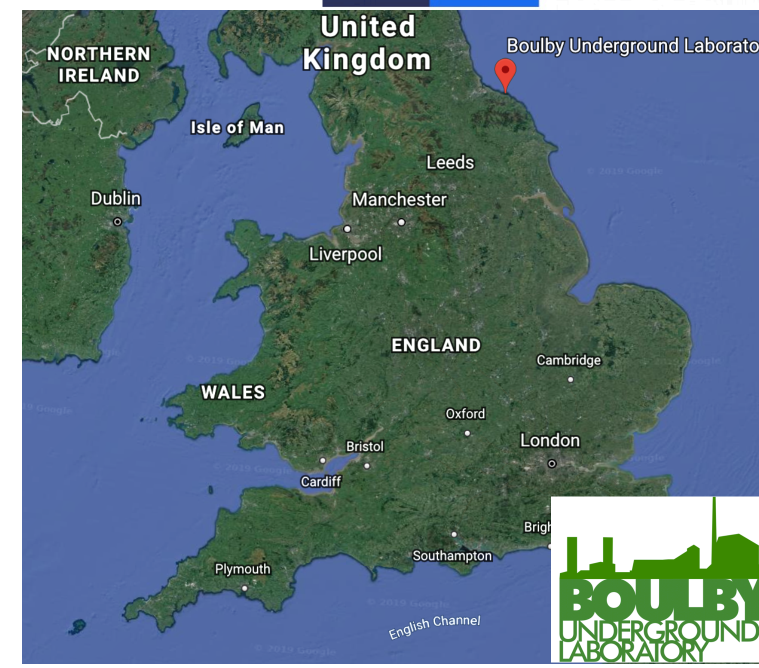

DarkSPHERE

Volume ×10: ⌀300cm intact underground electroformed spherical proportional counter with water-based shield

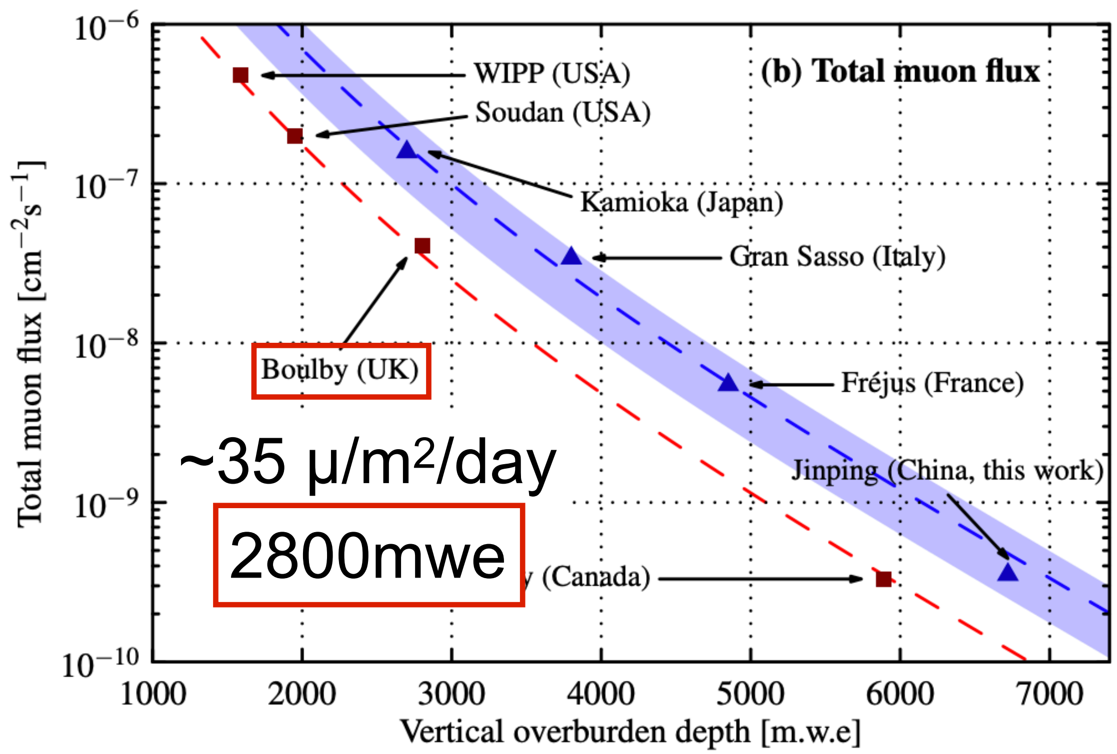

Science and Technology Facilities Council

DarkSPHERE

Volume ×10: ⌀300cm intact underground electroformed spherical proportional counter with water-based shield

UKRI Science and Technology Facilities Council

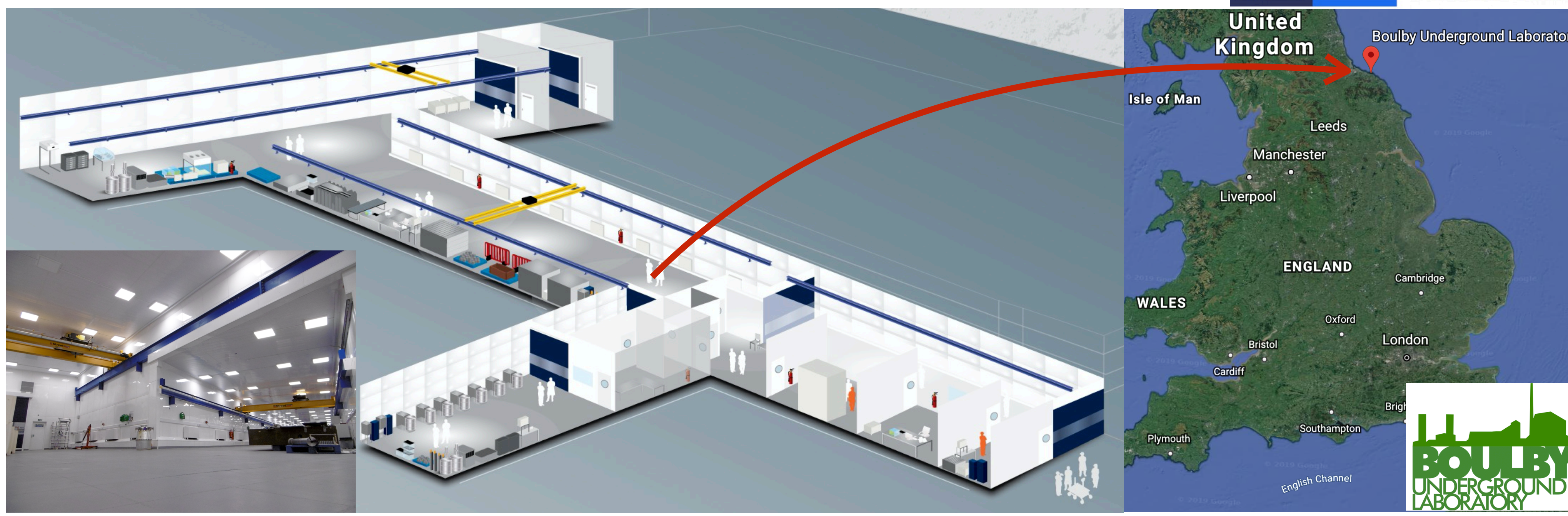

DarkSPHERE

Volume ×10: ⌀300cm intact underground electroformed spherical proportional counter with water-based shield

Science and Technology Facilities Counc

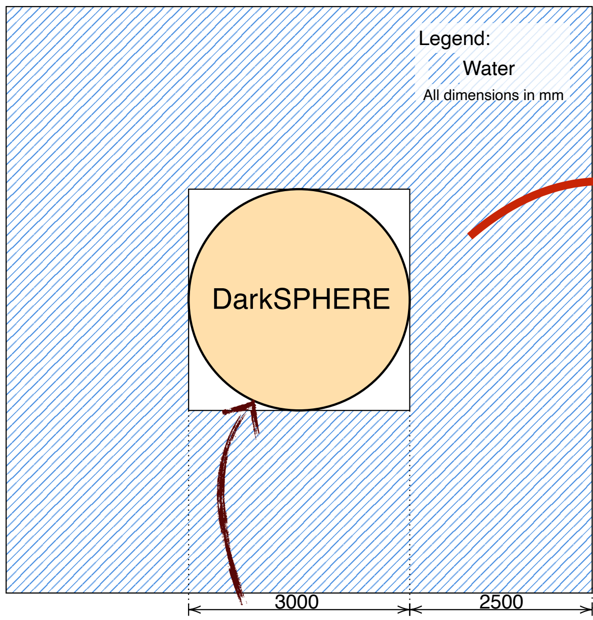

5 bar He:C_4H_{10} (90%:10%)
(27 kg target mass)

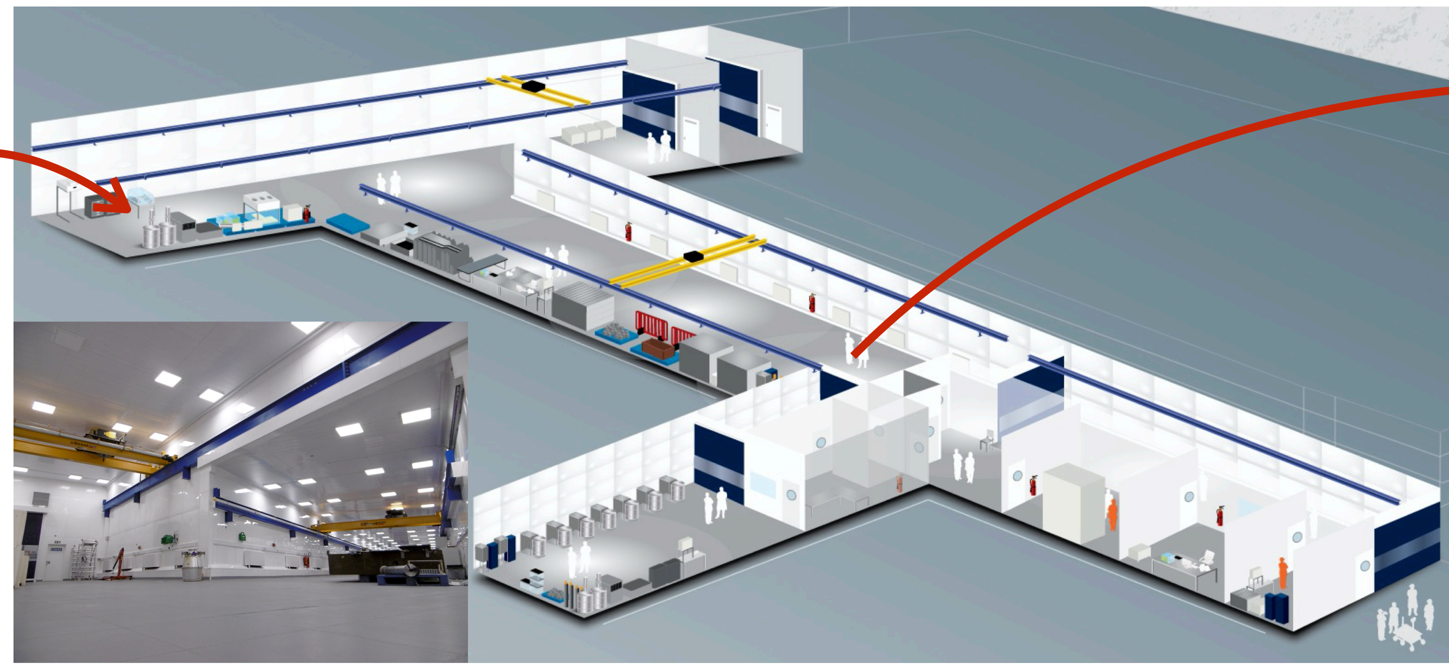

DarkSPHERE

Volume ×10: ⌀300cm intact underground electroformed spherical proportional counter with water-based shield

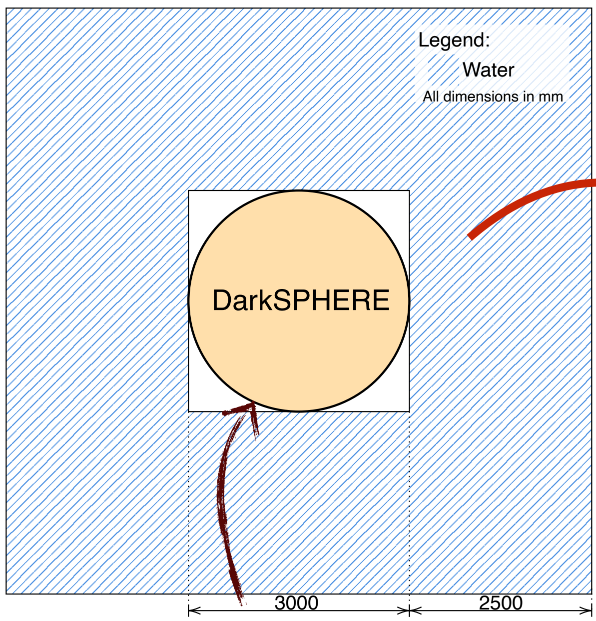

5 bar He:C_4H_{10} (90%:10%)
(27 kg target mass)

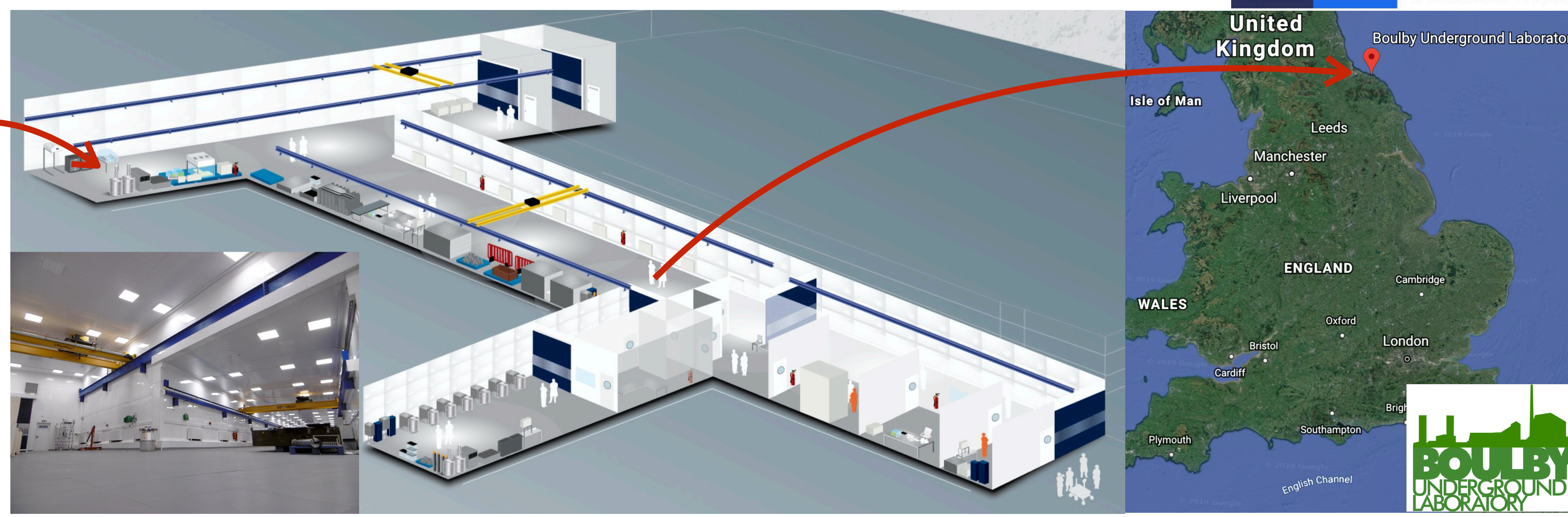

Possibility to host DarkSPHERE at Boulby's Large Experimental Cavern

- Possibility for a 8×8×8m^3 detector without further excavations
- Funding obtained for setting-up electroformation facility

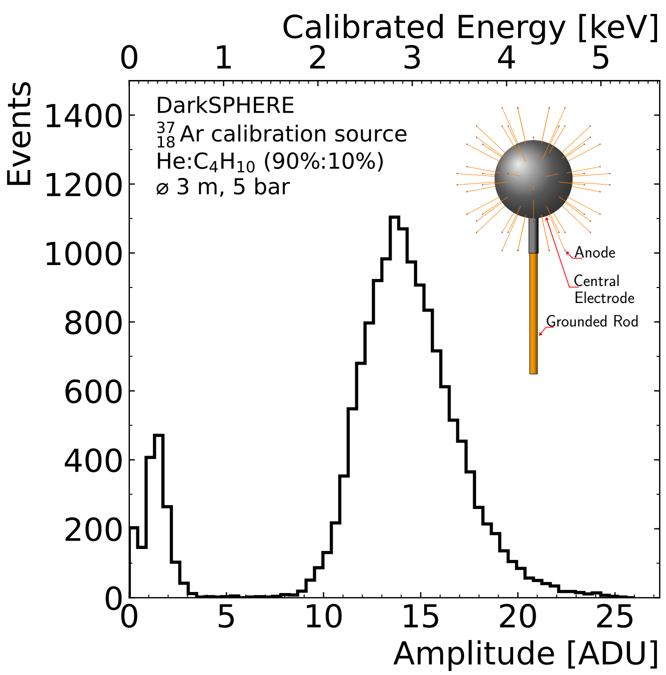

Simulation with 60-anode ACHINOS in DarkSPHERE

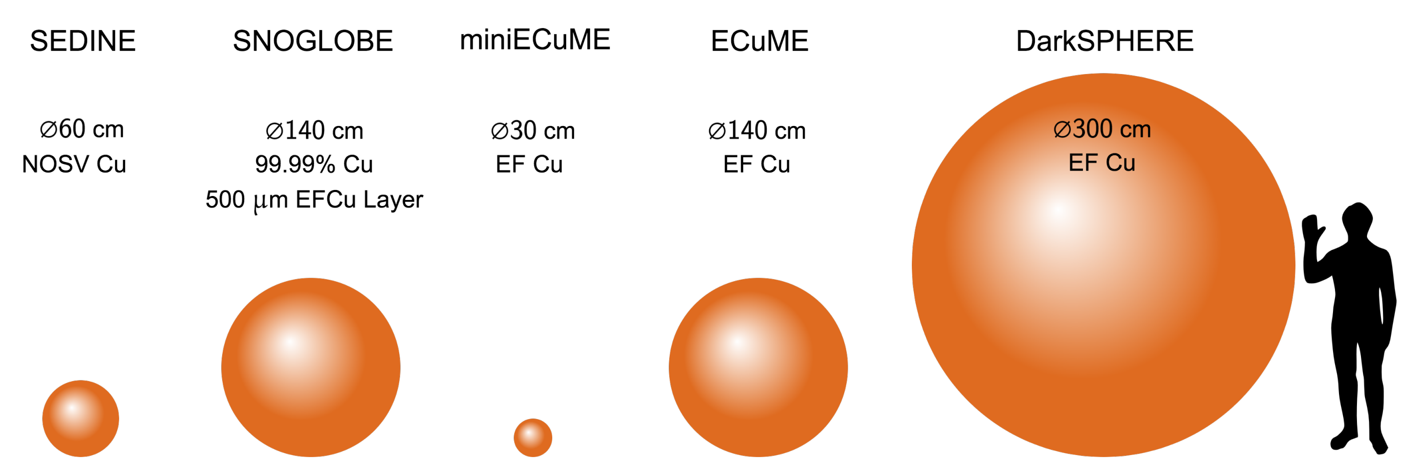

DarkSPHERE: Physics Potential

Nuclear Recoils

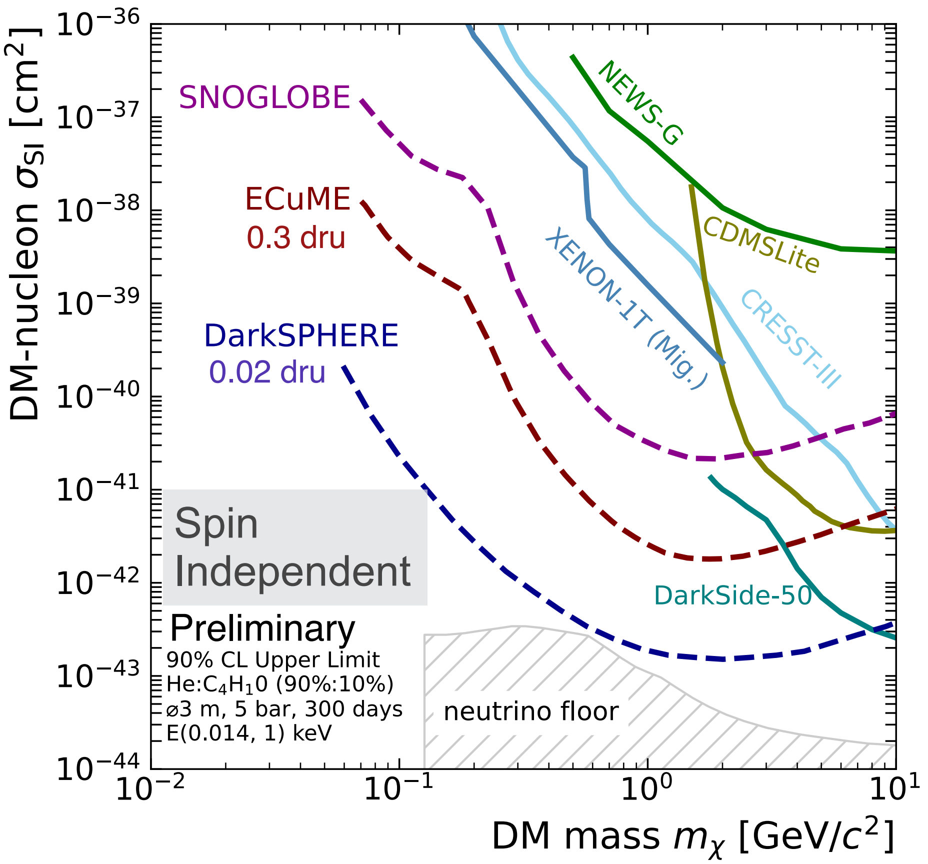

DarkSPHERE: Physics Potential

Nuclear Recoils

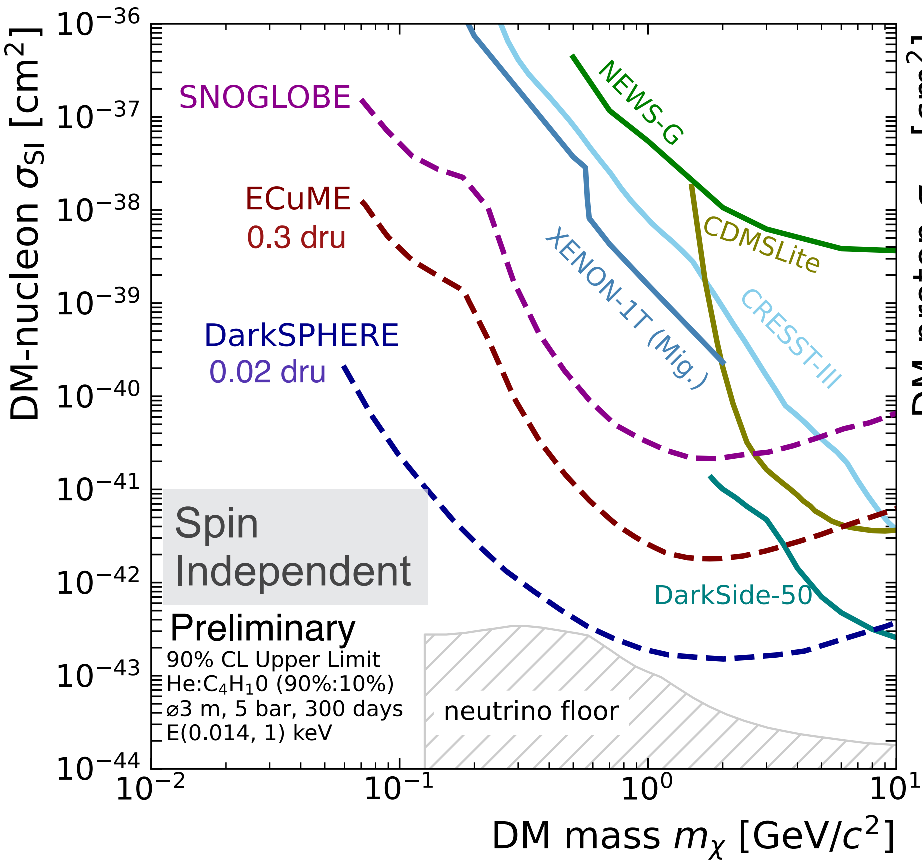

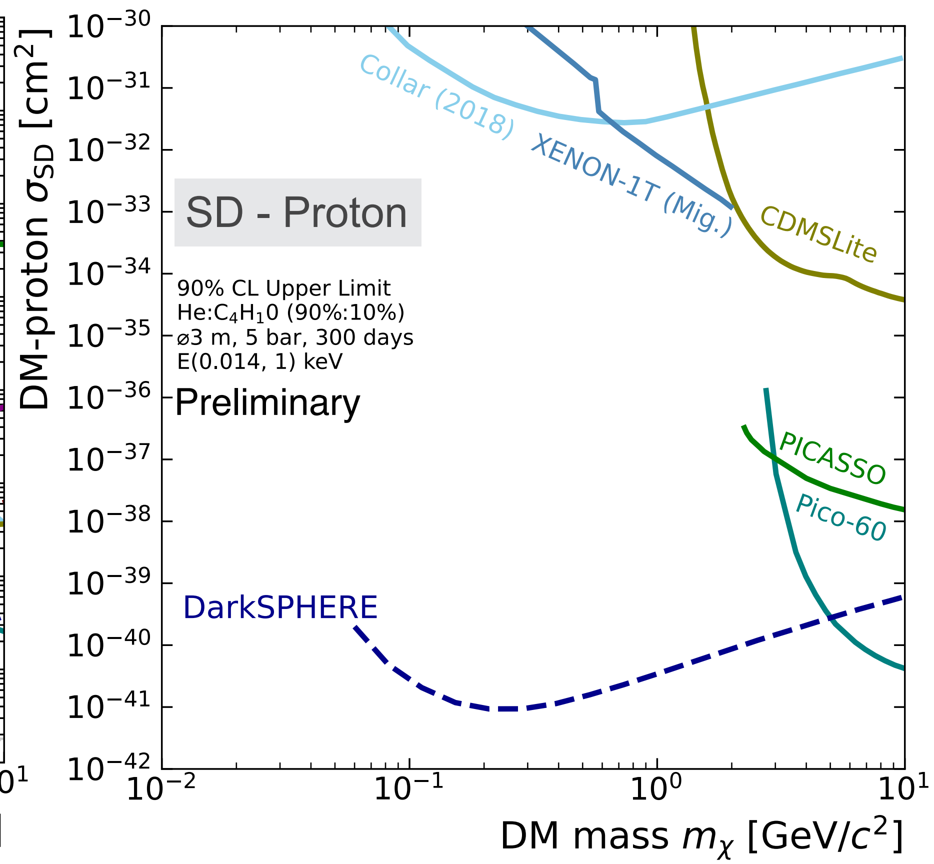

DarkSPHERE: Physics Potential

Nuclear Recoils

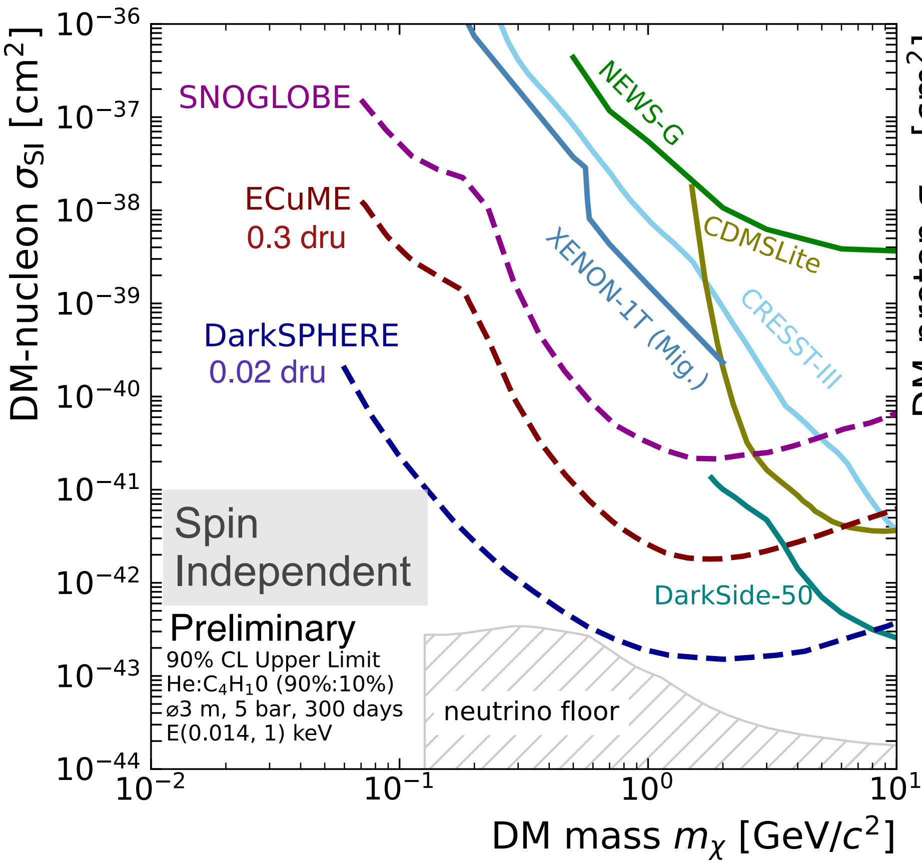

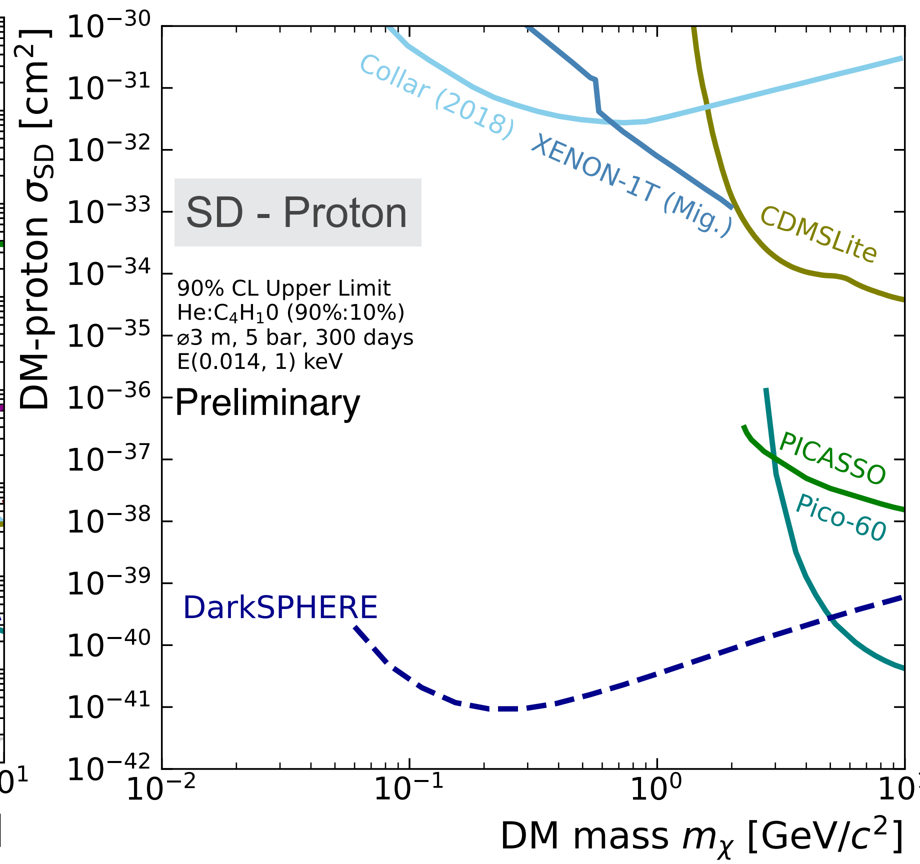

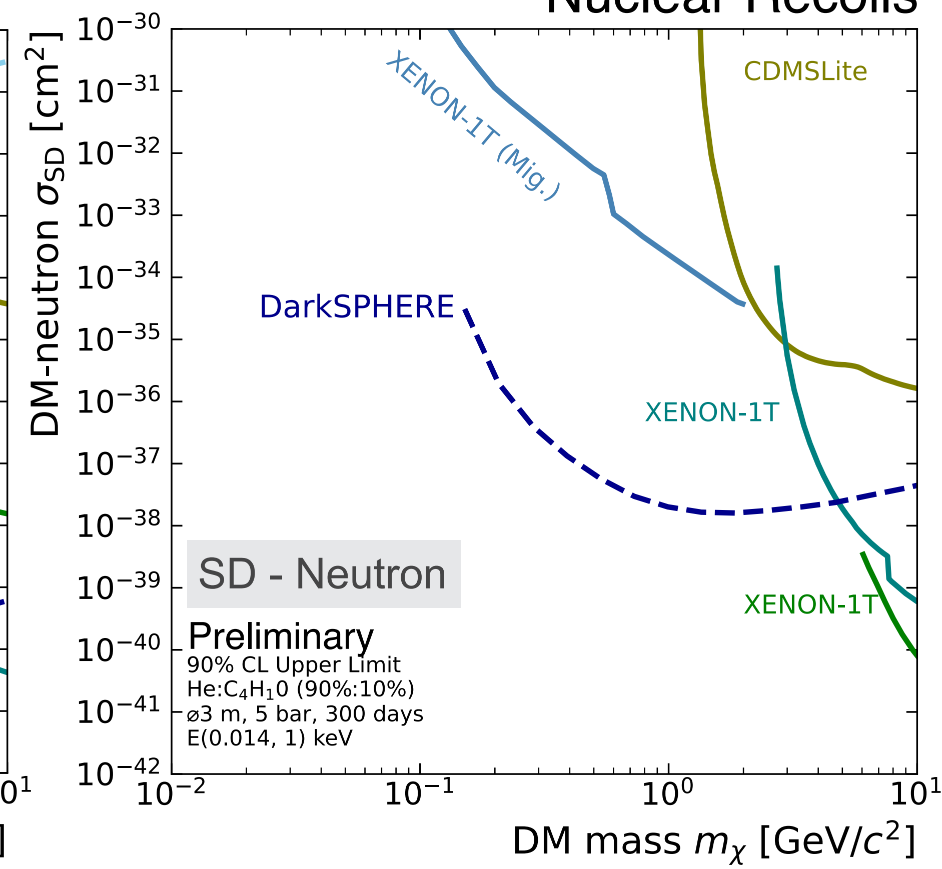

DarkSPHERE: Physics Potential

Nuclear Recoils

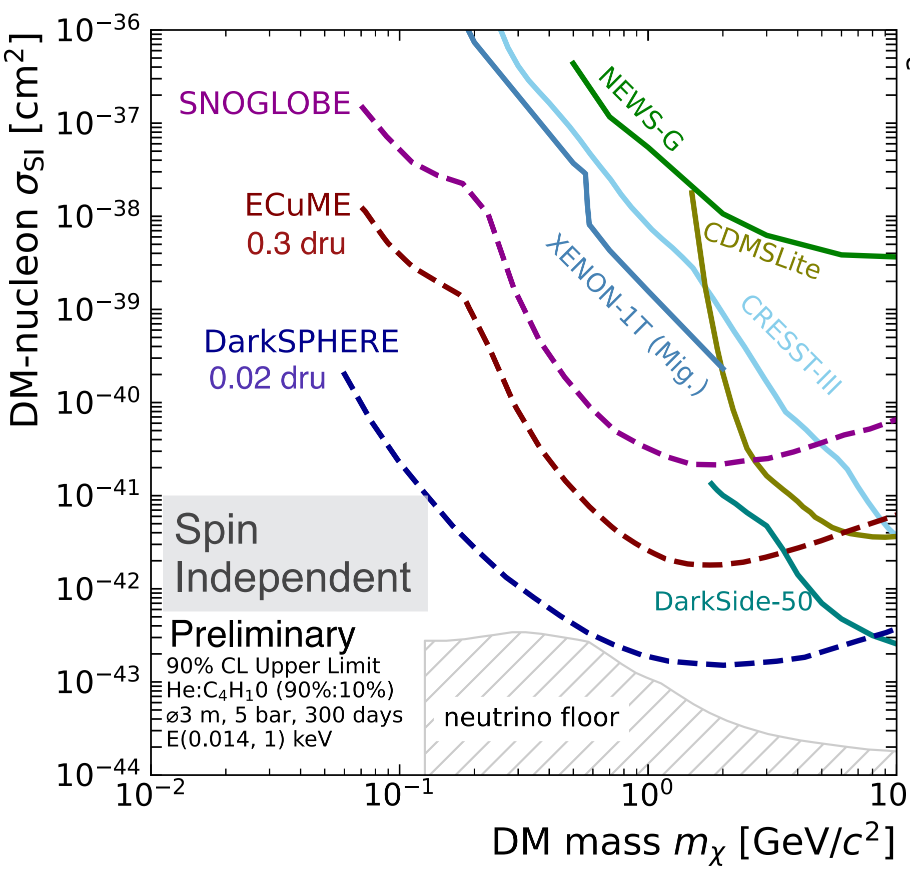

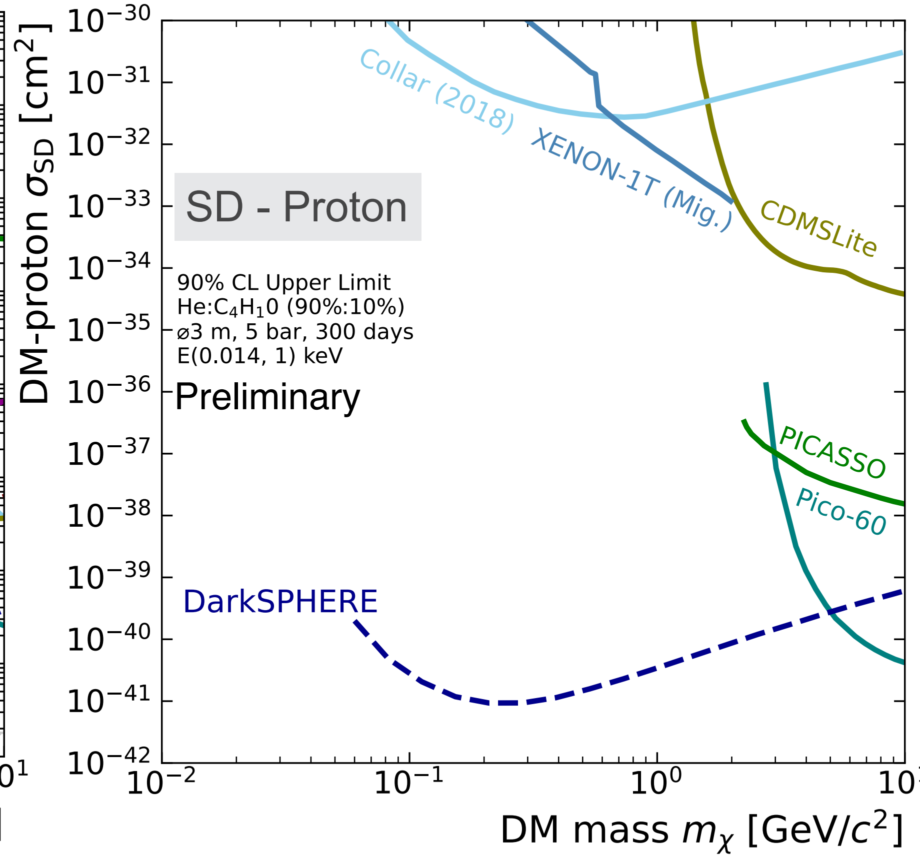

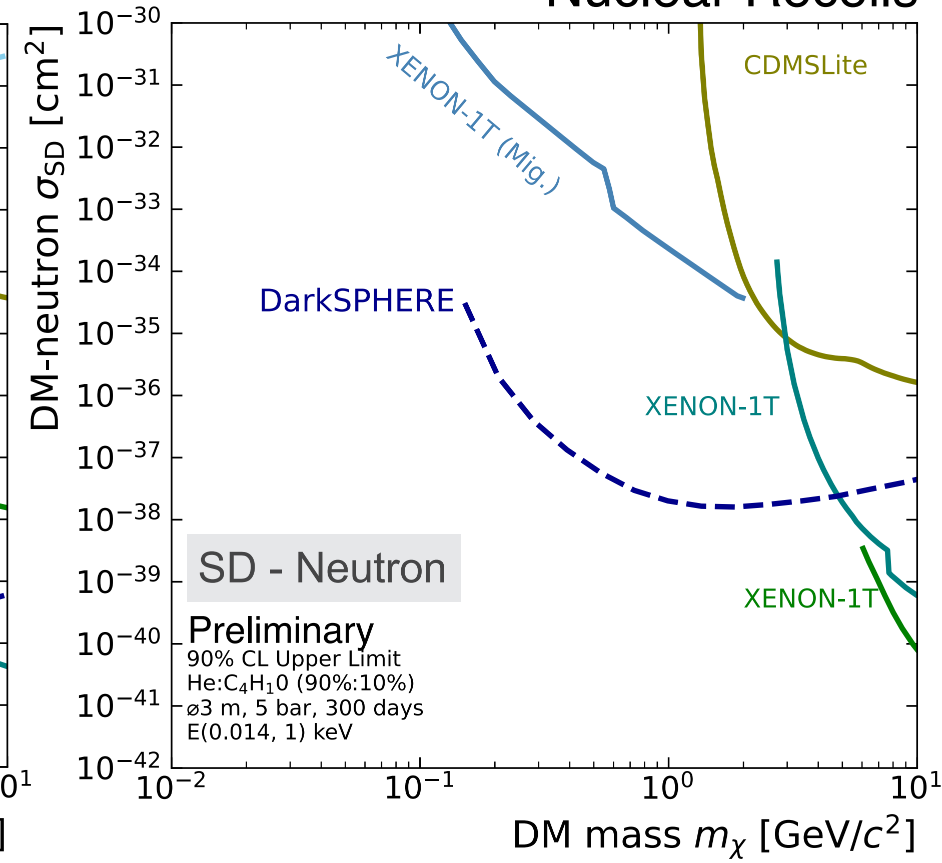

Electron Recoils

Based on arXiv:2110.02985

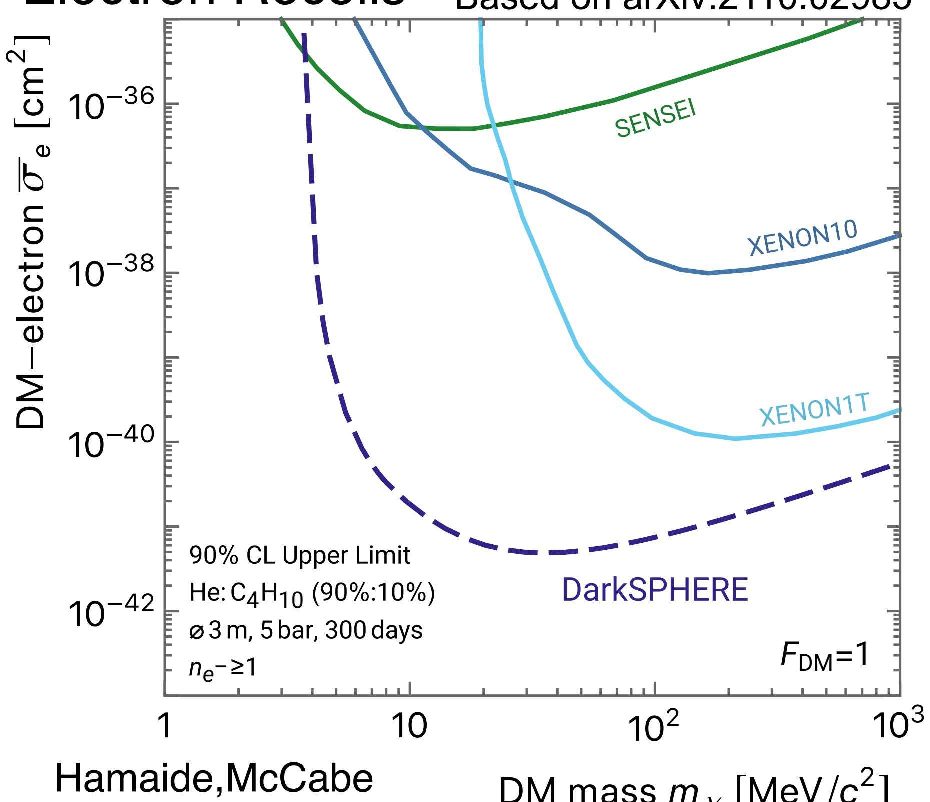

Hamaide,McCabe

DarkSPHERE: Physics Potential

Nuclear Recoils

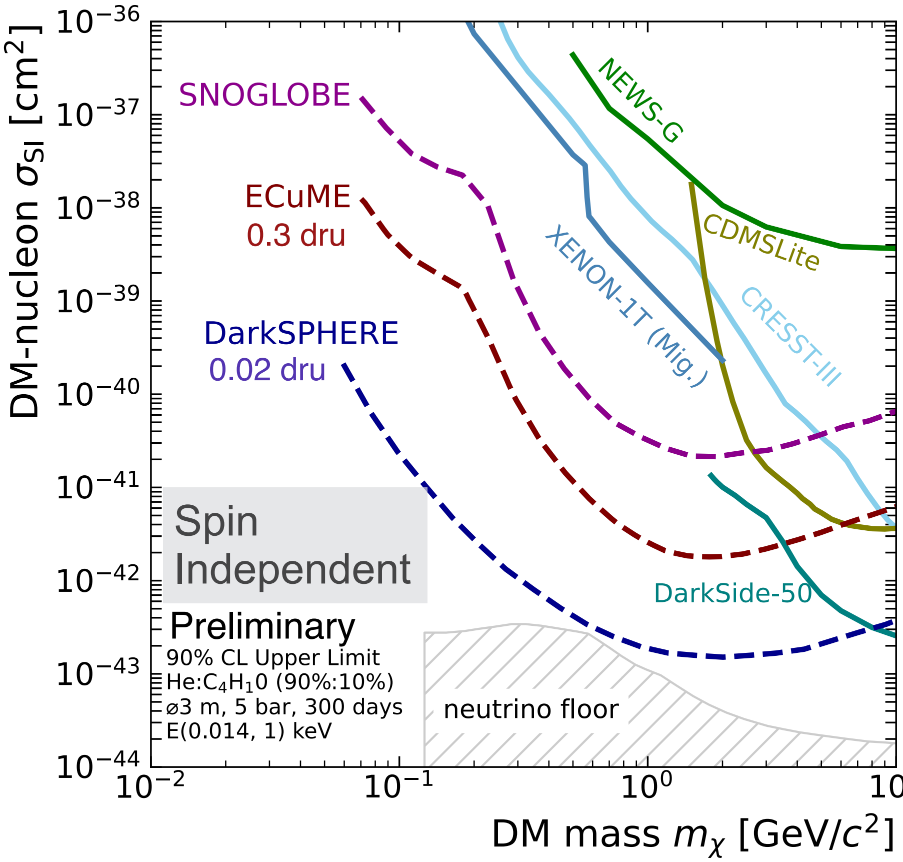

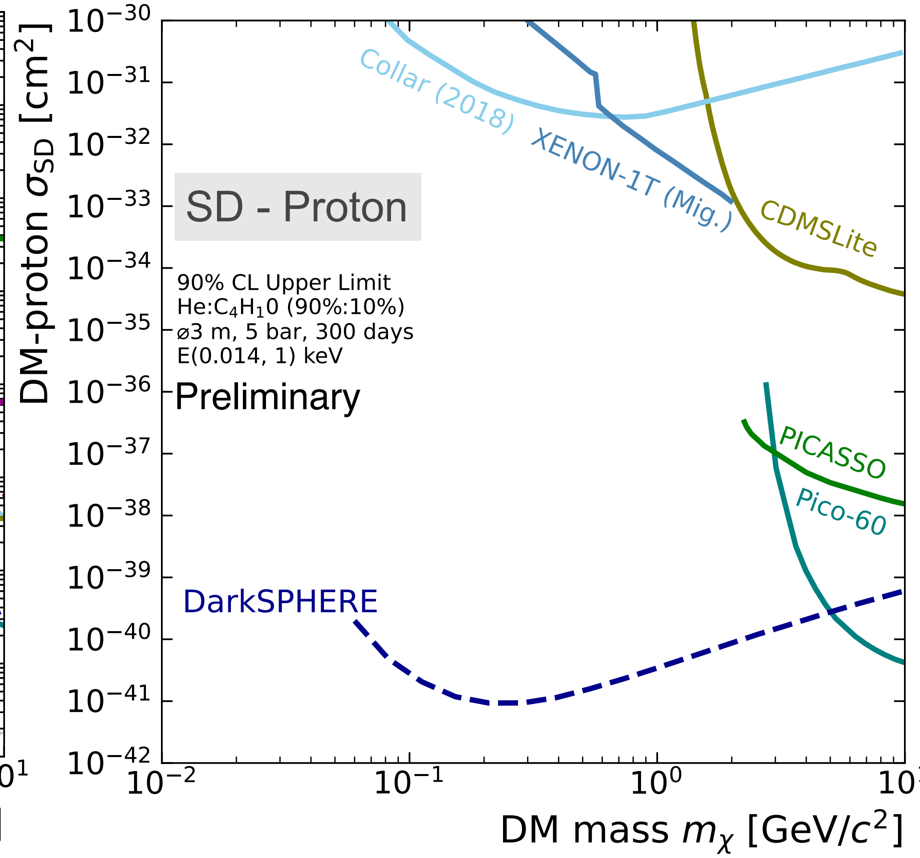

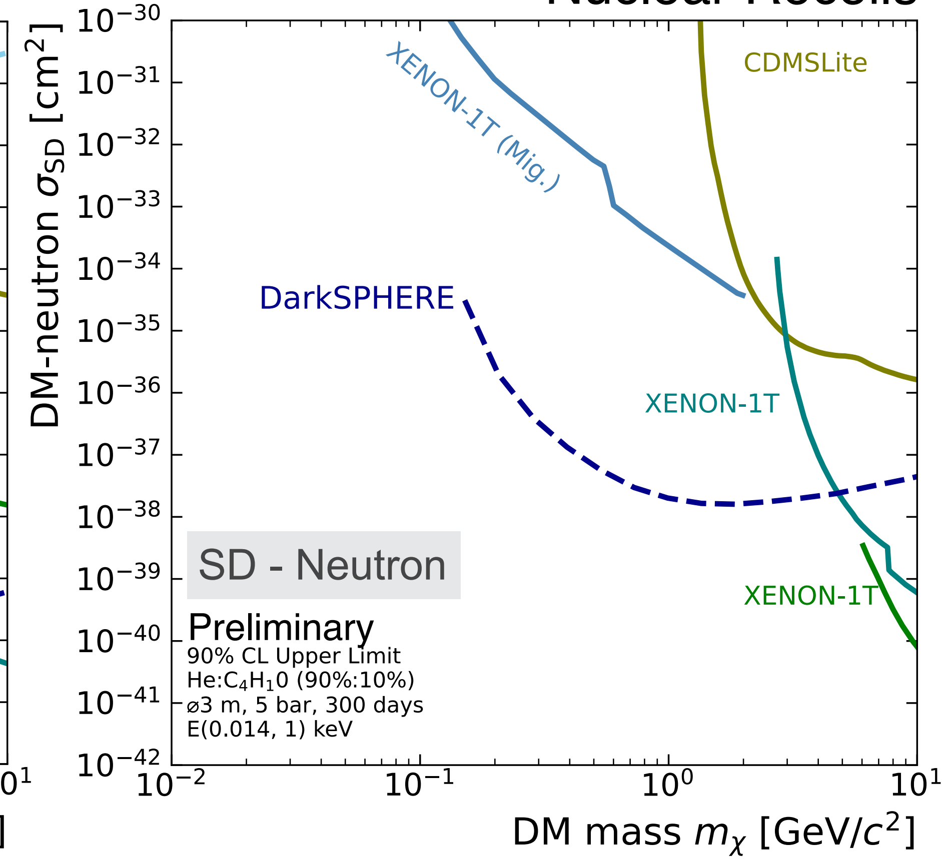

Electron Recoils

Based on arXiv:2110.02985

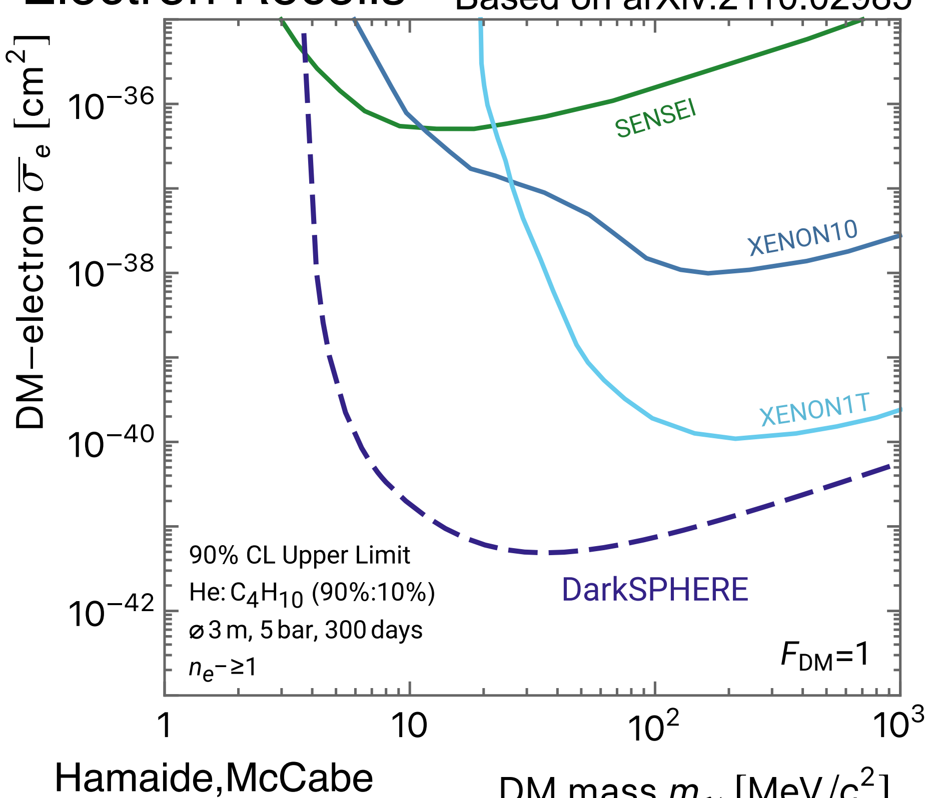

Hamaide,McCabe

DarkSPHERE has the potential to probe uncharted territory in light Dark Matter searches

- Nuclear recoils: Spin-independent and spin-dependent
- Electron recoils

DarkSPHERE: Physics Potential

Nuclear Recoils

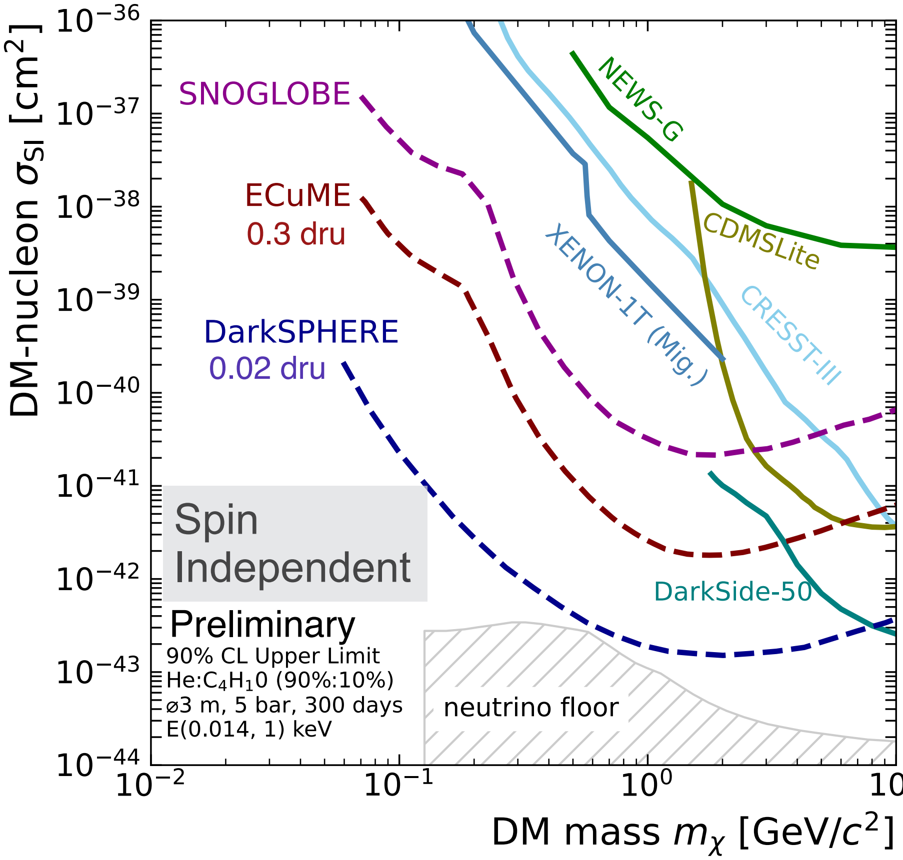

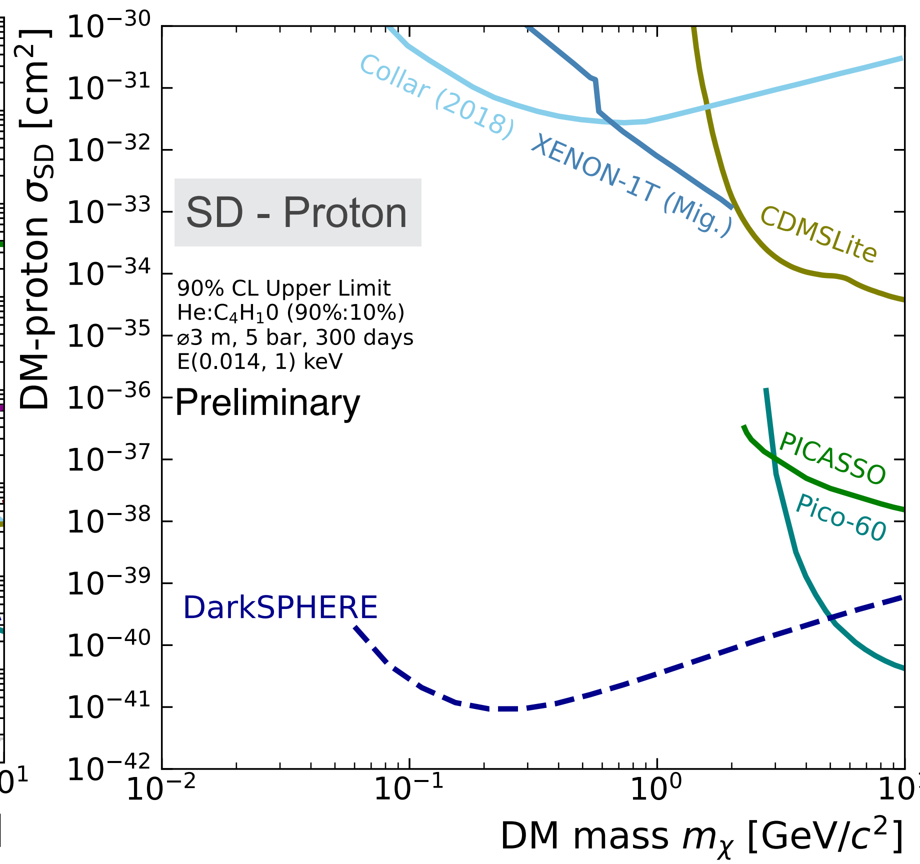

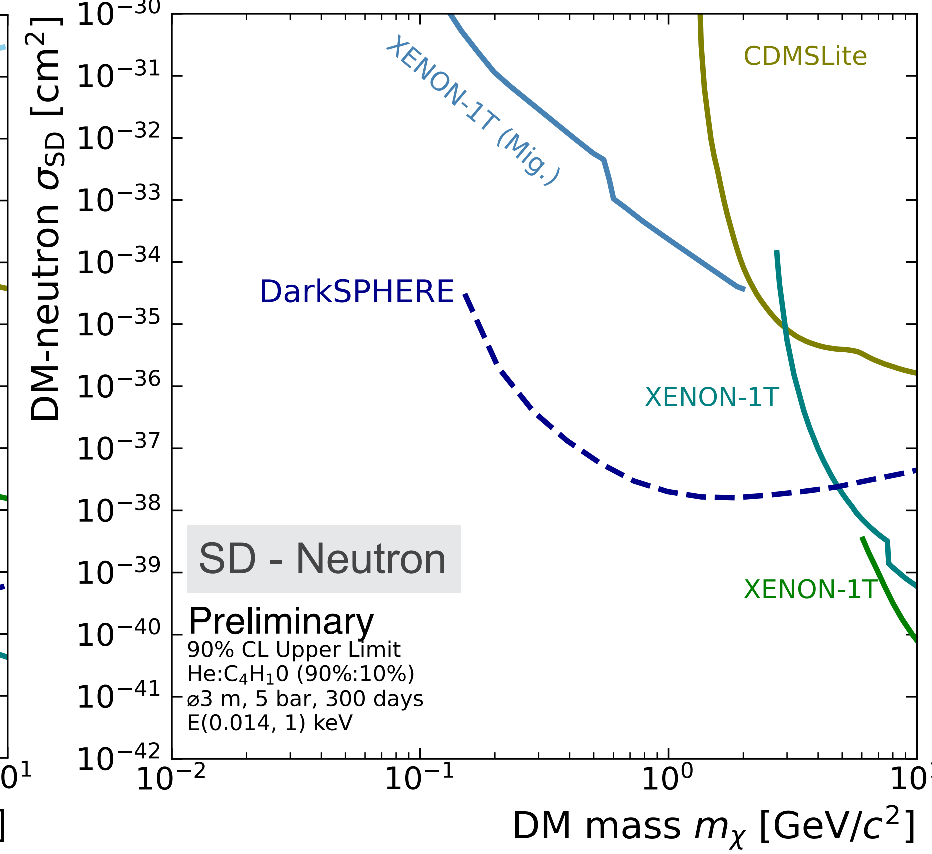

Electron Recoils

Based on arXiv:2110.02985

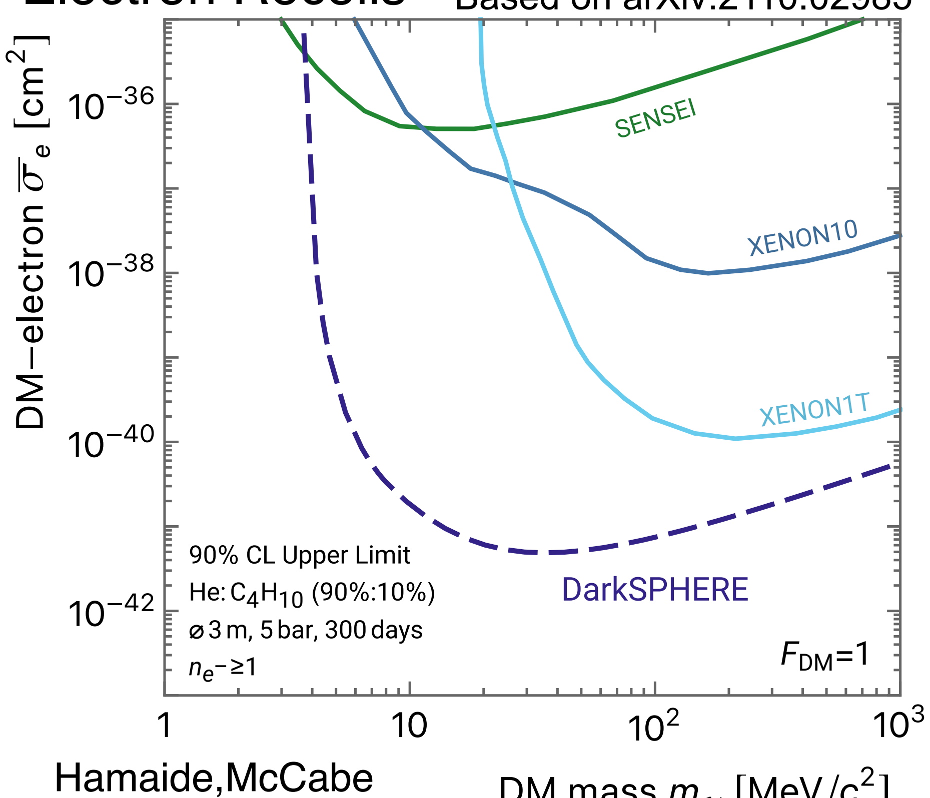

Hamaide,McCabe

DarkSPHER
in light Dark
- Nuclear re
- Electron re

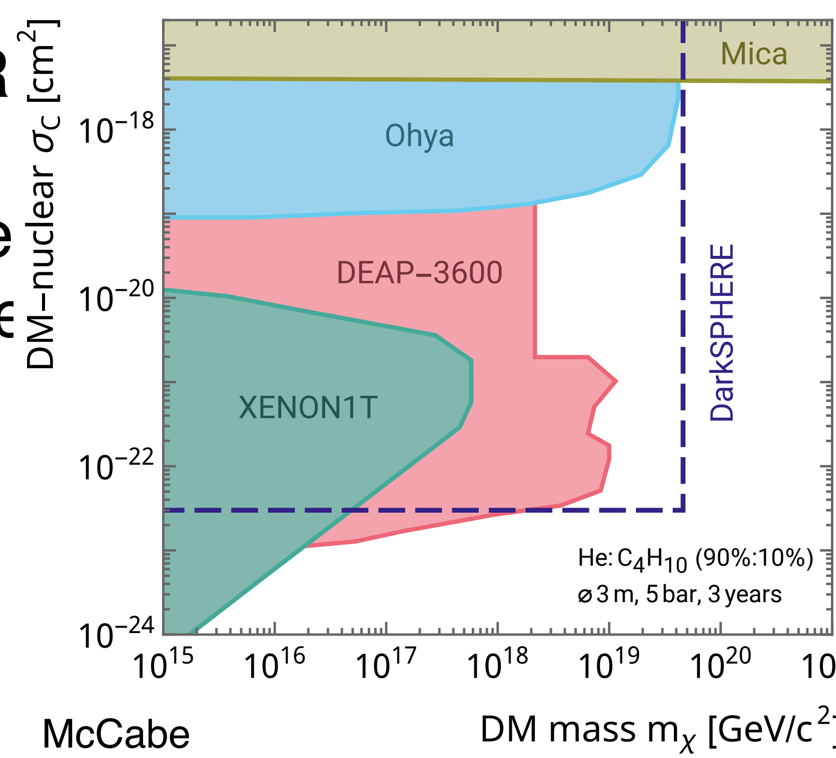

McCabe

uncharted territory

spin-dependent

Atypical searches: Solar Kaluza-Klein axions

- Kaluza-Klein axions produced in the sun
  - Gravitationally bound to the solar system
  - Potential explanation to:
    - Corona heating problem
    - Observed X-rays
  - Decays to two photons

Phys.Rev.D 105 (2022) 1, 012002

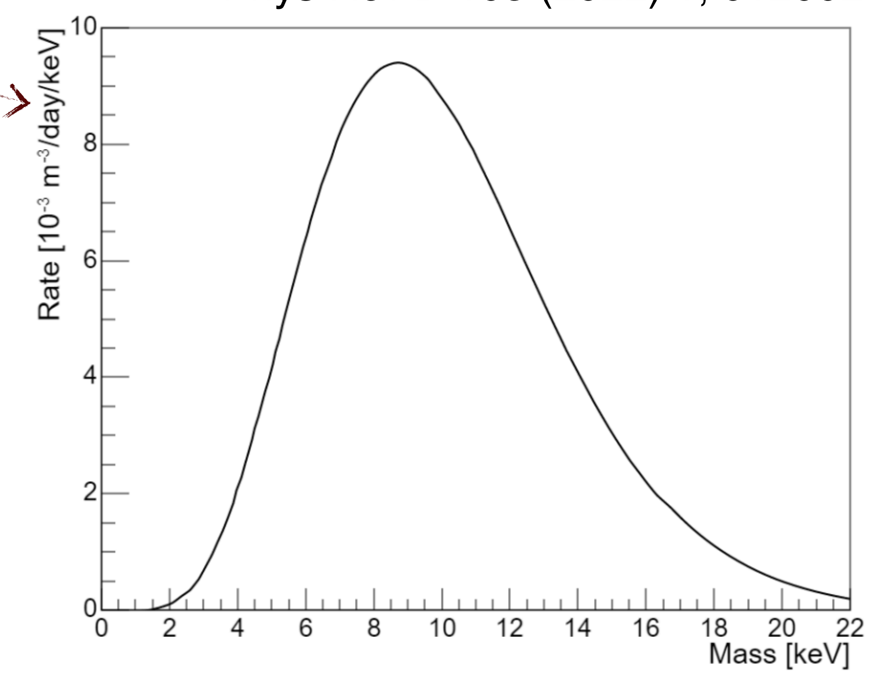

Atypical searches: Solar Kaluza-Klein axions

- Kaluza-Klein axions produced in the sun
  - Gravitationally bound to the solar system
  - Potential explanation to:
    - Corona heating problem
    - Observed X-rays
  - Decays to two photons

Phys.Rev.D 105 (2022) 1, 012002

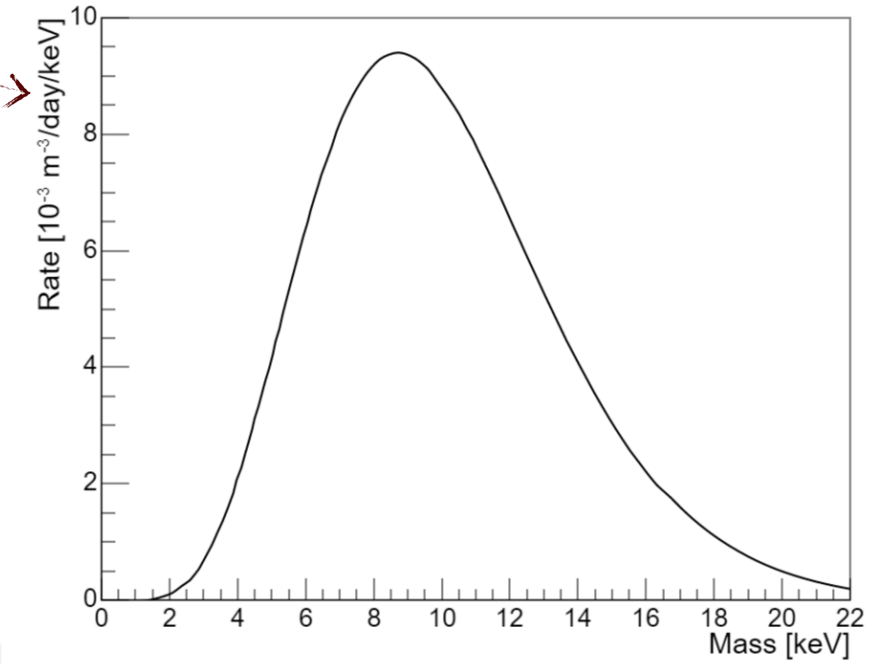

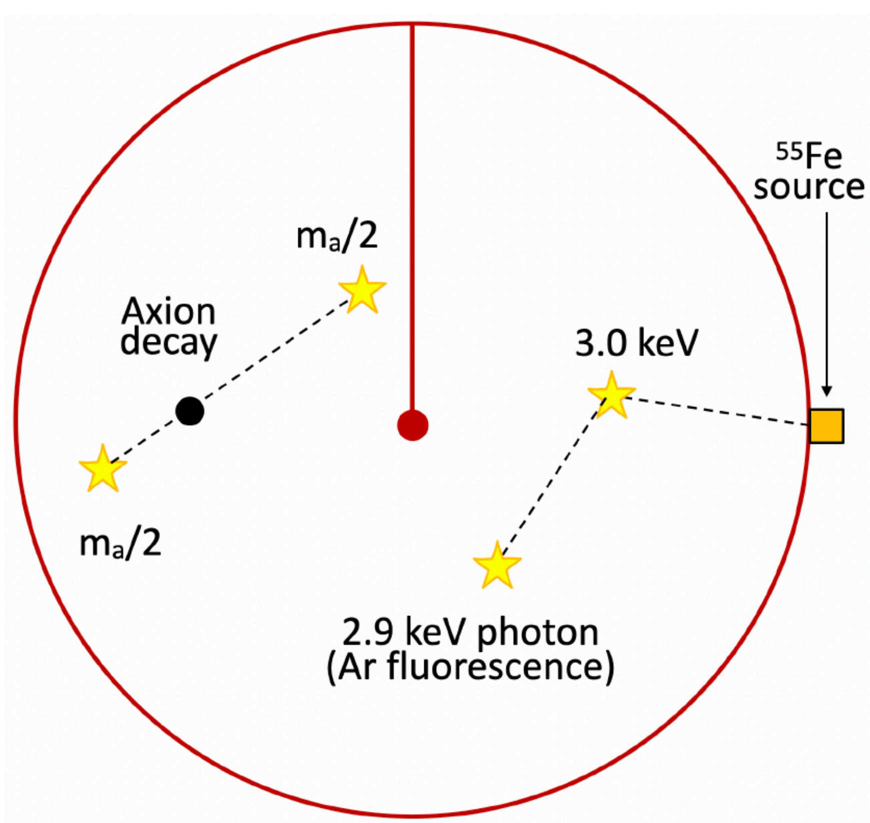

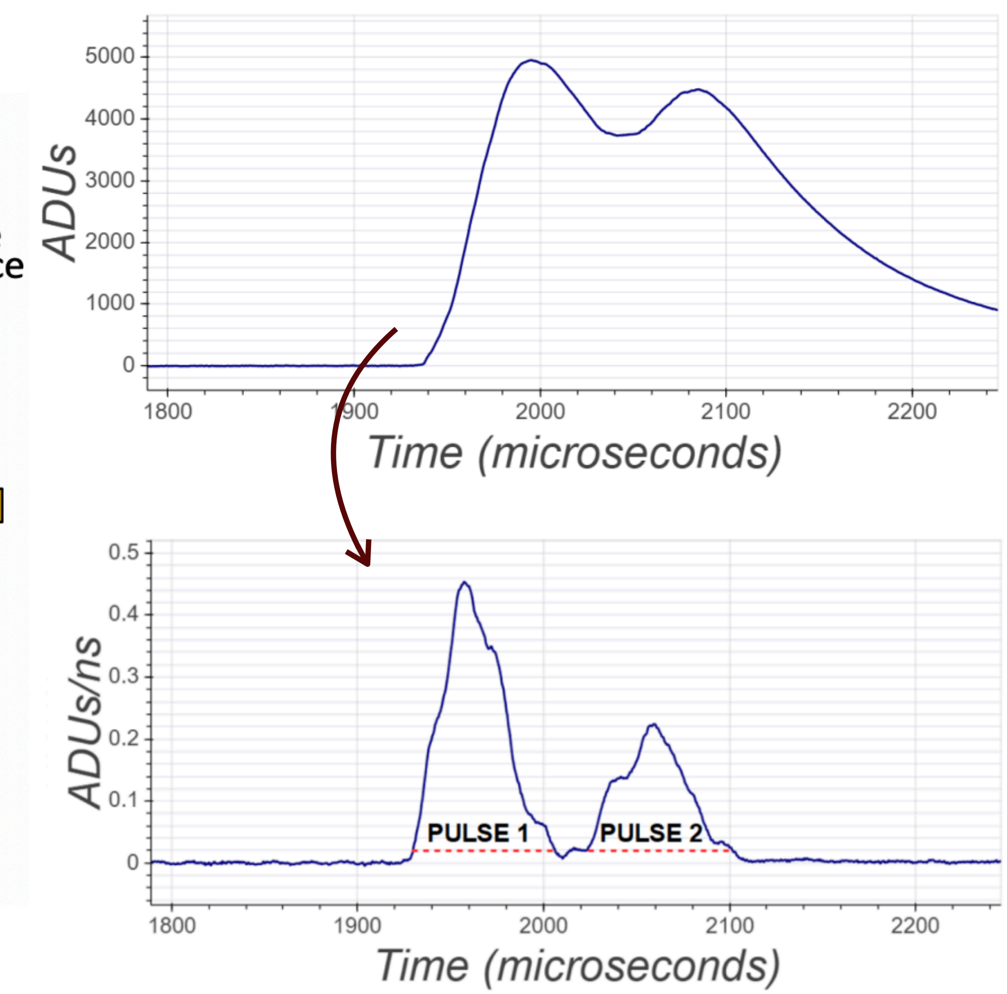

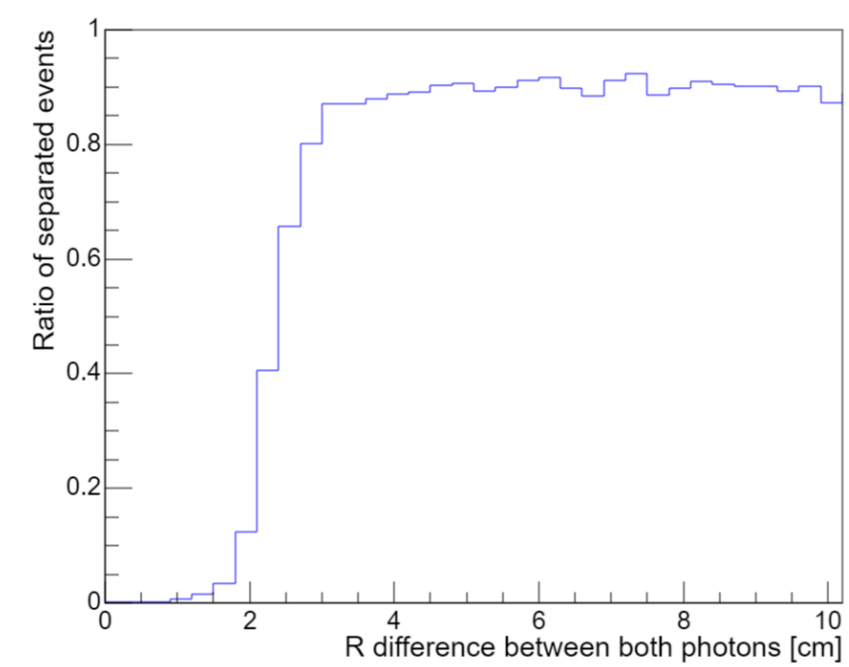

Atypical searches: Solar Kaluza-Klein axions

- Exposure: $4.3\ \mathrm{day} \cdot \mathrm{m}^3$
- Ne:CH_4(0.7%) at 3.1 bar

Phys.Rev.D 105 (2022) 1, 012002

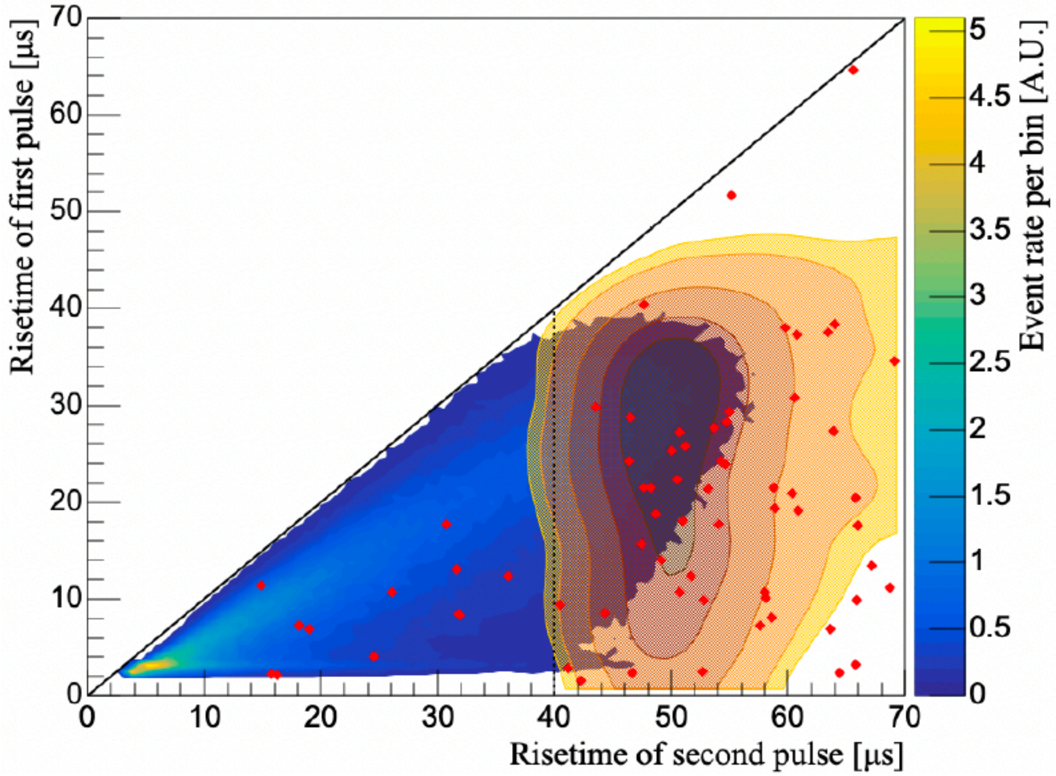

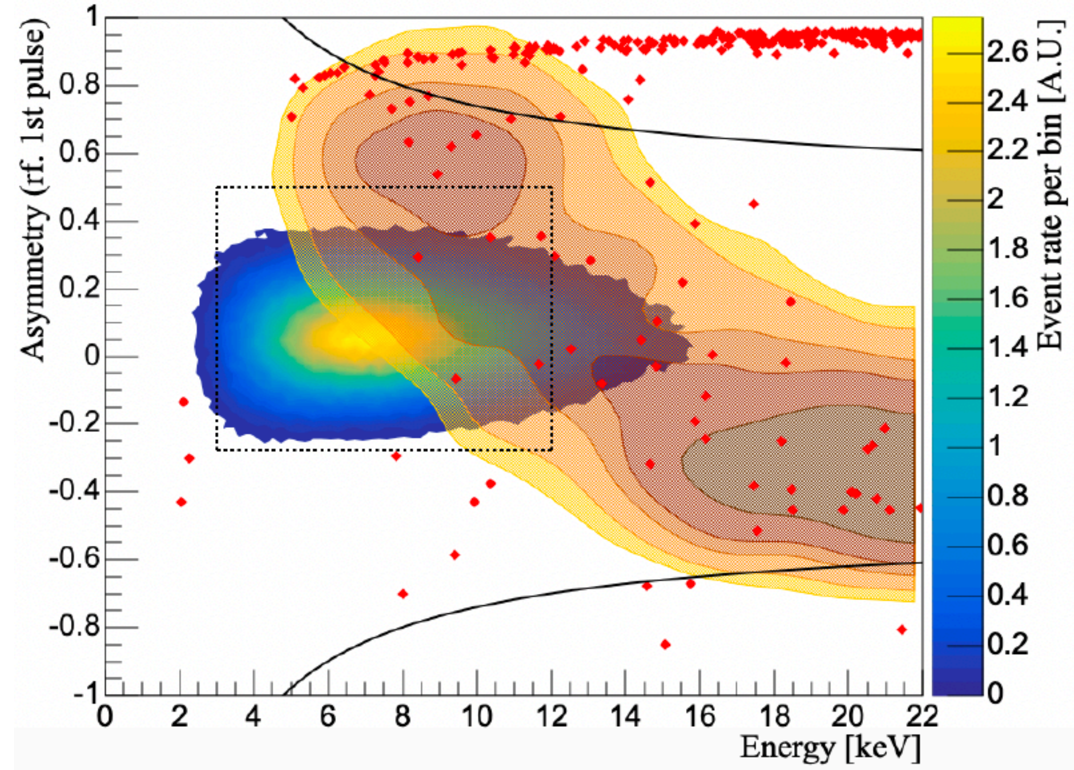

Atypical searches: Solar Kaluza-Klein axions

- Exposure: $4.3\ \text{day} \cdot \text{m}^3$
- Ne:CH_4(0.7%) at 3.1 bar

Phys.Rev.D 105 (2022) 1, 012002

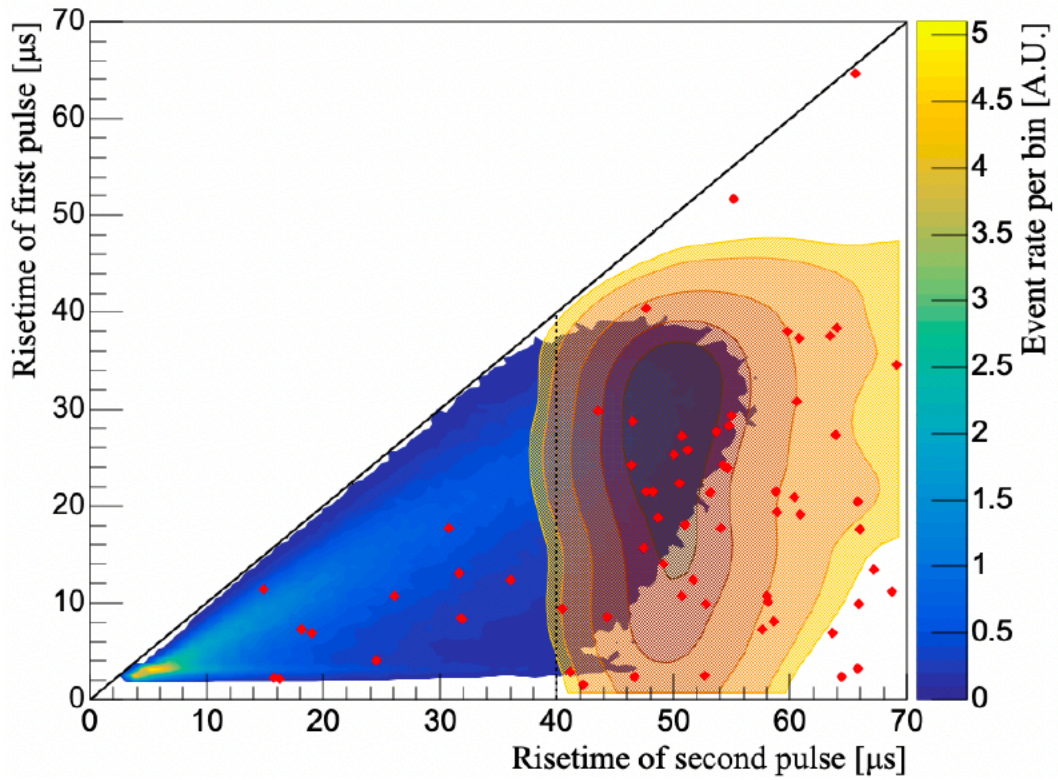

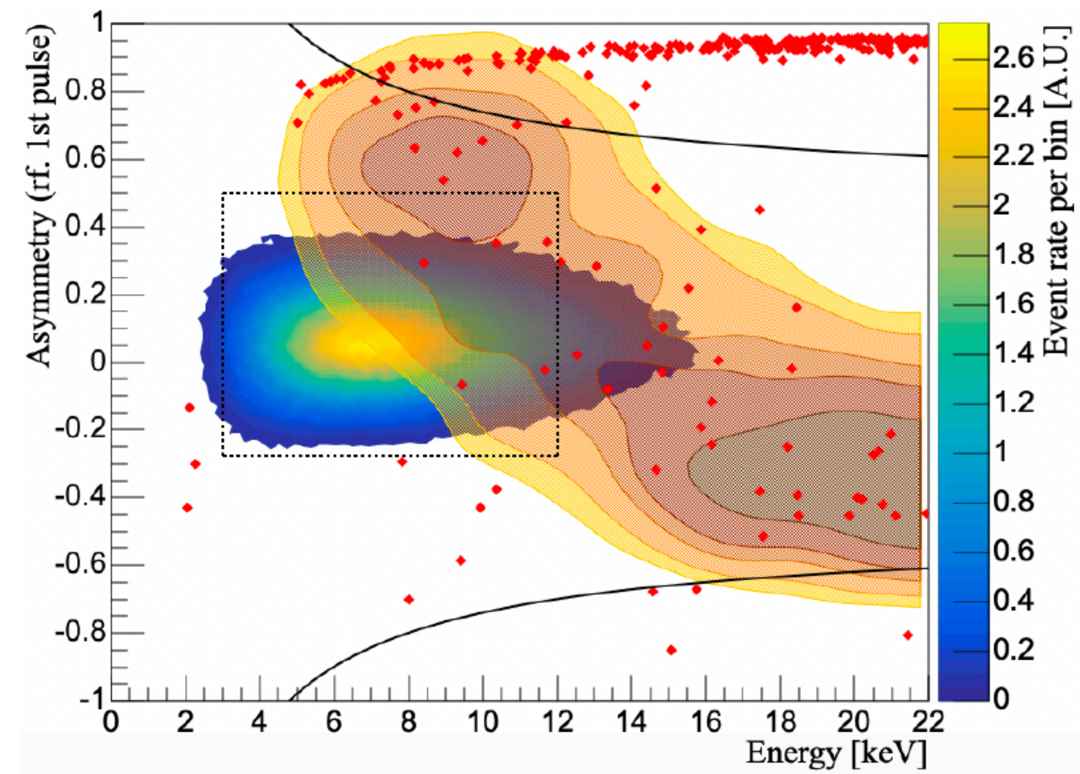

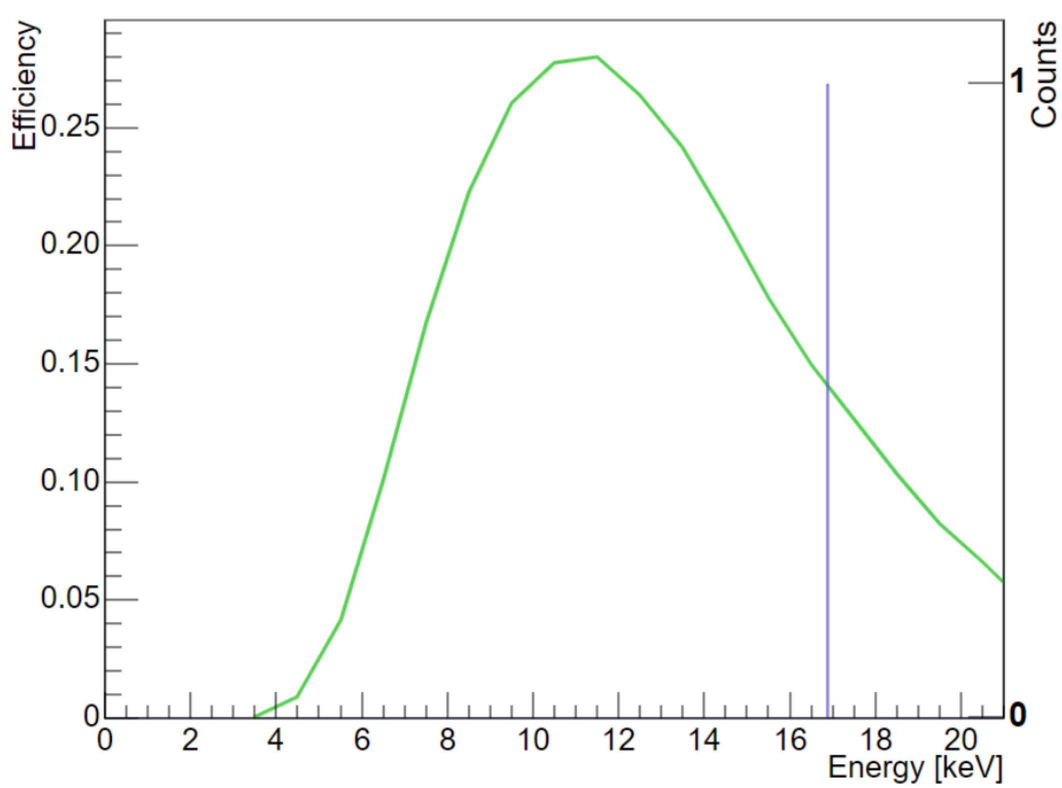

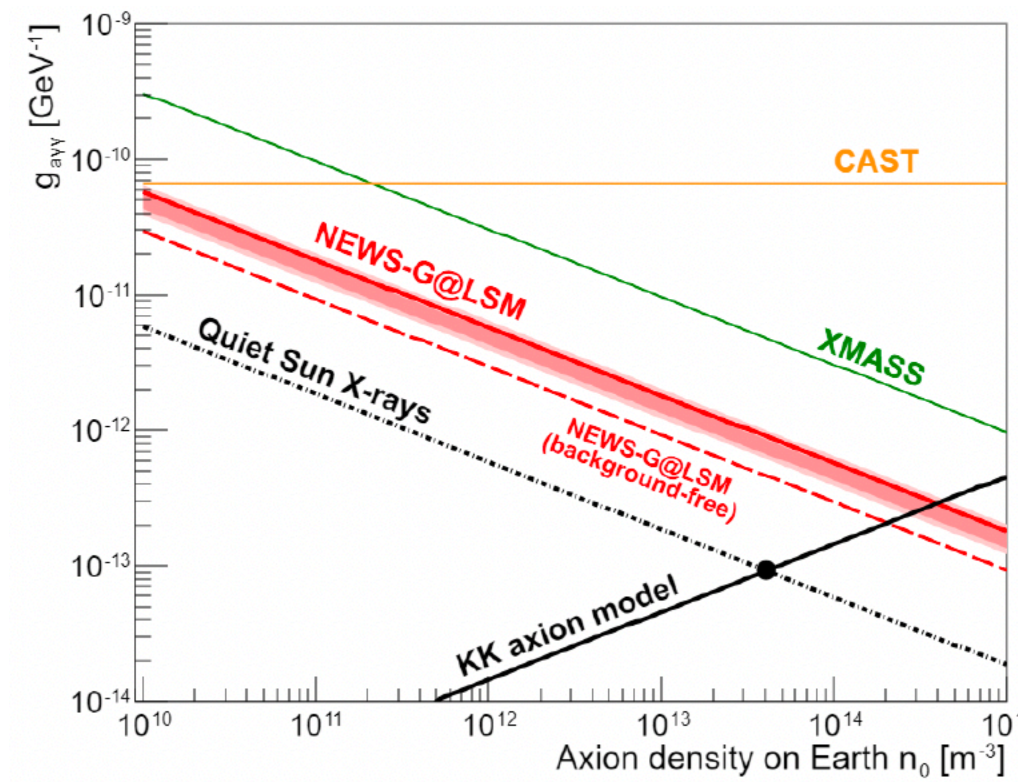

Coherent Elastic ν-Nucleus Scattering

- **CEνNS opens a window to investigation non-standard neutrino interactions**
  - First observations by COHERENT in NaI (2017) and Ar (2020)
  - Unique complementarity with DM searches as sensitivity reaches the neutrino floor
- **NEWS-G3: A low-threshold low-background sea-level facility**
  - Environmental and cosmogenic background studies towards reactor CEνNS studies
  - Shielding: Layers of pure copper, polyethylene, and lead, with active muon veto
  - Commissioning in 2021

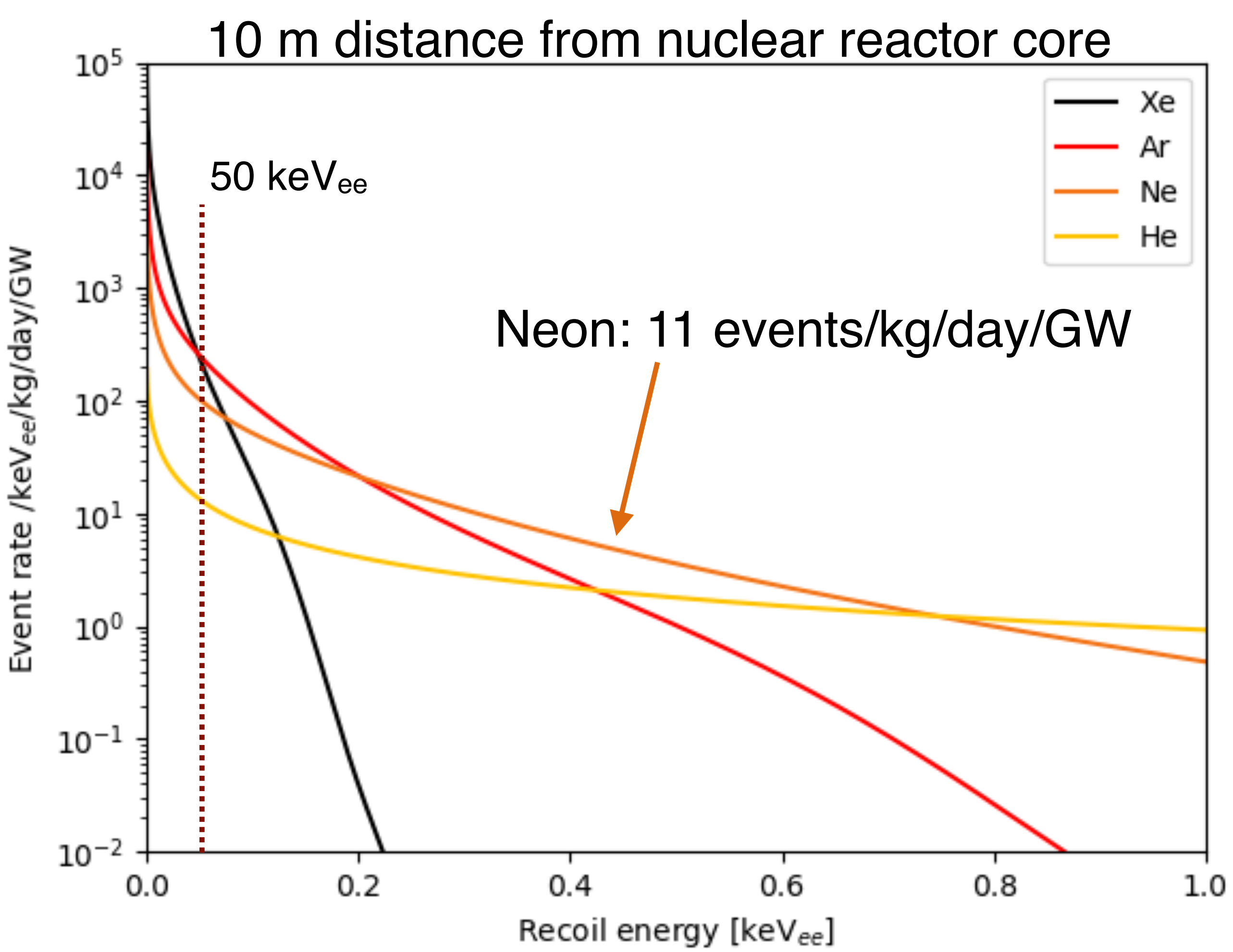

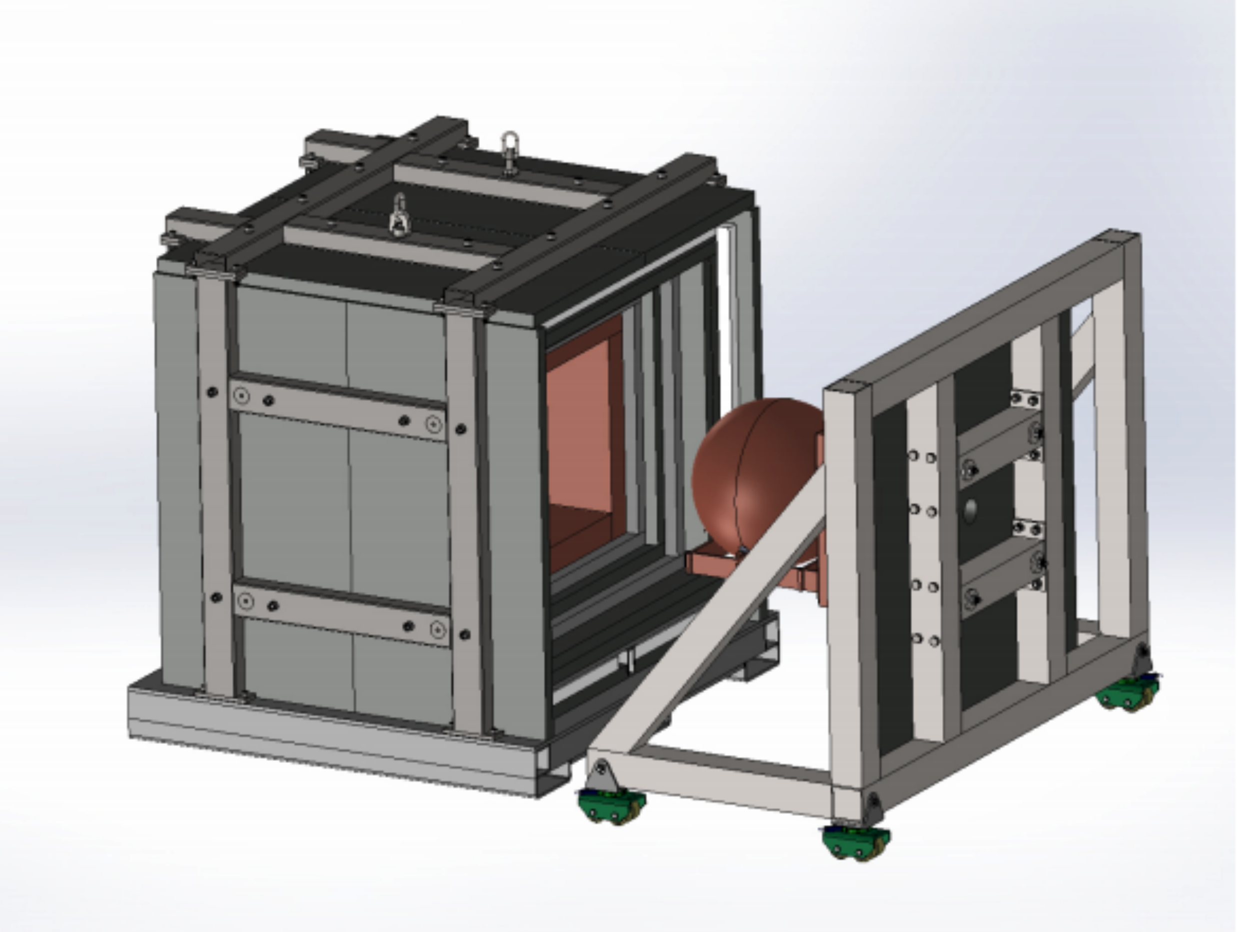

Summary

Particle nature of Dark Matter is unknown!

- Sub-GeV mass range is uncharted territory

NEWS-G probes this key mass range

- Enabled by instrumentation advances
- New detectors planned for the coming years
- Many physics opportunities
- Eventually sensitivity could reach neutrino floor

Exciting physics programme ahead!

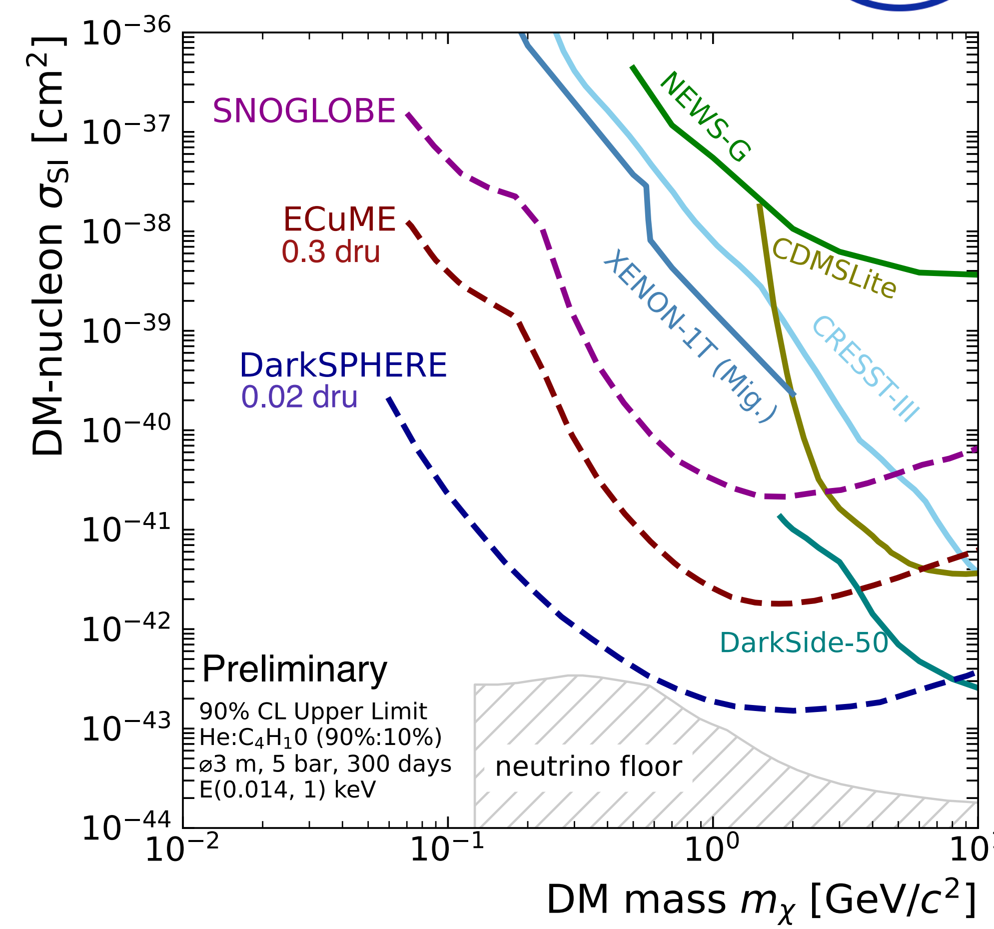

ECuME

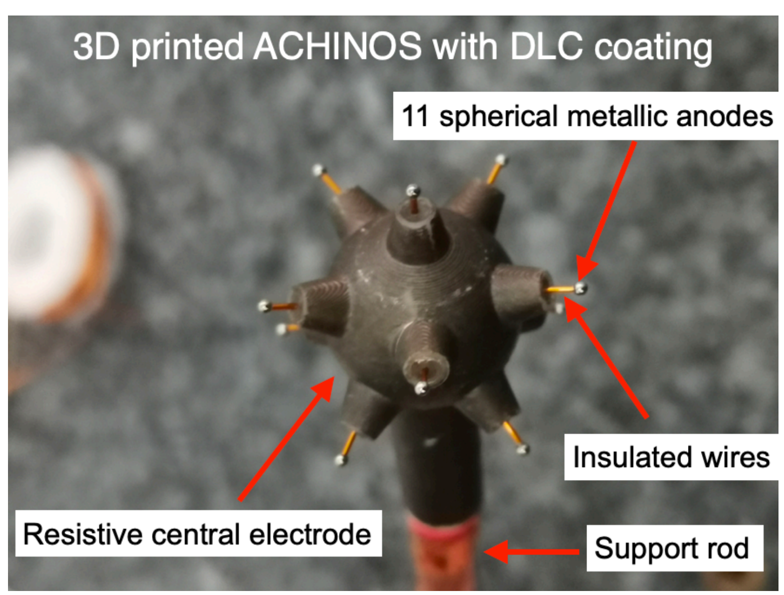

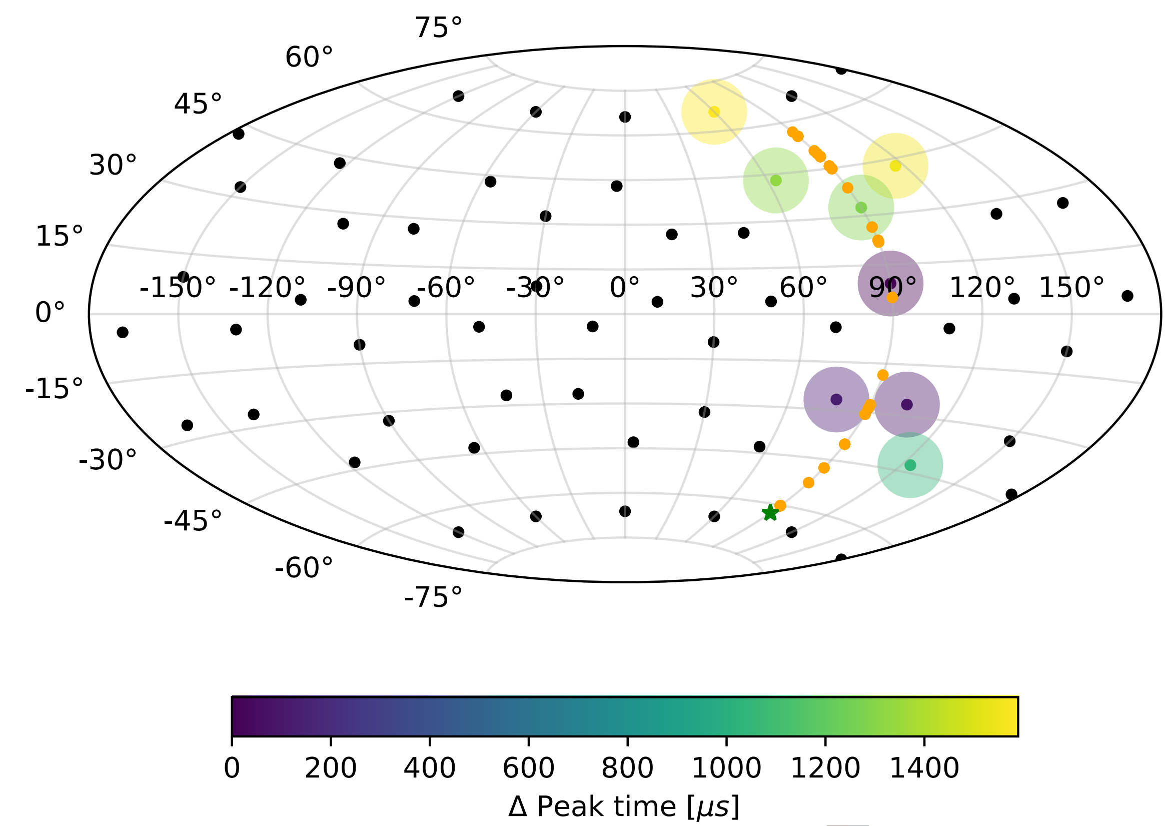

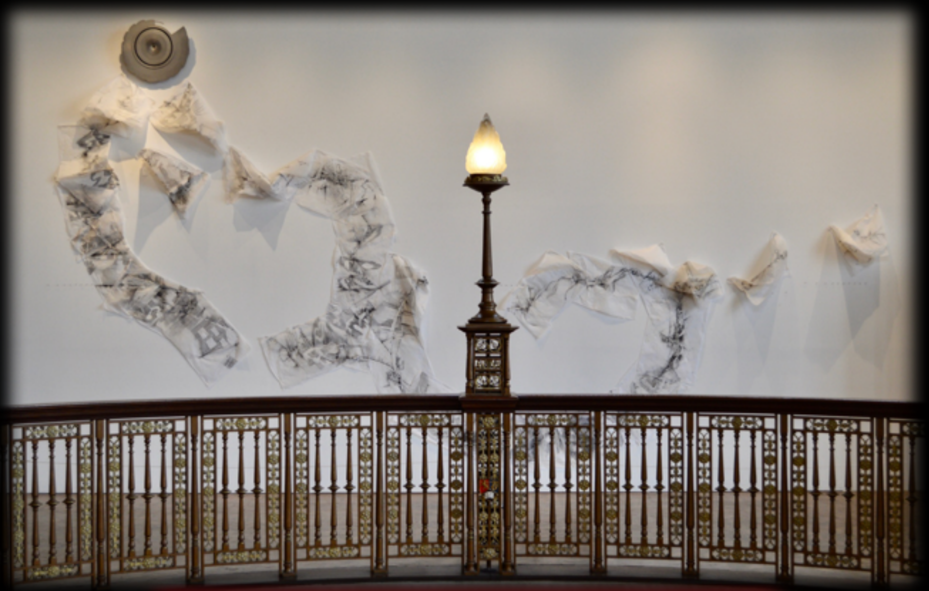


Volume 53 Number 5 September 2018
ISSN 0031-9120
Physicseducation
iopscience.org/physed
Picturing the invisible
Making sense of particle physics through art
Papers: Mercury, Pendulums Frontline: Kahoot!
IOP Publishing

Additional Slides

The Halo Model in the era of Gaia

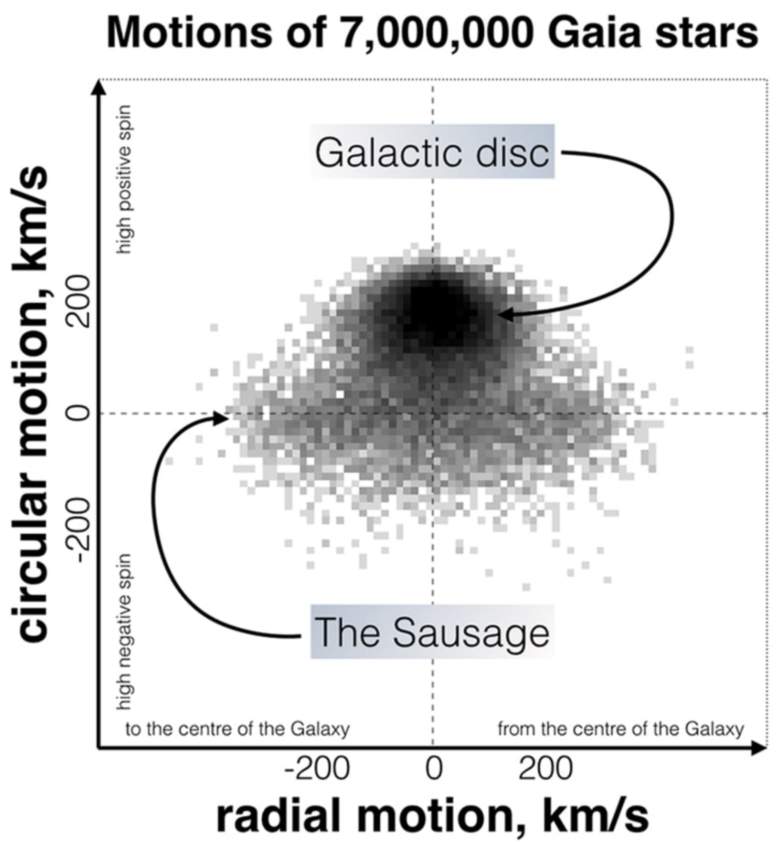

PRD99 (2019) 2, 023012

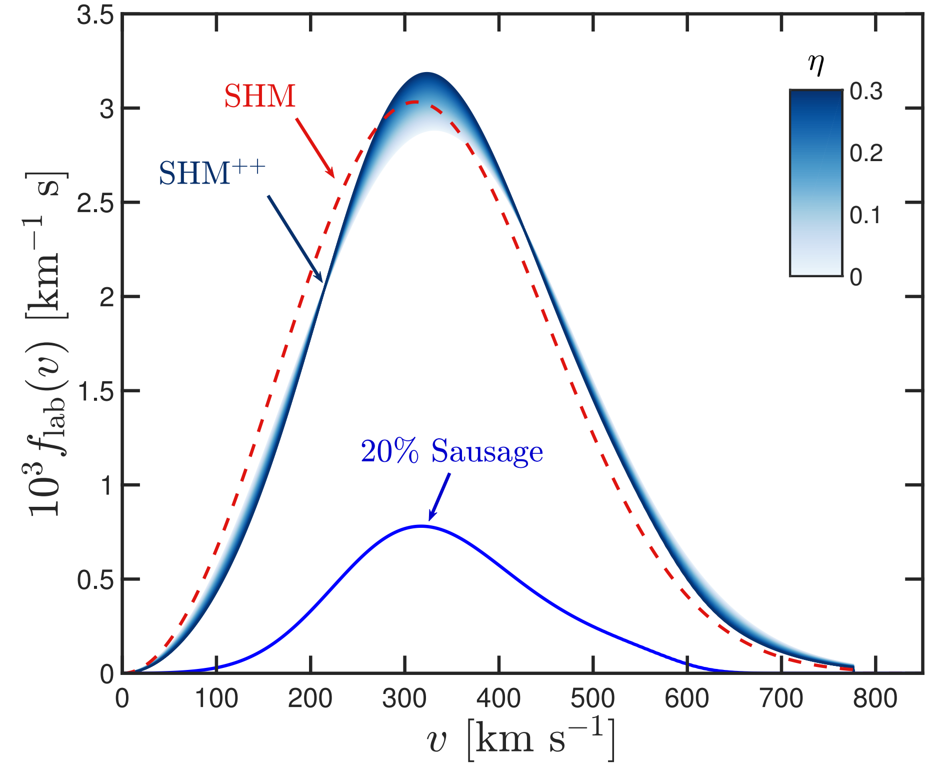

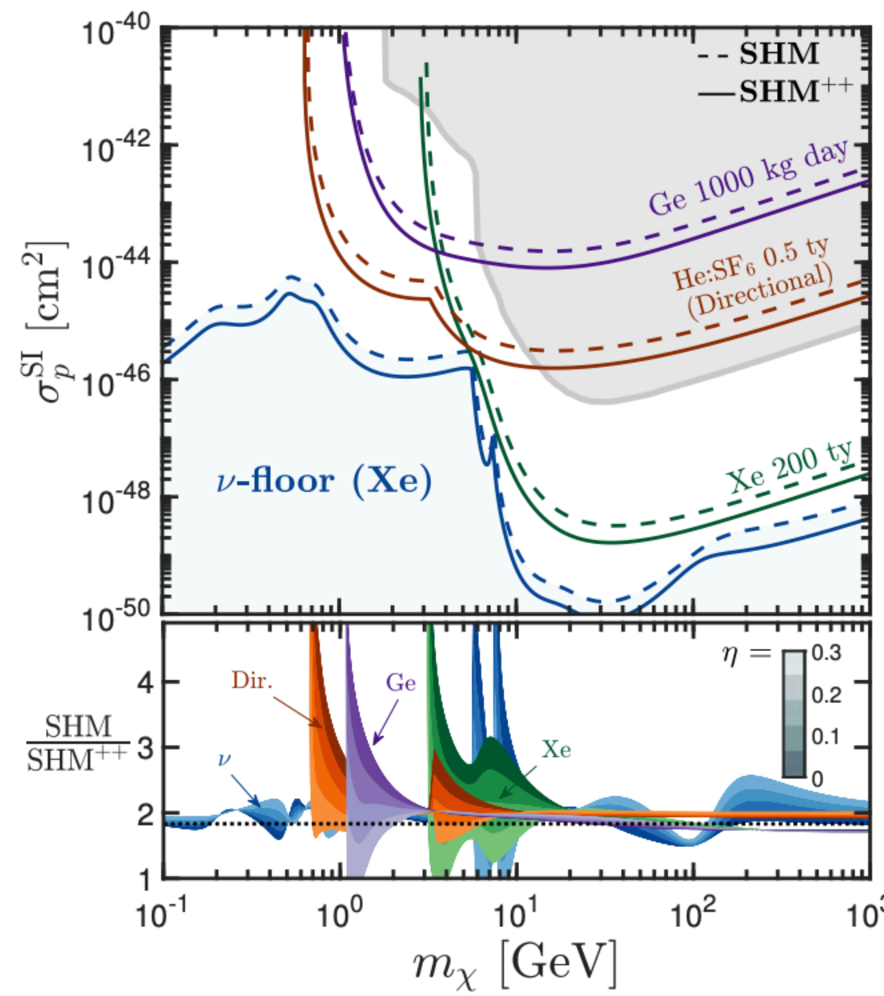

- Standard Halo Model (SHM)
  - Spherical and Isotropic
  - Maxwell velocity distribution
  - No substructure
- Gaia: new light on our galaxy
  - Gaia Sausage
  - Streams
  - …
- Modification of SHM
  - Typically, small effect for direct detection

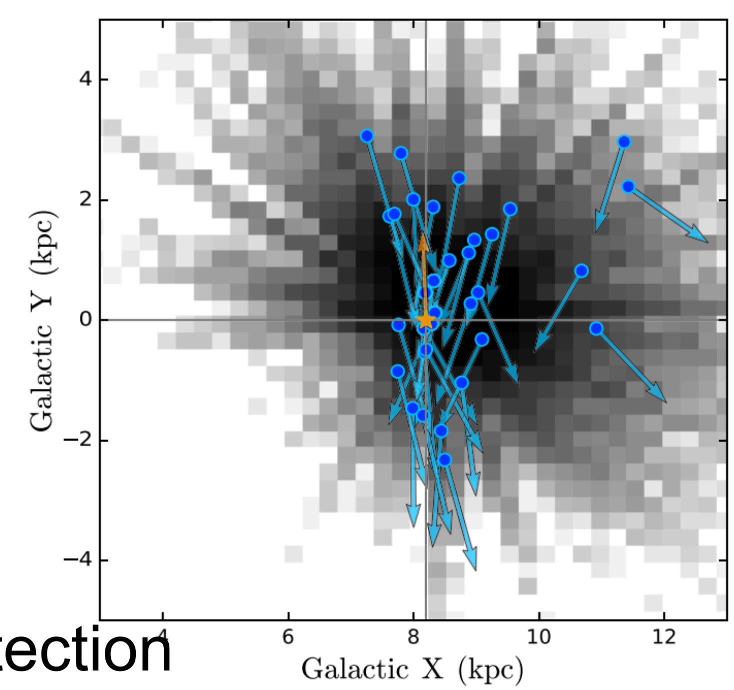

PRD 98 (2018) 10, 103006

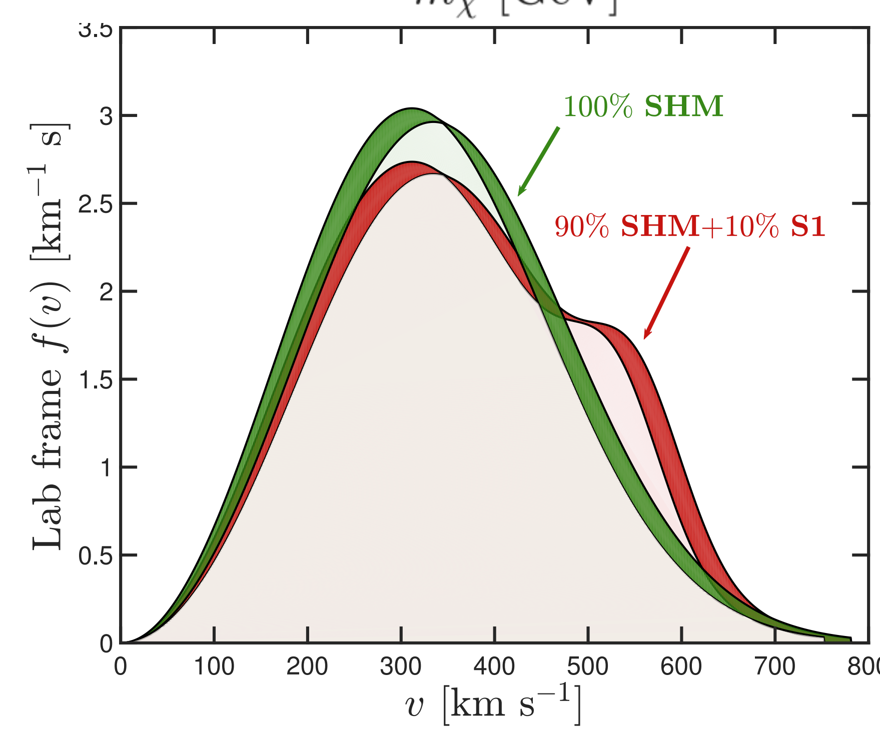

PRD 98 (2018) 10, 103006

SMH++

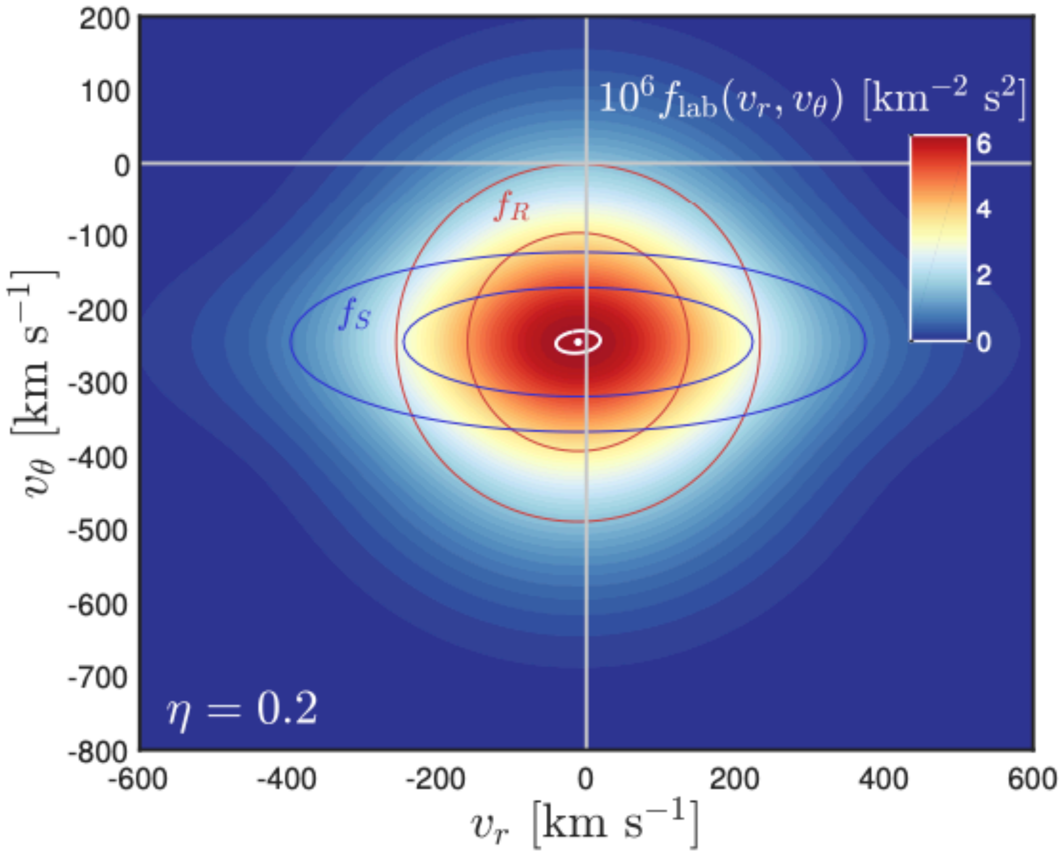

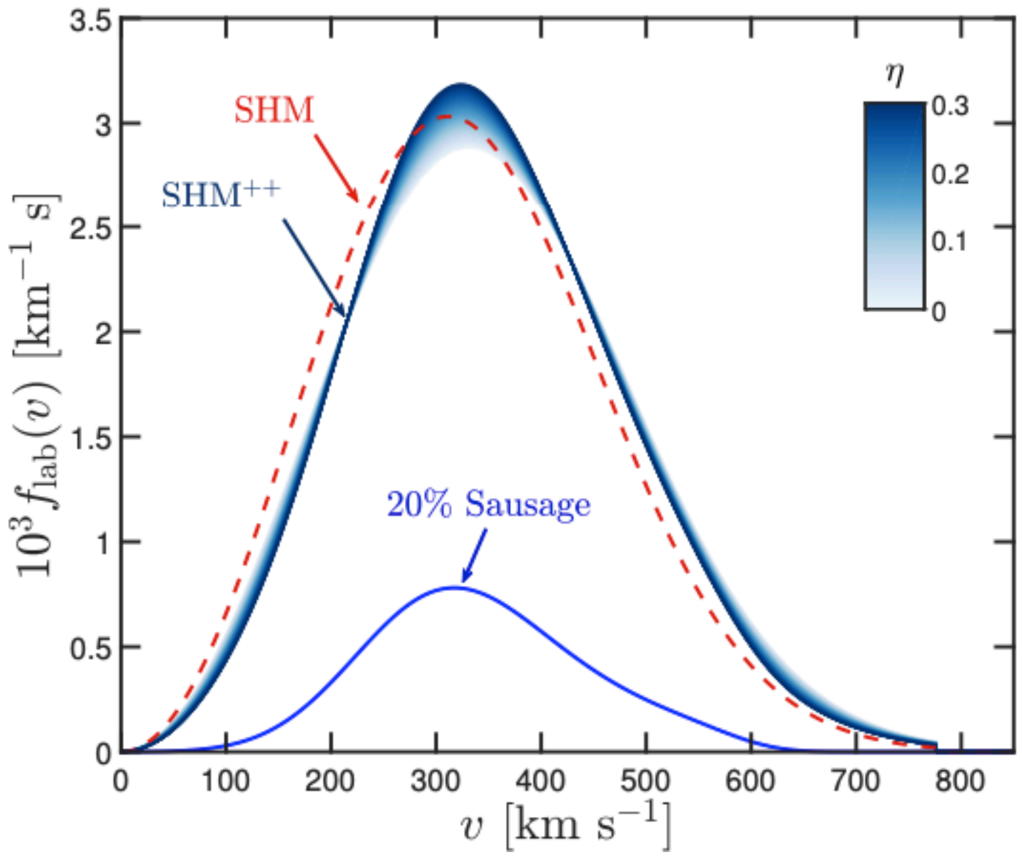

SHM	Local DM density	ρ_0	$0.3\,\text{GeV cm}^{-3}$
	Circular rotation speed	v_0	220 km s^{-1}
	Escape speed	$v_{\rm esc}$	544 km s^{-1}
	Velocity distribution	$f_{\rm R}(\mathbf{v})$	Eq. (1)
SHM^{++}	Local DM density	ρ_0	0.55 ± 0.17 GeV cm^{-3}
	Circular rotation speed	v_0	233 ± 3 km s^{-1}
	Escape speed	$v_{\rm esc}$	528^{+24}_{-25} km s^{-1}
	Sausage anisotropy	β	0.9 ± 0.05
	Sausage fraction	η	0.2 ± 0.1
	Velocity distribution	$f(\mathbf{v})$	Eq. (3)

Phys.Rev.D 99 (2019) 2, 023012

Dark Matter Detection

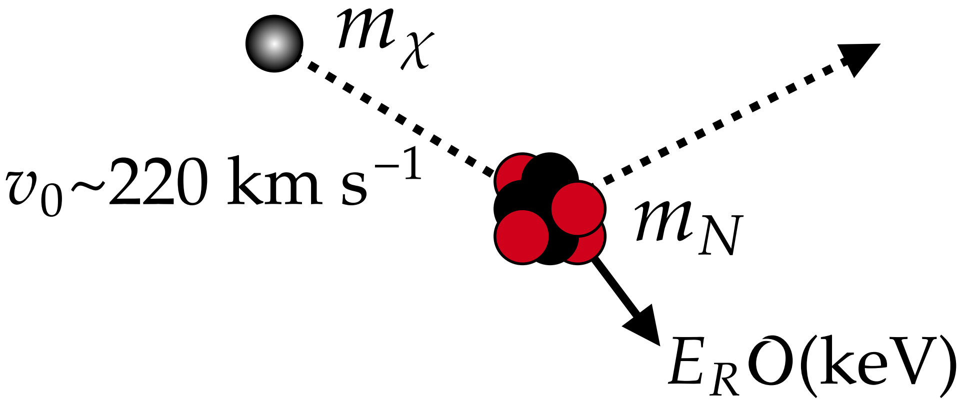

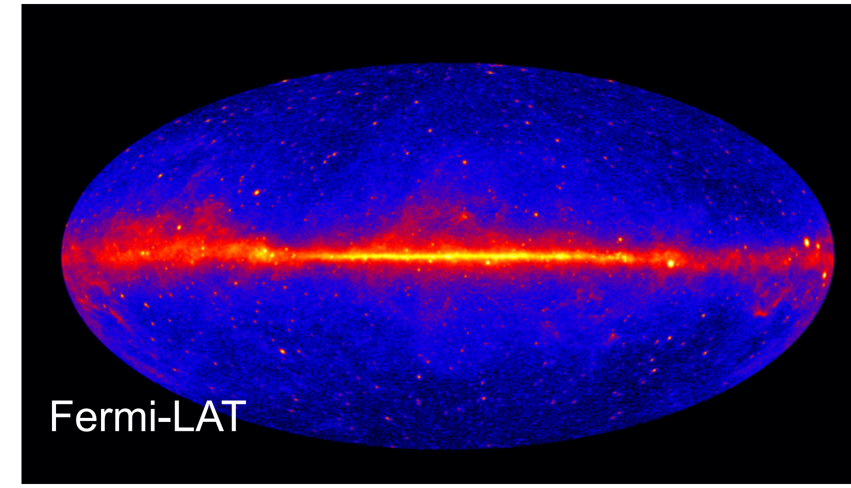

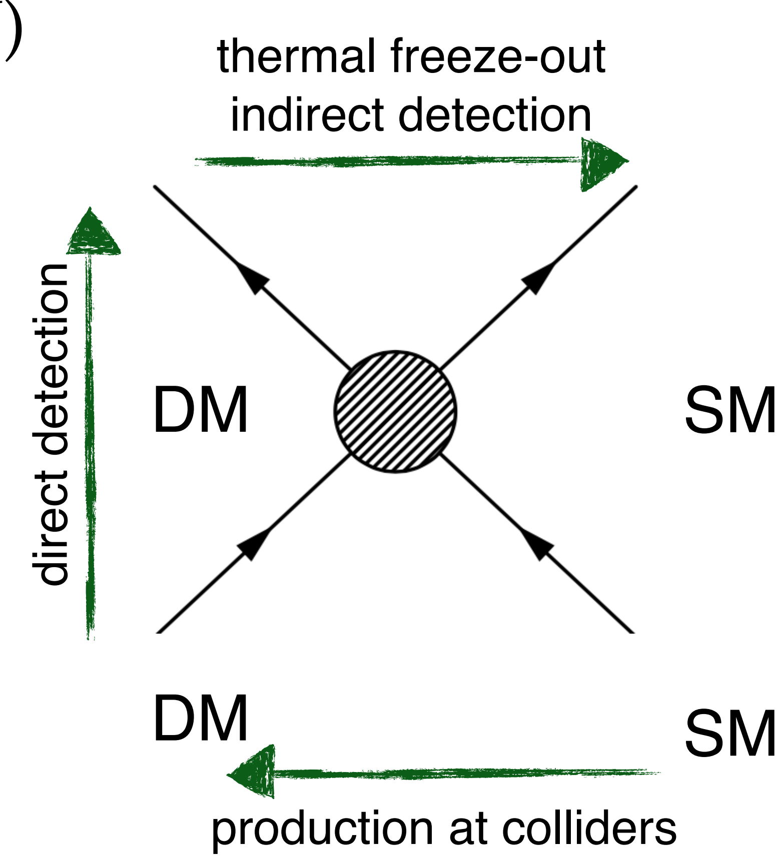

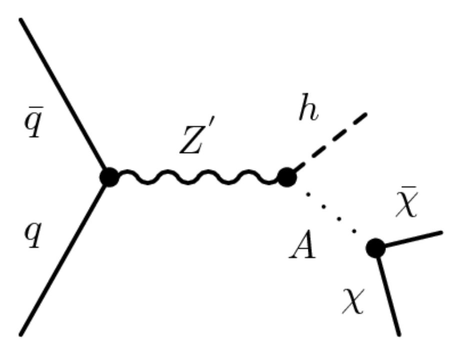

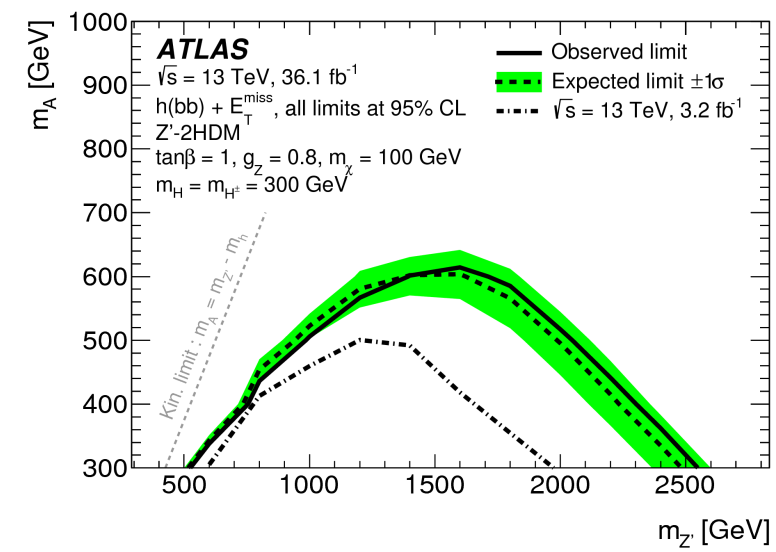

Phys. Rev. Lett. 119 (2017) 181804

Direct Detection: Light Dark Matter

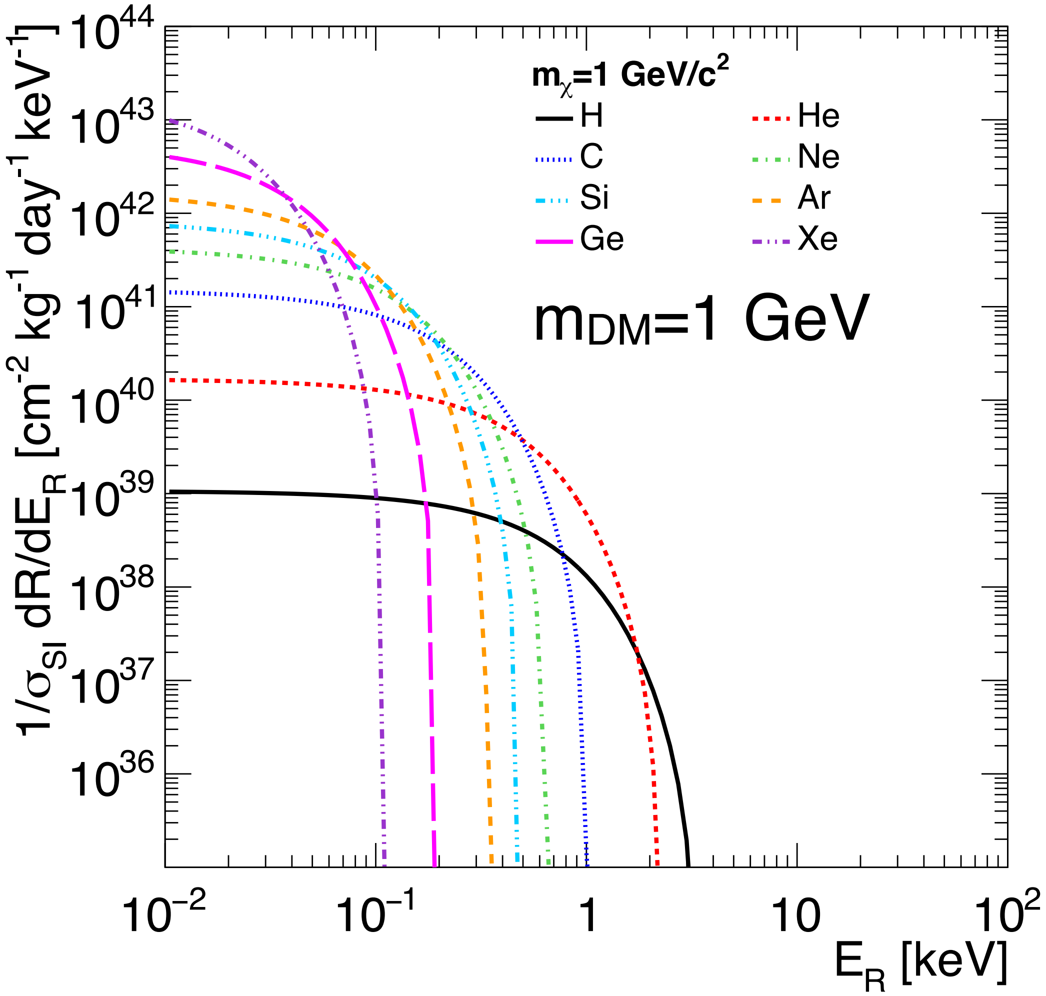

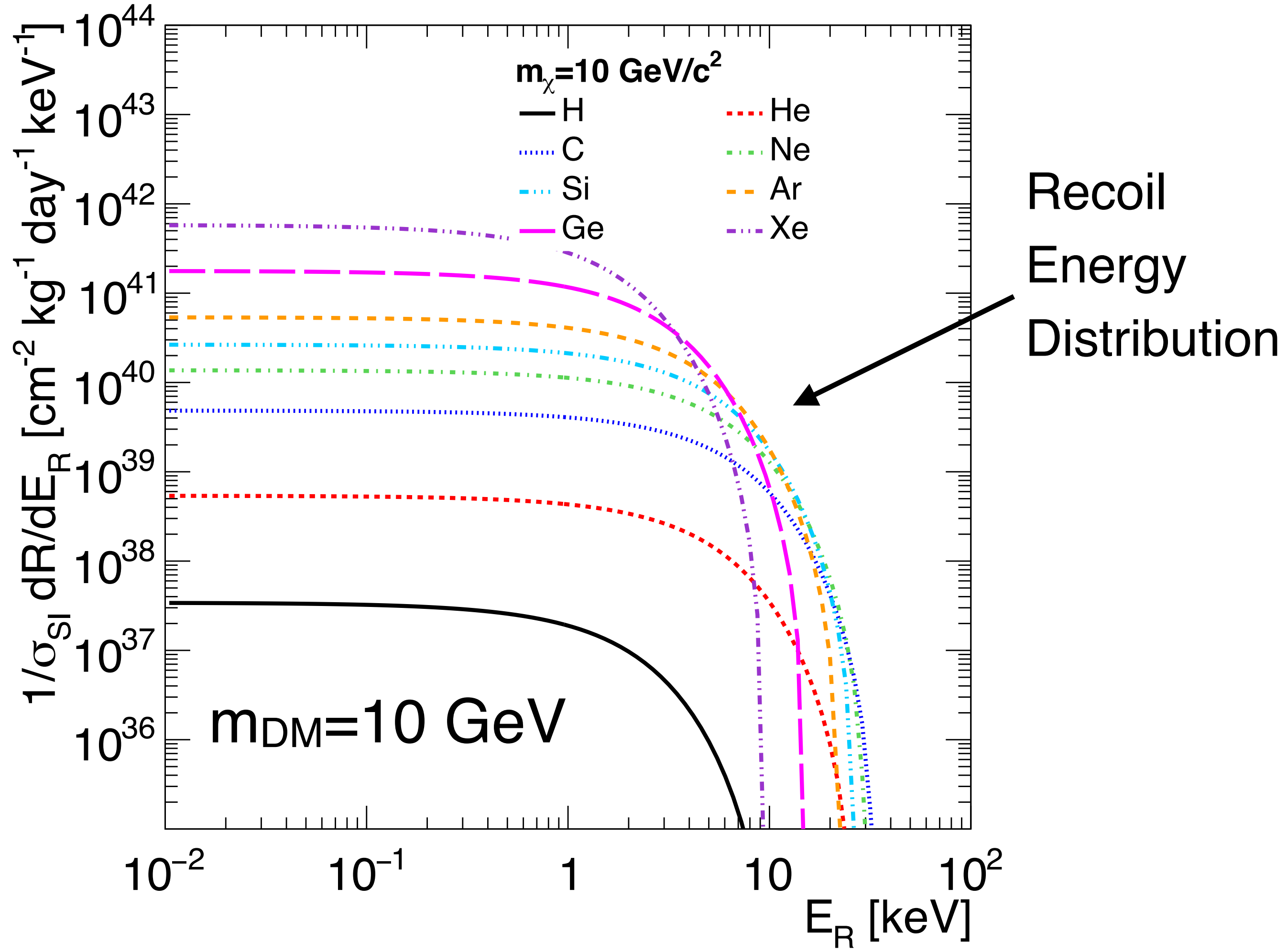

Favourable recoil energy distribution for lighter targets

^{238}U and ^{232}Th decay chains

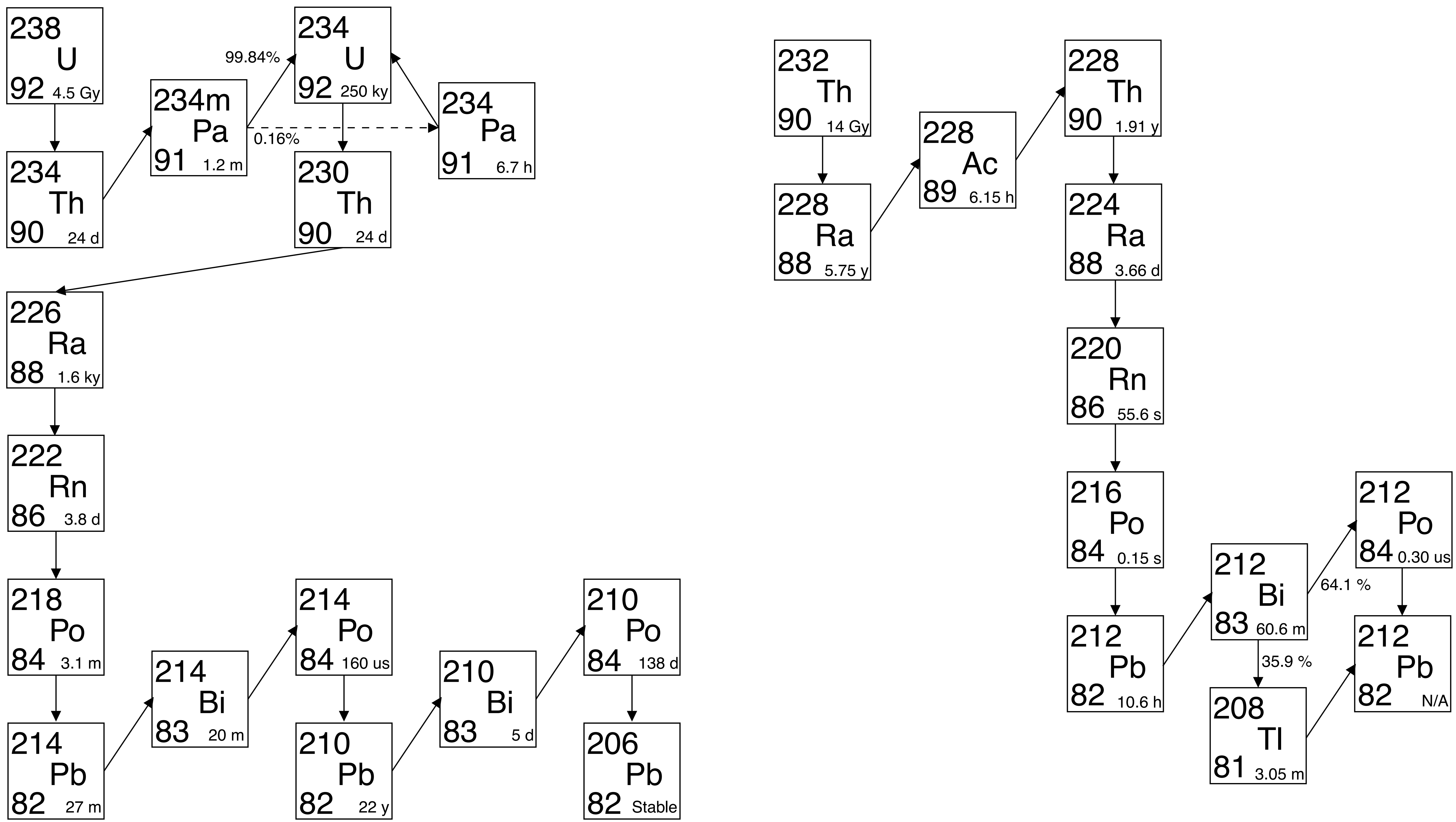

Simulation: Geant4 and Garfield

JINST 15 (2020) 06, C06013

- Detector is initialised and initial particle is generated
- ↓ Geant4 tracks particles and interactions
- ↓ Electrons with energy <2 keV are passed to Garfield++
- ↓ Heed calculates further ionisation and δ-electrons produced
- ↓ Using the gas transport parameters, ionisation electrons are transported up to the avalanche region
- ↓ Electron avalanche is simulated
- ↓ Ions and electrons produced in avalanche drift in electric field, and induced electric current is calculated
- ↓ Signal is processed through electronics module to form pulse

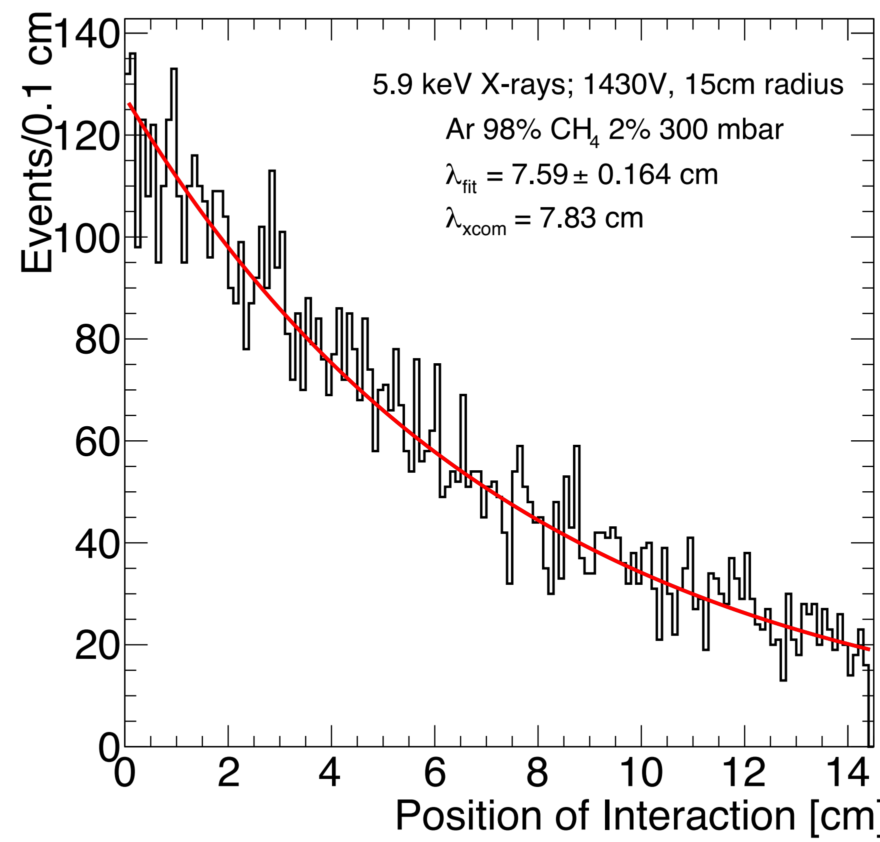

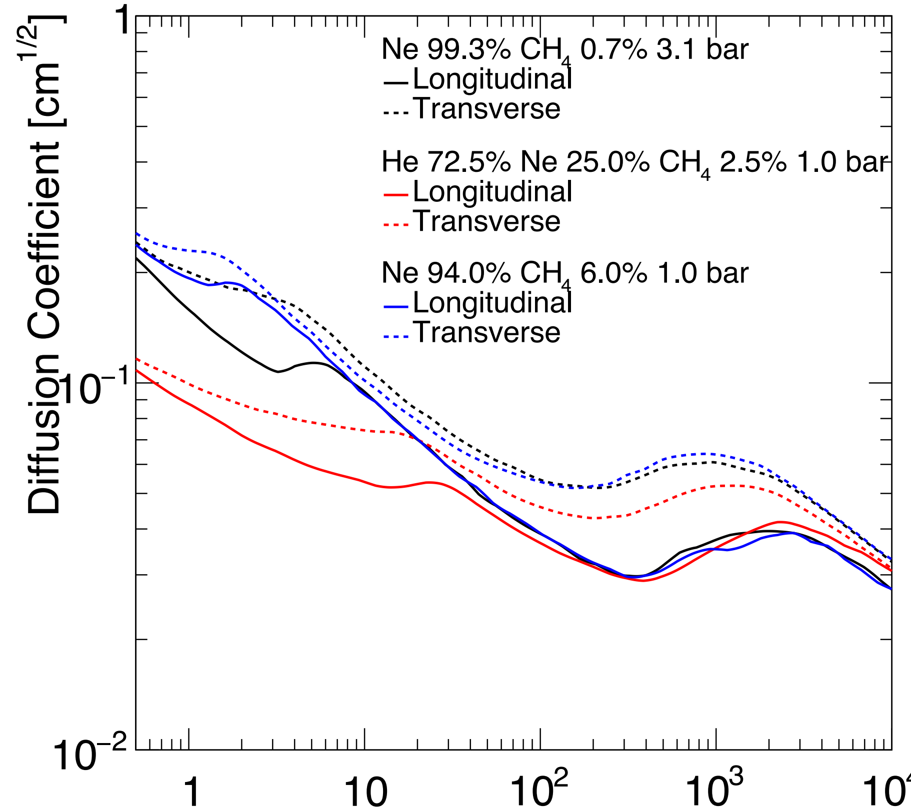

arXiv:20202.02718

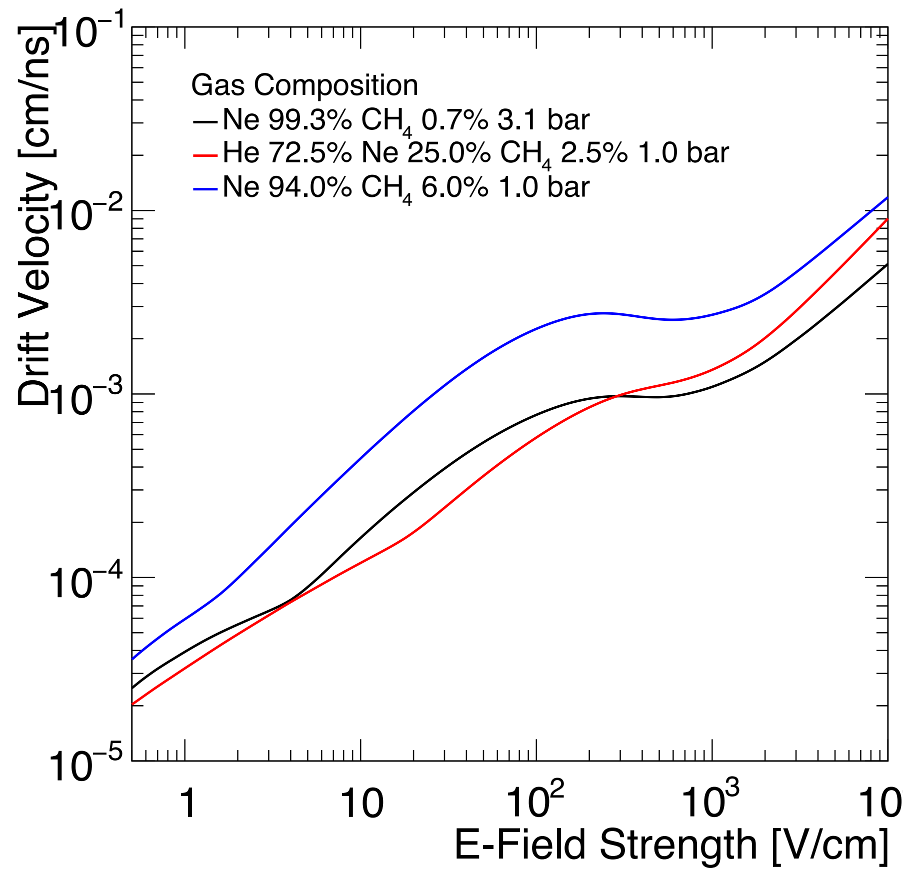

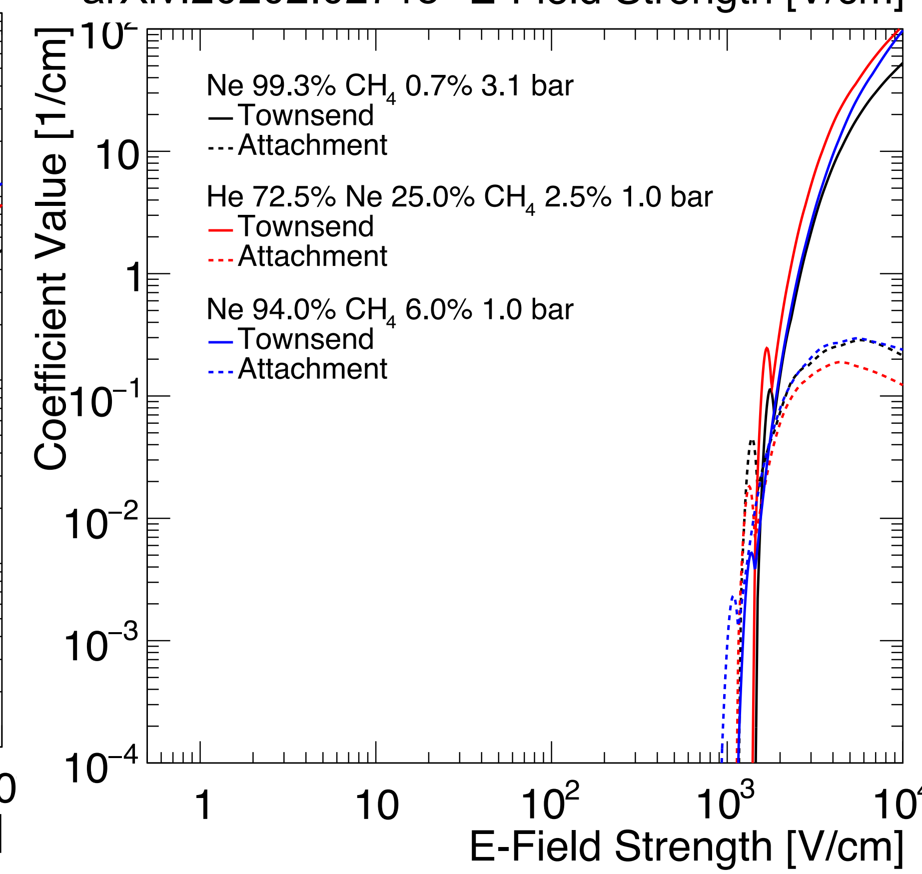

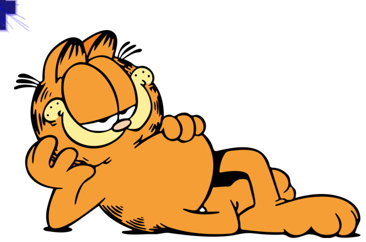

Towards individual anode readout

- Individual ACHINOS anode readout: interaction localisation and tracking

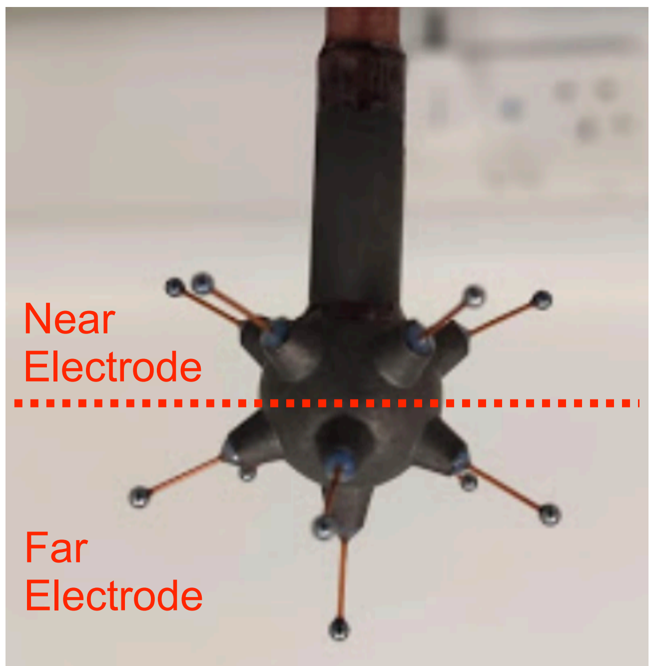

Near electrode weighting field on Far Side

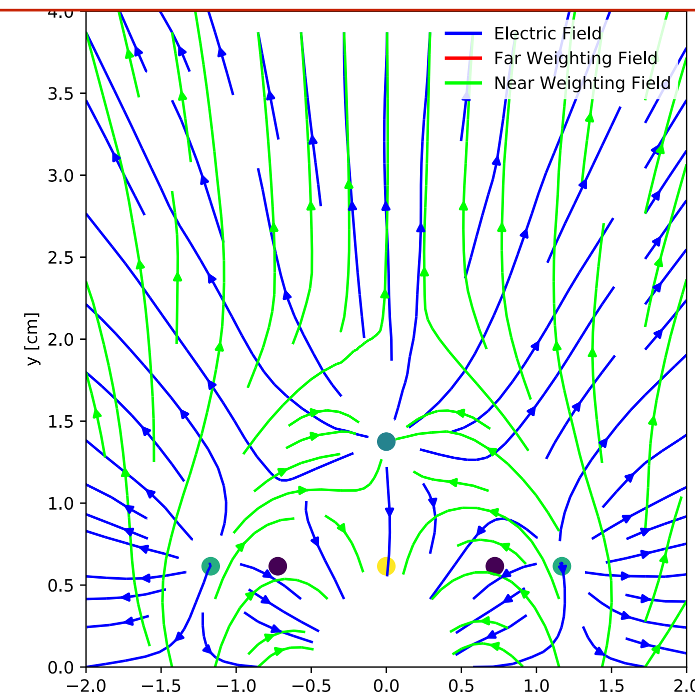

Far electrode weighting field on Far Side

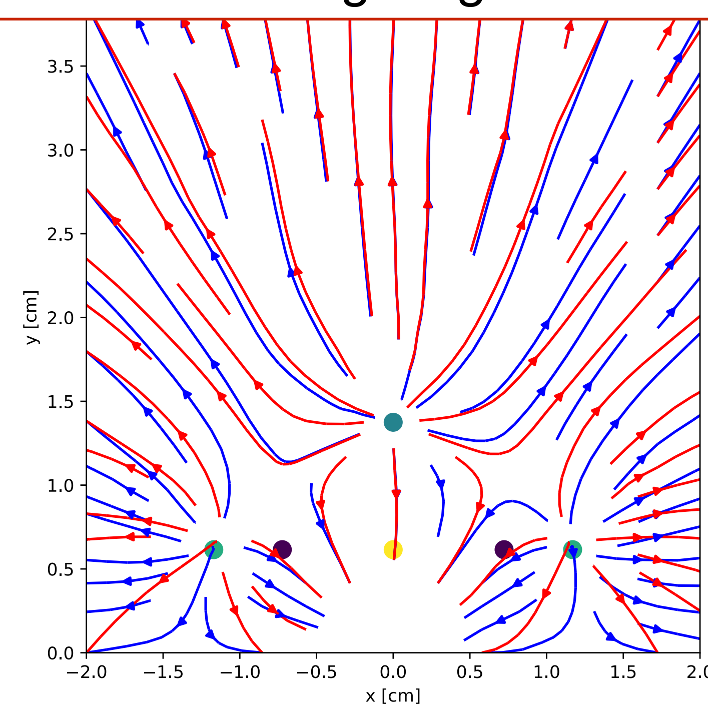

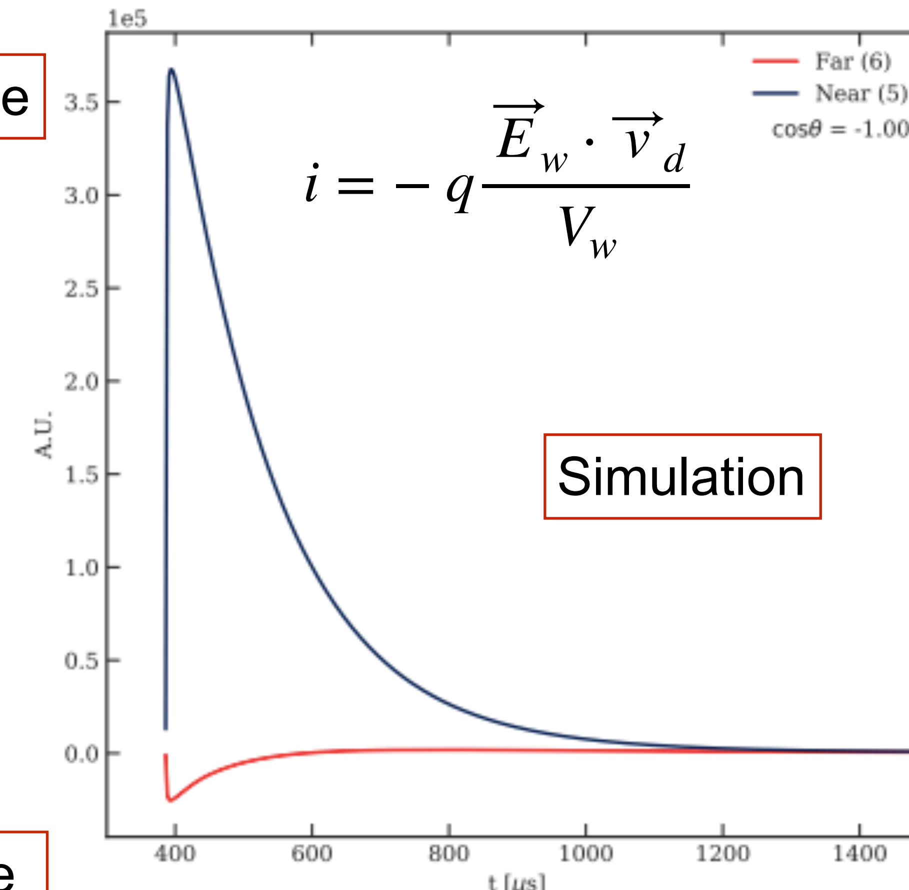

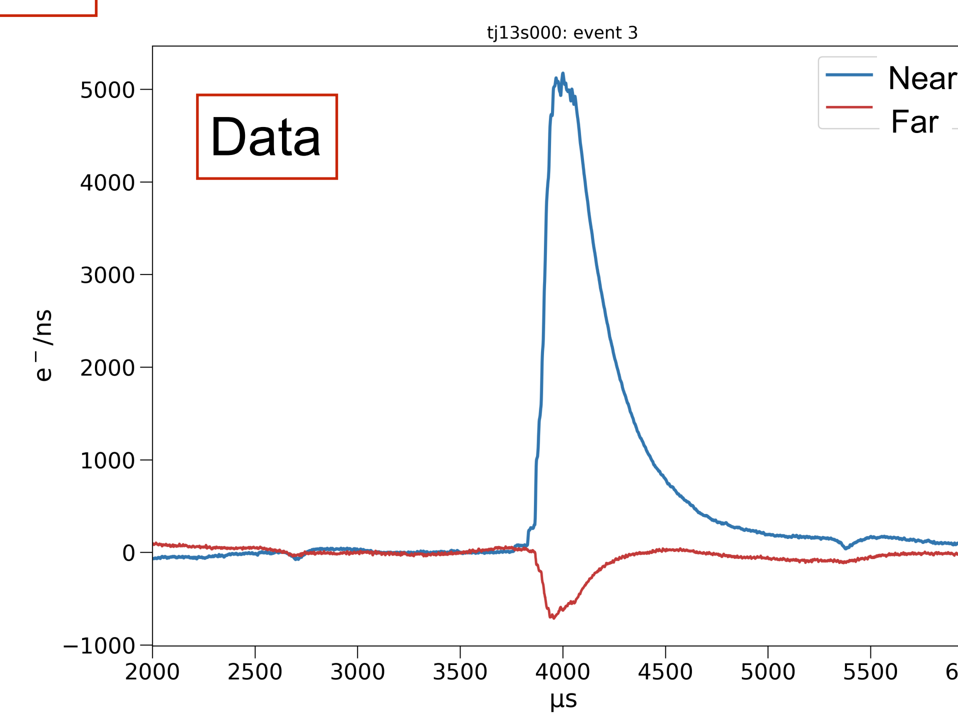

Ionisation quenching factor

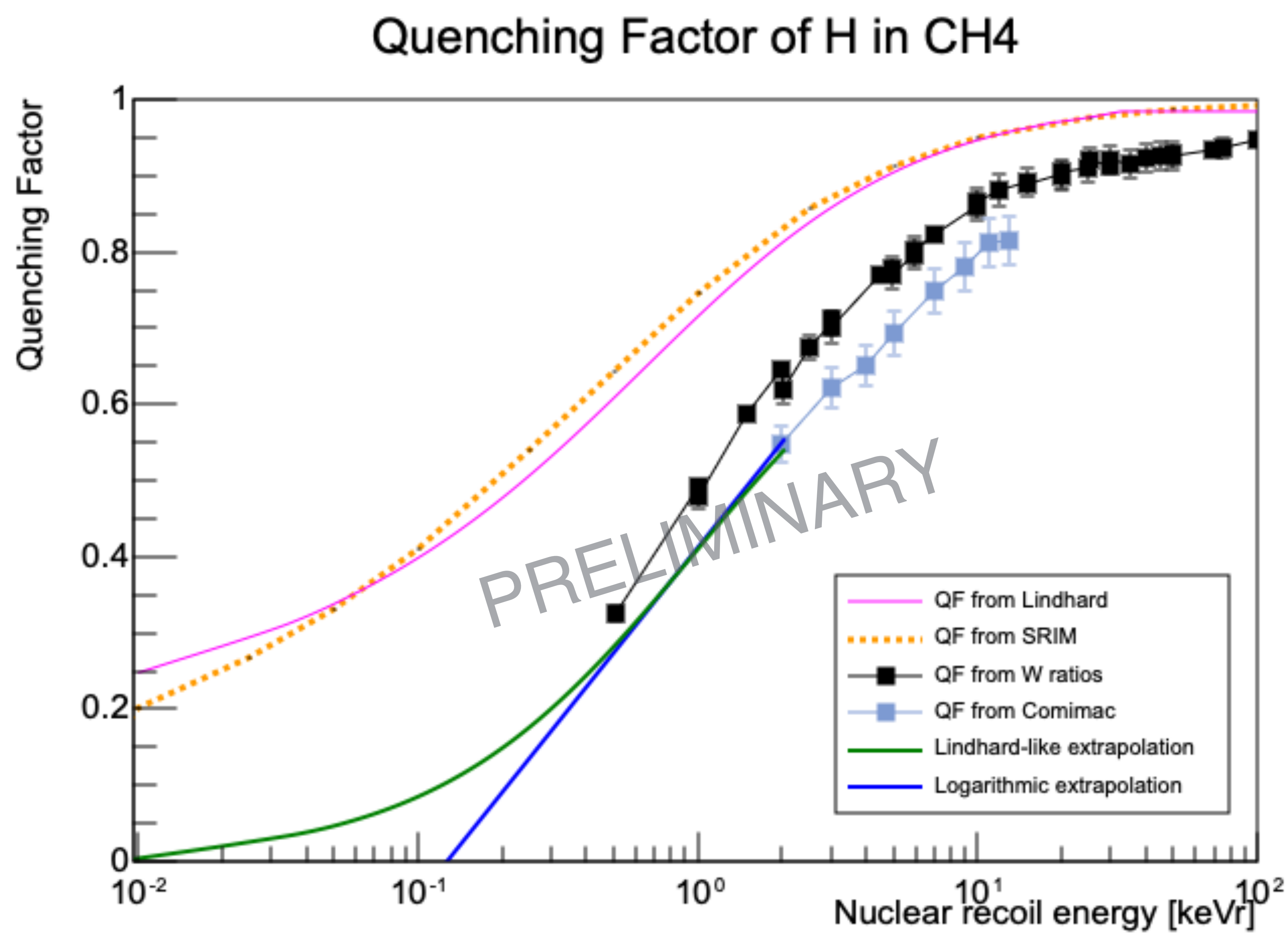

Electron counting characterisation

- Low-intensity, 213nm UV-laser extracts electrons from copper surface
  - Characterise avalanche gain and peak-counting
  - Electron detection efficiency: 60%
  - Separation of electron peaks above 8 μs
- ^{37}Ar injected at the end of physics campaign
  - (almost) mono-energetic lines at 200 eV, 270 eV, and 2.8 keV
  - detector response monitoring in physics runs

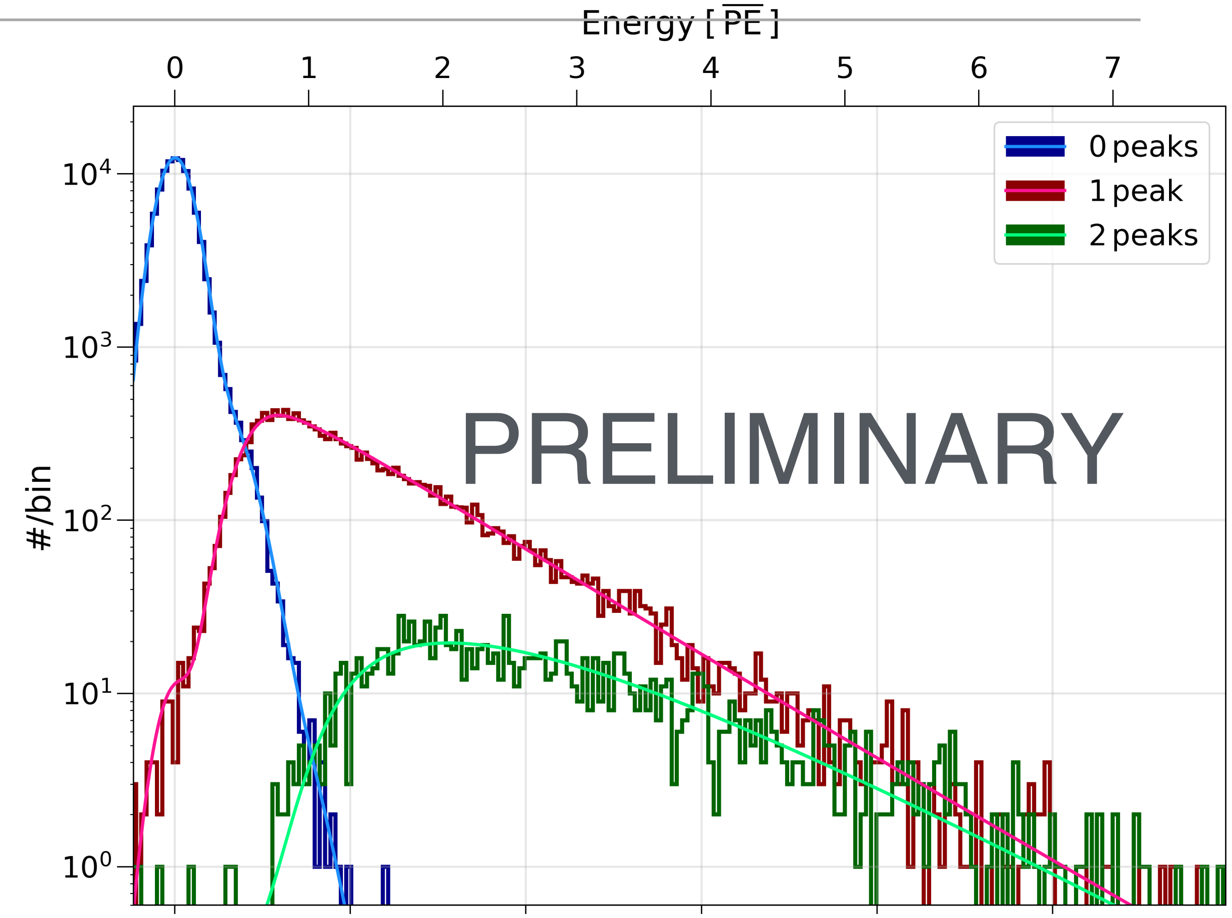

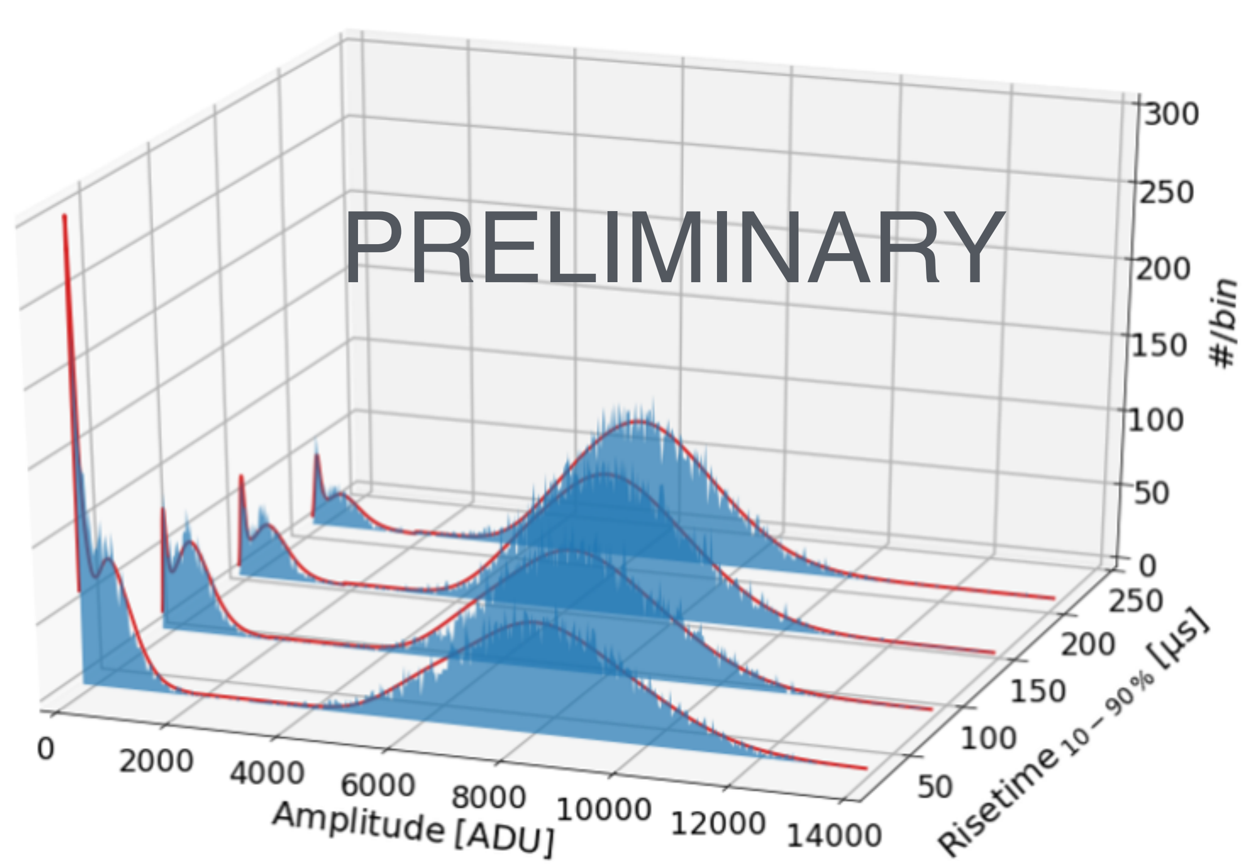

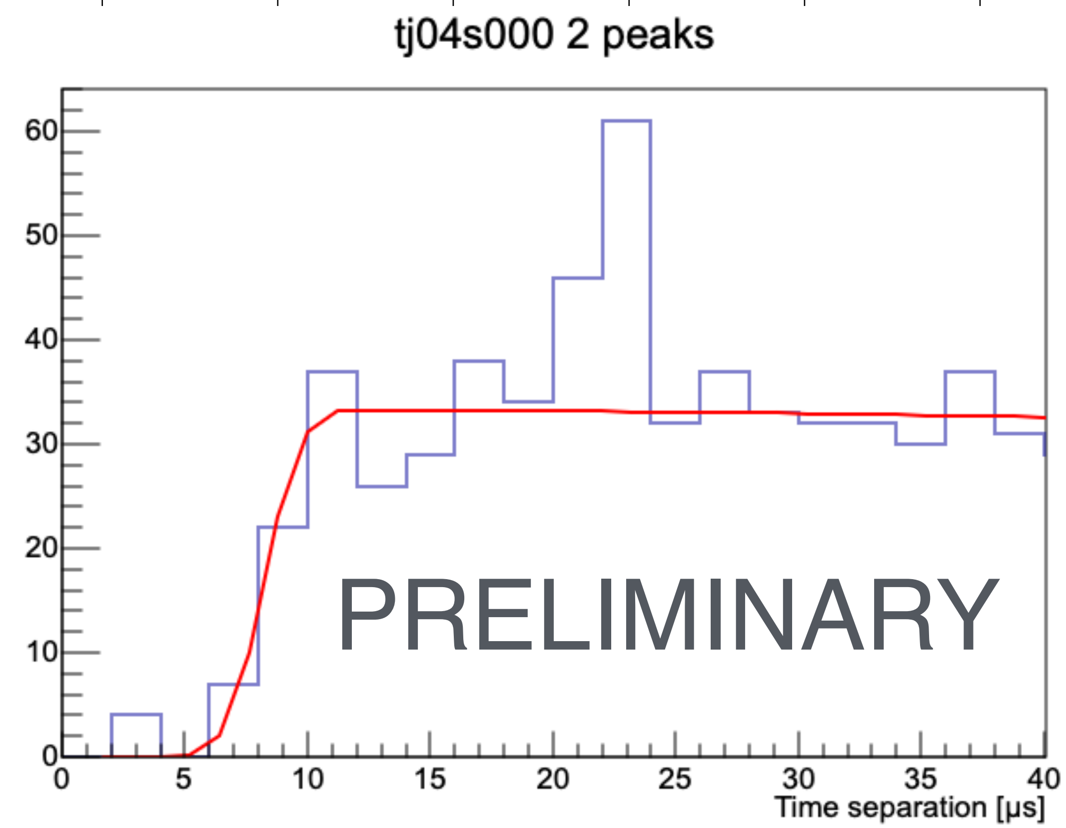

Quenching factor: W-value measurements

- Various quenching factor definitions in the literature
  - fraction of ion kinetic energy dissipated as ionisation electrons and excitation of atomic and quasi-molecular states
  - ratio of the "visible" energy in an ionisation detector to the recoil kinetic energy
  - conversion factor between kinetic energy of an electron and ion that result to the same "visible" energy in the ionisation detector

Astropart.Phys. 141 (2022) 102707

Quenching factor: W-value measurements

- Various quenching factor definitions in the literature
  - fraction of ion kinetic energy dissipated as ionisation electrons and excitation of atomic and quasi-molecular states
  - ratio of the "visible" energy in an ionisation detector to the recoil kinetic energy
  - conversion factor between kinetic energy of an electron and ion that result to the same "visible" energy in the ionisation detector
- Quenching factor intimately connected to W-value
  - W-value is the average energy required to liberate an e-ion pair
  - Typically, detector response calibrated with electrons of known energy

$$q_f(E) = \frac{E_{ee}}{E} = \frac{N_i^i \cdot W_e(E)}{E} = \frac{W_e(E)}{W_i(E)}$$

Astropart.Phys. 141 (2022) 102707

Quenching factor: W-value measurements

- Various quenching factor definitions in the literature
  - fraction of ion kinetic energy dissipated as ionisation electrons and excitation of atomic and quasi-molecular states
  - ratio of the "visible" energy in an ionisation detector to the recoil kinetic energy
  - conversion factor between kinetic energy of an electron and ion that result to the same "visible" energy in the ionisation detector
- Quenching factor intimately connected to W-value
  - W-value is the average energy required to liberate an e-ion pair
  - Typically, detector response calibrated with electrons of known energy

$$q_f(E) = \frac{E_{ee}}{E} = \frac{N_i^i \cdot W_e(E)}{E} = \frac{W_e(E)}{W_i(E)}$$

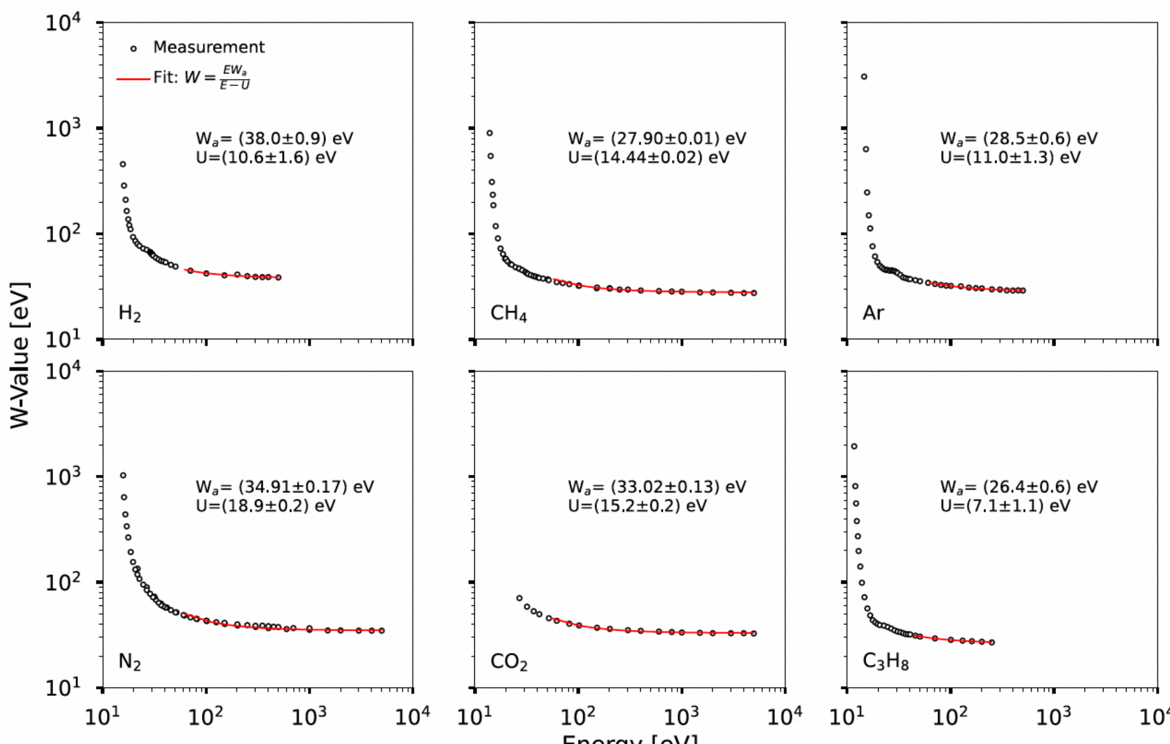

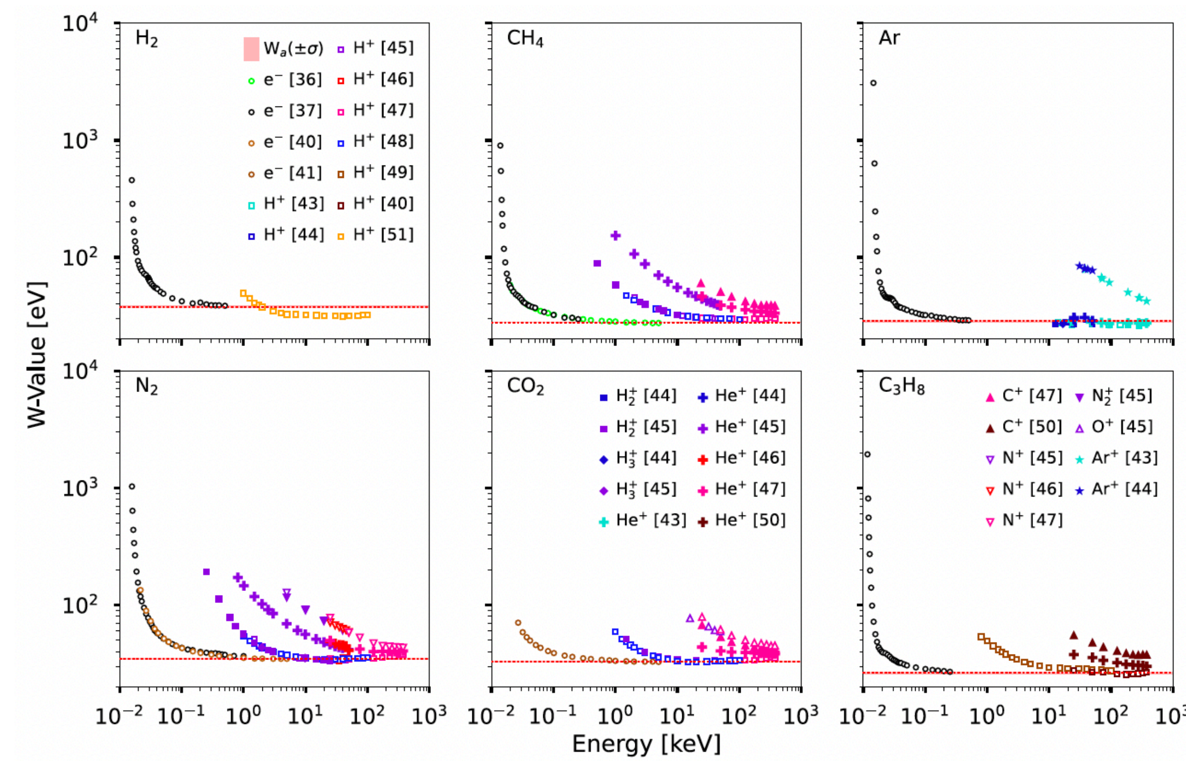

Astropart.Phys. 141 (2022) 102707

$$W(E) = \frac{W_a}{1 - U/E}$$

Gas Purification

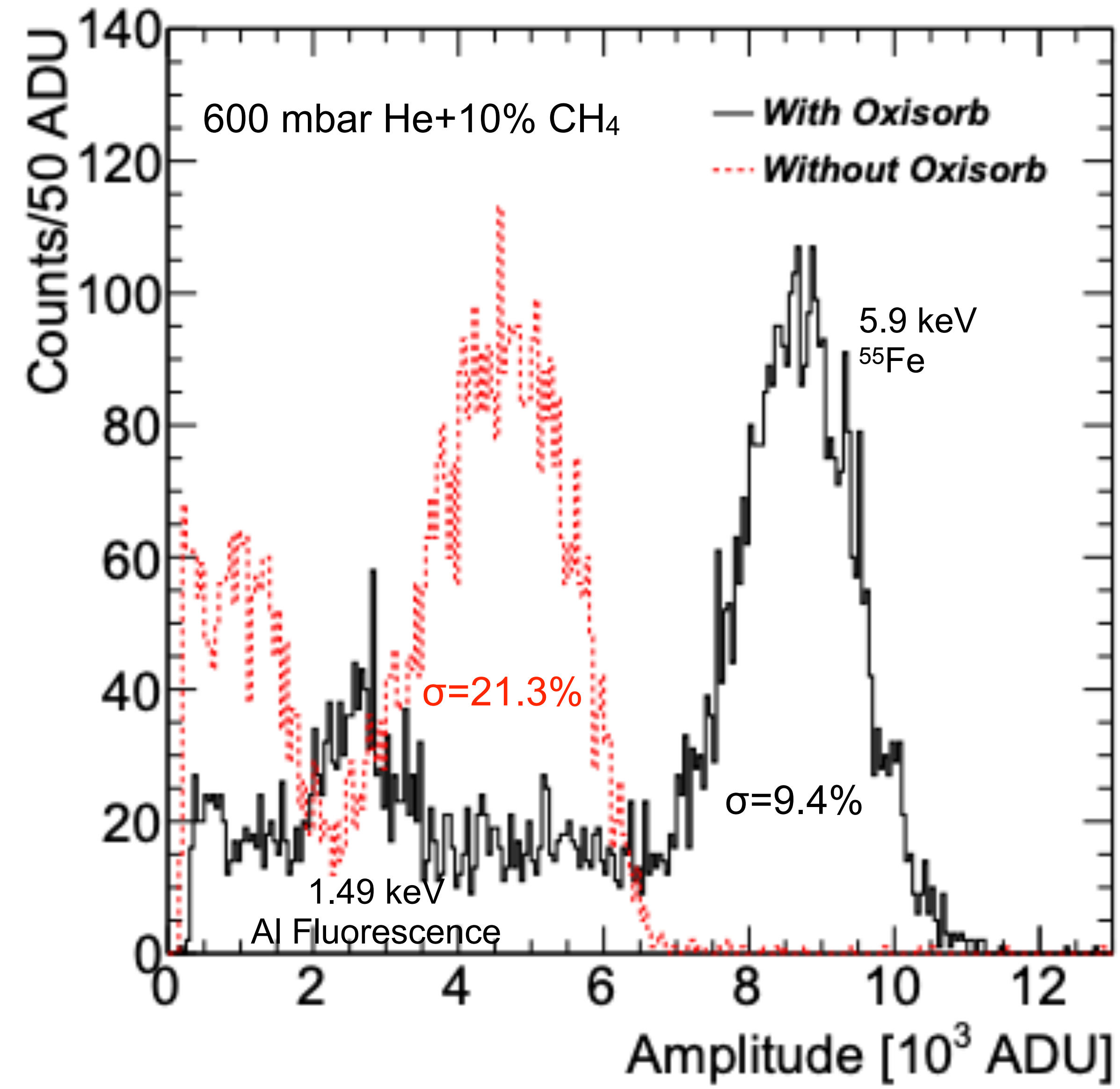

- Contaminants: O_2, H_2O, electronegative gases
- Filtering with: Getter, Oxysorb
  - Crucial improvement in gas quality

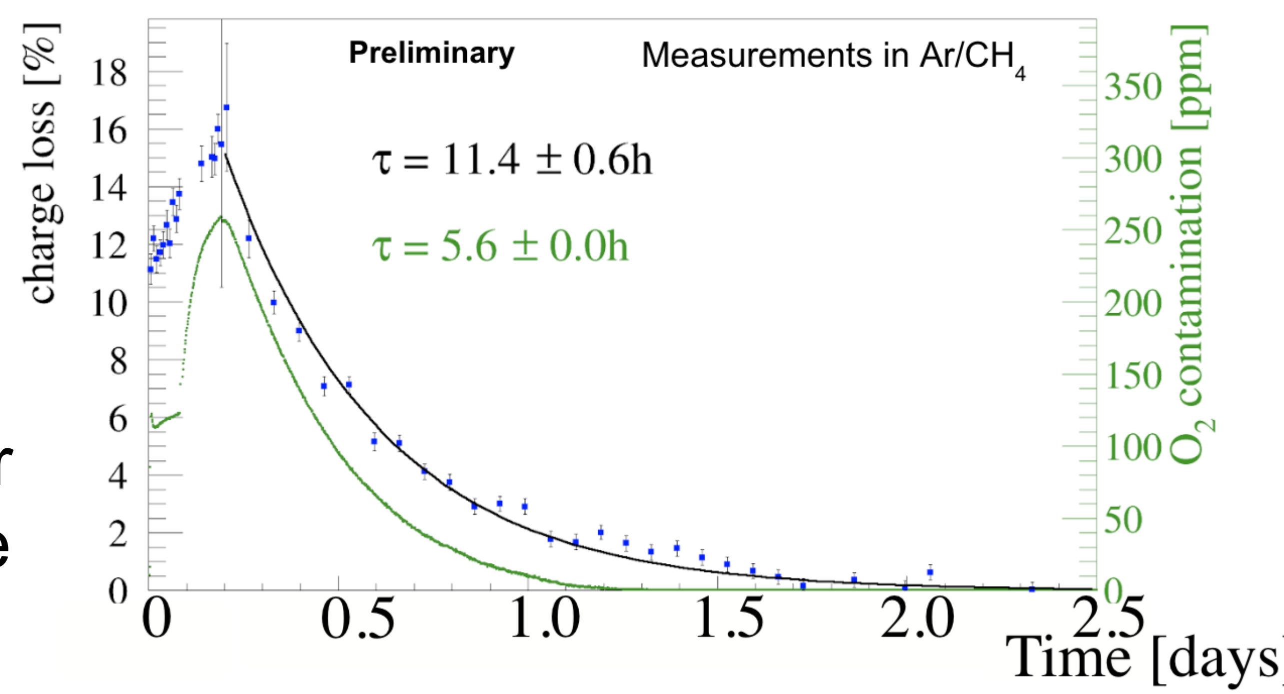

- Filtering in a gas re-circulation system
  - SAES MicroTorr Purifier (MC700 902-F)
  - Incorporated with Residual Gas Analyser
- Improved filtering efficiency in large sphere

Detector Calibration

Phys. Rev. D 99, 102003 (2019)

Parallel photo-detector to tag laser events

Tunable transmission to control the mean number of electrons

Common DAQ for timing analysis between two channel

Scheme of the experimental set-up

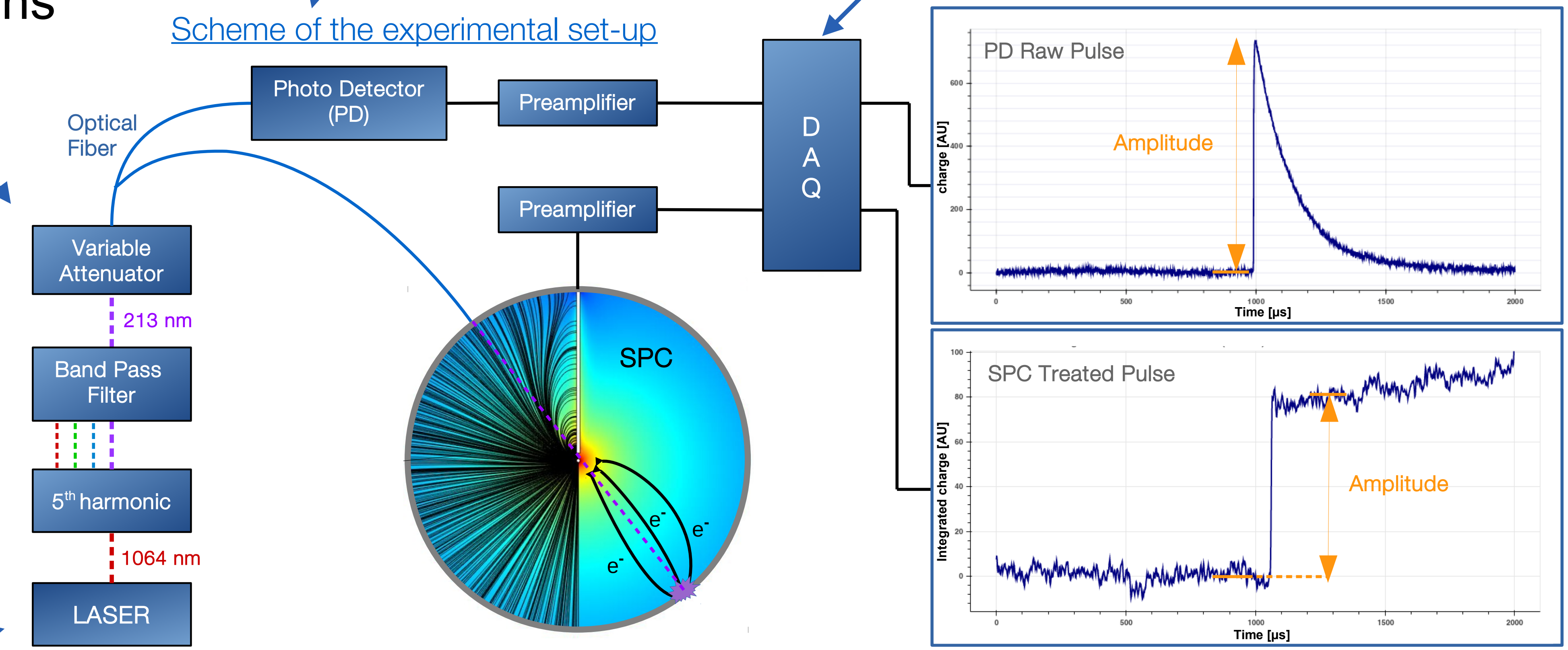

A powerful UV laser capable of extracting 100s of electrons

- 213 nm laser used to extract primary electrons from detector wall
- Photo-detector in parallel tags events and monitors laser power
- Laser intensity can be tuned to extract 1 to 100 photo-electrons

Modelling Single Electron Response

Phys. Rev. D 99, 102003 (2019)

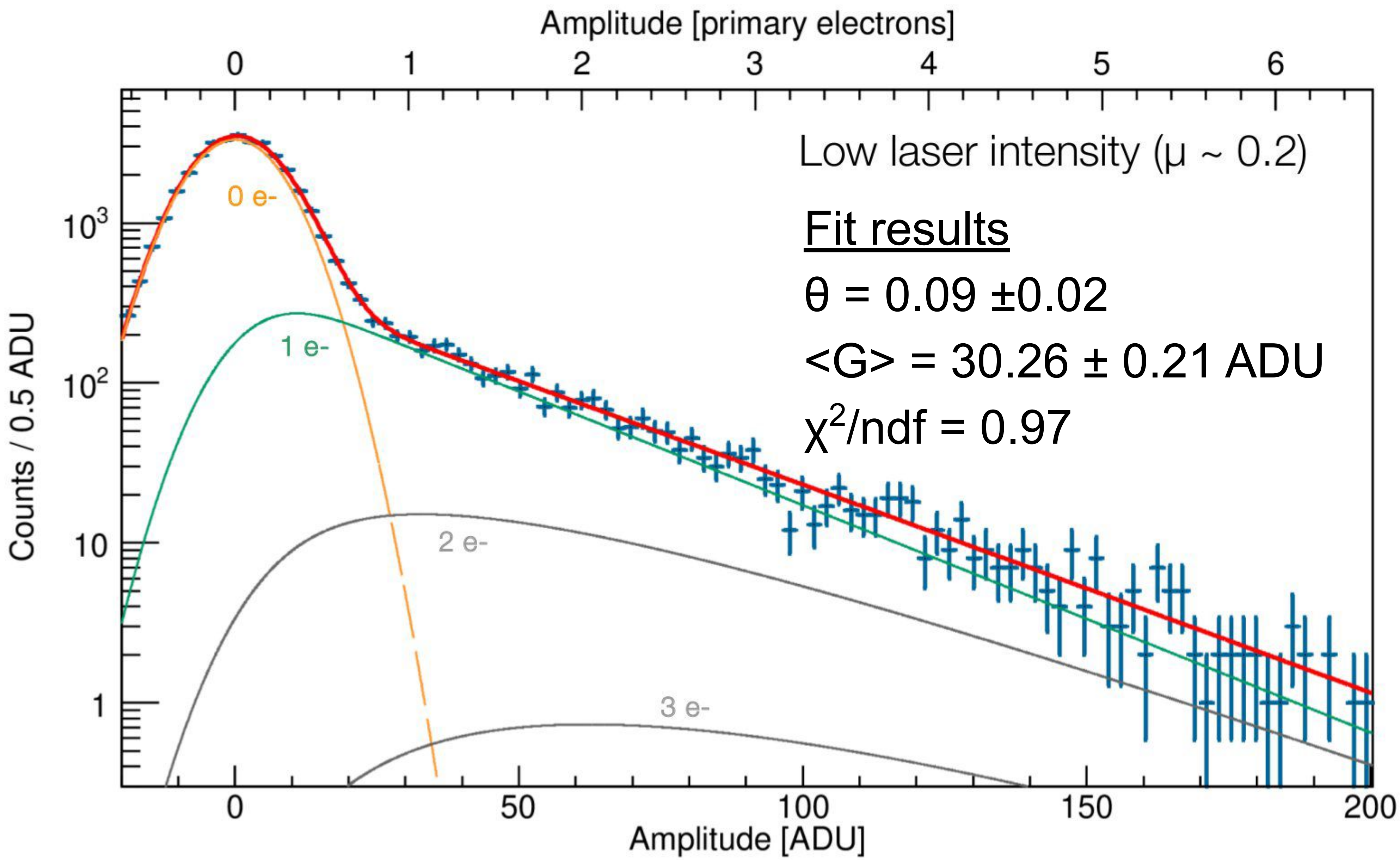

- N photo-electrons are extracted from the surface of the sphere: Poisson
- Each photo-electron creates S avalanche electrons
- Sum the contributions of all N photo-electrons: N^{th} convolution of Polya
- The overall response is convolved with a Gaussian to model baseline noise

Detector Monitoring

Phys. Rev. D 99, 102003 (2019)

- Long runs, response fluctuations induced by:
  - temperature/pressure changes
  - O_2 contamination
  - sensor damage
  - …
- ^{37}Ar calibrations
  - crucial information
  - can only be used at the end of a run
- Laser system
  - detector response monitoring in physics runs

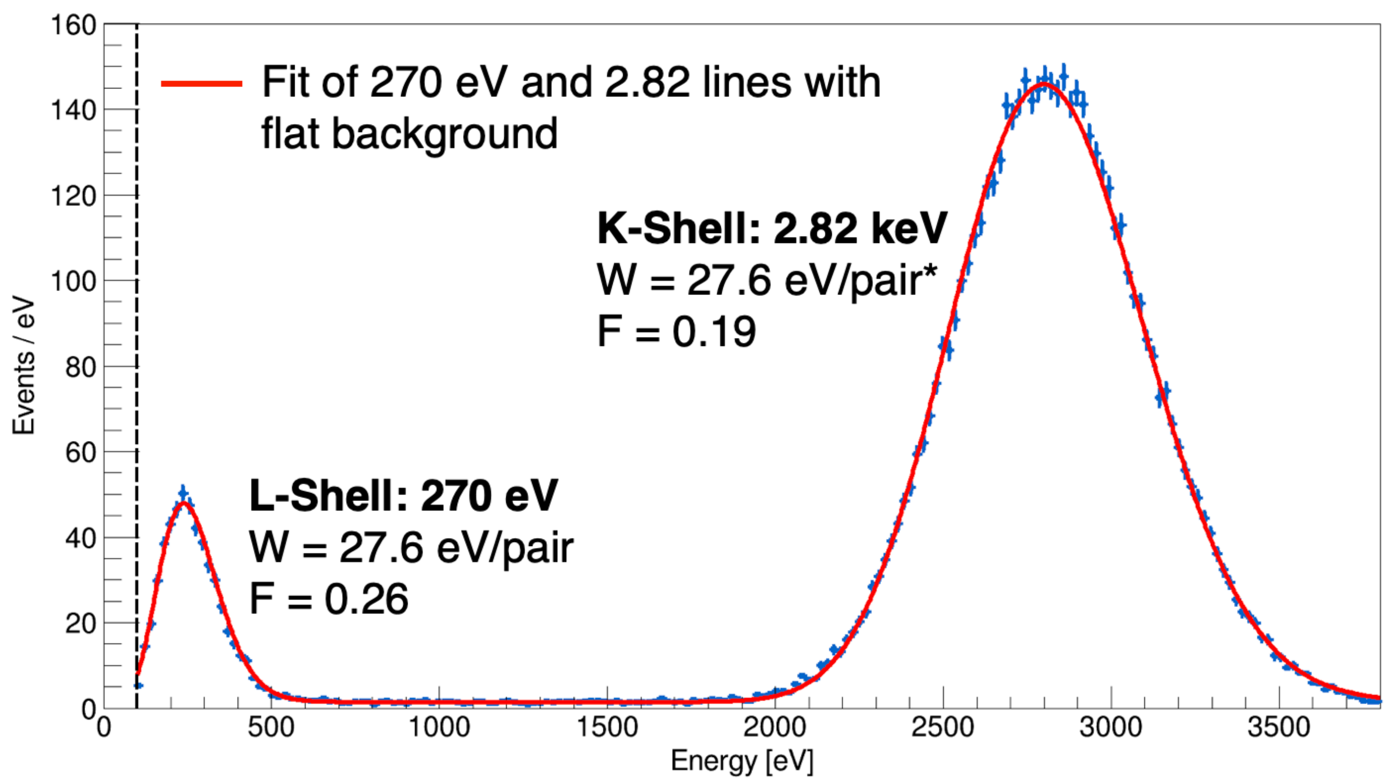

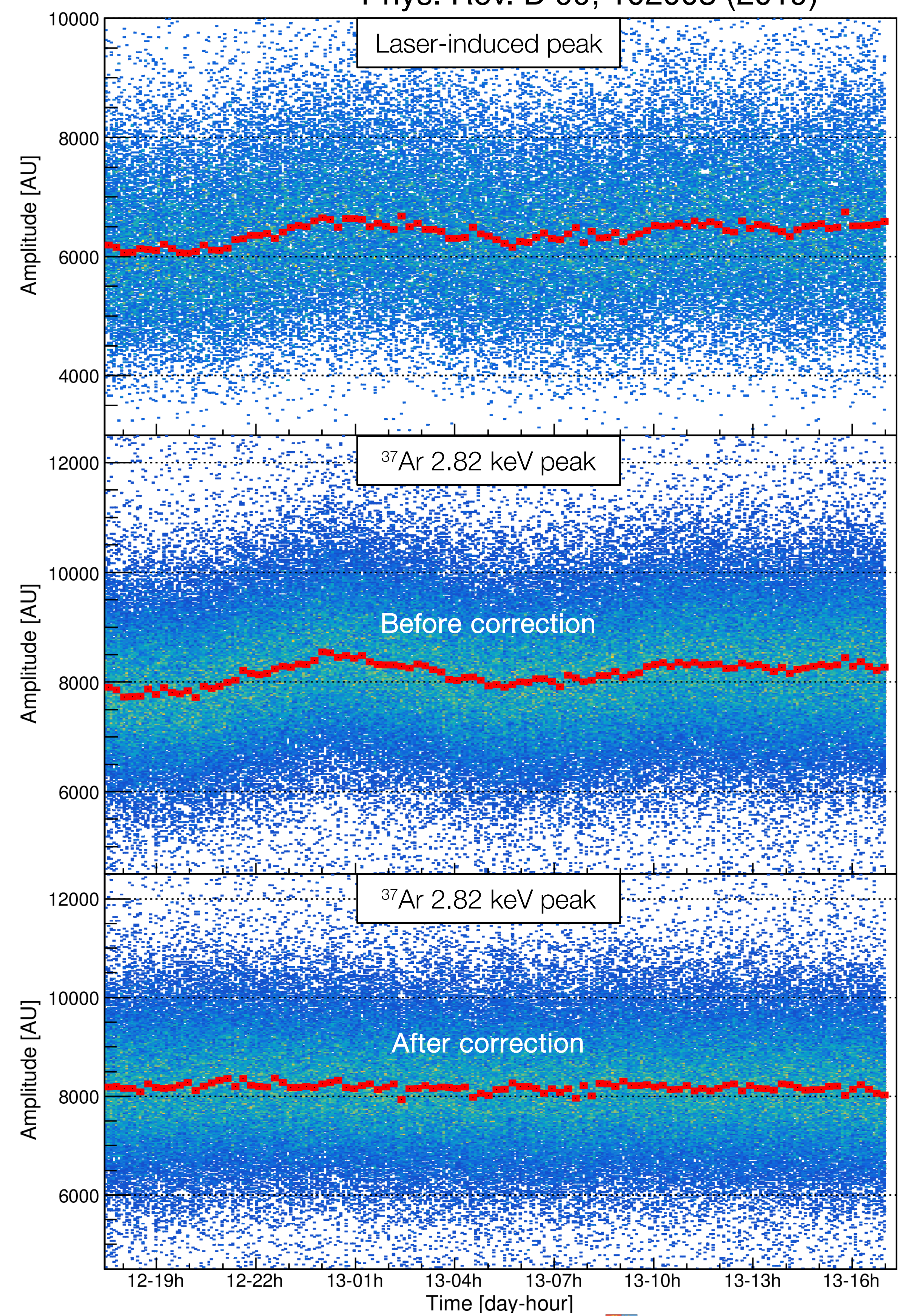

SEDINE: Data taking conditions

- **Target:** Neon + 0.7% CH_4 at 3.1 bar (282 gr)
- **Run time:** Continuous data taking for 42.7 days
  - **Exposure:** 34.1 live-days x 0.282 kg =9.6 kg.days
- Anode high voltage 2520 V, no sparks
  - Absolute Gain ~3000.
  - Loss of gain 4% throughout the period
- Sealed mode, no recirculation.
- **Read-out:** Canberra charge sensitive preamplifier (τ_{RC}=50 μs)
- **Calibration:** ^{37}Ar gaseous source,8 keV Cu fluorescence line, AmBe neutron source

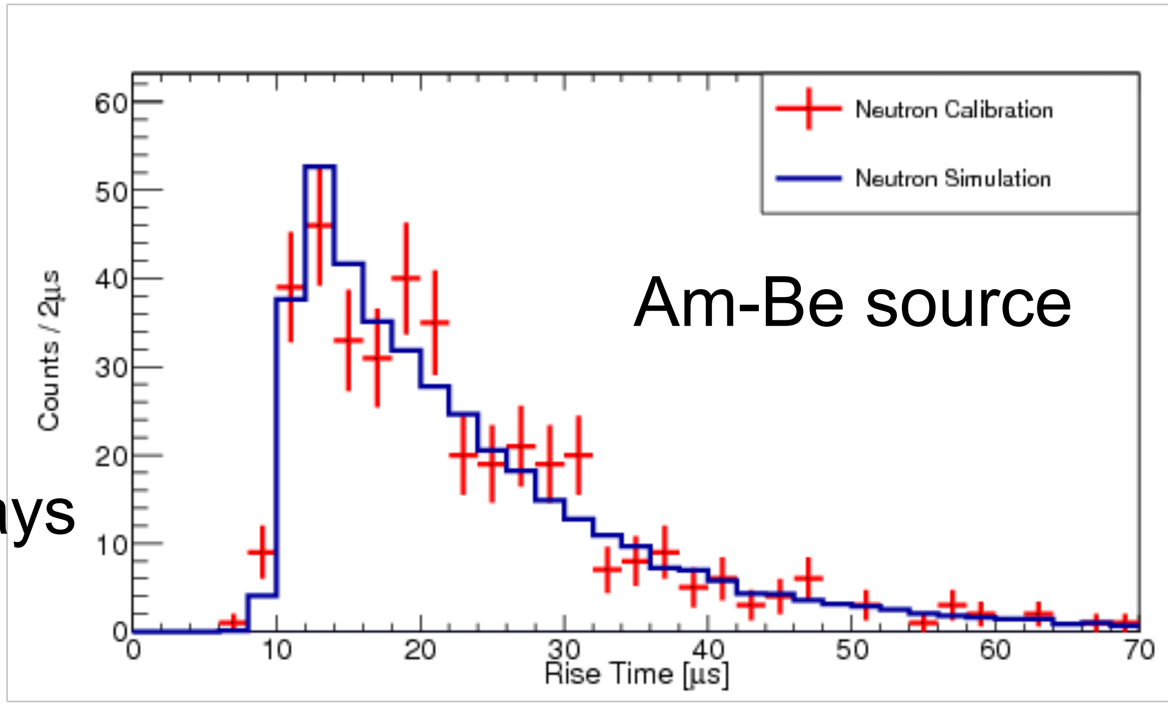

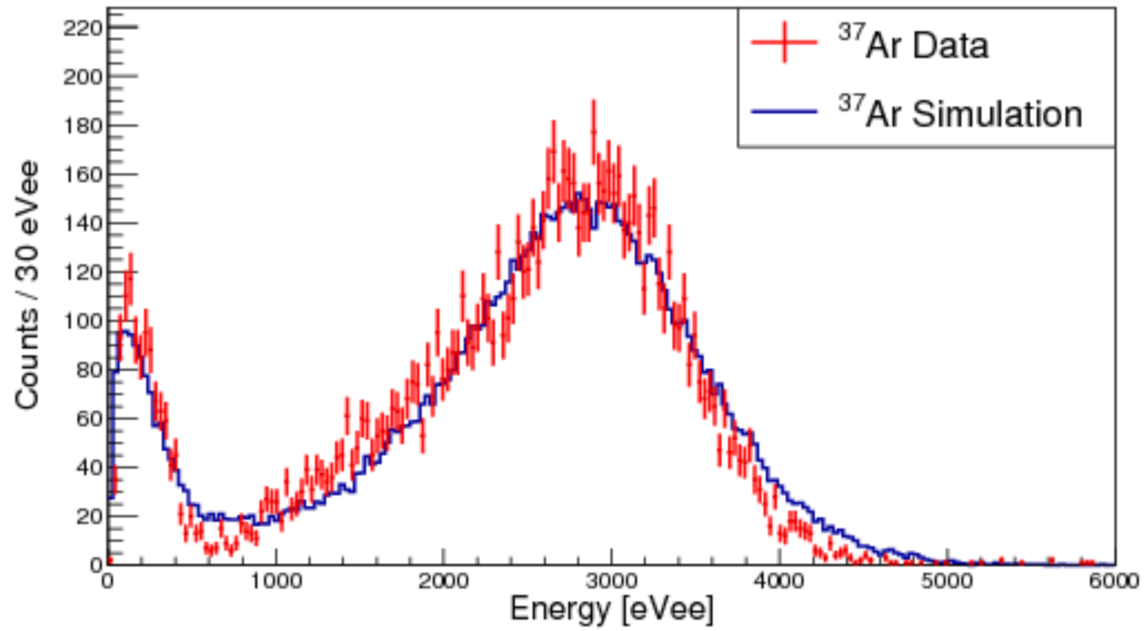

Astropart.Phys. 97 (2018) 54-62

SEDINE: Background simulation

- Anticipated main backgrounds:
  - Volume: Compton electrons
    - ^{208}Tl and ^{40}K in the rock
    - ^{238}U, ^{232}Th, and ^{60}Co copper shell/shielding
  - Surface: Radon decay products
  - Chemical Cleaning (nitric acid)
    - >200eV: 180 mHz → ~2mHz
    - <200eV: 400 mHz → ~20mHz
- Pulse simulations include:
  - Electric field (FEM)
  - Diffusion (Magboltz)
  - Avalanche process
  - Signal induction
  - Preamplifier response

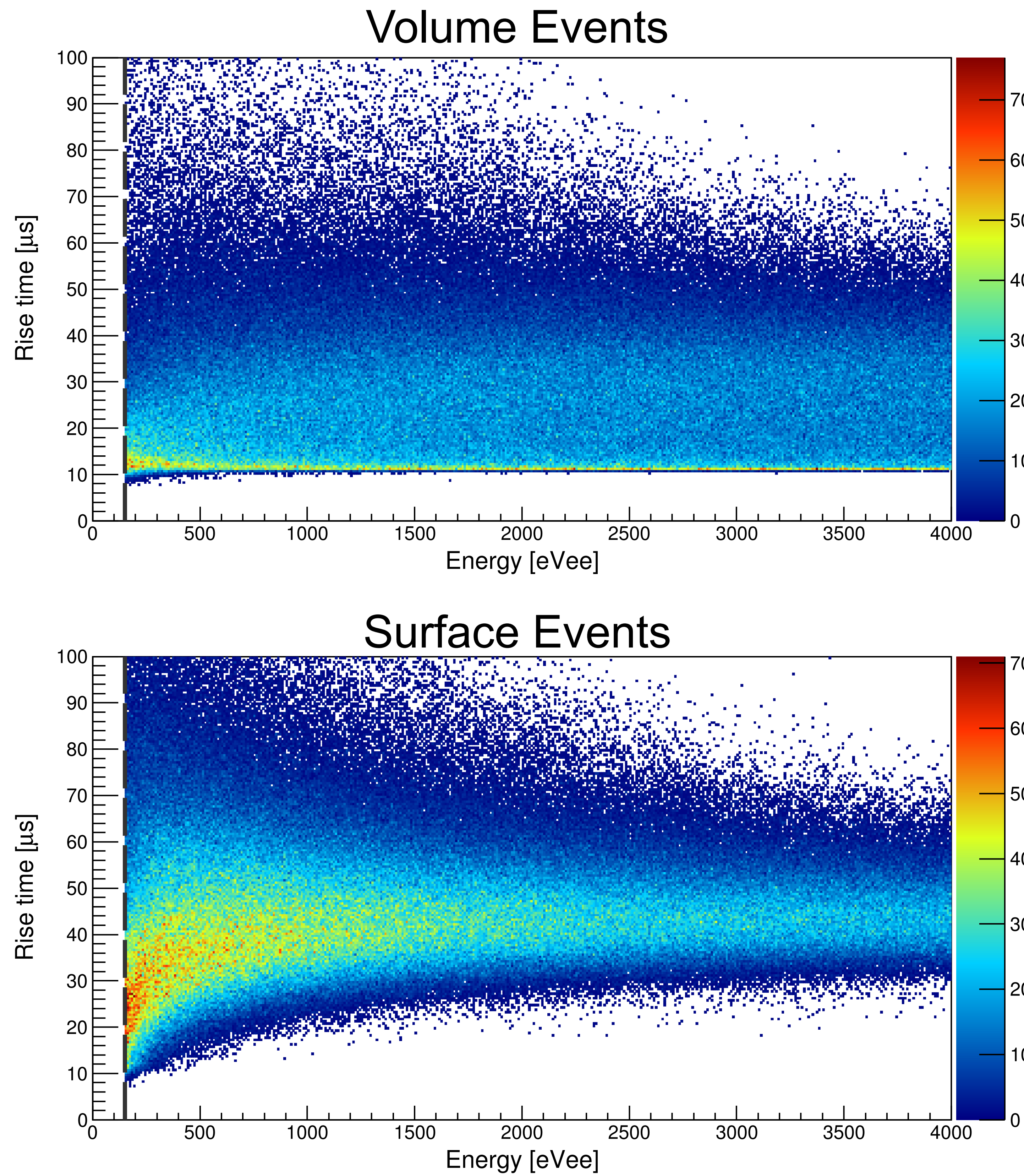

Astropart.Phys. 97 (2018) 54-62

SEDINE: Event Selection

- Analysis threshold: 150 eVee (~720 eVnr)
- 100% trigger efficiency (threshold @ ~35 eVee)
- Optimised Signal Region determined with Boosted Decision Tree (8 candidate masses)
- 1620 events selected in preliminary ROI
  - Failed BDT
  - Pass 0.5 GeV BDT: 15 events
  - Pass 16 GeV BDT: 123 events
  - Pass BDT for other masses